

Heterologous expression of lignin-degrading enzymes for biological depolymerization of lignin

Heterologe Expression von Lignin-abbauenden Enzymen für die biologische Depolymerization von Lignin

Von der Fakultät für Mathematik, Informatik und Naturwissenschaften der RWTH Aachen University zur Erlangung des akademischen Grades einer Doktorin der Naturwissenschaften genehmigte Dissertation

vorgelegt von

Master of Science (MSc) Biochemikerin

Selin Ece

aus

Izmir (Türkei)

Berichter: Prof. Dr. Rainer Fischer
Prof. Dr. Lars M. Blank

Tag der mündlichen Prüfung:

19.04.2018

Diese Dissertation ist auf den Internetseiten der Universitätsbibliothek verfügbar.

Table of contents

Table of contents.....	I
Abbreviations	IV
Abstract	1
Zusammenfassung.....	2
1.0 Introduction	4
1.1 Lignocellulose.....	4
1.2 Lignin-degrading enzymes	11
1.3 Directed evolution of lignin-degrading enzymes	17
1.4 Objectives of the Research	18
2.0 Results.....	20
2.1 Expression of selected lignin-degrading enzymes in <i>E. coli</i>	20
2.2 Expression of selected lignin degrading enzymes in <i>P. fluorescens</i>	29
2.3 Characterization of the purified enzyme preparations.....	30
2.3.1 Analysis of heme B content and T1-copper incorporation	30
2.3.2 The effect of temperature and pH on enzyme activities and stabilities	33
2.4 Activity assays with common lignin-model substrates	37
2.5 Activity assays with complex lignin-model compounds	39
2.5.1 Phenolic and non-phenolic lignin-model compounds.....	42
2.6 Activity assays with Kraft lignin.....	46
2.7 Modifications of selected enzymes for higher stability and/or activity	48
2.7.1 Immobilization of ScLac by two distinct methods.....	48
2.7.2 Protein engineering for improved H ₂ O ₂ stability.....	50
3.0 Discussion.....	59
3.1 Heterologous expression of lignin-degrading enzymes	59
3.1.1 <i>E. coli</i> as the heterologous expression host	60
3.1.2 <i>P. fluorescens</i> as the heterologous expression host	62
3.2 Functional and structural characterization of the purified enzymes.....	67
3.3 Activity analyses of the purified recombinant lignin-degrading enzymes.....	70
3.3.1 Activity assays with common lignin-model compounds	70
3.3.2 Activity assays with complex lignin-model compounds.....	71
3.3.3 Activity assays with Kraft lignin	72
3.4 Modification of the selected enzymes for enzymes for higher stability and/or activity	73
3.4.1 Immobilization of ScLac.....	73
3.4.2 Protein engineering for improved H ₂ O ₂ stability.....	73

Table of contents

4.0	Conclusions	75
5.0	Outlook.....	79
6.0	Experimental procedures.....	81
6.1	Materials	81
6.1.1	Chemicals and consumables.....	81
6.1.2	Primers	81
6.1.3	Plasmids.....	81
6.1.4	<i>Escherichia coli</i> strains.....	82
6.1.5	<i>Saccharomyces cerevisiae</i> EBY100 cells and yeast display system	83
6.2	Methods	84
6.2.1	Vector construction.....	84
6.2.2	Genomic DNA extraction from <i>Thermobifida fusca</i> XY	86
6.2.3	Colony PCR.....	86
6.2.4	Transformation of competent <i>E. coli</i> cells.....	86
6.2.5	Preparation and transformation of competent <i>S. cerevisiae</i> EBY100 cells.....	87
6.2.6	Cultivation of <i>E. coli</i> and <i>P. fluorescens</i> cells for protein expression	87
6.2.7	Cultivation of <i>S. cerevisiae</i> EBY100 cells.....	88
6.2.8	Protein extraction from <i>E. coli</i> and <i>P. fluorescens</i> cells.....	88
6.2.9	IMAC purification of recombinant lignin-degrading enzymes	88
6.2.10	Sodium dodecyl sulfate polyacrylamide gel electrophoresis (SDS-PAGE)	89
6.2.11	Western blot.....	89
6.2.12	Zymography assays.....	89
6.2.13	Determination of protein concentration.....	90
6.2.14	UV-Vis Spectra for Soret band and T1-copper detection	90
6.2.15	Activity assays using simple lignin-model compounds.....	90
6.2.16	Synthesis of MUAV compound.....	91
6.2.17	Determination of enzyme kinetics	91
6.2.18	Activity assays using complex lignin-model compounds.....	91
6.2.19	Activity assays of ScLac towards veratryl alcohol.....	91
6.2.20	Activity assays using Kraft lignin.....	92
6.2.21	Characterization of the enzymes.....	92
6.2.22	Immobilization of ScLac.....	93
6.2.23	Creation of <i>TfuDyP</i> Libraries.....	94
6.2.24	High-throughput screening of <i>TfuDyP</i> libraries.....	95
7.0	References.....	98
8.0	Appendix	112

Table of contents

8.1	Primer list	112
8.2	List of equipment	113
8.3	Plasmid maps	114
8.4	Protein and DNA ladder	116
8.5	Standard calibration curve of 4-MU (MUAV product)	116
8.6	Representative IMAC chromatogram	117
8.7	Analysis of ScLac activity on veratryl alcohol by HPLC	118
8.8	Representative LC-MS analysis of ScLac reaction with the SS β -O-4 OH model	122
8.9	Activity analysis of commercial laccase from <i>T. versicolor</i> on phenolic SS β -O-4 OH lignin-model compound	124
8.10	Initial activity assays with Kraft lignin	125
8.11	Optimization of <i>TfuDyP</i> expression time in <i>S. cerevisiae</i>	126
8.12	Secondary structure of <i>TfuDyP</i>	126
8.13	Characterization of isolated mutant <i>TfuDyP</i> variants and WT- <i>TfuDyP</i>	127
8.14	List of publications	129
8.15	List of figures	130
8.16	List of tables	133
	Acknowledgements	135
	Declaration	137
	Curriculum vitae	138

Abbreviations

Au	Absorbance
CLEA	Cross-linked enzyme aggregate
DyP	Dye-decolorizing peroxidase
DyPB	Dye-decolorizing peroxidase from <i>Rhodococcus jostii</i> RHA1
DyP-type peroxidase	Dye-decolorizing peroxidase
<i>E. coli</i>	<i>Escherichia coli</i>
Ep-PCR	Error-prone PCR
EtOH	Ethanol
FACS	Fluorescence activated cell sorting
His ₆ -tag	Hexa histidine affinity tag
HPLC	High pressure liquid chromatography
HRP	Horseradish peroxidase
HTP	High-throughput
IMAC	Immobilized metal affinity chromatography
IPTG	Isopropyl β -D-1-thiogalactopyranoside
kDa	Kilo Dalton
LiP	Lignin peroxidase
LMS	Laccase mediator system
mAu	Milliabsorbance
MeOH	Methanol
mg	Milligram
MnP	Manganese peroxidase
MTP	Microtiter plate
MUAV	α -O-(β -methylumbelliferyl) acetovanillone
nm	Nanometer
Ni-NTA	Nickel-Nitrilotriacetic acid
OD	Optical density
PCR	Polymerase chain reaction
pelB	Pectate lyase B of <i>Erwinia carotovora</i> CE
Pf	<i>P. fluorescens</i>
RZ	Reinheitszahl ratio
SDS-PAGE	Sodium dodecyl sulfate-polyacrylamide gel electrophoresis
SSHGDyP	Dye-decolorizing peroxidase from <i>Streptomyces albus</i> J1074
T1-copper	Type 1 copper
Tat	Twin arginine translocation
<i>TfuDyP</i>	Dye-decolorizing peroxidase from <i>Thermobifida fusca</i> XY
<i>TfuDyP</i> -Tat	<i>TfuDyP</i> with Tat leader peptide
<i>TfuDyP</i> -pelB	<i>TfuDyP</i> with pelB leader peptide
UV-Vis	Ultraviolet-Visible
MEGAWHOP	Whole plasmid amplification using megaprimers
WT	Wild type
VA	Veratryl alcohol
VP	Versatile peroxidase

Abstract

The decrease in the amount of the fossil fuels and significant environmental issues arisen from their consumption drives our currently fossil fuel-based society towards more sustainable sources. Lignocellulose is the most abundant sustainable biomass on earth. It has a very promising potential for the production of renewable fuels and chemicals. Two of the main components of lignocellulosic material, cellulose and hemicellulose, are evaluated for the use in industrial processes since they can be degraded easily by identified enzymes and chemical hydrolysis. However, at present very little is known about lignin, the third component of the lignocellulosic material. Insufficient knowledge and technology in lignin degradation, in part due to its recalcitrant nature, prevents industry from fully exploiting the potential of this polymer. The effort shown in the last decades about enzymatic lignin degradation has provided many bacterial and fungal organisms, eventually specific enzymes, which take part in efficient lignin degradation in the nature. Promising enzymes from bacteria and fungi have been identified; however, many drawbacks and difficulties stand between these enzymes and efficient exploitation of them in the industrial processes.

The main objective of this dissertation was to establish a versatile set of knowledge-based lignin-degrading enzymes from oxidoreductases to β -etherases and to achieve the heterologous expression of those enzymes to develop efficient methods for enzymatic lignin degradation. For this purpose, individual lignin-degrading enzymes were selected and heterologously expressed initially in *E. coli*. Expression yields of certain enzymes were improved by changing the host to *P. fluorescens*. The recombinant enzymes were purified via immobilized metal affinity chromatography and characterized using simple lignin-model substrates. Following basic characterization assays, which helped to understand the best conditions for the activity assays, the recombinant enzymes were tested with more complex lignin-model compounds and polymeric Kraft lignin. Two different immobilization methods were applied successfully to a laccase as a model for the recycling of these enzymes to reduce the production costs. Eventually a directed evolution library for a DyP-type peroxidase was created and an ultra-high-throughput method based on FACS was developed to screen the library for the variants with higher H₂O₂ stability.

This dissertation presents efficient heterologous expression of bacterial lignin-degrading enzymes and offers ways to obtain a decent amount of recombinant enzymes. Most of the expression yields reported here represent the highest yields achieved so far in the literature, which gives the flexibility of performing a wide range of activity assays with simple and complex lignin-model compounds and polymeric lignin samples from different sources. Immobilization and protein engineering were applied to the selected enzymes to develop advanced methods for improving the activity and stability of lignin-degrading enzymes economically.

Zusammenfassung

Die Abnahme der Menge an fossilen Brennstoffen sowie erhebliche Umweltprobleme, die sich aus ihrem Verbrauch ergeben, treiben unsere derzeit auf fossilen Brennstoffen basierende Gesellschaft zu nachhaltigeren Quellen. Lignocellulose ist die am häufigsten vorkommende nachhaltige Biomasse auf der Erde und besitzt ein vielversprechendes Potenzial für die Produktion von erneuerbaren Kraftstoffen und Chemikalien. Zwei der Hauptbestandteile des Lignocellulosematerials, Cellulose und Hemicellulose, werden für die Verwendung in industriellen Prozessen verwendet, da sie leicht durch identifizierte Enzyme und chemische Hydrolyse abgebaut werden können. Über Lignin, die dritte Komponente des Lignocellulosematerials, ist derzeit jedoch nur sehr wenig bekannt. Unzureichendes Wissen und Technologie im Ligninabbau, zum Teil aufgrund seiner widerspenstigen Natur, verhindert, dass die Industrie das Potenzial dieses Polymers vollständig ausnutzt. In den letzten Jahrzehnten konnte bereits gezeigt werden, dass viele bakterielle und pilzliche Organismen spezifische Enzyme bereitstellen, die an einem effizienten Ligninabbau in der Natur beteiligt sind. Vielversprechende Enzyme aus Bakterien und Pilzen wurden identifiziert; es bestehen jedoch viele Nachteile und Schwierigkeiten zwischen diesen Enzymen und ihrer effizienten Verwendung in den industriellen Prozessen.

Das Hauptziel dieser Dissertation war es, ein vielseitige Set wissensbasierter Lignin-abbauender Enzyme von Oxidoreduktasen zu β -Etherasen bis zu etablieren und heterolog zu exprimieren, um effiziente Methoden für den enzymatischen Ligninabbau zu entwickeln. Zu diesem Zweck wurden einzelne ligninabbauende Enzyme ausgewählt und zunächst heterolog in *E. coli* exprimiert. Die Ausbeuten bestimmter Enzyme wurden verbessert, indem *P. fluorescens* als Expressionssystem verwendet wurde. Die rekombinanten Enzyme wurden über immobilisierte Metallaffinitätschromatographie gereinigt und unter Verwendung von einfachen Ligninmodells substraten charakterisiert. Nach den grundlegenden Charakterisierungsassays, die dazu dienen, die optimalen Bedingungen für die Aktivitätsassays zu identifizieren, wurden die rekombinanten Enzyme mit komplexeren Lignin-Modells substraten und polymerem Kraft-Lignin getestet. Um die Produktionskosten zu senken, wurde eine Laccase exemplarisch mittels zweier unterschiedlicher Methoden immobilisiert, sodass eine Möglichkeit zum Recycling besteht. Schließlich wurde eine gerichtete Evolutionsbibliothek für eine DyP-Peroxidase geschaffen und eine Ultra-Hochdurchsatz-Methode auf FACS-Basis entwickelt, um die Bibliothek auf Varianten mit höherer H_2O_2 -Stabilität zu untersuchen.

Diese Dissertation präsentiert eine effiziente heterologe Expression von bakteriellen Lignin-abbauenden Enzymen und bietet Möglichkeiten, um eine ausreichende Menge an rekombinanten Enzymen zu erhalten. Die meisten der hier angegebenen Expressionsausbeuten stellen die höchsten

Zusammenfassung

bisher erzielten Ausbeuten in der Literatur dar, was die Flexibilität der Durchführung eines breiten Spektrums von Aktivitätsassays mit einfachen und komplexen Lignin-Modellsubstraten und polymeren Ligninen aus verschiedenen Quellen ermöglicht. Immobilisierung und Protein-Engineering wurden auf die ausgewählten Enzyme angewendet, um fortgeschrittene Verfahren zur wirtschaftlichen Verbesserung der Aktivität und Stabilität ligninabbauender Enzyme zu entwickeln.

1.0 Introduction

1.1 Lignocellulose

The energy and feedstock requirements of modern society have traditionally been dependent on petroleum-based fuels such as oil, coal, gas and various petrochemicals. However, nowadays these energy sources are approaching severe depletion, which is accompanied by the proportional increase in the prices (Bauer et al., 2016). In addition to this fact, there are many evidences showing that these energy sources are not environmentally friendly and there is an unequivocal correlation between the consumption of fossil energy sources and increasing greenhouse effects with increasing carbon dioxide emissions. Adverse consequences such as increase in land temperature and sea levels can be also counted as some of the many negative contributions of fossil sources to nature (Brecha, 2008; Zakzeski et al., 2012). Together with the aforementioned effects of fossil fuels (Figure 1), decreasing amounts of the reserves have directed the society into the search for sustainable energy, including alternative carbon sources as novel feedstocks (Marechal et al., 2005).

Biofuels, most commonly bioethanol and biodiesel, offer plant-based solutions for energy requirement and a chance to reverse the environmental deterioration. However, biofuels are majorly produced from corn kernels, sugarcane or soybean oil (Schubert, 2006). The increasing consumption of agricultural products and lands for the production of biofuels brings the discussion of water-land-food competition forward. Approximately 4% of the actual agricultural land, accompanied by almost equal amount of world's fresh water, is being used to supply the needs for biofuel production. The given amount of land and water could be sufficient to feed one-third of the malnourished population of the world (Rulli et al., 2016). Increasing competition between food and energy, together with the unfavorable outcomes contributing to the climate change, attentions has been given to changing the type of sustainable feedstock, which can also supply the demands for biofuel production or even for building blocks heavily used for industrially important chemicals.

Lignocellulose is the most sustainable biomass on earth (Moreno et al., 2015). The exploitable fractions of this valuable biomass are cellulose, hemicellulose and lignin (Isikgor & Becer, 2015). Unlike the aforementioned agricultural products, lignocellulose does not compete with the food supply (Valentine et al., 2012). Lignocellulose as a potential feedstock for biofuels and building blocks comprises the non-edible part of almost all plants including the agricultural waste. Lignocellulose is expected to substitute fossil-based fuels in the near future (Van Dyk & Pletschke, 2012).

Introduction

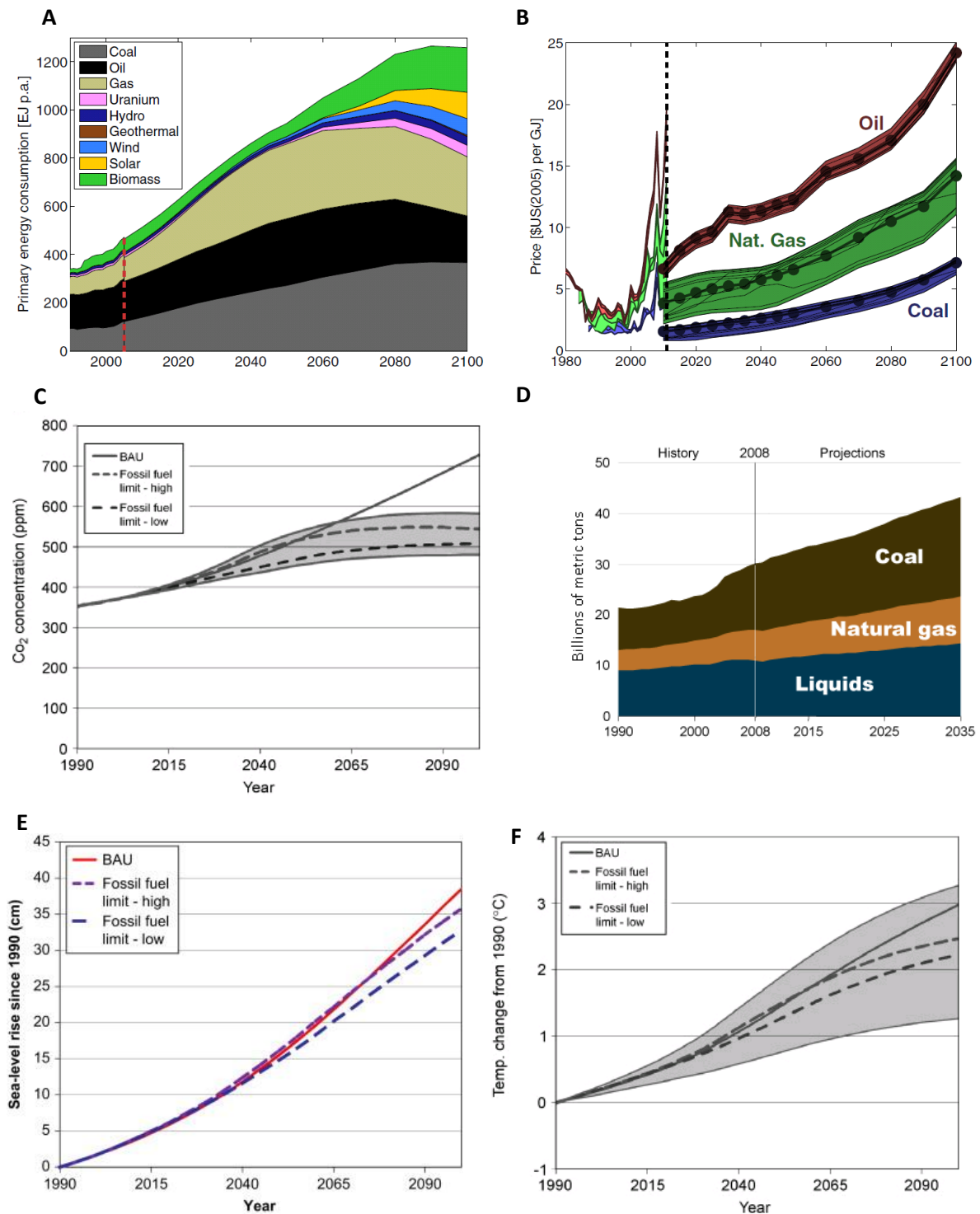


Figure 1: The big picture of energy consumption and its adverse outcomes on economics and environment (Bauer et al., 2016; Statistics, 2011). A: Primary energy consumption (before dashed line: 1990-2005, after dashed line: 2005-2100), B: Increase in the prices of the fossil fuels oil natural gas and coal (before dashed line: 1980-2011, after dashed line: 2011-2100), C: Carbon dioxide (CO₂) concentration scenarios in the next century (Bauer et al., 2016), D: Fossil fuel energy-related CO₂ emissions between 1990 and 2035 (Statistics, 2011). Projections of E: Sea-level increase and F: Temperature change since 1990 (Bauer et al., 2016). BAU: Business-as-usual scenario.

Introduction

Cellulose, a homopolymer of β -1,4-linked glucose, is the main structural polysaccharide of the plant cell wall (Figure 2). It comprises 30-50% of the dry mass of lignocellulose. The linkages between the glucose units, which build up the polymer, can be depolymerized by microbial cellulases (Sukumaran et al., 2005). Hemicellulose comprises 15-30% of the plant cell wall. It consists of pentoses and hexoses such as xylose, arabinose and mannose. Hemicelluloses can be degraded into their monomers by diluted acid or base hydrolysis and also by microbial hemicellulases (Abdel-Hamid et al., 2013). The third component, which occupies up to 15-30% of the plant cell wall, is lignin (Figure 2). Lignin has a very complex nature, in that it is resistant to degradation. It evolved to give plants the structural rigidity during the adaptation to the terrestrial life (Vanholme et al., 2010).

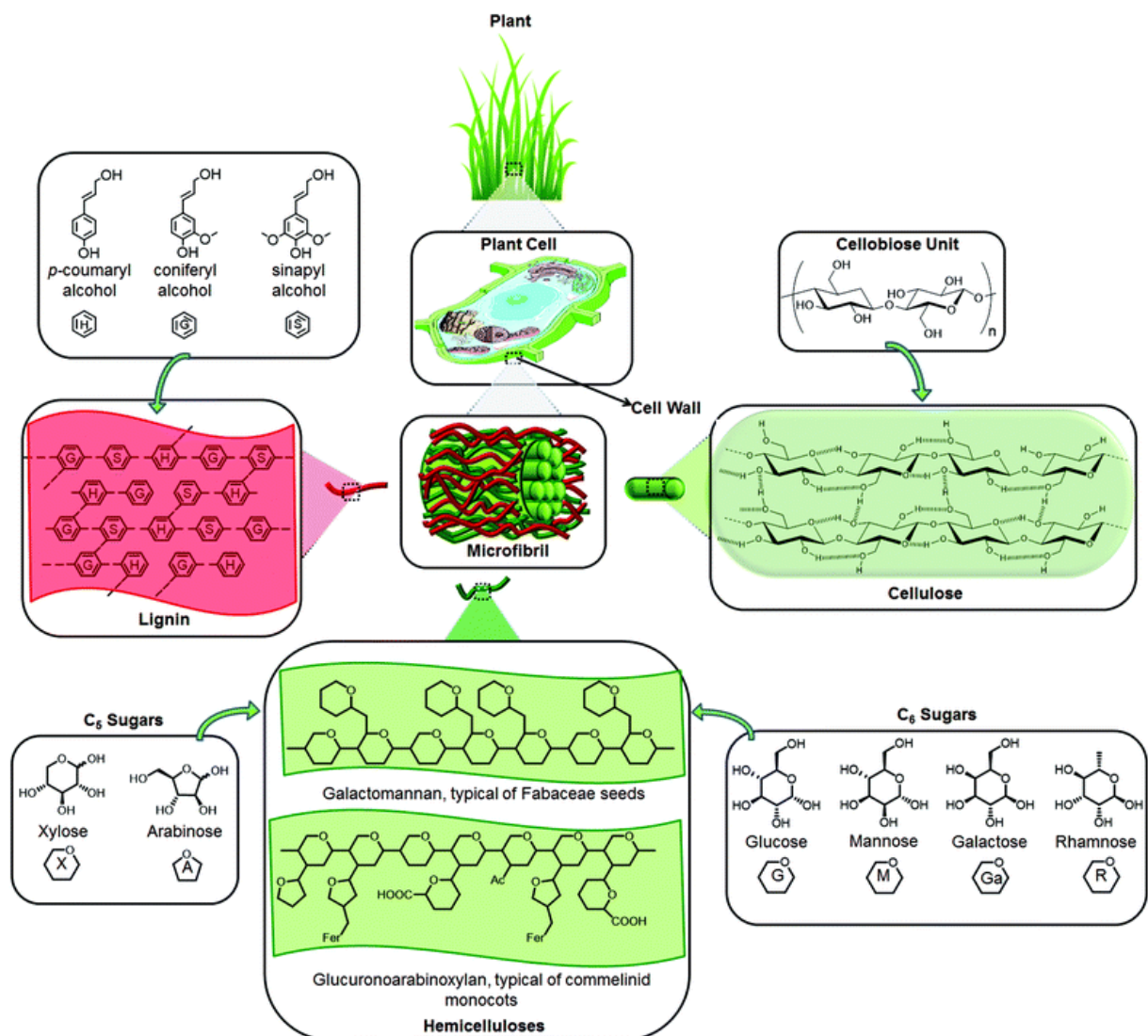


Figure 2: The main components of lignocellulose and their building blocks (Isikgor & Becer, 2015). The most sustainable and abundant biomass on earth is lignocellulose. Lignocellulose is made of three components: cellulose, hemicellulose and lignin. Cellulose is a β -1,4-linked glucose homopolymer. Hemicellulose consists of C₅ and C₆ sugars connected by various linkages. Lignin is the sole non-carbohydrate component of lignocellulose made of phenylpropanoid subunits.

Introduction

Unlike cellulose and hemicellulose, lignin is a non-carbohydrate aromatic polymer. Depending on the lignin source, one, two or three of the phenylpropanoid monomers come together by coupling reactions in order to build up the lignin polymer (Abdel-Hamid et al., 2013). The main phenylpropanoid monomers or monolignols are namely coniferyl alcohol, sinapyl alcohol and *p*-coumaryl alcohol (Figure 3), which are synthesized from phenylalanine obtained from the shikimate biosynthetic pathway in the plastid (Rippert et al., 2009; Vanholme et al., 2010). The monolignols incorporated into the lignin polymer structure are named as guaiacyl (G), syringyl (S), and *p*-hydroxyphenyl (H) units (Figure 3). Lignin polymers of different origins can contain different combinations of these three components. Hardwood lignins (dicotyledonous angiosperm) consist majorly of G and S units and trace amounts of H units, whereas softwood (gymnosperm) lignins are built mostly by G units with low levels of H units. Grasses (monocots) consist of almost equal amounts of G and S units and relatively more H units than dicots (Baucher et al., 1998). However, exceptions can be always encountered. There can be even one type of lignin polymer, which is built by merely one type of subunit such as lignins from gymnosperms that are built by only G-units (Uzal et al., 2009). Many different linkages exist in the incorporated structure of lignin polymer (Figure 4). The most abundant inter-unit linkage is the β -O-4 (β -aryl ether) linkage, which is also the one cleaved most easily by enzymes and chemical catalysts. Besides β -O-4 linkage, there are β -5, β - β , 5-5, 5-O-4 and β -1. These linkages are both chemically and enzymatically more difficult to break than the β -aryl ether linkage. The type of lignin monomer controls the amount of a certain linkage in the polymer. G-units tend to link via more resistant β -5, 5-5 and 5-O-4 linkages in comparison to the S-units (Boerjan et al., 2003).

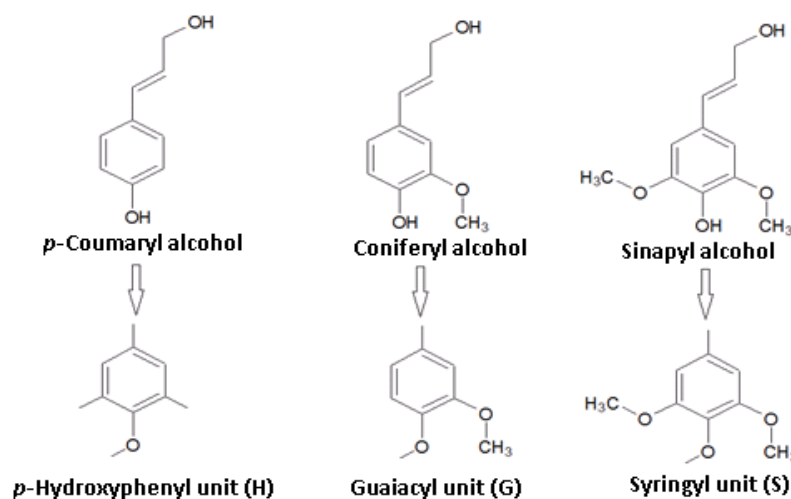


Figure 3: The monomers, which build lignin polymers and corresponding units within the incorporated lignin polymer structure (modified from Abdel-Hamid et al., 2013).

Introduction

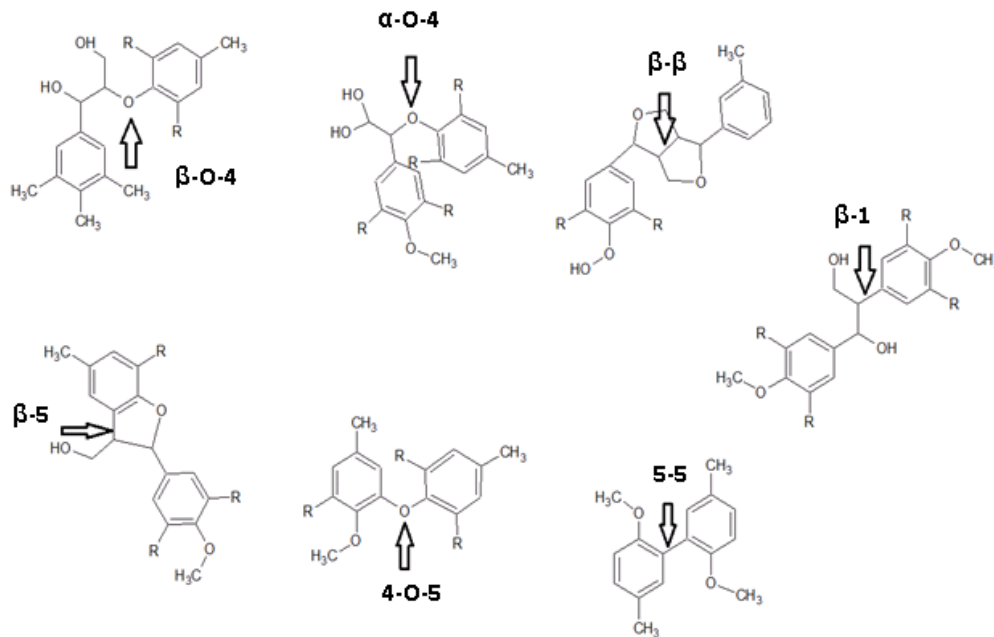


Figure 4: Phenylpropanoid linkages in lignin polymer structure (modified from Abdel-Hamid et al., 2013). β -O-4 linkage is the most abundant linkage found in lignin structures. The percentage of the linkages may vary among species and cells. An arrow indicates each related bond.

Nowadays most of the lignin polymer is obtained from the paper and pulp industries as a by-product. Lignocellulosic biomass including agricultural waste and biomass fractionation for various purposes also contribute to the amount of lignin obtained yearly, which is not valorized efficiently. However, an effective lignocellulosic biomass valorization strategy (Figure 5) should cover the exploitation of all three components (Jorgensen et al., 2007). Most of the lignin is either combusted in order to provide power for the cellulose fermentation plants (Schubert, 2006) or is chemically modified and used in chemical industry such as phenolic binder powder resins, polyurethane foams, epoxyresins, biodispersants and others (Lora & Glasser, 2002). The efficient depolymerization of this under-utilized highly-sustainable biopolymer has a potential to lead the industrial production of high value-added products such as vanillin, ferulic acid, vinyl guaiacol, optically active lignans, monolignol dimers (Ghaffar & Fan, 2014) and *p*-coumaric acid (Tapin et al., 2006). However, currently vanillin is the sole industrial product that is produced from lignin at a decent commercial scale and able to compete with the vanillin produced from the feedstocks of petrochemical origin (Balan, 2014). The major obstacle preventing the efficient industrial valorization of lignin is the lack of methods for the complete degradation of the polymer. Using an individual enzyme or a chemical catalyst for lignin degradation does not yield in complete depolymerization of the polymers, since each enzyme or catalyst is specific for merely one type of linkage breakdown in lignin.

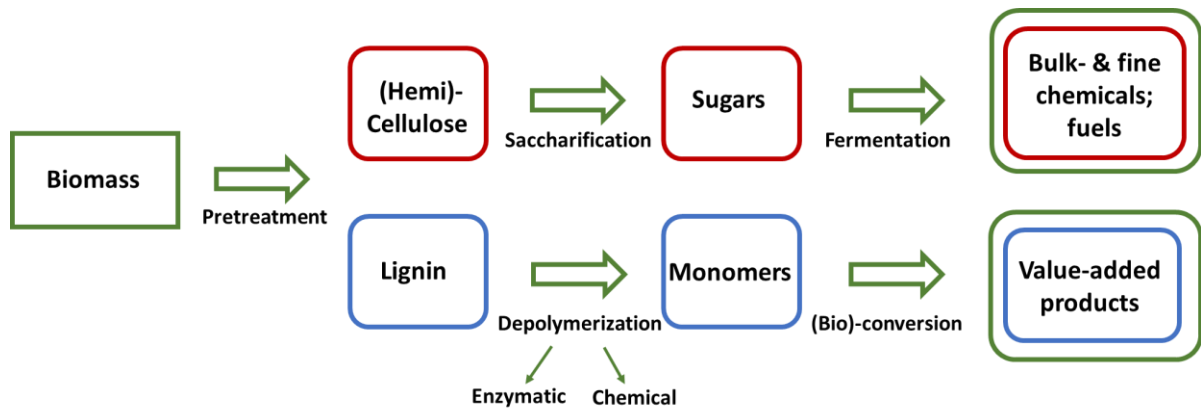


Figure 5: A scheme of ideal lignocellulosic biomass exploitation by the conversion of the subunits into the value-added products (adapted from Jorgensen et al., 2007). The (hemi)-cellulose part of the lignocellulosic biomass is pretreated and hydrolyzed to fermentable sugars and lignin is depolymerized to the monomers resulting in value-added products such as biofuel and bulk chemicals. Alternatively, the rest of lignin following the enzymatic or chemical cleavage can either be burned to provide energy to the whole biomass valorization plant or can be converted into chemicals to feed other processes.

The difficulties in the lignin valorization processes mostly arise from the heterogeneity in the monomer units and type of linkages. The type of linkages and physicochemical properties of isolated lignin polymer is majorly affected by the methodology used for extracting lignin from the total lignocellulose fraction. Therefore, following valorization procedures are also affected by the preparation techniques. Several techniques are used frequently for the extraction such as acidic and alkaline pulping. Acidic pulping is carried out with aqueous bisulfite and some additional chemicals such as either sodium, magnesium hydroxide or calcium hydroxide (Gratzl & Chen, 2000). At the end of the procedure lignin is obtained as lignosulfonate together with certain amount of degraded carbohydrates (Gierer & Ljunggren, 1979). Alkaline pulping can be achieved by two individual processes: Kraft process, being the most dominant one, and soda process (Chakar & Ragauskas, 2004). Alkaline pulping process resembles the acidic pulping process as lignin is dissolved in black liquor in both processes (Gierer & Wannstrom, 1986; Kondo & Sarkanen, 1984). In the Kraft process, aqueous sodium hydroxide is used together with sodium sulfide, thus lignin is obtained as lignin phenolate. The Bergius-Rheinau process uses concentrated hydrochloric acid at low temperatures resulting in a lignin sample that is insoluble in water and very poor in functional groups. The hydrochloric acid used in the acidic pulping can be recovered by an extraction process (Baniel & Eyal, 2010). Another common pretreatment method is steam explosion. This method is applied to redistribute lignin by exploding fibrous fraction. In a following step lignin can be extracted by an aqueous alkali or organic solvent (Jorgensen et al., 2007). Lignin can be also isolated relatively easier than other methods by treating the lignocellulosic biomass by mixture of an organic solvent and water. The drawback of the method, which is called organosolv pulping, is the requirement for elevated temperatures (Johansson et al., 1987; N, 1971). In addition to the methods described thus far, more methods are being developed at pilot-scale or even lab-scale i.e.

Introduction

using dilute acid for hydrolysis, by employing ionic liquids, superheated steam or supercritical water etc. (Liu, 2010; TAO, 2012; van Groenestijn et al., 2012; Yu et al., 2008). Mechanical comminution can be applied on lignocellulose samples in order to reduce the particle size and crystallinity, however, the methodology is not economically feasible because of the high energy requirements (Saritha et al., 2012). Lignin isolation techniques, types of lignin polymers and their properties are summarized in Figure 6.

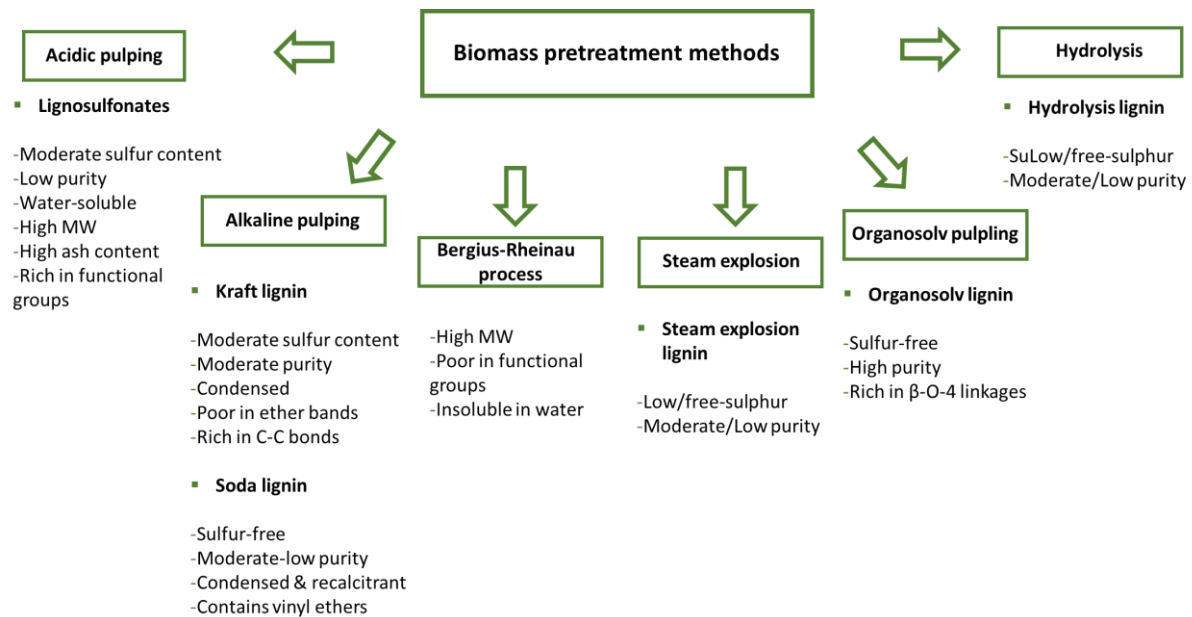


Figure 6: Biomass pretreatment methods and the type of lignin obtained from each method (adapted from Bruijninx et al., 2016).

In addition to the pretreatment techniques where the biomass is processed by chemical or physical forces, delignification can be also achieved biologically by the hydrolysis of the lignocellulosic sugars (Hatakka, 1984; Saritha et al., 2012; Woolridge, 2014). Biological delignification offers several advantages over the abovementioned techniques such as no harsh effects for environment, mild reaction conditions, low energy requirement, less complicated reactor design, higher product yield and lower side products which can have inhibiting effects on ongoing reactions or in further fermentation steps (Moreno et al., 2015). However, it can be difficult to achieve effective hydrolysis of the sugars because of the poor accessibility caused by the recalcitrant lignin barrier. Therefore, additional steps might be required to increase the accessibility to hemicellulose and cellulose and to increase the solubility of the given components.

1.2 Lignin-degrading enzymes

In nature, degradation of lignocellulosic biomaterial takes place by the participation of various enzymes from a certain organism or most of the time by the synergism of different enzymes of different origins (Bornscheuer et al., 2014). The depolymerization of lignin is among all other components the bottleneck as it is also the case for the pretreatment processes. Studies focused on the biological degradation of lignin go back to the 1980s. The first identified lignin degrading enzymes were peroxidases from the white rot fungus *Phanerochaete chrysosporium* (Glenn et al., 1983; Tien & Kirk, 1983). Afterwards, many different enzymes were identified and characterized. Although, it is known that both bacteria and fungi can take part in lignin degradation, only one class of organisms, White-rot Basidiomycetes, is able to achieve a complete lignin depolymerization and the mineralization of the degradation products. White-rot Basidiomycetes have a set of extracellular enzymes consisting of unspecific peroxidases, oxidases and reductases, which show activity in the presence of certain low molecular mass compounds mediating the reactions (Isroi et al., 2011; Martinez et al., 2005). Mediators are important for local lignin modification, because the lignin-degrading enzymes might be too large to penetrate in the condensed biomass structure (Pollegioni et al., 2015).

Particularly in the last decades, many bacterial and fungal lignin-degrading organisms and even insects have been identified as lignin-degrading organisms. Promising enzymes of bacterial and fungal origin have been expressed in order to characterize them further and to understand the function of these enzymes (Alam et al., 2014; Bugg et al., 2011b; Call, 1992; Farrell et al., 1987). Today, lignin-degrading enzymes (Figure 7) are divided into two major groups; heme peroxidases and laccases. As an additional group, β -etherases have also been shown to be effective lignin-degrading biocatalysts (Picart et al., 2015). There are more enzymes such as glucose oxidases, glyoxal oxidases and veratryl alcohol oxidases, which do not participate directly in lignin depolymerization, however, they help other enzymes by providing required molecules as hydrogen peroxide for example, or by reducing methoxy radicals generated by the peroxidases and laccases (Green, 1977). Esterases are another significant group of supporting enzymes that act on the junction groups between lignin and carbohydrates (d'Errico et al., 2015). Thus, the esterases are required for efficient total biomass depolymerization or biological delignification through the degradation of lignin-carbohydrate complexes (LCC) (Jeffries, 1990).

Heme peroxidases consist of two sub-groups that belong to different superfamilies. The first heme peroxidase superfamily comprises lignin peroxidase (LiP; EC 1.11.1.14), manganese peroxidase (MnP; EC 1.11.1.13) and versatile peroxidase (VP; 1.11.1.16), which are typically produced by fungi. (Hofrichter et al., 2010).

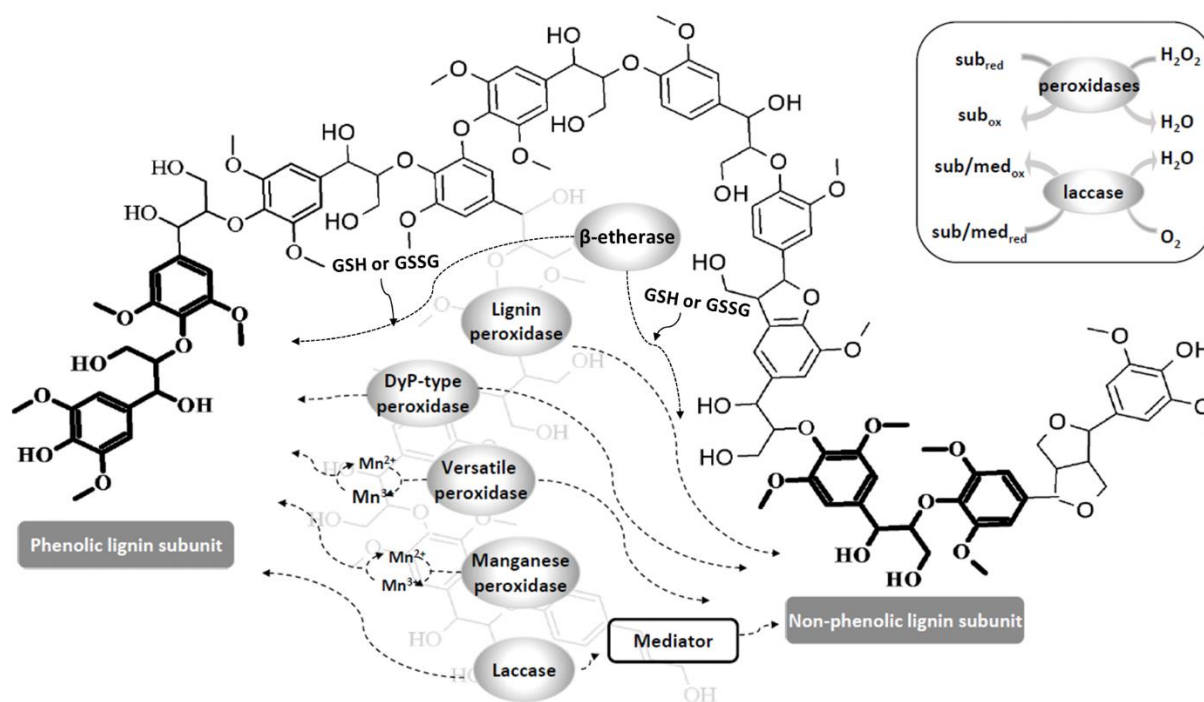


Figure 7: The lignin subunits that are attacked by lignin-degrading enzymes and the most common reaction mechanisms for each enzyme (modified from Lambertz et al., 2016). The bulky lignin polymer structure represents part of an organosolv lignin. Both superfamilies of lignin-degrading enzymes (heme peroxidases and laccases) can oxidize phenolic lignin subunits. Laccase requires the presence of a mediator to oxidize non-phenolic lignin subunits successfully. Lignin peroxidase, versatile peroxidase and DyP-type peroxidase do not require a mediator to attack non-phenolic structures. Manganese peroxidase and versatile peroxidase oxidize phenolic lignin subunits via the oxidation of manganese ($Mn^{2+} \rightarrow Mn^{3+}$). The inset box shows heme peroxidases reducing H_2O_2 to water to catalyze the oxidative reactions, whereas laccases reduce molecular oxygen to water, which is accompanied by the oxidation of the substrates or mediators. β -etherases act on aryl ether linkages independent of the phenolic or non-phenolic character of the groups. Depending on the type of β -etherase, glutathione (GSH) or glutathione disulfide (GSSG) is required for the reaction. The atoms and bonds of the phenolic and non-phenolic lignin subunits are highlighted in bold within the bulky structure. med: mediator, sub: substrate.

Non-phenolic structures are thought to be degraded by LiP due to its high redox potential. MnP can oxidize phenolic model compounds via the oxidation of Mn^{2+} to Mn^{3+} . VP is so called because it combines the catalytic properties of LiP and MnP (Abdel-Hamid et al., 2013). The second heme peroxidase superfamily comprises the dye-decolorizing peroxidases (DyP; EC 1.11.1.19), which also oxidize non-phenolic and phenolic β -O-4 lignin-model compounds (Sugano, 2009). Although the first DyP was isolated from fungi, subsequent genome sequence analysis has revealed that this superfamily of enzymes is also prominent in bacteria (Colpa et al., 2014). DyPs typically require hydrogen peroxide to form the oxo-ferryl intermediates of the enzymes, which subsequently oxidize the mediator or the substrate.

Unlike peroxidases, laccases (EC 1.10.3.2) reduce molecular oxygen to water using the copper atoms located within the active center to oxidize the mediator or substrate. Phenolic lignin units are oxidized directly whereas non-phenolic subunits are oxidized via a redox mediator system to overcome the low

Introduction

redox potential of laccases. The potential applications of laccases in lignocellulose degradation have been reviewed comprehensively in comparison to other lignin-degrading enzymes (Munk et al., 2015; Roth & Spiess, 2015).

β -etherases are members of glutathione-S-transferases. As non-radical ligninolytic enzymes being able to cleave the most dominant intermolecular linkage arylglycerol- β -aryl ether bond (Adler, 1957), β -etherases hold a great potential for biological lignin valorization (Picart et al., 2014). Despite their potential and catalytic properties, the number of studies about the identification and characterization of fungal or bacterial β -etherases is very limited. The reported β -etherases consist of a fungal member from the genus *Chaetomium* (Otsuka et al., 2003), bacterial members from the soil α -proteobacterium *Sphingobium paucimobilis* SYK-6, and some other from different bacterial species (Picart et al., 2014). The fungal enzyme was reported to be extracellular and active on β -aryl ether bonds in two lignin model dimers and a polymeric synthetic lignin (Otsuka et al., 2003). LigE, LigF and LigP are three enantioselective β -etherases from *S. paucimobilis* (EC 2.5.1.18) and are able to cleave β -aryl ether bond in the presence of glutathione (Masai et al., 2007; Masai et al., 1999; Tanamura et al., 2011).

In the last years, enzymes from fungi have been studied more comprehensively than those from bacteria since fungi had been shown to be more effective in lignin degradation and mineralization. However, recent studies suggest that, bacteria are also able to degrade lignin and that they produce potentially important bacterial peroxidases, laccases and β -etherases.

DyP-type peroxidases: *TfuDyP*, *DyPB*, *SSHGDyP*

DyP-type peroxidases comprise a relatively novel class of heme-containing lignin-degrading peroxidases (Singh & Eltis, 2015). The first member of the superfamily that had been described was a fungal DyP. However, further genomic studies have asserted that the number of DyPs in bacteria is even higher than the counterparts in eukaryotes (Colpa et al., 2014). Currently, DyPs are divided into four main sub-groups. Class A DyPs contain a Tat-type signal sequence, class B and C DyPs are known to be cytoplasmic and class D DyPs represent the fungal members of the family (Yoshida & Sugano, 2015). There is an additional sub-group, which is not always included in the classification. DyPs in this sub-group, class E, are relatively less characterized and have a stress-response function (Singh & Eltis, 2015). DyPs were initially known by their ability to degrade anthraquinone dyes and to oxidize a range of phenolic substrates (Sugano, 2009). Following studies revealed the potential of DyPs in lignin degradation. Several members of DyPs were shown to be responsible for lignin degradation in nature and activities on lignin-model compounds were also confirmed (Ahmad et al., 2011; Rahmanpour & Bugg, 2015a).

Introduction

TfuDyP represents one of the most comprehensively characterized bacterial DyPs from the thermophilic organism *Thermobifida fusca* XY. It was first described by van Bloois and colleagues and shown to bear a Tat-type signal peptide, which is a particular feature for class A DyP-type peroxidases (van Bloois et al., 2010). The enzyme possesses the typical structural DyP properties such as the conserved GXXDG motif, which is a part of the heme-binding region and crucial for the peroxidase activity (Colpa et al., 2014). Further characterization and crystallization studies revealed significant structural and catalytic properties and showed that *TfuDyP* can oxidize Kraft lignin and a β -aryl ether lignin model compound to a dimer. Regarding its broad substrate specificity and activity on complex model compounds and polymeric lignin, *TfuDyP* is a promising biological catalyst for further biomass valorization applications.

DyPB was identified by bioinformatical analysis of the genome sequence of *Rhodococcus jostii* RHA1 (Roberts et al., 2011). Further characterization and activity analyses showed that DyPB is active on lignin-model compounds and Kraft lignin (Ahmad et al., 2011). Just like *TfuDyP*, DyPB has also been investigated comprehensively. The specificity of the enzyme was analyzed for a wide range of organic substrates. Different from other DyPs, DyPB was shown to be able to oxidize Mn^{2+} by kinetic and spectroscopic analyses, which is a feature for fungal MnPs. The X-ray crystal structure of DypB was also determined, revealing the substrate access and putative active site residues.

The *SSHGDyP* gene was revealed following the genome analysis of *Streptomyces albus* JA10 genome (Zaburannyi et al., 2014). *SSHGDyP* was annotated to be an extracellular DyP; however, the expression of the enzyme in *S. albus* was not reported yet. There is also no report about the heterologous expression of the enzyme in other organisms.

SclLac

Laccases are the largest subgroup of the multi-copper oxidase protein superfamily (Ihssen et al., 2015). They can oxidize a broad range of substrates including phenolic compounds, azo dyes, aromatic amines, non-phenolic substrates (mostly with the help of mediators), anilines and aromatic thiols, and recalcitrant environmental pollutants (Canas & Camarero, 2010; Majumdar et al., 2014; Margot et al., 2013; Widsten & Kandelbauer, 2008). Each monomeric laccase contains four copper atoms located at three different positions, namely the type 1 (T1), type 2 (T2) and the binuclear type 3 (T3) copper sites. All of them are involved in the oxidation of substrate molecules accompanied by the reduction of molecular oxygen to two molecules of water (Thurston, 1994). The copper atoms bind histidine residues that are conserved among the laccases of different organisms (Claus, 2003; Luis et al., 2004). The T1 copper gives the laccase its blue color and is responsible for the final oxidation of the substrate. Electrons are transferred from the T1 copper site to the T2/T3 sites, where molecular oxygen is

Introduction

reduced to water. The T1 copper is characterized by its absorbance at 610 nm whereas the T3 copper shows a weak absorbance at 330 nm. The T2 copper is colorless but it can be detected by electro-paramagnetic resonance spectroscopy (Gunne & Urlacher, 2012a; Thurston, 1994).

Laccases are used in many biotechnological processes in the paper and pulp, textile, pharmaceutical and petrochemical industries, and for the bioremediation of industrial wastes (Chandra & Chowdhary, 2015; Morozova et al., 2007; Munk et al., 2015; Rodriguez Couto & Toca Herrera, 2006; Roth & Spiess, 2015). Laccases can be combined with laccase mediator systems (LMS) such as 1-hydroxybenzotriazole (HBT) and 2, 2'-azino-bis (3-ethylbenzothiazoline-6-sulfonic acid) (ABTS) for the pretreatment and depolymerization of lignocellulosic biomass (Call & Mucke, 1997; Canas & Camarero, 2010). Digestion of the cellulose fraction of a lignocellulose sample can be increased after decomposing the lignin fraction by laccases (Chen et al., 2012a). In the presence of HBT, lignin can be removed from woody and non-woody feedstocks to increase sugar and ethanol yields (Gutierrez et al., 2012). By combining ABTS with a laccase, the lignin fraction of a wheat straw sample can be degraded selectively after applying a steam explosion pretreatment (Qiu & Chen, 2012).

Although laccases are ubiquitous, research has focused mainly on fungal laccases because many different isozymes have been identified, particularly among the white-rot fungi. Following the identification of the first bacterial laccase (Givaudan et al., 1993) many further examples were discovered (Chandra & Chowdhary, 2015). The properties of bacterial laccases, such as their enantioselectivity, stability at high pH and high temperatures, and a broader pH range are advantageous for industrial applications. Further, the large-scale production of fungal laccases is challenging because of the slow growth rates of fungi. These factors have made bacterial laccases a valuable alternative to fungal laccases (Ausec et al., 2011; Bugg et al., 2011b; Chandra & Chowdhary, 2015).

The extracellular expression of Sclac in its native host was previously carried out in the submerged culture for 10 days and the laccase was purified by 5 sequential steps (Arias et al., 2003). The enzyme showed activity on a range of phenolic substrates, on veratryl alcohol via ABTS as the mediator (Arias et al., 2003), and even in Kraft pulp biobleaching (Arias et al., 2003) and micropollutant degradation for waste water treatment (Margot et al., 2013). However, the activity of the enzyme was 20 times lower when compared to the fungal laccase from *Trametes versicolor* (Margot et al., 2013). Although, the enzyme presented promising catalytic properties against phenolic and non-phenolic substrates, the heterologous expression of the enzyme and applications towards biological lignin valorization have not been reported in the literature so far.

β -etherases: LigE and LigF

LigE and LigF are two well-characterized bacterial β -etherases from *S. paucimobilis* that are dependent on glutathione and belong to the glutathione-S-transferase (GST) superfamily. Enzymes in the superfamily of GSTs are involved in a broad range of detoxifying processes, including xenobiotics (Allocati et al., 2009; Hayes et al., 2005). LigE and LigF genes are tandemly located together with another GST LigG in the genome of *S. paucimobilis* SYK-6 (Masai et al., 1999). However, in the β -aryl ether cleavage pathway of *S. paucimobilis* there are more enzymes including several stereospecific alcohol dehydrogenases that are dependent on four nicotinamide adenine dinucleotide (NADH) (Figure 8). Masai et al. used a lignin-model compound, α -(2-methoxyphenoxy)- β -hydroxypropiovanillone (MPHPV), to understand the exact function of LigE and LigF in lignin degradation mechanism achieved by the organism. According to the assays, LigF and LigE catalyze the nucleophilic attack of glutathione on the carbon atom at the β position of MPHPV, however, each enzyme attacks a different enantiomer of the racemic MPHPV preparation (Picart et al., 2015). Picart et al. recently used LigF and LigE to mine the databases and obtained four novel β -etherases. The group provided more evidences that LigF and LigE are active on various β -aryl ether lignin-model compounds and artificial polymeric lignin structures (Picart et al., 2014). Further assays towards the lignin-degrading activities and stereoselectivities of the β -etherases were also carried out by Gall et al. It was shown that with racemic β -aryl ether-linked model substrates, LigE cleaves only the (R)-enantiomer, whereas LigF cleaves only the (S)-stereoisomer (Gall et al., 2014).

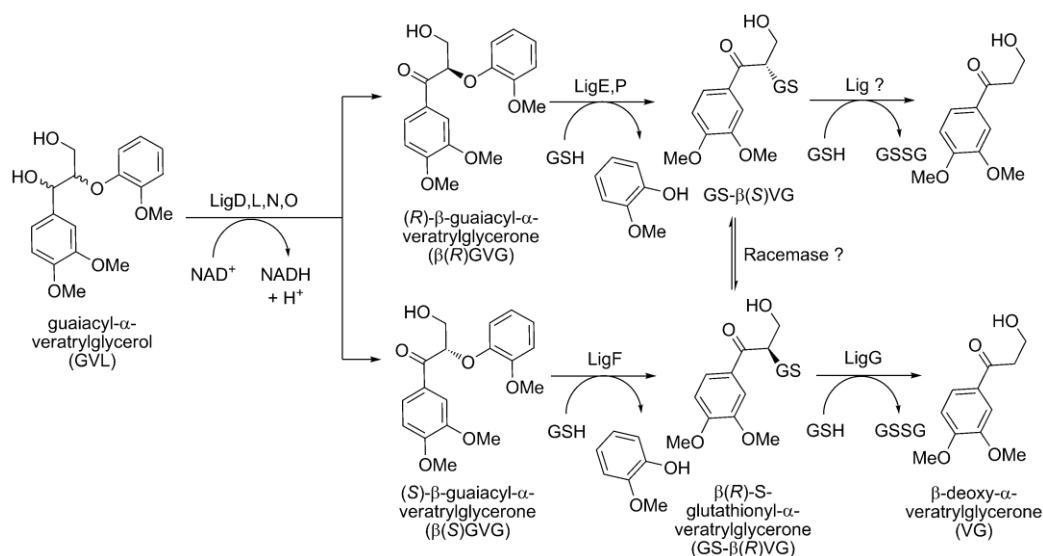


Figure 8: β -aryl ether cleavage pathway in *S. paucimobilis* via guaiacyl- α -veratrylglycerol (GVL) model compound (Picart et al., 2014). NADH-dependent LigD, LigL, LigN, and LigO oxidize the Ca-hydroxyl group of the GVL diastereomers that are subsequently cleaved by the β -etherases LigE, LigF, and LigP, which yield two enantiomeric glutathione (GSH) conjugates (GS- β VG). LigG is the glutathione lyase that uses GSH to liberate veratrylglycerone (VG) from GS- β (S)VG through the formation of glutathione disulfide.

1.3 Directed evolution of lignin-degrading enzymes

Directed evolution is a technology platform, which is used to modify or improve certain characteristics of enzymes without necessarily requiring prior knowledge about the protein structure (Garcia-Ruiz et al., 2014). It can be applied to an enzyme by following four main experimental steps: generation of the diversity, cloning and transformation in heterologous host, screening for improved variants, and isolation of the mutant and the gene responsible for the enhanced property (Matsuura & Yomo, 2006). Random mutagenesis by error-prone PCR or recombination by DNA shuffling are two frequently used methods for the generation of diversity (Shivange et al., 2009; Wong et al., 2006). Based on the performance of the variants obtained from the screening of each library, diversity generations can be repeated as many times as required to obtain an even better and improved variant. To detect the best performing variants creating a high-quality mutant library and developing an efficient screening system that reflects the property of interest are very important and essential steps. In most of the directed evolution studies, lack of an effective high-throughput screening method is the main bottleneck in finding improved variants (Wong et al., 2005). Microtiter plate (MTP) and agar plate assays for enzymatic activity detection are most commonly used screening methods. MTP assays can be easy to develop and carry out, however, the number of the variants that can be screened is restricted (10^3 - 10^5) and they can be expensive and time consuming (Becker et al., 2004; Longwell et al., 2017; Olsen et al., 2000; Ostafe, 2013). Agar plate assays are straightforward and economic, but the activity of the variants cannot be assayed quantitatively (Leemhuis et al., 2009). As an alternative to MTP and agar plate assays, flow cytometry makes it possible to screen more than 10^7 variants in a very short time (Aharoni et al., 2005) with a rate of 100,000 cells per second (Givan, 2001). The technique provides detection and analysis of fluorescent signals generated by particles as they flow in a liquid stream past an illuminating laser beam. Optical and fluorescence characteristics of cells can be measured and resolved for a certain sample population (Brown & Wittwer, 2000). The signal detection, however, is limited to fluorescence and the product of the enzymatic reaction needs to stay connected to the cells responsible for producing it. This can be achieved by binding or the intercalation of the fluorescent dyes (Becker et al., 2004) or creating artificial compartments around the cells. Lipovsek et al. used the tyramide-fluorescein assay to stain yeast cells by binding fluorescence-labeled tyramine. This fluorescent assay combined with the display of a horseradish peroxidase (HRP) on the yeast surface provided a high-throughput (HTP) screening assay based on fluorescence activated cell sorting (FACS) without the requirement of cell compartmentalization and decreased the possibility of cross-activity between the cells (Lipovsek et al., 2007).

Directed evolution of lignin-degrading oxidoreductases promises great improvements towards industrial applications by changing their substrate specificity, increasing their stability at the elevated

Introduction

temperatures or in the presence of industrial denaturants and against high concentrations of hydrogen peroxide (Rahmanpour & Bugg, 2016). Nevertheless, the number of studies about the engineering of bacterial lignin-degrading enzymes are very low due to lack of suitable heterologous expression hosts and HTP assays. A few studies have been conducted recently on a bacterial laccase CotA, and the substrate specificity and functional expression of the enzyme was improved successfully (Brissos et al., 2009; Gupta & Farinas, 2009; Gupta et al., 2010; Gupta et al., 2011; Koschorreck et al., 2009). Neither fungal nor bacterial DyPs were used previously in directed evolution experiments for improving the enzyme characteristics. So far, only a small number of fungal heme-peroxidases were used in directed evolution studies to improve the stability against higher concentrations of hydrogen peroxide, the stability in the presence of organic solvents, the stability at elevated temperatures, the catalytic activity, and the functional expression and secretion (Cherry et al., 1999; Garcia-Ruiz et al., 2012; Houborg et al., 2003; Miyazaki-Imamura et al., 2003; Morawski et al., 2001; Patel & Hecht, 2012; Ryu et al., 2008a; Ryu et al., 2008b). In all cases *S. cerevisiae* had been chosen as heterologous expression host and sometimes also for the generation of the diversity (Gonzalez-Perez et al., 2012). The host facilitates the introduction and recombination of point mutations and provides an efficient secretory machinery and possibility for complex post-translational modifications (Garcia-Ruiz et al., 2014). It is also possible to display the proteins on the surface of *S. cerevisiae* cells by using a special plasmid called pCTcon2 (Chao et al., 2006), which can accelerate the high-throughput screening processes and keeps the connection between genotype and phenotype.

1.4 Objectives of the Research

Lignin is the most under valorized component of lignocellulosic biomass due to the lack of knowledge and technologies for degradation. One of the major problems in the field of biological lignin depolymerization is to obtain sufficient amount of biological catalysts to investigate efficient methods. The main objective of this thesis is to develop high-yield heterologous expression strategies for a versatile set of lignin-degrading enzymes in suitable host system/s to investigate efficient methods for biological lignin depolymerization. The experiments described in this thesis constitute a comprehensive comparison of different heterologous expression strategies based on the application of leader peptides, changing the position of the affinity tags and changing expression host from most commonly used bacterial host *Escherichia coli* to *Pseudomonas fluorescens*. The following work will discuss the ways to produce lignin-degrading enzymes efficiently and will provide assays using bacterial recombinant enzymes against complex model substrates and polymeric lignin samples. The methods for modifying the recombinant enzymes via immobilization or protein engineering will be also discussed as an alternative platform to obtain enhanced biocatalysts to develop advanced methods for efficient biological lignin valorization. The outline of the objectives are summarized in Figure 9.

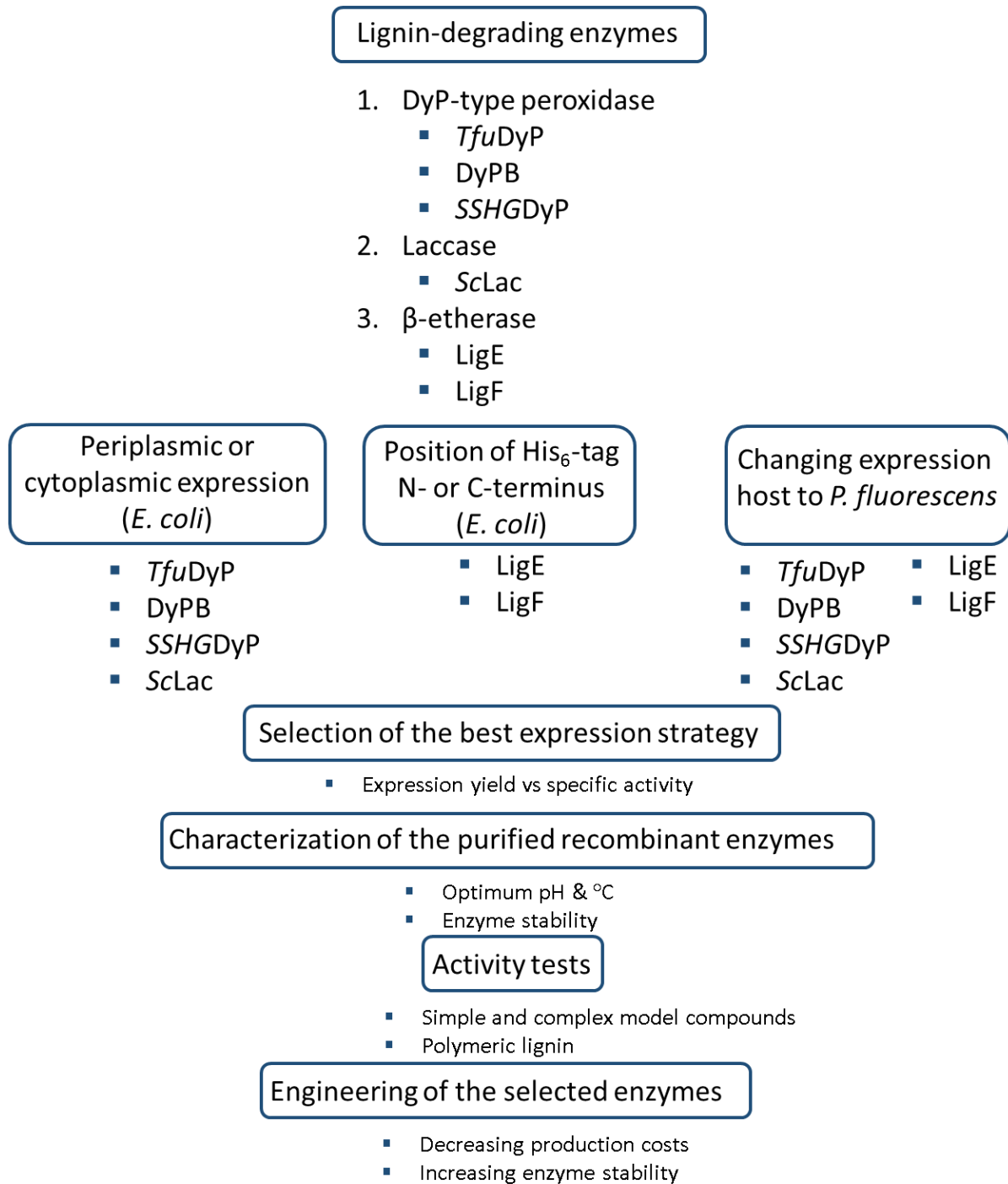


Figure 9: The flowchart of the work described in this thesis. The experimental steps of the thesis are summarized for each main point of the experimental procedures. It starts with the selection of the lignin-degrading enzymes, followed by three heterologous expression strategies, the characterization of the enzyme's properties and specific activities and leads into an engineering approach for enhanced features.

2.0 Results

2.1 Expression of selected lignin-degrading enzymes in *E. coli*

Considering the structure of lignin and the linkages that build it up, a versatile set of lignin degrading enzymes were selected. Particular emphasis has been placed on the enzymes which are able to modify β -O-4 linkages because they are ubiquitous in lignin sources from many different species (Nichols et al., 2010). At least one member of each major group (heme-containing peroxidases, laccases and β -etherases) was included in the enzyme set to achieve a comprehensive catalysis of the complex model substrates and polymeric lignin samples. The progress indicating the significance of the bacterial lignin-degrading enzymes and the ease to produce these enzymes influenced the selection of certain enzymes in this thesis. Therefore, three bacterial DyP-type peroxidases, one bacterial laccase and two bacterial β -etherases were selected to be used in further experiments. The selected enzymes, their origin organisms and properties were summarized in the following table (Table 1).

Table 1: Enzymes that have been chosen for heterologous expression in an *E. coli* and a *Pseudomonas fluorescens* host system. The enzymes, their origin and the type of lignin linkage they are capable of modifying are given.

Enzyme	Origin	Reaction
DyP-type peroxidase (<i>TfuDyP</i>)	<i>Thermobifida fusca</i> TM51	Oxidation of non-phenolic lignin model compounds and β -O-4 linkages
DyP-type peroxidase (<i>SSHGDyP</i>)	<i>Streptomyces albus</i> J104	Oxidation of non-phenolic lignin model compounds and β -O-4 linkages
Peroxidase DyPB (<i>DyPB</i>)	<i>Rhodococcus jostii</i> RHA1	Oxidation of non-phenolic lignin model compounds
Laccase (<i>ScLac</i>)	<i>Streptomyces cyaneus</i> CECT 3335	Catalysis of both phenolic and non-phenolic lignin model compounds
β -etherase (<i>ligE</i>)	<i>Sphingobium paucimobilis</i> SYK-6	Degradation of β -aryl ether linkages
β -etherase (<i>ligF</i>)	<i>Sphingobium paucimobilis</i> SYK-6	Degradation of β -aryl ether linkages

The *TfuDyP* encoding nucleotide sequence (UniProt Q47KB1) was amplified from the isolated genomic DNA of *Thermobifida fusca* YX. The coding sequences of *DyPB* (UniProt Q0SE24), *SSHGDyP* (UniProt D6B600) and *ScLac* (UniProt F6L7B5) were codon optimized for the expression in *E. coli* and obtained by gene synthesis. In order to transport the DyPs and the laccase into the periplasmic space of *E. coli*, further modifications were carried out when required and the genes were cloned into the pET-22b(+) bacterial expression vector system. The native Tat signal peptide within the *TfuDyP* coding sequence and the *pelB* leader peptide of the pET-22b(+) plasmid were implicated in the expression cassettes of

Results

two individual expression constructs. In addition, another construct lacking any kind of leader peptides (*TfuDyP*-cp) was prepared to check the effect of the signal sequences on the heterologous expression levels *TfuDyP*. The DyPB coding sequence comprised no native signal peptide, therefore, merely the *pelB* leader peptide of the pET-22b(+) vector was used to direct the protein in the periplasmic space of *E. coli*. *SSHGDyP* and *ScLac* were reported to be secreted enzymes (Arias et al., 2003; Zaburannyi et al., 2014). Thus, the codon optimized synthetic nucleotide sequences of these enzymes were cloned into pET-22b(+) initially without any leader peptides in the expression cassette. However, in a parallel strategy, the enzymes were also cloned with the *pelB* leader peptide into the pET-22b(+) vector to compare the expression yields. Codon optimized and synthesized sequences of the β -etherases, *LigE* and *LigF*, were cloned into pET-22b(+) without any leader peptides since they are known to be cytoplasmic enzymes. All constructs harbored a His₆-tag at the C-terminus for later immunodetection and purification. In addition, *LigE* and *LigF* were also designated to harbor an N-terminus His₆-tag as individual constructs. Test expressions were carried out in small scale (20 ml) for each enzyme to determine the optimal culture conditions (Table 2) for the following protein expression in higher volumes (500 ml). The temperature was varied between 12°C and 37°C, the expression time was varied between 3 h and 20 h, and the IPTG concentration was varied between 0.04 mM and 0.5 mM. Various *E. coli* strains were also used as host systems to optimize the expression yields: *E. coli* BL21-CodonPlus(DE3)-RIL, BL21 Star(DE3), SHuffle Express, ArcticExpress, Rosetta-gami 2(DE3)pLysS, and NiCo21(DE3).

The enzymes were expressed under optimal conditions in 500 mL culture volume and purified by one-step IMAC. The elution fractions obtained from the IMACs were analyzed by SDS-PAGE (5-12% polyacrylamide gels) and western blot (detection by using an α -His antibody and GAR^{AP}). The fractions, for which strong protein signals were detected, were pooled and dialyzed to remove the imidazole. Protein concentrations were determined and expression yields were calculated.

The IMAC chromatograms of *TfuDyPs* show that all enzymes were eluted from the column at approximately same imidazole concentration independent of the used construct (type of signal leader peptide). However, the strength of the eluted protein bands might vary depending on the expression yield and purification efficiency.

Results

Table 2: Optimal culture conditions (Induction OD₆₀₀, IPTG concentration, expression temperature and expression duration), *E. coli* strain used for the heterologous expression of the lignin-degrading enzyme constructs and the corresponding expression yields. cp: Cytoplasmic, pelB: Pectate lyase B of *Erwinia carvotora* CE, Tat: Twin-arginine translocation pathway.

Enzyme	His ₆ -tag position	Leader peptide	<i>E. coli</i> strain	Induction OD ₆₀₀	IPTG mM	Expression temperature °C	Expression time h	Expression yields ~mg protein L ⁻¹ expression culture
TfuDyP	C-terminus	Tat	BL21-CodonPlus(DE3)-RIL	0.6	0.5	30	16	6.0
	C-terminus	pelB	BL21-CodonPlus(DE3)-RIL	0.6	0.5	30	16	6.0
	C-terminus	cp	BL21-CodonPlus(DE3)-RIL	0.6	0.5	30	16	20.0
DyPB	C-terminus	pelB	BL21 Star (DE3)	0.6	0.04	20	20	18.0
	C-terminus	cp	BL21 Star (DE3)	0.6	0.04	20	20	4.0
SSHGDyP	C-terminus	pelB	BL21 Star (DE3)	0.6	0.04	20	20	3.5
	C-terminus	cp	BL21 Star (DE3)	0.6	0.04	20	20	5.0
ScLac	C-terminus	pelB	BL21 Star (DE3)	0.6	0.04	20	20	3.5
	C-terminus	cp	BL21 Star (DE3)	0.6	0.04	20	20	104.0
LigE	C-terminus	no	BL21-CodonPlus(DE3)-RIL	0.6	0.5	30	16	2.0
	N-terminus	no	BL21-CodonPlus(DE3)-RIL	0.6	0.5	30	16	5.5
LigF	C-terminus	no	BL21-CodonPlus(DE3)-RIL	0.6	0.5	30	16	3.0
	N-terminus	no	BL21-CodonPlus(DE3)-RIL	0.6	0.5	30	16	16.0

Results

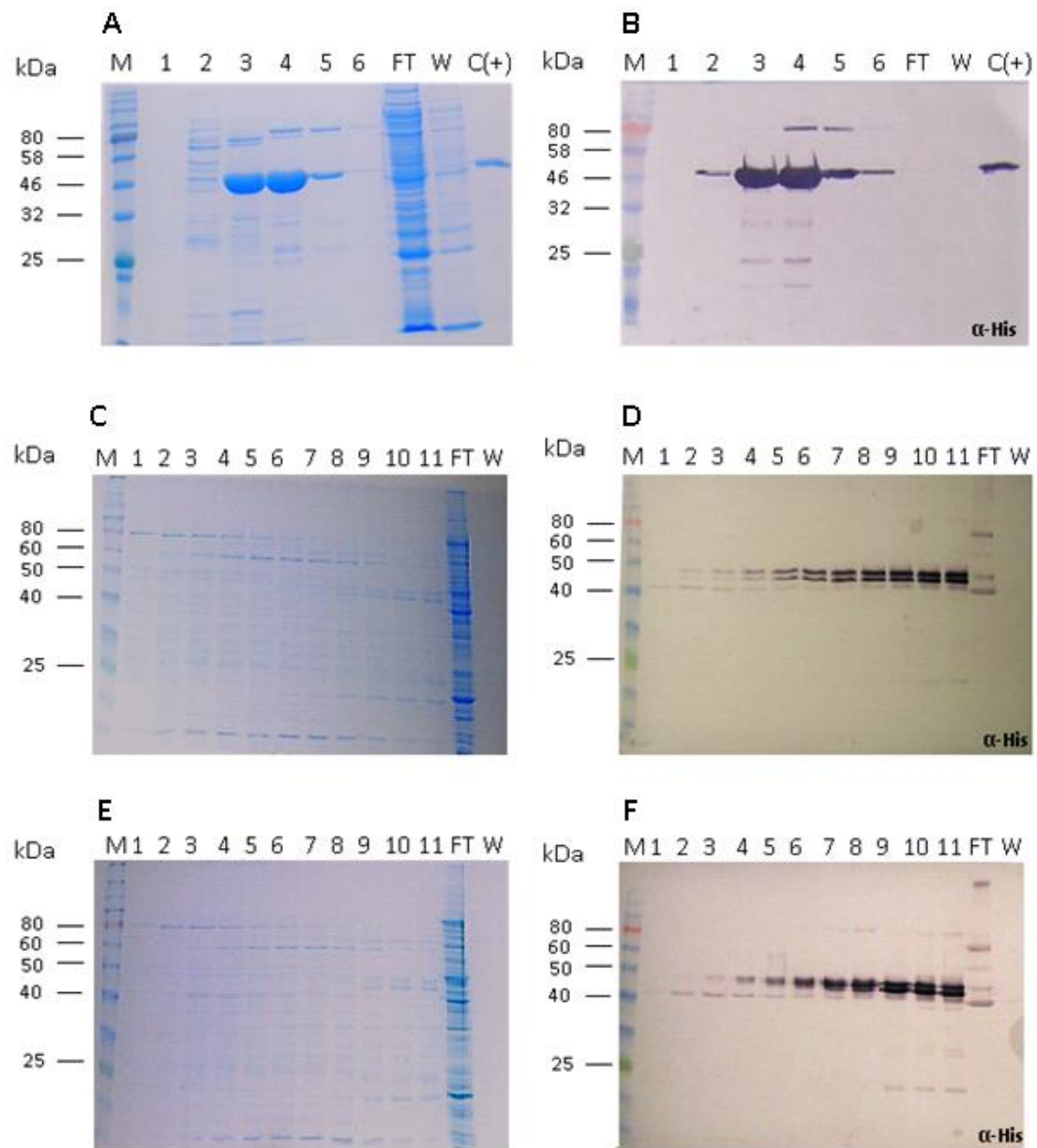


Figure 10: SDS-PAGE and western blot analysis of the IMAC purification fractions of *TfuDyP-cp* (A, B), *TfuDyP-Tat* (C, D) and *TfuDyP-pelB* (E, F). Elution fractions: 1-6 for *TfuDyP-cp*, 1-11 for *TfuDyP-Tat* and *TfuDyP-pelB*, FT: Flow through, W: Washing after sample application, M: Molecular mass marker (A-B: P7711S, C-F: P7712S, NEB) and C(+): Positive control (a His₆-tagged recombinant protein sample). SDS-PAGE analyses (A, C, E) were carried out using 12% polyacrylamide gels (6.2.10) and the detections for western blot analyses (B, D, F) were done with an α -His antibody and GAR^{AP} (6.2.11). The number indicated above each well corresponds to different elution fraction for each IMAC. SDS-PAGE and western blot for the IMAC purifications of the *TfuDyP-cp* construct was carried out by Laura Grabowski as a part of her Bachelor thesis.

Both SDS-PAGE and western blot analyses of the elution fractions revealed a dominant band around 46 kDa for *TfuDyP-cp*, which corresponds to its calculated mass (Figure 10A, B). The eluted protein sample bands of *TfuDyP-Tat* and *TfuDyP-pelB* cannot be distinguished easily by Coomassie staining because of lower amounts of purified proteins. However, western blot analyses revealed two distinct but very close bands for both constructs (Figure 10C-F). This shows that two different forms of *TfuDyP-Tat* and *TfuDyP-pelB* were present in the expression cultures. The first form is the unprocessed

Results

precursor of the protein, which has a higher molecular mass. The one, which has a lower molecular mass, results after signal peptide cleavage and transportation to the periplasmic space of *E. coli* (van Bloois et al., 2010). Other minor signals on the SDS-PAGE gels or western blot membranes might be degradation or aggregation products of the proteins of interest or contaminating proteins from the host lysate that retained in the column via unspecific interaction even after excess washing. The expression yields were determined as ~20 mg, ~6 mg, and ~6 mg purified protein per L of expression culture for *TfuDyP*-cp, *TfuDyP*-Tat and *TfuDyP*-pelB, respectively. The results show that *TfuDyP* was expressed best when there was no leader peptide included at the N-terminus of the protein coding sequence. However, the type of signal sequence did not have any influence on the expression yields.

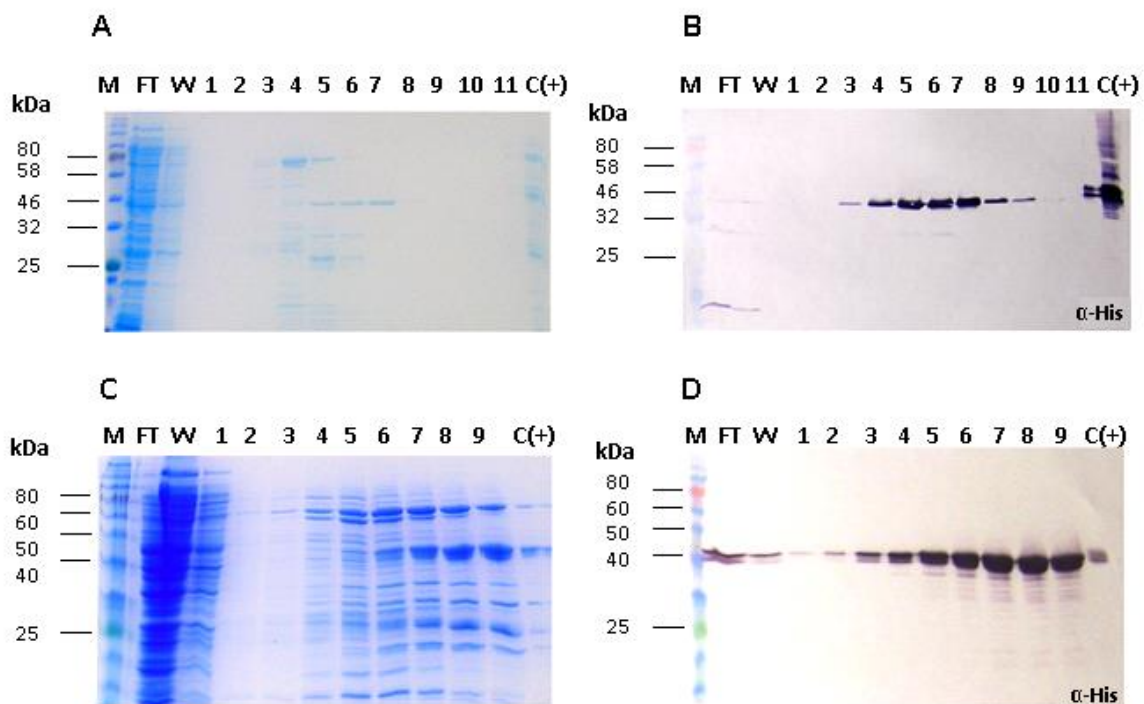


Figure 11: SDS-PAGE and western blot analyses of the IMAC purification fractions of DyPB-cp (A, B) and DyPB-pelB (C, D). Lanes 1-11 or 1-9: Elution fractions, FT: Flow through, W: Washing after sample application, M: Molecular mass marker (A-B: P7712S, C-D: P7711S, NEB), C(+): Positive control (a His₆-tagged recombinant protein sample). SDS-PAGE analyses (A, C) were carried out using 12% polyacrylamide gels (6.2.10) and the detections for western blot analyses were done with an α -His antibody and GAR^{AP} (6.2.11). The number indicated above each well corresponds to different elution fraction for each IMAC.

DyPB was expressed successfully in the soluble phase both with pelB leader peptide and without any leader peptide. The purification of the construct with the pelB leader peptide resulted in two forms of the protein (Figure 11C, D) like *TfuDyP*-Tat or -pelB. The products of both constructs were purified by IMAC successfully and prominent bands were detected around 40 kDa (Figure 11A-D), which is slightly higher than the calculated molecular mass of DyPB (37 kDa). The signals obtained for the flow through and washing fractions of DyPB-pelB show that some parts of the protein of interest did not bind to the column efficiently, therefore, washed away before the elution. Additional bands obtained in the

Results

elution fractions can be aggregation and/or degradation products of DyPB-cp and DyPB-pelB or contaminating proteins from the host lysate that retained in the column via unspecific interaction even after excess washing. The expression yields of DyPB-cp and DyPB-pelB were determined as ~4 mg and ~18 mg purified protein per L of expression culture, respectively.

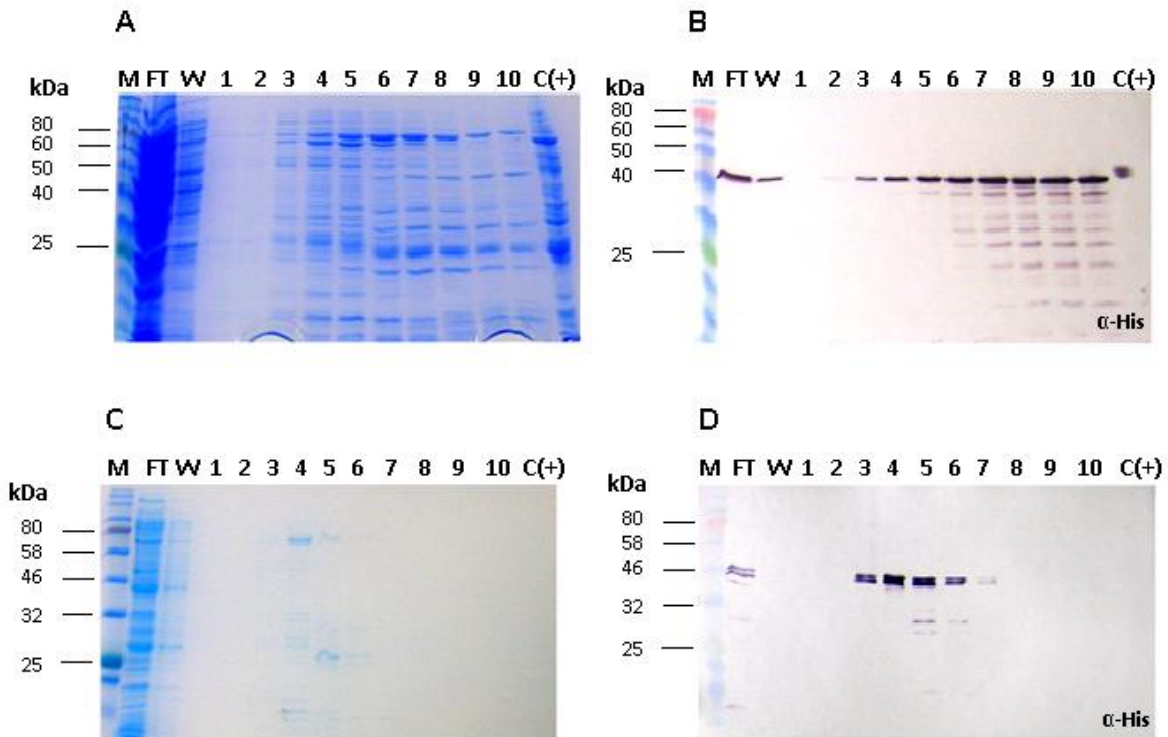


Figure 12: SDS-PAGE and western blot analyses of the IMAC purification fractions of *SSHGDyP*-cp (A, B) and *SSHGDyP*-pelB (C, D). Lanes 1-10: Elution fractions, FT: Flow through, W: Washing after sample application, M: Molecular mass marker (P7711S, NEB), C(+): Positive control (a His₆-tagged recombinant protein sample). SDS-PAGE analyses (A, C) were carried out using 12% polyacrylamide gels (6.2.10) and the detections for western blot analyses (B, D) were done with an α -His antibody and GAR^{AP} (6.2.11). The number indicated above each well corresponds to different elution fraction for each IMAC.

The SDS-PAGE and western blot analyses of the purified enzyme preparations of cytoplasmic and periplasmic *SSHGDyP* confirmed the expression of soluble proteins for both variants (Figure 12). Stronger signals detected by western blot analyses and higher number of elution fractions where protein of interest was detected suggested higher expression yields for *SSHGDyP*-cp (~36 kDa). When *SSHGDyP* was expressed with the pelB leader peptide, two individual bands were detected as proteins of interests. This is expected as observed for previous constructs. However, the heterologous expression of the enzyme, which was reported as extracellular, yielded merely single bands (Figure 12B). Heterologous expression yields were calculated as ~5.0 mg and ~3.5 mg purified protein per L of expression culture for *SSHGDyP*-cp and *SSHGDyP*-pelB, respectively. Several bands were observed below the proteins of interest on the western blot membranes, which could be degradation products. Signals obtained for flow through and wash fractions indicate weak interaction of *SSHGDyP* with the column resin.

Results

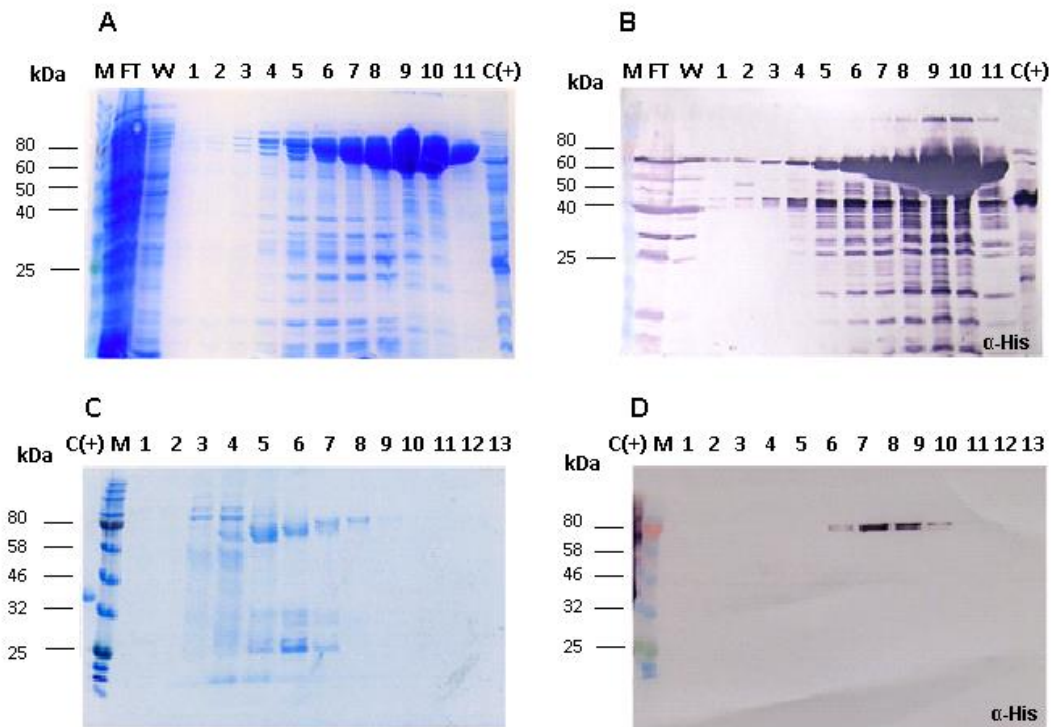


Figure 13: SDS-PAGE and western blot analyses of the IMAC purification fractions of Sclac-cp (A, B) and Sclac-pelB (C, D). Lanes 1-11 or 1-13: Elution fractions, FT: Flow through, W: Washing after sample application, M: Molecular mass marker (A-B: P7711S, C-D: P7712S NEB), C(+): Positive control (a His₆-tagged recombinant protein). SDS-PAGE analyses (A, C) were carried out using 12% polyacrylamide gels (6.2.10) and the detections for western blot analyses (B, D) were done with an α -His antibody and GAR^{AP} (6.2.11). The number indicated above each well corresponds to different elution fraction for each IMAC. SDS-PAGE and western blot analyses for the IMAC purifications of Sclac-pelB construct was carried out by Louisa Kauth as a part of her Bachelor thesis.

An SDS-PAGE analysis of the purified enzyme revealed strong bands for the elution fractions of Sclac-cp near the 70 kDa marker agreeing with the predicted molecular mass of 69.5 kDa. High expression yields up to 104 mg L⁻¹ purified protein per L of expression culture were achieved by heterologous expression. However, both SDS-PAGE (Figure 13A) and western blot analysis (Figure 13B) show many additional bands, which might be degradation products of the protein of interest. On the contrary, the IMAC of Sclac-pelB resulted in only a few elution fractions where the recombinant protein was detected. The lesser number of elution fractions and weaker signals of protein of interest obtained by western blot analysis correlated with the calculated expression yield of up to 3.5 mg purified protein per L expression culture.

Results

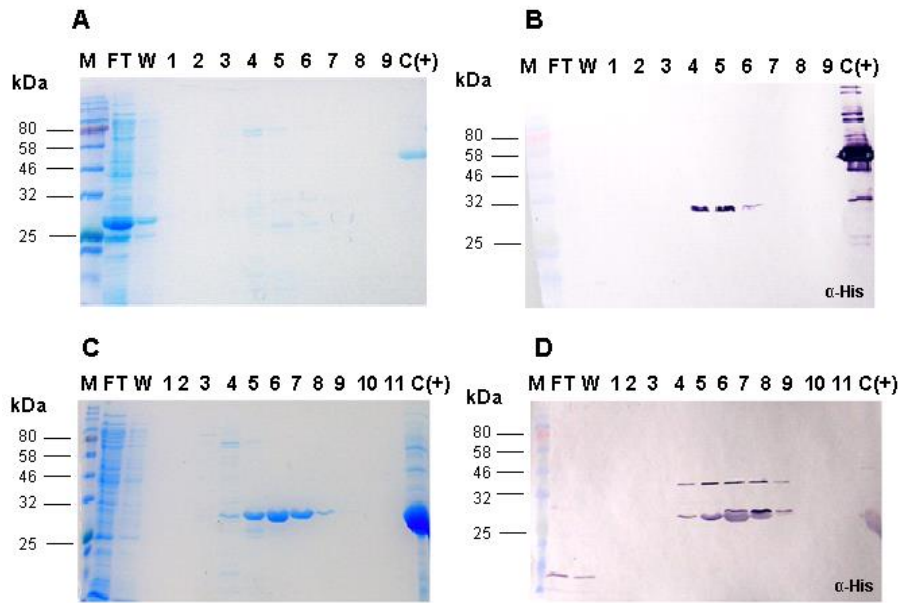


Figure 14: SDS-PAGE and western blot analyses of the IMAC fractions of LigE with C-terminus His₆-tag (A, B) and with N-terminus His₆-tag (C, D). SDS-PAGE (left) and western blot analysis (right) of the fractions obtained from the IMAC. Lanes 1-9: Elution fractions, FT: Flow through, W: Washing after sample application, M: Molecular mass marker (P7712S, NEB), C(+): Positive control (a His₆-tagged recombinant protein sample). SDS-PAGE analyses (A, C) were carried out using 12% polyacrylamide gels (6.2.10) and the detections for western blot analyses (B, D) were done with an α -His antibody and GAR^{AP} (6.2.11). The number indicated above each well corresponds to different elution fraction for each IMAC.

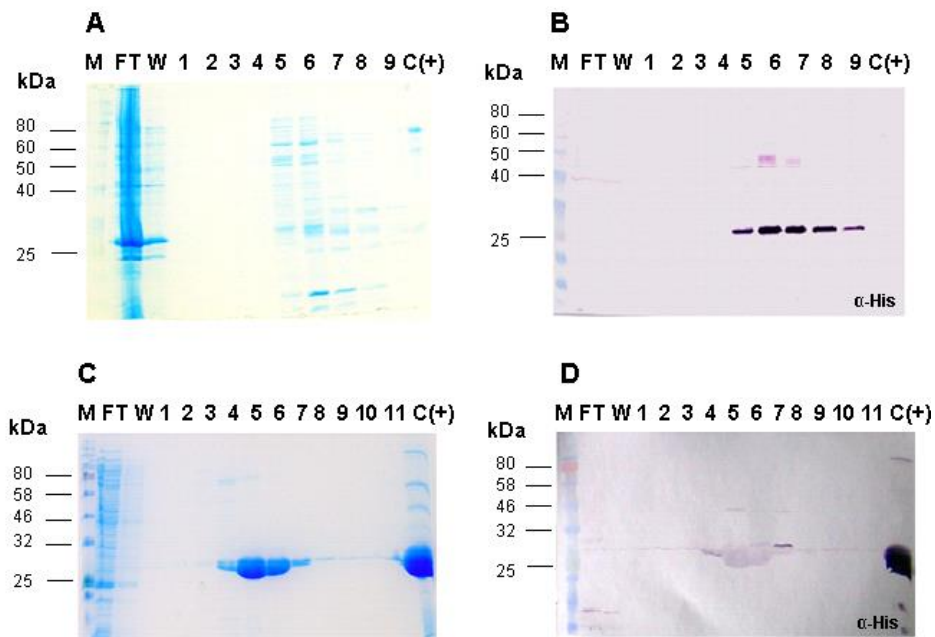


Figure 15: SDS-PAGE and western blot analyses of the IMAC purification fractions of LigF with C-terminus His₆-tag (A, B) and LigF with N-terminus His₆-tag (C, D). Lanes 1-9 or 1-11: Elution fractions, FT: Flow through, W: Washing after sample application, M: Molecular mass marker (A-B: P7711S, C-D: P7712S, NEB), C(+): positive control (a His₆-tagged recombinant protein sample). SDS-PAGE analyses (A, C) were carried out using 12% polyacrylamide gels (6.2.10) and the detections for western blot analyses (B, D) were done with an α -His antibody and GAR^{AP} (6.2.11). The number indicated above each well corresponds to different elution fraction for each IMAC.

Results

Both β -etherases, ligE and ligF, were expressed successfully in the soluble fractions and purified by IMAC via the His₆-tag located on both of the termina (Figure 14 and Figure 15). Wider bands on SDS-PAGE gels and stronger signals on western blot membranes were detected for both of the β -etherases containing the affinity tag at the N-terminus. When the affinity tag was located at the C-terminus, the expression yields were calculated as \sim 2.0 and \sim 3.0 mg purified protein per L of expression culture for LigE and LigF, respectively. When the affinity tag was placed at the N-terminus, the expression yields increased up to 5.5 and 16.0 mg purified protein per L of expression culture for LigE and LigF, respectively. Changing the location of the affinity tag from C-terminus to the N-terminus led to an increase of about 2-3 fold.

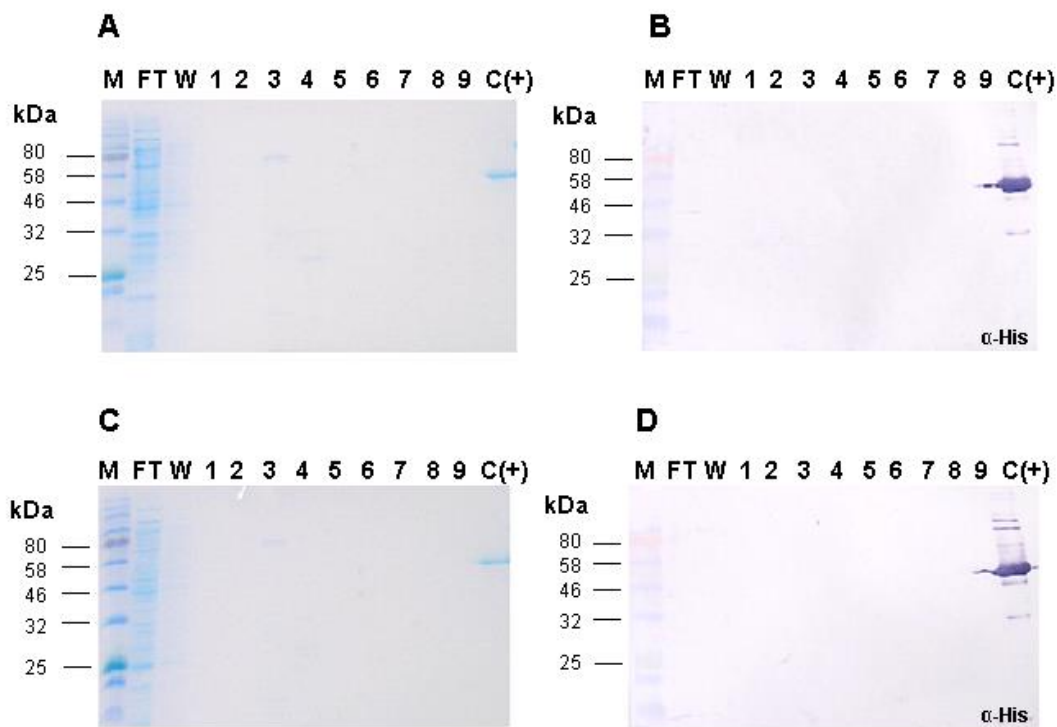


Figure 16: SDS-PAGE and Western-Blot analyses of the IMAC purification fractions of *E. coli* BL21 Star (DE3) cells (A, B) and *E. coli* BL21-CodonPlus(DE3)-RIL (C, D) carrying the empty pET-22b(+) vector. Lanes 1-9: Elution fractions, FT: Flow through, W: Washing after sample application, M: Molecular mass marker (P7712S, NEB), C(+): Positive control (a His₆-tagged recombinant protein sample). SDS-PAGE analyses (A, C) were carried out using 12% polyacrylamide gels (6.2.10) and the detections for western blot analyses (B, D) were done with an α -His antibody and GAR^{AP} (6.2.11). The number indicated above each well corresponds to different elution fraction for each IMAC.

E. coli BL21-CodonPlus(DE3)-RIL and BL21 Star(DE3) cells were transformed with the empty pET22b(+) vector as negative controls. As observed in the western blot analyses, no signals were detected using α -His antibodies, which is an expected outcome. However, several bands were detected in certain elution fractions on the Coomassie stainings for both strains. This shows that endogenous proteins bind to the column resin unspecifically and are eluted together with the protein of interest. That

Results

explains the additional bands observed in the Coomassie stainings of certain IMAC fractions given above for the recombinant enzymes.

Expression yields based on different expression strategies described for the heterologous expression of the selected lignin-degrading enzymes in *E. coli* were summarized together with the strategies and *E. coli* strains used in the experiments in Table 2.

2.2 Expression of selected lignin degrading enzymes in *P. fluorescens*

Due to the restrictions of the expression vector pD1 and the commercial *P. fluorescens* system, all enzymes, *TfuDyP*, *DyPB*, *SSHGDyP*, *ScLac*, *LigE* and *LigF*, were expressed in *P. fluorescens* without any signal sequences. Therefore, the *DyPs* and the laccase were expressed without any additional leader peptide. The native signal sequence in the *TfuDyP* coding sequence was removed at the gene synthesis step. The expression of *LigE* and *LigF* resulted in higher expression yields when the His₆-tag was located at the N-terminus for the expression in *E. coli*. Thus, the constructs of the β -etherases for the expression in *P. fluorescens* were designed to carry the His₆-tag at the N-terminus. All sequences were codon optimized for expression in *P. fluorescens*. *TfuDyP*, *ScLac*, *LigE* and *LigF* were initially expressed in 50 mL scale successfully in the soluble phase. *SSHGDyP* was expressed in the form of inclusion bodies and the expression of *DyPB* could not be approved neither in the soluble form nor in the inclusion body form. The enzymes that were expressed successfully were purified by one-step IMAC and the purified enzyme preparations were analyzed by SDS-PAGE (Figure 17). Afterwards, the heterologous expressions were optimized for 2 L culture volume. The recombinant enzymes (*TfuDyP*, *ScLac*, *LigE* and *LigF*) were purified by one-step IMAC for further analyses.

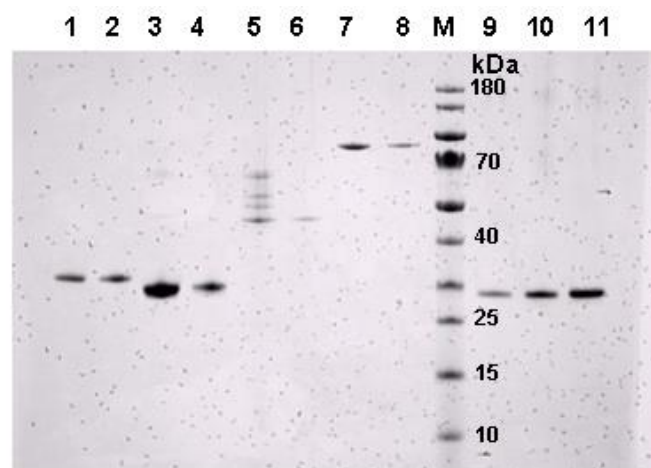


Figure 17: SDS-PAGE of IMAC purified *TfuDyP*, *ScLac*, *LigE* and *LigF* expressed in *P. fluorescens*. All IMAC-purified enzyme preparations were analyzed in 2 different dilutions on a coomassie stained SDS-gel (5-12%) (6.2.10). Lane 1-2: *LigE* (1:5 and 1:10); lane 3-4: *LigF* (1:5 and 1:10); lane 5-6: *TfuDyP* (1:2 and 1:5); lane 7-8: *ScLac* (1:2 and 1:5); lane M: Molecular mass marker (PageRuler, Thermo Fisher); lane 9-11: Protein standard (250/500/1000ng). The figure represents the IMAC purified enzyme samples after initial expressions. Due to license issues of the strain and the expression vector, the cloning and heterologous gene expression in *P. fluorescens* and the subsequent IMAC purifications were carried out by Dr. Stefan Rasche and his group at Fraunhofer IME (Aachen).

Results

The protein concentrations after the first and second IMAC purifications were determined densitometrically using a well-characterized and quantified protein standard. The initial and optimized expression yields after one-step IMAC are summarized in Table 3.

Table 3: The initial and optimized heterologous expression yields of the lignin-degrading enzymes in *P. fluorescens*. The position of His₆-tag was optimized for each enzyme in *E.coli* (6.2.1). IB: Inclusion body, NE: Not expressed successfully.

Enzyme	His ₆ -tag position	Initial expression yields ~mg protein L ⁻¹ expression culture	Optimized expression yields ~mg protein L ⁻¹ expression culture
<i>TfuDyP</i>	C-terminus	6.4	130
<i>DyPB</i>	C-terminus	NE	NE
<i>SSHGDyP</i>	C-terminus	IB	IB
<i>ScLac</i>	C-terminus	27.2	234
<i>LigE</i>	N-terminus	53.2	490
<i>LigF</i>	N-terminus	169.4	1123.5

2.3 Characterization of the purified enzyme preparations

2.3.1 Analysis of heme B content and T1-copper incorporation

DyP-type peroxidases are a novel group of heme-containing peroxidases and possess a heme B (iron protoporphyrin IX) group as a cofactor (Rahmanpour & Bugg, 2016). The prosthetic heme group is important for the oxidation activity of DyPs on the substrates and it can be detected by Ultraviolet-visible (UV-Vis) spectrophotometry due to their electronic absorption (Giovannetti, 2012). The heme group gives an intensive peak around 400-436 nm, which is called Soret or B band (Dayer et al., 2010). Using the absorbance value of the Soret band together with the absorbance of the enzyme sample at 280 nm, a ratio is calculated called "Reinheitszahl (RZ) value" (Harreither et al., 2011). RZ value of an enzyme preparation indicates the purity of the sample and gives an idea about the enzymatic activity. However, it is not a measure of the catalytic activity quantitatively. The higher the RZ values, the greater the purity of the sample (Deshpande, 2012).

The heme content of the DyPs were quantified by carrying out Soret band scans of the purified enzyme samples. The Soret scans yielded observable peaks for *TfuDyP* and *DyPB* around 400-410 nm (Figure 18A-C). However, *SSHGDyP* samples expressed either with or without pelB leader peptide did not show any peaks. This indicates that during the protein folding, the heme B group was not incorporated correctly into the protein structure and thus, inactivity of the enzyme. The RZ numbers of the enzyme samples were calculated and the resulting values indicated that the recombinant enzymes represented higher RZ values when they were expressed without the leader peptides. The RZ values were summarized in Table 4.

Results

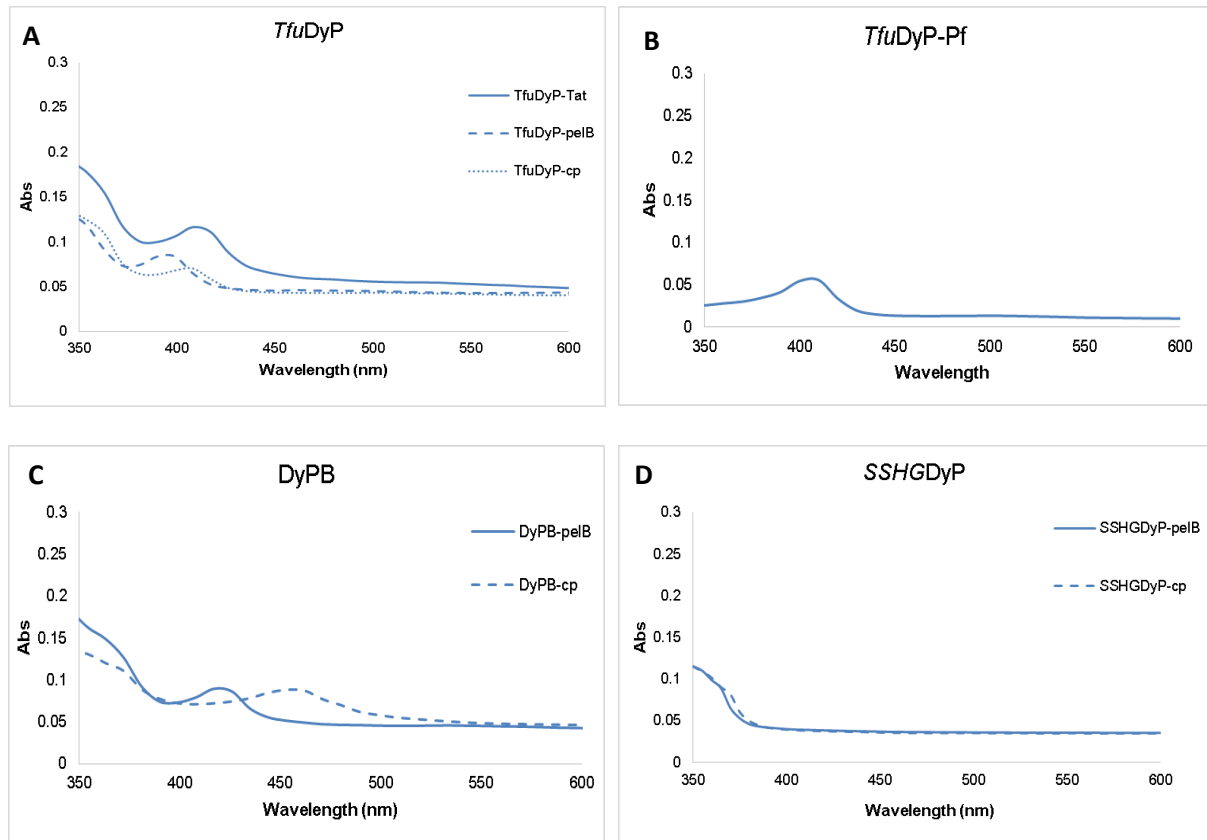


Figure 18: Soret band analyses of DyP-type peroxidases expressed in *E. coli* and *P. fluorescens* (Pf). The UV-Vis spectra of 1 μ M purified enzyme preparation was recorded between the wavelengths of 350 and 600 nm (6.2.14). A: *TfuDyP* expressed with or without leader peptides in *E. coli*. B: *TfuDyP* expressed in *P. fluorescens* without leader peptide. C: *DyPB* expressed with or without leader peptide in *E. coli*. D: *SSHGDyP* expressed with or without leader peptide in *E. coli*. Tat: Twin-arginine translocation pathway signal peptide. pelB: Pectate lyase B (*Erwinia carotovora* CE) leader peptide. cp: Cytoplasmic expression (no leader peptide).

Table 4: Reinheitszahl (RZ) values (6.2.14) calculated for DyP-type peroxidases expressed in *E. coli* and *P. fluorescens* with or without leader peptides. ND: Not detected. Tat: Twin-arginine translocation pathway signal peptide. pelB: Pectate lyase B (*Erwinia carotovora* CE) leader peptide. cp: Cytoplasmic expression (no leader peptide).

Expression host	DyP-type peroxidase	Leader peptide	Reinheitszahl value (A_{406}/A_{280})
<i>E. coli</i>	<i>TfuDyP</i>	Tat	1.00
		pelB	1.00
		cp	2.06
	<i>DyPB</i>	pelB	0.28
		cp	0.52
	<i>SSHGDyP</i>	pelB	ND
cp		ND	
<i>P. fluorescens</i>	<i>TfuDyP</i>	cp	1.36

Results

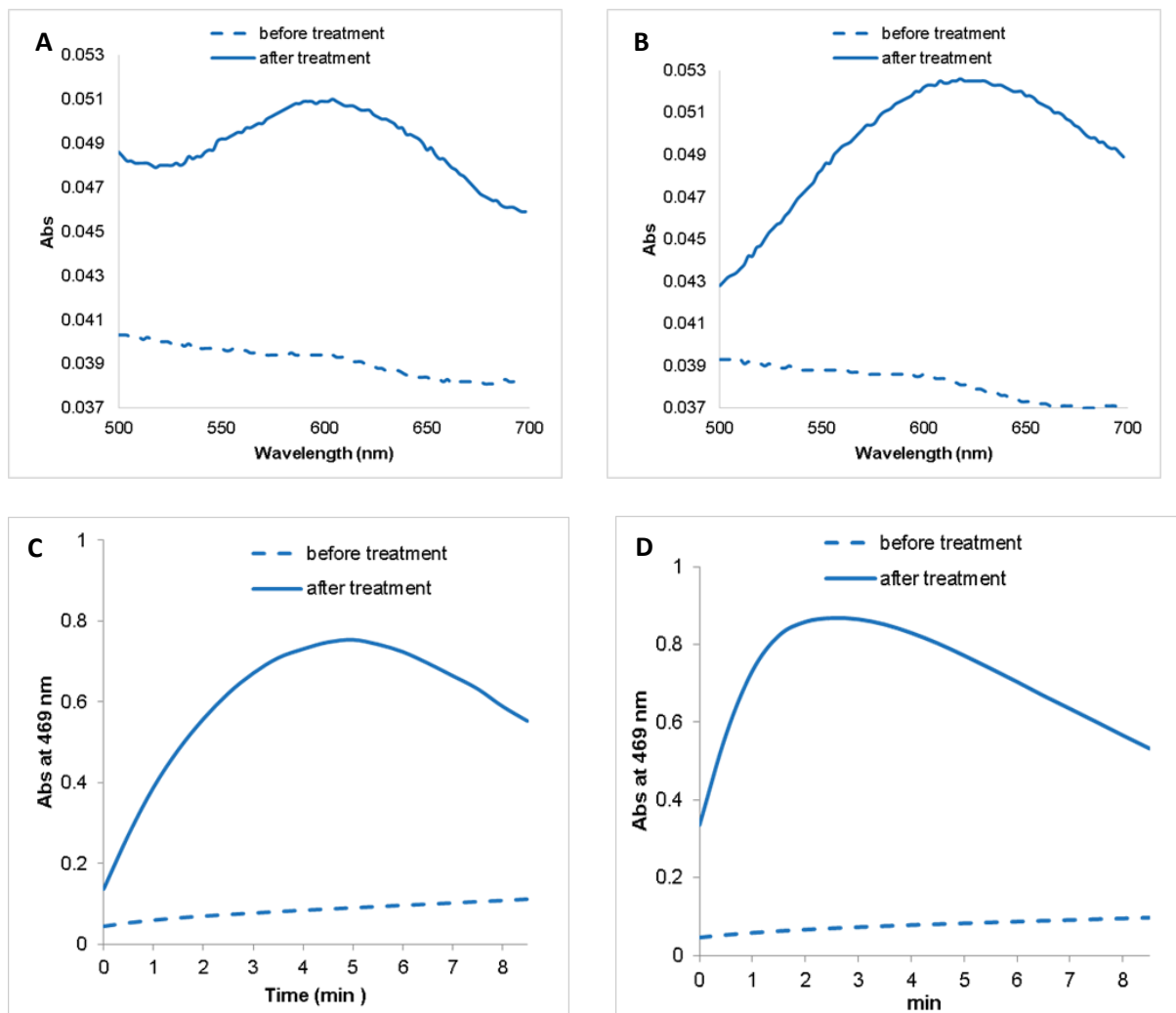


Figure 19: Visible spectra analyses and activity assays of Sclac-cp expressed in *E. coli* (A, C) and in *P. fluorescens* (B, D). The visible spectra and the activity assays were recorded before (dashed lines) and after CuSO₄ (0.1 mM) treatment (solid lines). 1 μ M of each enzyme was used to record the visible spectra between 500 nm and 700 nm (6.2.14). Activity assays were carried out using DMP (6.2.15) before and after CuSO₄ treatment with 0.4 μ M of Sclac-cp expressed in *E. coli* and 1 μ M of Sclac-cp expressed in *P. fluorescens*. The reactions were followed spectrophotometrically for 8.5 min at 465 nm.

The detection of the T1-copper gives information about the proper folding and the activity of the enzyme. Just like the heme B group of the DyP-type peroxidase, the T1-copper in the laccase can be detected by the analysis of the visible spectra. The visible spectra of the recombinant Sclac-cp, expressed in *E. coli* and *P. fluorescens* were initially recorded after IMAC purification. None of the samples gave a peak around 600 nm, which would show the successful incorporation of the T1-copper (Figure 19A-B dashed lines). Thereupon, protein samples were incubated in the presence of 0.5 mM CuSO₄ and the visible spectra were recorded again (Figure 19A-B solid lines). The visible spectra following the CuSO₄ treatments correlated with the typical spectra of blue laccases. A peak around 600 nm was observed for both enzyme samples. This indicates that the type 1 copper atom is incorporated into the protein structure (Thurston, 1994), however only after the CuSO₄ treatment. Activity assays were carried out with both CuSO₄ treated and non-treated enzyme samples using DMP as the substrate (Figure 19C-D). A significant increase in the absorbance at 469 nm was observed only with the CuSO₄

Results

treated samples (Figure 19C-D solid lines). The activity of the CuSO₄ treated recombinant Sclacs were also checked via zymography using ABTS, L-DOPA and caffeic acid as substrates (Figure 20). For Sclac expressed in *E. coli*, it was possible to detect the activity against three of the substrates on native gels whereas Sclac expressed in *P. fluorescens* showed a visible activity signal merely against L-DOPA.

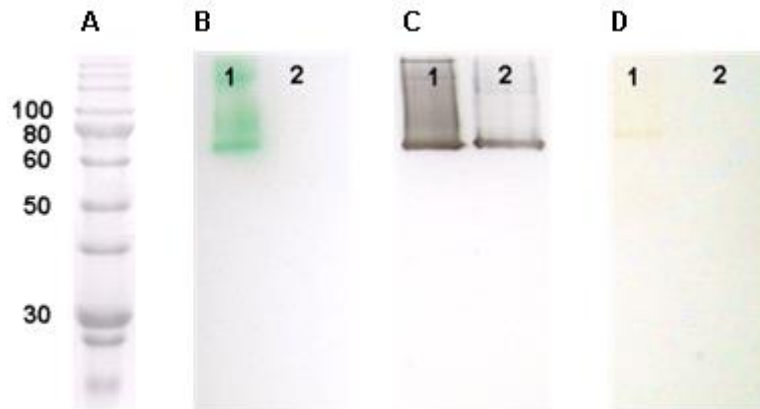


Figure 20: Zymogram analysis of purified laccases expressed in *E. coli* (lane 1) and in *P. fluorescens* (lane 2). 25 µg of each laccase was loaded onto native gels for electrophoresis and the gels were stained with ABTS (B), L-DOPA (C) and caffeic acid (D). Molecular mass marker is shown in the lane A (6.2.12).

2.3.2 The effect of temperature and pH on enzyme activities and stabilities

In order to assess the optimal reaction conditions of the purified recombinant enzymes, the optimum pH value (Figure 21A) and temperature (Figure 21B) for each enzyme were determined. If not otherwise stated, Sclac-cp and DyPB-peIB expressed in *E. coli* and TfuDyP-cp, LigE (N-terminus His₆-tag) and LigF (N-terminus His₆-tag) expressed in *P. fluorescens* were assayed in the characterization and detailed activity analysis studies given from here on. DMP was used as substrate for the DyPs and the laccase, whereas α-O-(b-methylumbelliferyl) acetovanillone (MUAV) was used to assay the optimal conditions for the etherases. Sclac showed a very broad pH range from 3.5 to 8.5 with a maximum at pH 5.5 (Figure 21A), however, after pH 8.5, a significant decrease was observed in the activity. TfuDyP showed high activity levels at acidic pH range (3.5 to 5.5) with a constant decrease in the activity at pH values under pH 5.5.

DyPB was also active at acidic pH values and showed the highest activity at pH 4.5. The pH profile of the enzyme resembled the one from TfuDyP. LigE and LigF showed no activity at acidic pH values. The substantive activity levels were first observed at neutral pH values. The highest activities were observed at pH 9.5 and 9.0 for LigE and LigF, respectively.

Results

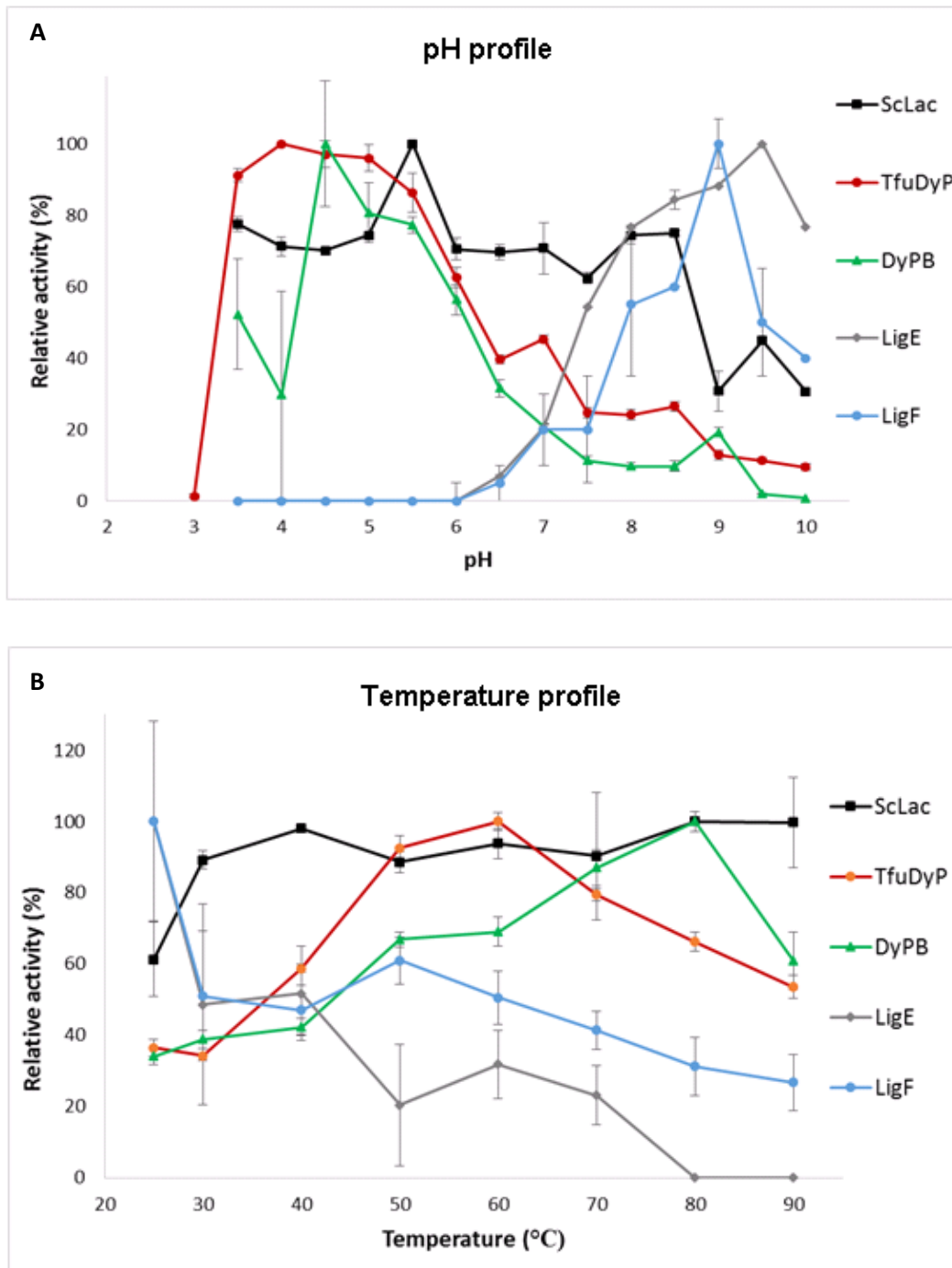


Figure 21: pH (A) and temperature (B) profiles of the recombinant lignin-degrading enzymes. A: The activities of the purified recombinant enzymes were measured against 20 μ M DMP (6.2.15) for *TfuDyP*, *DyPB* and *ScLac* and 100 μ M MUAV (6.2.15) for *LigE* and *LigF* at 30°C in buffers with various pH values ranging from pH 3.5 to 10.0 at 25°C (6.2.21). B: In order to assay the optimum temperatures, the activities towards 20 μ M DMP were followed spectrophotometrically for *TfuDyP*, *DyPB* and *ScLac* and towards 100 μ M MUAV for *LigE* and *LigF* after incubation for 5 min in the optimal buffer system of each enzyme in a temperature range from 25°C to 90°C (6.2.21). The highest activity was assigned as 100% and the lower activities were calculated as % of the highest activity. All measurements were performed in triplicate (n = 3). Error bars indicate standard deviation ($x \pm SD$) from arithmetic mean.

Following the determination of the optimum pH values, optimum temperature assays (Figure 21B) were carried out in the buffer systems in which the enzymes performed best at a temperature range from 25°C to 90°C. Therefore, *ScLac* was assayed in 100 mM MES pH 5.5 and the enzyme showed

Results

constant activity levels from 30°C to 90°C. *TfuDyP* was assayed in 100 mM sodium acetate buffer pH 4.0. The maximum *TfuDyP* activity was observed at 60°C. The optimum temperature assay of DyPB was carried out in 100 mM sodium acetate buffer with pH 4.5. The recombinant enzyme reached its maximum activity at 80°C. The β -etherases performed best at approximately 25°C. Rapid loss of activity was observed by increasing the temperature from 25°C to 30°C. However, LigF showed better stability than LigE at the temperatures higher than 40°C but lost its activity at 80°C.

The effect of temperature on lignin degrading enzymes were assayed by short and long term thermal stability assays. In order to assay the short term thermal stabilities, the enzymes were incubated in their optimal pH buffer systems for 5 min at the given temperature range (Figure 22A) from 25°C to 90°C and the residual activities were measured towards the substrates as mentioned in the assays for optimum pH and temperature. As given in Figure 22A, *TfuDyP*, DyPB and ScLac showed activity after 5 min of incubation at all temperatures. Interestingly, ScLac demonstrated an increasing profile of the residual activities by increasing temperature. Its residual activity at 90°C was increased by approximately 5-folds in comparison to its initial activity (control). *TfuDyP* and DyPB also showed heat activation, thus increase in the residual activities up to approximately 150% and 200% at 40°C. From this point on, the enzymes started losing their activities. LigE kept half of its initial activity at 30°C but showed no activity at higher temperatures. LigF showed approximately 80% of residual activity at 60°C and lost its whole activity from 70°C on. Long term thermal stability assay results (Figure 22B) correlated in general with the ones from the short term. However, the heat activation was only observed for ScLac after incubation at 30°C. The enzyme kept 64% of its initial activity after incubation at 60°C and lost almost its activity completely after incubation at 90°C. *TfuDyP* and DyPB showed no heat activation in the long term thermal stability assay. *TfuDyP* preserved 88% and 16% of its initial activity at 30°C and 60°C, respectively, and lost almost all activity at 90°C. DyPB maintained approximately 34% and 9% of its initial activity at 30°C and 60°C, respectively. The enzyme showed no activity after incubation at 90°C. LigE showed very low activity (7% of its initial activity) after incubation at 30°C and stayed inactive at the temperatures higher than that point. LigF stayed active after incubation at 30°C (~58% and ~24%) and 60°C, correlating with the short term stability assay results, however it showed no activity after incubation at 90°C.

Results

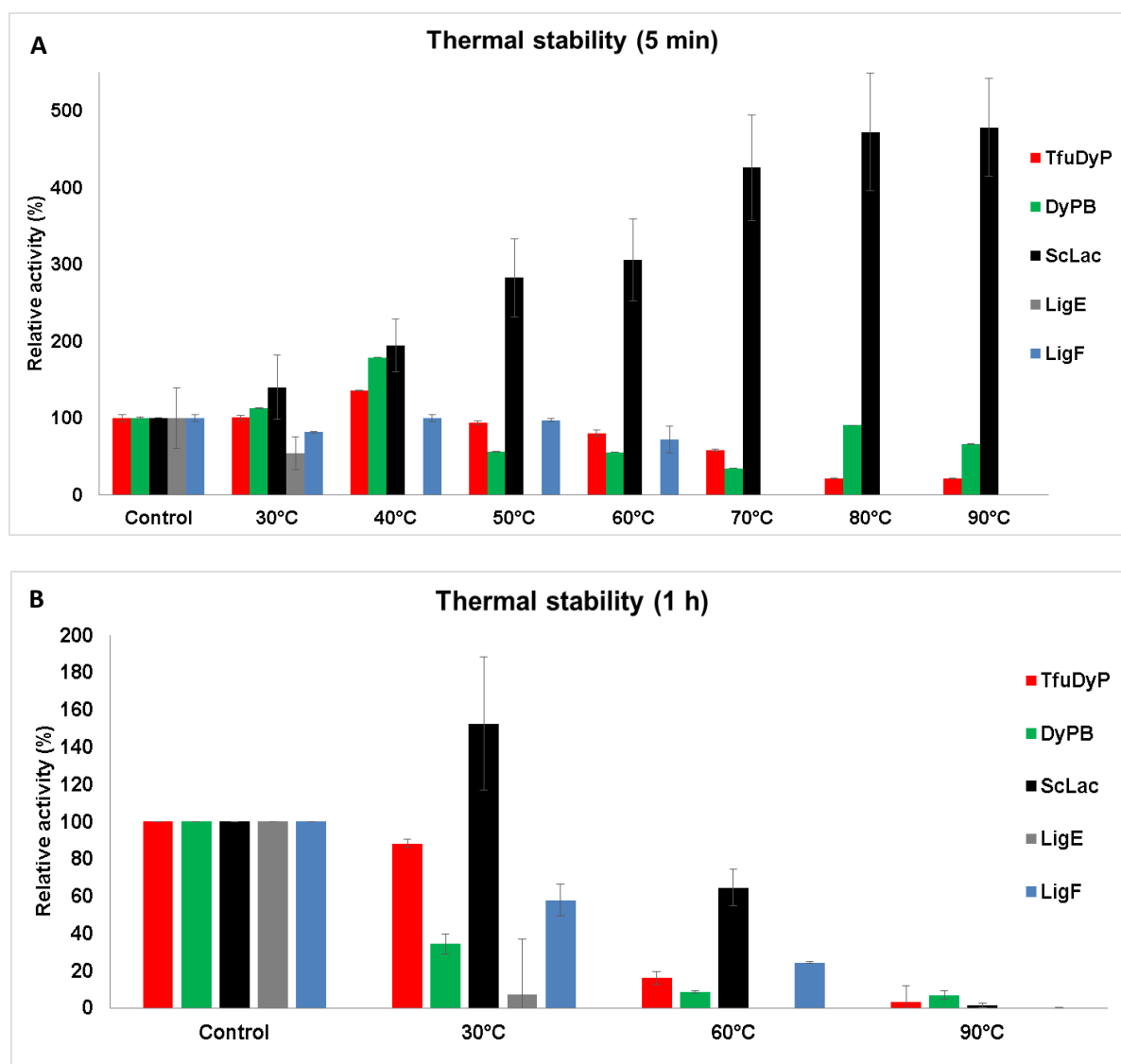


Figure 22: Short term (A) and long term (B) thermal stability assays of the recombinant lignin-degrading enzymes. A: 1 μ M of each enzyme was incubated for 5 min at 25°C, 30°C, 40°C, 50°C, 60°C, 70°C, 80°C and 90°C. After incubations, the samples were cooled down to the room temperature and the residual activities were assayed using 20 μ M DMP (6.2.15) for *TfuDyP*, *DyPB* and *ScLac* or using 100 μ M MUAV (6.2.15) for *LigE* and *LigF* (6.2.21). B: 1 μ M of each enzyme was incubated for 1 h at 25°C, 30°C, 60°C and 90°C. After the incubation the samples were cooled down to the room temperature and the residual activities were assayed as described for the short term thermal stability assay (6.2.21). Control assays were carried out as mentioned above skipping the heat incubation step. Each enzyme's control was assigned to 100% and the heat-incubated sample's relative activity was calculated as % of the corresponding control. n = 3; \bar{x} ±SD.

The effect of pH on the enzyme stabilities was assayed by incubating the enzymes in their optimal pH buffer systems at approximately 25°C for 1, 6, and 24 h and assaying the residual activities (Figure 23). In general, the enzymes kept the major percentage of their initial activity after 1 h incubation. *DyPB* only kept ~17% of its initial activity after 1 h incubation. Except *LigF*, all enzymes preserved some part of their initial activity after 24 h incubation. Approximately 76%, 6%, 39%, 62% of their initial activities were assayed for *TfuDyP*, *DyPB*, *ScLac* and *LigE*, respectively.

Results

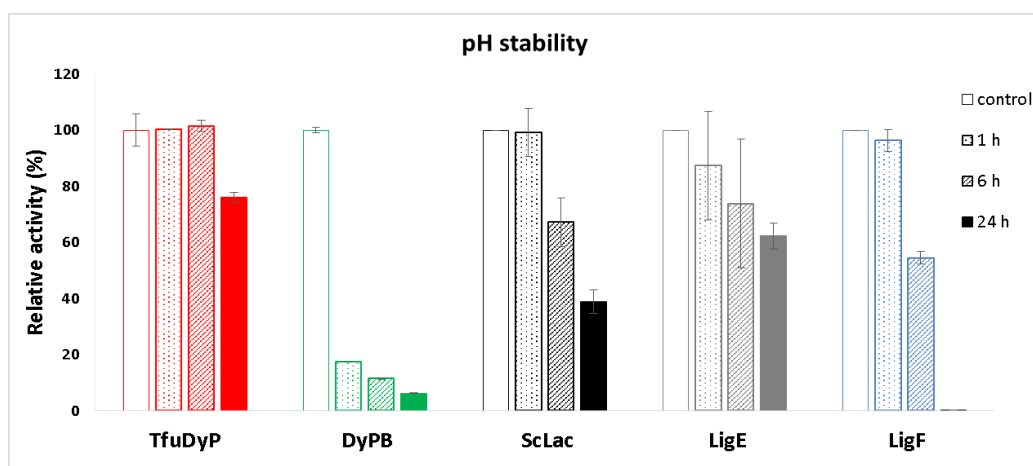


Figure 23: pH stability profiles of the recombinant lignin-degrading enzymes. 1 μ M of each enzyme was incubated at 25°C for 1, 6, and 24 h and the residual activities were assayed using 20 μ M DMP (6.2.15) for *TfuDyP*, *DyPB* and *ScLac* or using 100 μ M MUAV (6.2.15) for *LigE* and *LigF* (6.2.21). The control represents the initial activity of each enzyme prior to pH incubation. n = 3; \bar{x} ±SD.

2.4 Activity assays with common lignin-model substrates

The activities of the purified enzymes were assayed towards most commonly used substrates by microtiter plate (MTP) assays (6.2.15). Specific activities and/or kinetic parameters of the enzymes were calculated based on the MTP assay results. The specific activities of DyPs towards DMP is summarized in Table 5, the specific activities of *ScLac* towards DMP are summarized in Table 6 and the specific activities of the β -etherases towards MUAV are summarized in Table 7.

Table 5: Specific activities of recombinant DyP-type peroxidases towards DMP (6.2.15) expressed by various heterologous expression strategies. NA: Not applicable, ND: Not detected. Tat: Twin-arginine translocation pathway signal peptide. pelB: Pectate lyase B (*Erwinia carotovora* CE) leader peptide. cp: cytoplasmic expression (no leader peptide). n = 3; \bar{x} ±SD.

Expression host	DyP-type peroxidase	Leader peptide	Specific activity (mU mg ⁻¹)
<i>E. coli</i>	<i>TfuDyP</i>	Tat	55.0 ± 0.5
		pelB	96.0 ± 1.0
		cp	60.0 ± 0.0
	<i>DyPB</i>	pelB	77.9 ± 5.2
		cp	7.7 ± 0.53
	<i>SSHGDyP</i>	pelB	ND
cp		ND	
<i>P. fluorescens</i>	<i>TfuDyP</i>	cp	38.2 ± 0.67
	<i>DyPB</i>	cp	NA
	<i>SSHGDyP</i>	cp	NA

Results

Table 6: Specific activities of the recombinant Sclac towards DMP (6.2.15) expressed by various heterologous expression strategies. Tat: Twin-arginine translocation pathway signal peptide. pelB: Pectate lyase B (*Erwinia carotovora* CE) leader peptide. cp: Cytoplasmic expression (no leader peptide). n = 3; x±SD.

		Leader peptide	Specific activity (mU mg ⁻¹)
<i>E. coli</i>	Sclac	pelB	630.0 ± 20.0
		cp	540.0 ± 20.0
<i>P. fluorescens</i>	Sclac	cp	127.0 ± 4.9

Table 7: Specific activities of the recombinant β-etherases towards MUAV (6.2.15) expressed by various heterologous expression strategies. ND: Not detected. n = 3; x±SD.

	β-etherases	His ₆ -tag location	Specific activity (mU mg ⁻¹)
<i>E. coli</i>	LigE	C-terminus	ND
		N-terminus	11.0 ± 3.3
	LigF	C-terminus	4.3 ± 0.2
		N-terminus	422.1 ± 8.7
<i>P. fluorescens</i>	LigE	N-terminus	20.9 ± 10.2
	LigF	N-terminus	302.2 ± 17.8

The spectral assays were performed with DMP, ABTS and guaiacol for the DyPs and the laccase, and with MUAV for the β-etherases to determine the steady state kinetics K_M , k_{cat} and k_{cat}/K_M (6.2.17). The values are given in Table 8 -Table 12.

Table 8: Kinetic parameters (6.2.17) of TfuDyP towards DMP, ABTS and guaiacol. n = 3; x±SD.

TfuDyP	K_M (μM)	k_{cat} (s ⁻¹)	k_{cat}/K_M (M ⁻¹ s ⁻¹)
DMP	2.178 ± 0.8439	0.026 ± 0.001425	1.19 × 10 ⁴
ABTS	13.72 ± 4.721	0.9249 ± 0.1977	6.70 × 10 ⁴
Guaiacol	89.48 ± 33.59	0.02132 ± 0.01389	0.0238 × 10 ⁴

Table 9: Kinetic parameters (6.2.17) of DyPB towards DMP, ABTS and guaiacol. n = 3; x±SD.

DyPB	K_M (μM)	k_{cat} (s ⁻¹)	k_{cat}/K_M (M ⁻¹ s ⁻¹)
DMP	109.9 ± 123.2	0.1088 ± 0.08361	0.099 × 10 ⁴
ABTS	1.552 ± 1.514	0.001719 ± 0.0008578	0.11 × 10 ⁴
Guaiacol	163 ± 17.56	0.0549 ± 0.00155	0.034 × 10 ⁴

Results

Table 10: Kinetic parameters (6.2.17) of ScLac towards DMP, ABTS and guaiacol. n = 3; x±SD.

ScLac	K_M (μM)	k_{cat} (s^{-1})	k_{cat}/K_M ($\text{M}^{-1} \text{s}^{-1}$)
DMP	201.6 ± 34.79	0.955 ± 0.135	0.473 × 10 ⁴
ABTS	33.52 ± 27.85	0.057 ± 0.031	0.17 × 10 ⁴
Guaiacol	5.373 ± 1.946	0.028 ± 0.00146	0.52 × 10 ⁴

Table 11: Kinetic parameters (6.2.17) of LigE towards MUAV. n = 3; x±SD.

LigE	K_M (μM)	k_{cat} (s^{-1})	k_{cat}/K_M ($\text{M}^{-1} \text{s}^{-1}$)
MUAV	0.4287 ± 1.186	0.001076 ± 0.000152	0.25 × 10 ⁴

Table 12: Kinetic parameters (6.2.17) of LigF towards MUAV. n = 3; x±SD.

LigF	K_M (μM)	k_{cat} (s^{-1})	k_{cat}/K_M ($\text{M}^{-1} \text{s}^{-1}$)
MUAV	9.292 ± 2.974	0.06253 ± 0.004758	0.67 × 10 ⁴

In addition to the substrates DMP, ABTS and guaiacol, ScLac expressed in *E. coli* and *P. fluorescens* was tested against the non-phenolic substrate veratryl alcohol (VA). The activities were tested in the presence of two different mediator systems ABTS and HBT. According to the HPLC analyses (Appendix Figure 49), ScLac converted some part of the substrate into the aldehyde product veratraldehyde preferably in the presence of ABTS. Although a quantification was not performed, the area of the veratraldehyde peak obtained out of the reaction with ABTS is apparently larger than the peak obtained out of the reaction with HBT (Appendix Figure 49-Figure 52). No peak was obtained for veratric acid, which could have been obtained as a second product.

2.5 Activity assays with complex lignin-model compounds

The phenolic and non-phenolic complex lignin-model compounds used in this study (Figure 26) are poorly soluble in water. In order to dissolve the compounds in the reaction mixtures completely, the stock solution of the compounds should be dissolved in an organic solvent such as DMSO, ethanol or methanol. However, the presence of organic solvents in a reaction mix affects the catalytic efficiency of most enzymes and even causes denaturation (Kumar et al., 2016). Therefore, it has to be avoided to use them as long as there is no special requirement such as increased thermostability, higher substrate solubility or lower microbial contamination risks (Anbu, 2016; Gupta, 1992). Prior to the activity assays using the complex lignin-model compounds, the stability of the enzymes was assayed in the presence of three of most commonly used organic solvents, DMSO, ethanol and methanol, to determine the best (less harmful) organic solvent (Figure 24 and Figure 25). The activity assays using DMP or MUAV as the substrates were carried out in the presence of increasing amounts of the abovementioned solvents. The behavior of the enzymes in the presence of the solvents showed a wide

Results

variety depending on the combination of the solvent and enzyme. The reproducibility of the activity assays in the presence of ethanol and methanol for LigE and LigF was very low (results not shown). According to the overall results, more than 10% of the organic solvents resulted in rapid decrease in the enzyme activities.

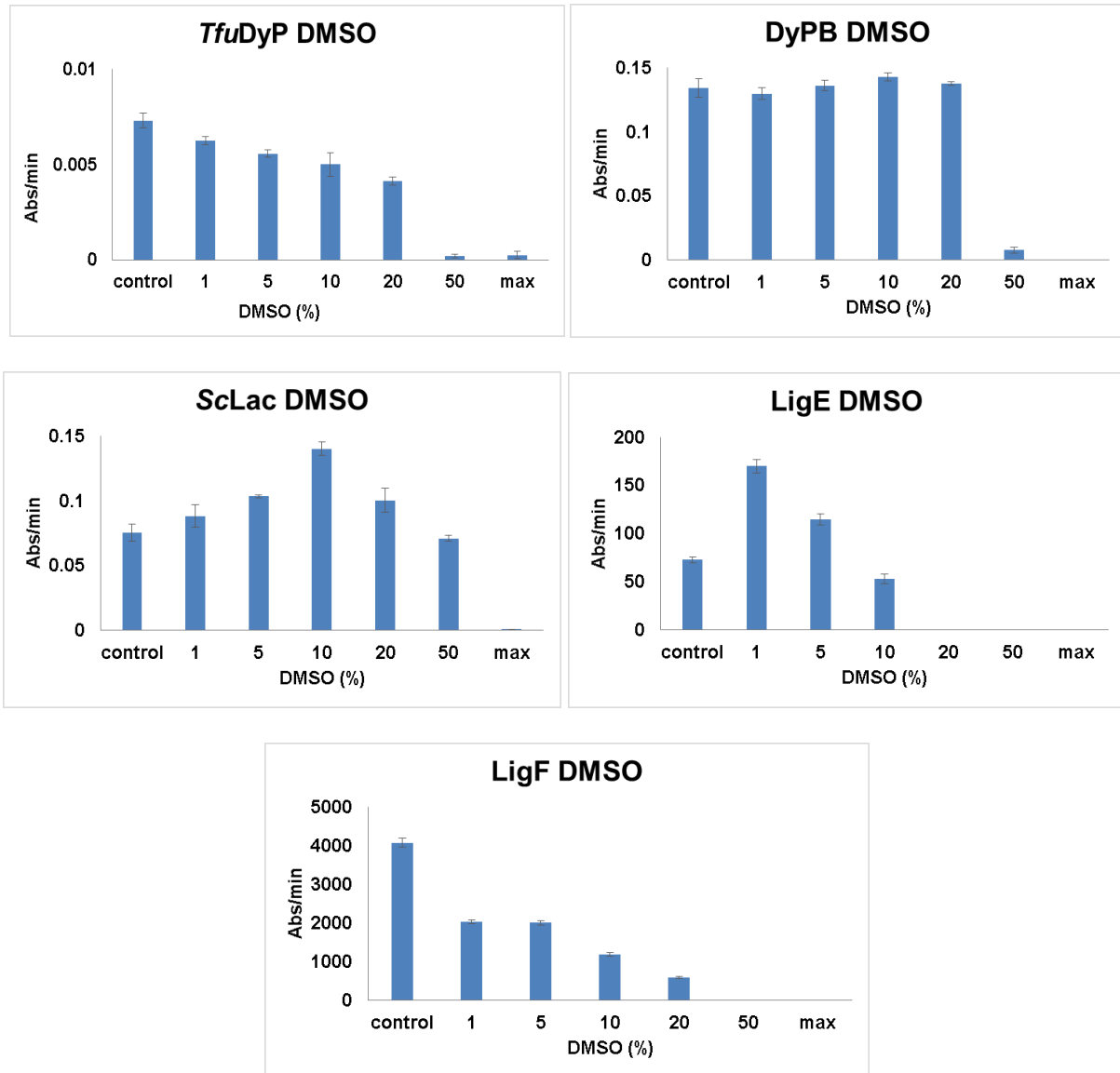


Figure 24: Stability profiles of the recombinant lignin-degrading enzymes in the presence of DMSO. Activity assays were carried out using DMP or MUAV as the substrates in the presence of 0% (control), 1%, 5%, 10%, 20%, 50% and approximately 67% (max) of DMSO (6.2.21). $n = 3$; $\bar{x} \pm SD$.

Results

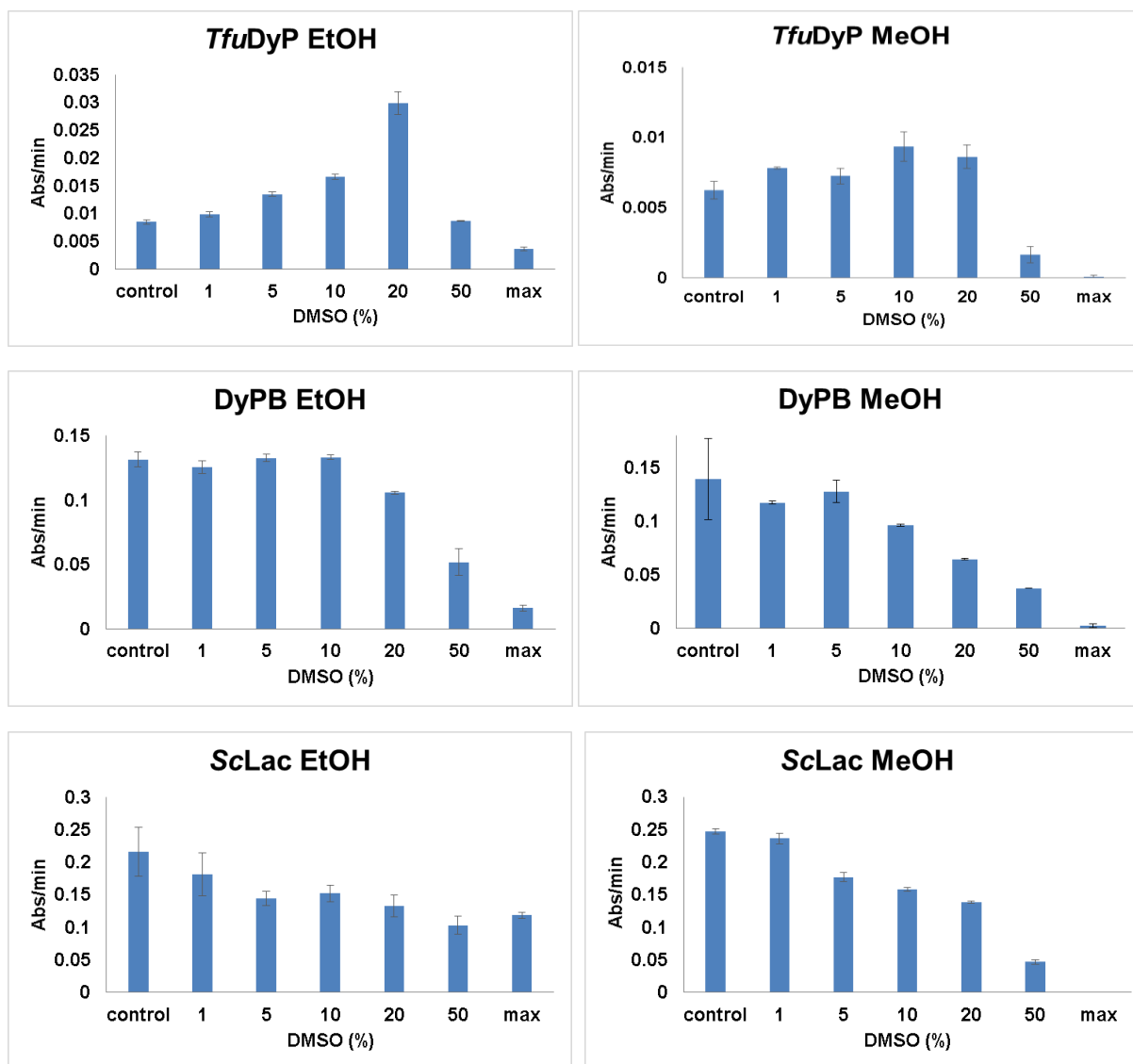


Figure 25: Stability profiles of the recombinant lignin-degrading enzymes in the presence of ethanol and methanol. Activity assays were carried out using DMP or MUAV as the substrates in the presence of 0% (control), 1%, 5%, 10%, 20%, 50% and approximately 67% (max) of DMSO (6.2.21). $n = 3$; $\bar{x} \pm \text{SD}$.

2.5.1 Phenolic and non-phenolic lignin-model compounds

Purified recombinant *TfuDyP*, *DyPB*, *ScLac*, *LigE* and *LigF* expressed in *E. coli* or/and *P. fluorescens* were tested against phenolic and non-phenolic lignin-model compounds (Figure 26) that were synthesized by the group of Prof. Nicholas Westwood (School of Chemistry, University of St Andrews, Scotland). Reactions were set up under the optimal conditions determined for each enzyme (2.3). The possible products of the reactions were extracted from the water phase to the organic phase using ethyl acetate as the solvent and analyzed by NMR.

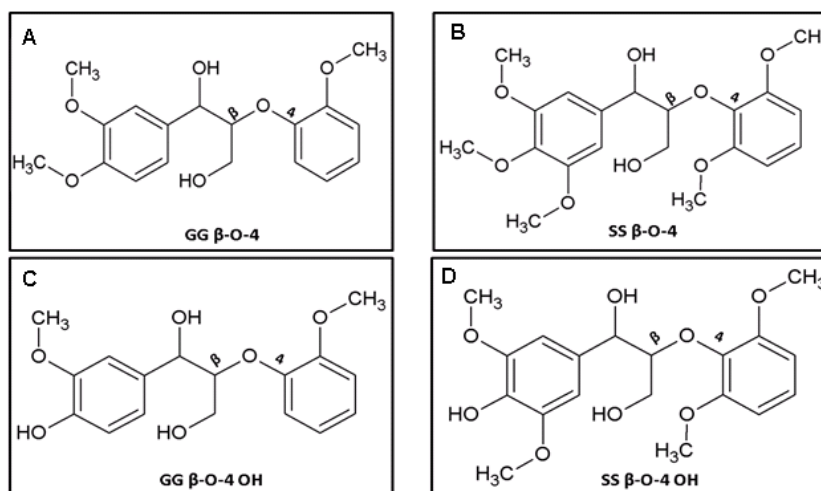


Figure 26: The phenolic and non-phenolic, aromatic complex lignin-model compounds. A and B are non-phenolic β -O-4 lignin model compounds whereas C and D are phenolic β -O-4 lignin model compounds. Depending on the number and the position of the methoxy groups on the structure, the compounds are called either GG- (A and C) or SS- (B and D). All compounds comprise the β -aryl ether linkage, which is the most dominant linkage type in lignin polymer. The compounds presented here were synthesized by Dr. Christopher S. Lancefield (former affiliation; School of Chemistry, University of St Andrews, Scotland and current affiliation; Chemistry - Debye Institute for Nanomaterials Science - Inorganic Chemistry and Catalysis, Utrecht University).

Among the model compounds that have been tested (Figure 26) with the purified recombinant DyPs and the laccase, significant activity levels were detected merely towards phenolic SS β -O-4 OH. Common mediators such as ABTS and HBT were used in the *ScLac* reactions with non-phenolic model compounds (Figure 26 A and B), however, in the NMR analyses only the starting materials were detected. According to the NMR and LC-MS analyses (8.7) of the reactions with the phenolic model compound SS β -O-4 OH (Figure 26 D), the enzymes catalyzed the conversion of the secondary alcohol moiety of the SS- β -O-4 OH to the corresponding SS- β -O-4 ketone (Figure 27). The distinct formation of aldehydes was also detected in each assay including the control reactions. The ketone formation yields were calculated by adding known concentrations of an internal standard, 4-nitrophenol, into the reaction mixtures after the reaction time was ended and before starting the extraction procedure. The analysis of the resulting ketone by NMR and the quantification of the ketone formation by *ScLac* using the internal standard is demonstrated in Figure 28 and Figure 29 as a representative example for *TfuDyP*, *DyPB* and *ScLac* reactions.

Results



Figure 27: Conversion of the secondary alcohol moiety of the SS-β-O-4 OH (left) to the corresponding SS-β-O-4 ketone (right) in the presence of laccase enzymes. The group that goes through the oxidation by the enzymatic activities is indicated by a red circle.

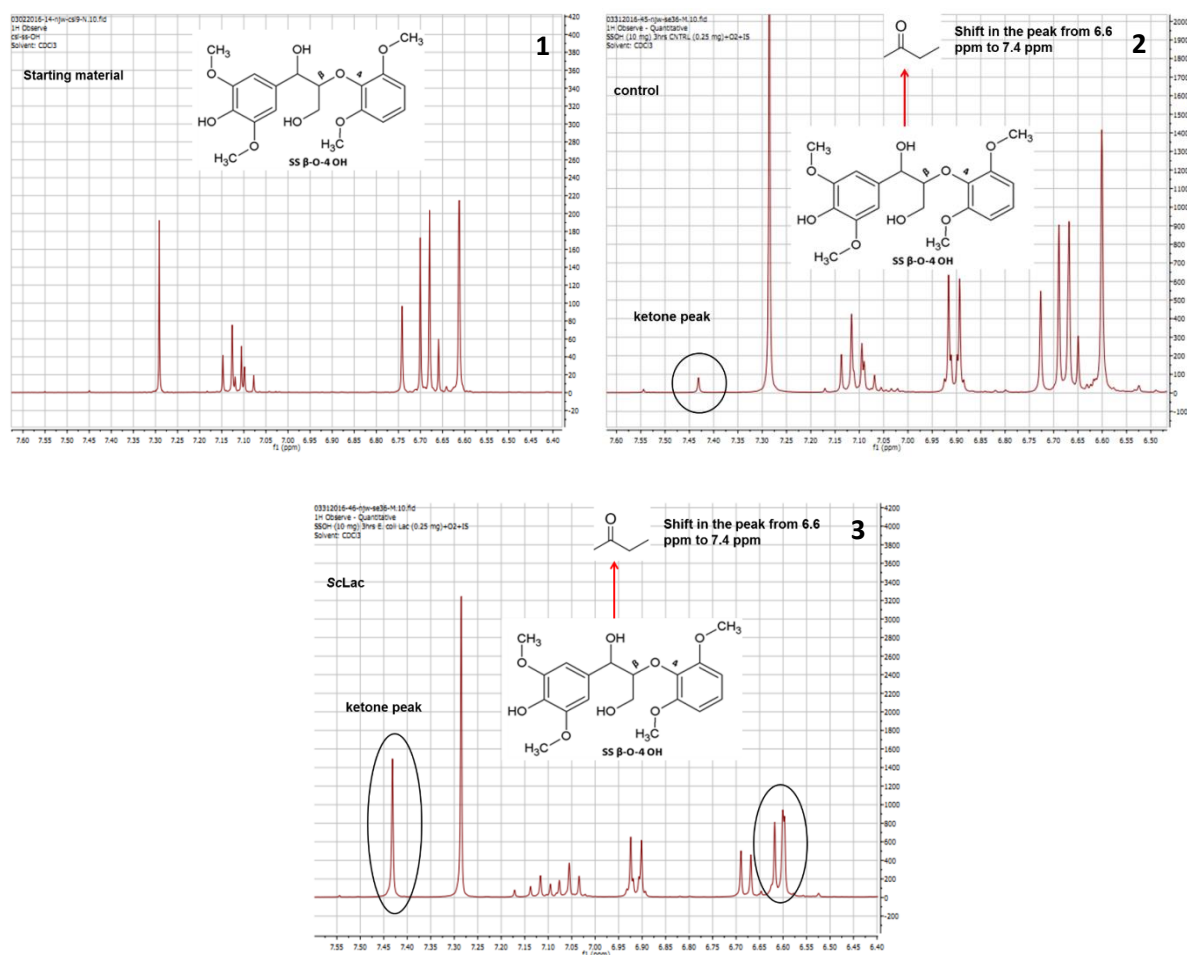


Figure 28: Representative analysis of the activity against the SS-β-O-4 OH model compound by NMR using ScLac. The formation of the ketone product was shown by the comparison of the NMR analysis (6.2.18) of the starting material with the control and the enzymatic reaction. 1: NMR analysis of SS-β-O-4 OH as the starting material, 2: NMR analysis of the control reaction (identical to the enzymatic reaction except the presence of the enzyme) where small amount of ketone formation is observed due to the reaction conditions (temperature, pH etc.), 3: NMR analysis of ScLac reaction with the model compound using 0.25 mg purified recombinant enzyme with 10 mg starting material after incubating the reaction mix at 90°C for 3h. All conditions were kept the same for control and enzymatic reactions and the same extraction protocol was used in order to separate the ketone product from the aqueous phase prior to the NMR analysis. Black circles indicate the peaks that correspond to the ketone products formed from the starting material.

Results

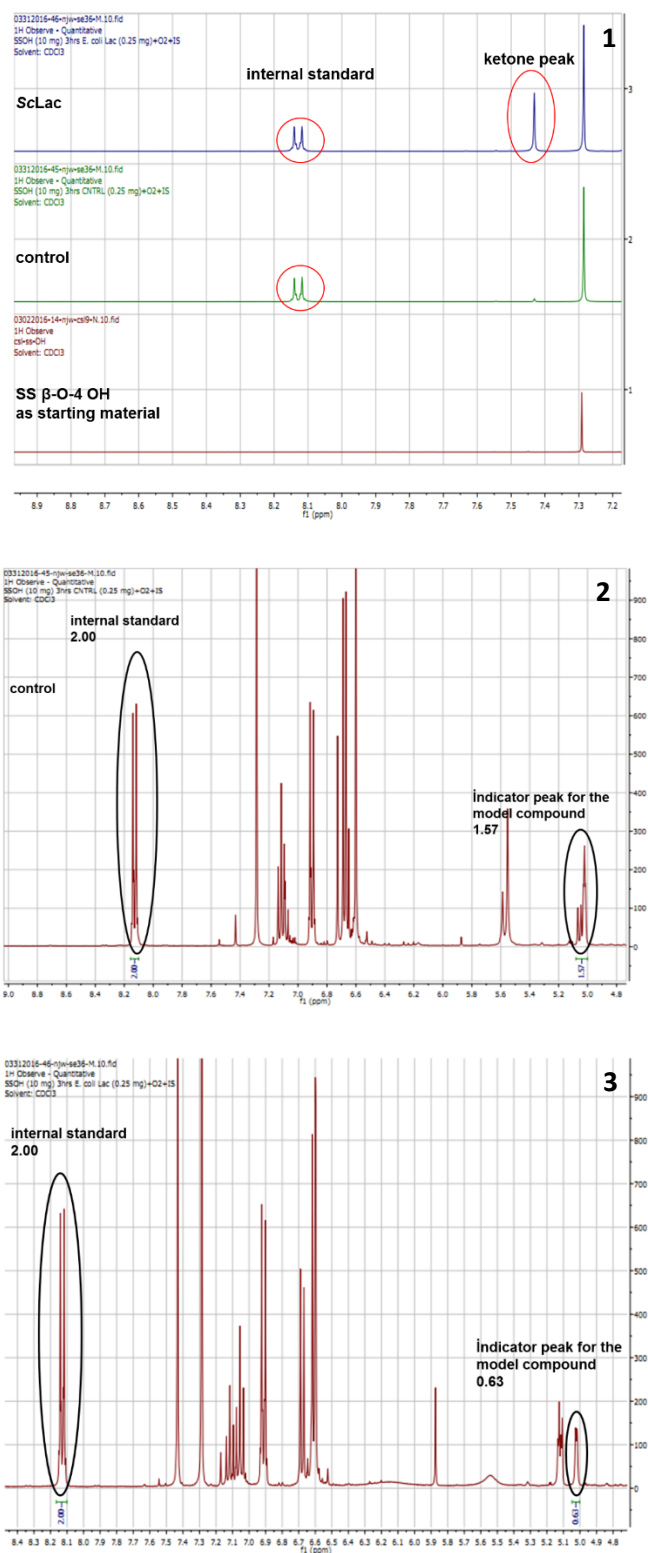


Figure 29: Demonstration of the quantification of the phenolic SS β-O-4 OH model compound conversion to the corresponding ketone product by the addition of an internal standard to the reaction mixtures after the reactions are stopped. The peak areas of the internal standard and the model compound were indicated in circles. Calculations were performed depending on those peak areas for all the reactions (6.2.18). 1: Demonstration of internal standard peaks in control and enzymatic reactions, 2: Peak area comparison for the control reaction, 3: Peak area comparison for the SCLac reaction.

Results

After confirming that the recombinant enzymes show activity towards the phenolic SS β -O-4 OH model compound, several conditions such as enzyme : starting material ratio (1:200 to 1:40), duration of the reaction (3 days to 3 hours) or saturation of the reaction mix with O₂ for laccase reactions in order to reach higher ketone formation yields were optimized. Both the DyPs and the laccase showed the highest activity at a ratio of 1:40 enzyme : starting material. ScLac showed improved activity levels, when the reaction mix was saturated with O₂ prior to the incubation. The ketone formation yields (%) for *TfuDyP*, *DyPB* and *ScLac* for different conditions are summarized in Table 13 and Table 14.

The ketone product, which was obtained from the DyPs and laccase reactions were collected together for separation via Silica column. The purified ketone product was characterized by NMR and used as a dimeric model compound to test the activities of LigE and LigF. The initial assays of LigE and LigF indicated no cleavage of the dimeric ketone product (data not shown).

Table 13: Percentage formation of SS β -O-4 OH ketone by purified *ScLac* expressed in *E. coli* or *P. fluorescens*. n = 3; $\bar{x} \pm \text{SD}$.

	<i>ScLac</i> -cp (<i>P. fluorescens</i>)	<i>ScLac</i> -cp (<i>E. coli</i>)		
Enzyme : starting material	1:200	1:200	1:40	1:40 + O ₂
Ketone formation (%)	6.0 \pm 1.24	11.0 \pm 0.81	40.0 \pm 2.05	58.0 \pm 1.41

Table 14: Percentage formation of SS β -O-4 OH ketone by purified *TfuDyP* and *DyPB* expressed in *E. coli* or *P. fluorescens*. n = 3; $\bar{x} \pm \text{SD}$.

	<i>TfuDyP</i> -cp		<i>DyPB</i> -pelB
Enzyme : starting material (1:40)	<i>E. coli</i>	<i>P. fluorescens</i>	<i>E. coli</i>
Ketone formation (%)	6.0 \pm 0.81	8.0 \pm 0.81	6.0 \pm 1.24

The closer inspection of the NMR data revealed that *ScLac* seems to react with one of the SS- β -O-4 OH diastereoisomers preferentially. The more the enzyme : starting material ratios is increased, the higher conversion of the related diastereoisomer was achieved. At the highest enzyme : starting material ratio, almost complete disappearance of the diastereoisomer was observed. Because of the highest ketone formation yields of *ScLac*, the reaction with the phenolic SS β -O-4 OH model compound was investigated in more detail by kinetic measurements. The previous measurements were done as dead-end reactions with the duration of 3 h. For the kinetic measurements, the reaction mixture was incubated for 3 h at 30°C and interval samples were collected for NMR analyses at the time points 0, 2.5, 5, 10, 15, 20, 30, 45, 60, 120, and 180 min. The ketone formed (mmol) was plotted vs time and the resulting diagram is given in Figure 30. The activity of *ScLac* towards the phenolic model compound increased and reached its maximum activity in the first 30 min. The amount of ketone formed at t= 30

Results

min corresponds to the whole amount of the preferred diastereoisomer added into the reaction mix in the beginning. After 30 min of incubation, the amount of ketone steadily decreased, which shows that the compound is most probably converted into another product that has not been characterized yet.

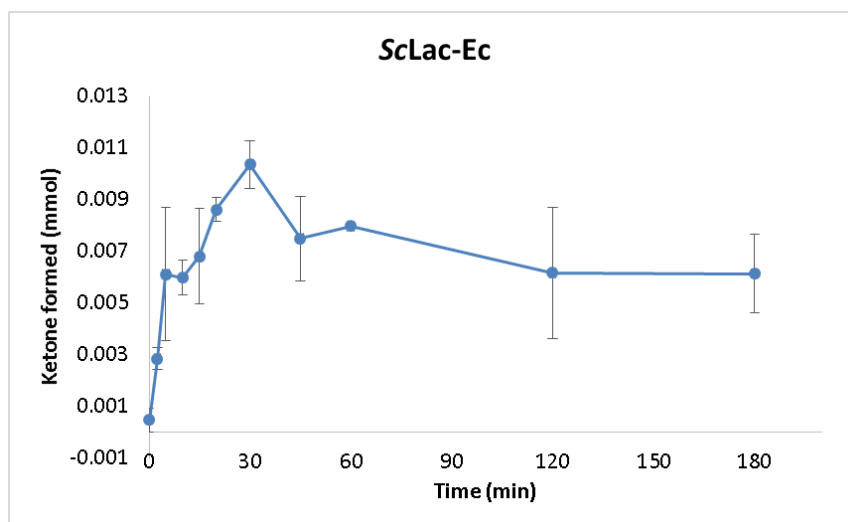


Figure 30: Kinetic analysis of the ScLac-Ec activity on the phenolic SS β -O-4 OH model compound. The reaction mix is prepared with approximately 0.0095 mmol model compound and 0.25 mg ScLac in the optimal buffer system of the enzyme. The mixture was saturated with O₂ prior to incubation at 30°C for 3 h. Interval samples were collected at time points 0, 2.5, 5, 10, 15, 20, 30, 45, 60, 120, and 180 min. The reaction products were extracted using ethyl acetate and quantified using an internal standard via NMR (6.2.18). The forming ketone (mmol) was plotted against the time. n = 3; x \pm SD.

2.6 Activity assays with Kraft lignin

The oxidation assays using alkali Kraft lignin were carried out as described previously (Rahmanpour & Bugg, 2015b; Rahmanpour et al., 2016) with *TfuDyP*-cp expressed in *P. fluorescens*, *DyPB*-pelB and *ScLac*-cp expressed in *E. coli*. Initial assays were carried out with 5 μ M Kraft lignin to check if the enzymes show activity on the polymeric lignin sample and to determine the effect of MnCl₂ on the activities of DyPs (Appendix Figure 56). The initial assays demonstrated the increase in the absorbance at 465 nm, which shows that some parts of the substrate went through oxidation in the presence of the enzymes. After confirmation of the enzymatic activities on Kraft lignin, more activity assays were carried out with varying concentrations of the substrate. The increasing concentrations of the substrate resulted in saturation kinetic behavior (Figure 31). The apparent K_M was determined as 20.42 μ M, 10.00 μ M and 3.33 μ M (All measurements were performed in triplicate (n = 3). Error bars indicate standard deviation (x \pm SD) from arithmetic mean.

Table 15) for *TfuDyP*, *DyPB* and *ScLac*, respectively. Michaelis-Menten models of the enzymatic activities by increasing Kraft lignin concentrations are given in Figure 31 and the kinetic parameters, V_{max} and K_M , were calculated based on these models are given in Table 15.

Results

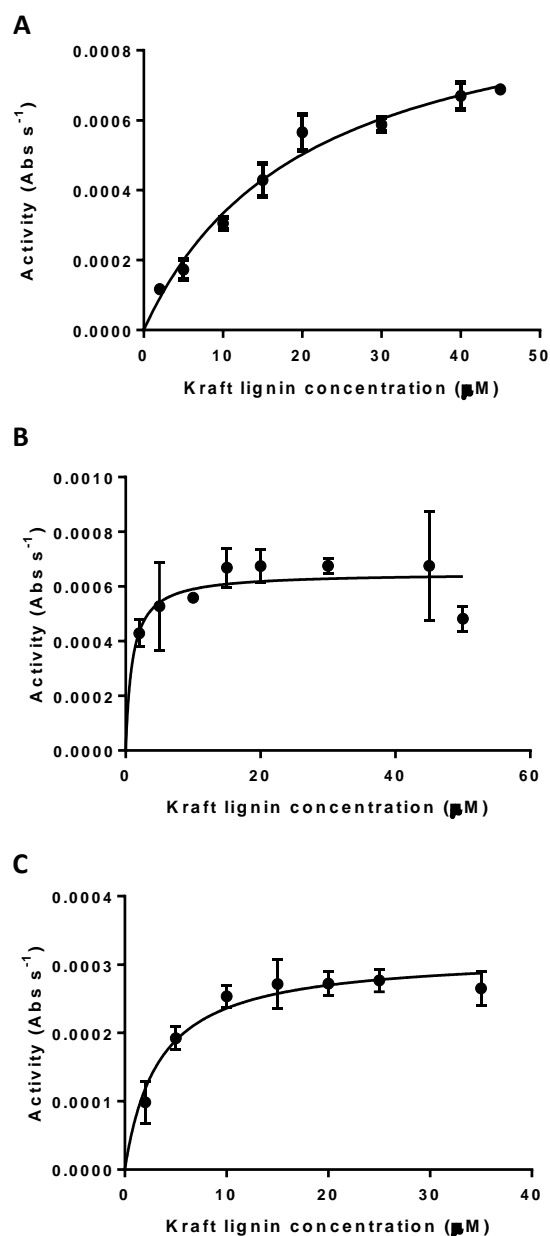


Figure 31: Change of *TfuDyP*, *DyPB* and *ScLac* activity (Abs s⁻¹) by increasing Kraft lignin concentration (μM). Specific activities of purified *TfuDyP* (A), *DyPB* (B) and *ScLac* (C) depending on varying concentrations of Kraft lignin were determined at 25°C, using 225 μg mL⁻¹ of each enzyme (6.2.17). 100 mM sodium acetate (pH 4.0) was used for *TfuDyP* assays, 100 mM sodium acetate (pH 4.5) was used for *DyPB* assays and 100 mM MES (pH 5.5) was used for *ScLac* assays as the buffer system (6.2.17). Michaelis-Menten model was fitted to the experimental data by non-linear curve fitting function of GraphPad Prism 6 software. All measurements were performed in triplicate (n = 3). Error bars indicate standard deviation (x"±" SD) from arithmetic mean.

Table 15: Kinetic parameters of *TfuDyP*, *DyPB* and *ScLac* towards Kraft lignin (6.2.17). n = 3; x±SD.

Construct	Vmax (Abs s ⁻¹)	K _M (mM)
<i>TfuDyP</i>	0.001015 ± 8,506x10 ⁻⁵	0.02042 ± 0.003902
<i>DyPB</i>	0.000649 ± 23.4x10 ⁻⁵	0.001 ± 0.0004679
<i>ScLac</i>	0.000315 ± 1.34x10 ⁻⁵	0.003338 ± 0.0006396

2.7 Modifications of selected enzymes for higher stability and/or activity

2.7.1 Immobilization of ScLac by two distinct methods

ScLac was immobilized on agarose beads and by the preparation of cross-linked enzyme aggregates (CLEAs), the latter mediated by PEG precipitation and glutaraldehyde cross-linking. At the end of the CLEA procedure, 71.5% of the initial activity was recovered. The immobilization of ScLac on agarose beads based on a Schiff base reaction was achieved by 33% immobilization efficiency (the proportion of bound protein). The reusability of the immobilized enzyme preparations was tested by performing 5 sequential activity assays using DMP as the substrate. The laccase immobilized on agarose beads maintained approximately 80% of its initial activity after five steps. The activity of the CLEAs declined to ~60% of the initial activity over the five steps, but the heat activation detected in the free enzyme sample was also observed for the CLEA preparation (Figure 32). Both methods made it possible to reuse immobilized ScLac samples at least five times in the sequential activity assays.

The stability of the immobilized ScLac was tested after 1 h incubation at 30°C and compared to the free ScLac sample. The laccase immobilized on agarose beads retained 70% of its initial activity whereas the CLEAs retained 88% of their initial activity (Figure 33 A). The pH optima of the immobilized enzymes were also determined and found to differ from the free enzyme preparation. The laccase immobilized on agarose beads reached its maximum activity at pH 6.5 and the CLEAs reached the maximum activity at pH 4.5 (Figure 33 B).

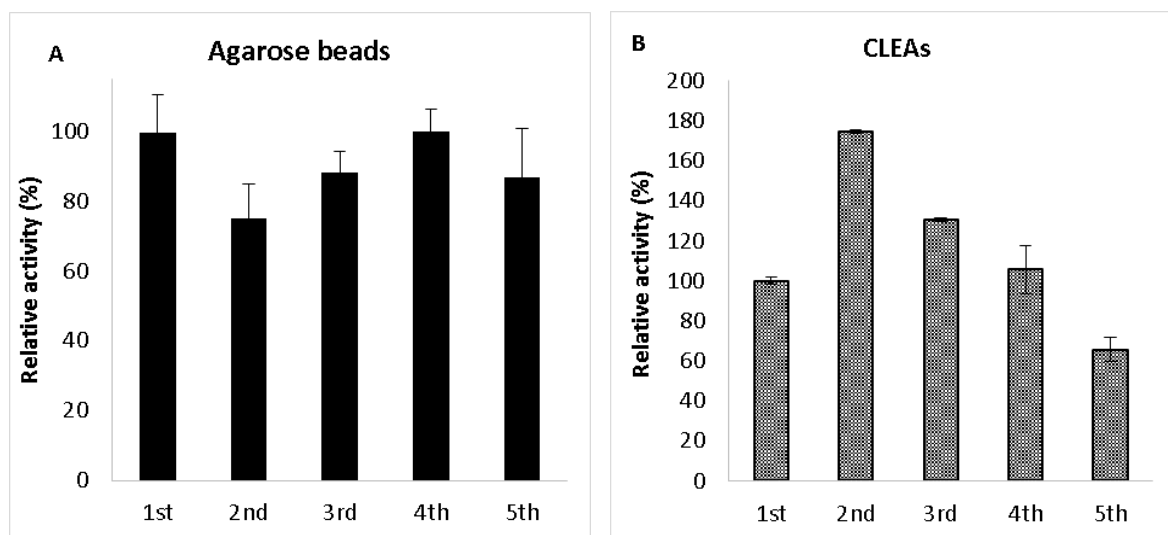


Figure 32: The reusability of immobilized ScLac samples. The remaining activity of immobilized ScLac on agarose beads (A) or as CLEAs (B) was analyzed in sequential activity assays for five cycles using DMP as the substrate (6.2.22). $n = 3$; $x \pm SD$.

Results

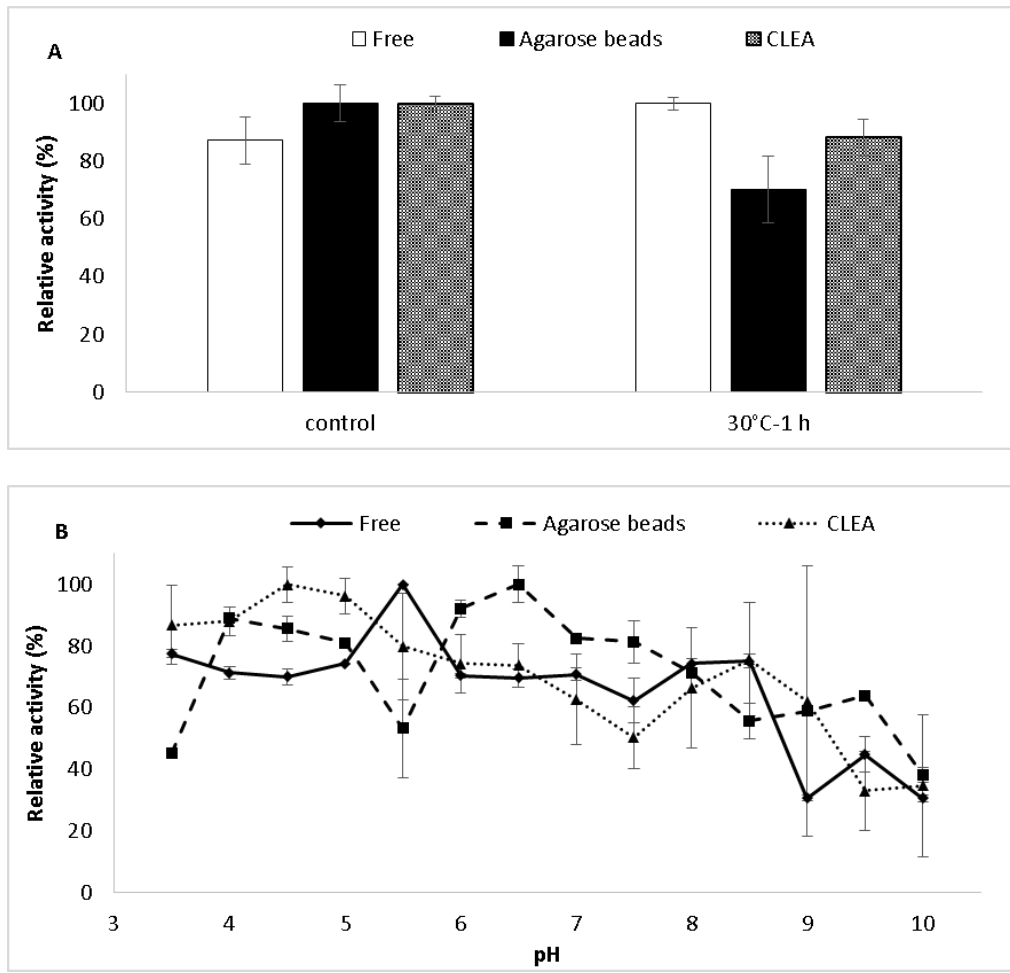


Figure 33: Characterization of immobilized and free Sclac samples. A: Thermal stability was determined by incubating the free and immobilized enzyme samples at 30°C for 1 h and measuring the residual activities. Control assays were set up without heat treatment, B: Optimum pH profiles of immobilized and free Sclac samples (6.2.22). n = 3; $\bar{x} \pm \text{SD}$.

2.7.2 Protein engineering for improved H₂O₂ stability

2.7.2.1 Development of an ultra-high-throughput screening method via fluorescence activated cell sorting

A modified version of the ultra-high-throughput screening method reported by (Ostafe et al., 2014) was adapted to screen the mutant libraries of *TfuDyP*. For this purpose, *TfuDyP* was cloned into the pCTcon2 vector system for expression in EB100 strain of *S. cerevisiae* cells. The pCTcon2 vector together with EB100 cells construct the yeast display system, which provides the expression of *TfuDyP* on the cell surface via α -agglutinin receptor of *S. cerevisiae* cells (Boder & Wittrup, 1997). The anchoring of *TfuDyP* on the cell surface is achieved by disulfide bridge formation between two subunits, AGA1 and AGA2 (Lu et al., 1995). A c-myc tag positioned at the C-terminus of *TfuDyP* was used to stain the cells with a fluorescent secondary antibody, facilitating the detection of the expression level of *TfuDyP* per cell (Figure 34).

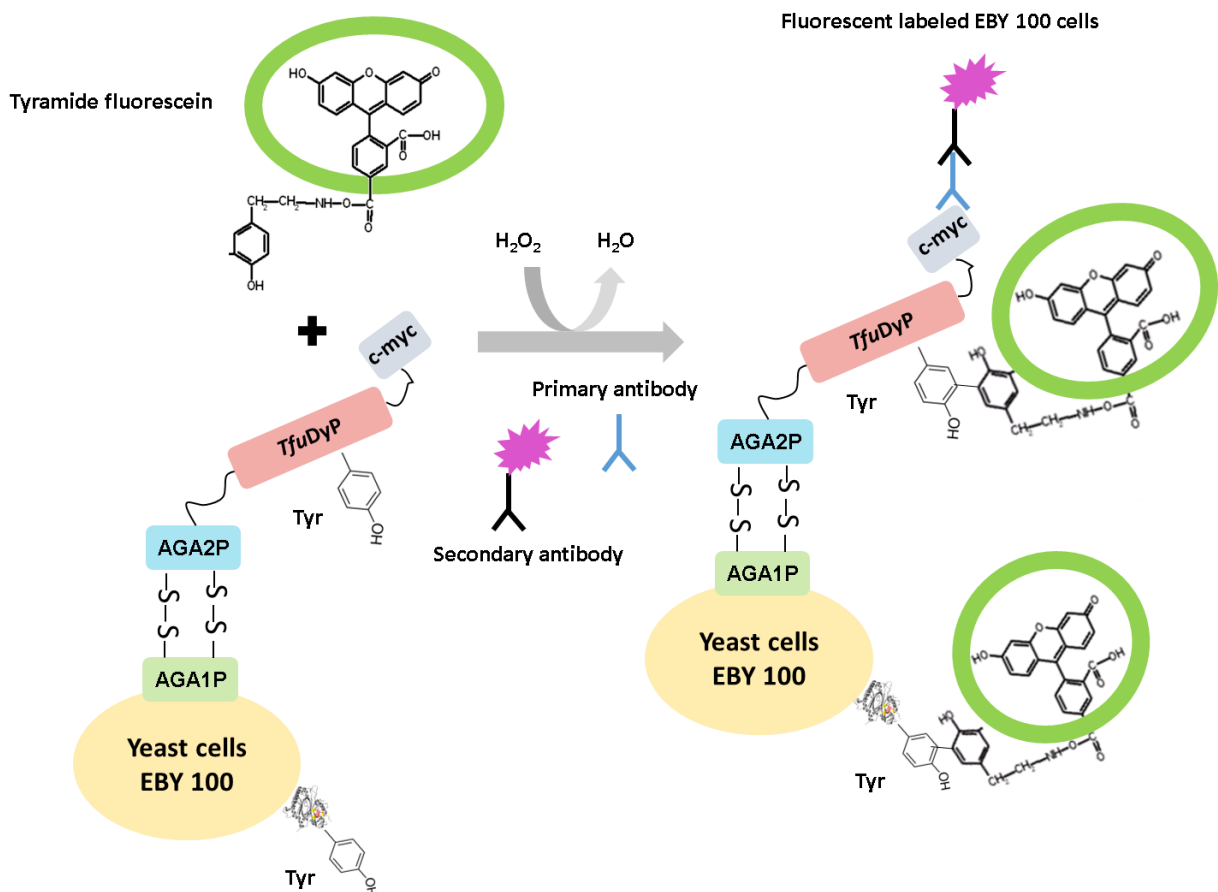


Figure 34: Ultra-high-throughput screening method for FACS. *TfuDyP* is expressed in EB100 cells using pCTcon2 vector. The vector system and the host facilitate the presentation of the enzyme on the cell surface through AGA1P and AGA2P peptides. The vector system harbors a C-terminus c-myc tag, which can be used for determining the expression level of the protein by staining the cells using a fluorescent antibody. Tyramide-fluorescein is used as the fluorescent substrate for the FACS screening experiments. When the enzyme oxidizes the substrate in the presence of H₂O₂, the substrate binds to the surface of the cell covalently via the tyrosine residues from the protein present on the surface of cells, thus staining the cells with the fluorescence. Adapted from Ostafe, 2013 and Boder & Wittrup, 1997.

Results

A fluorescent substrate, tyramide-fluorescein, was chosen to stain the EBY100 cells based on *TfuDyP* activity expressed on the cell surface. When the enzyme showed activity on the substrate in the presence of H₂O₂, the fluorescent substrate stained the cells by binding to proteins on the surface of the cells via tyrosine residues (Figure 34). In addition to staining the cells with tyramide-fluorescein, a fluorescent secondary antibody was used to double stain the cells in order to detect the amount of enzyme expressed on the cell surface (Figure 34). By using the two colors we could detect the specific activity of the enzyme determining the activity on one fluorescent channel and the amount of the expressed protein on another.

The successful cloning of *TfuDyP* into pCTcon2 was confirmed by sequence analysis. The expression of the enzyme in EBY100 cells was verified by a MTP assay using ABTS as the substrate. The optimal expression time for further studies was determined by evaluating the enzyme activity at different times of expression in YNB CAA galactose medium. The highest activity towards tyramide was tested using FACS analysis and was observed to be after 20 h of expression (Figure 57).

2.7.2.2 *TfuDyP* mutant library creation by random mutagenesis

The mutant libraries of *TfuDyP* were created by error-prone (ep) PCR using the commercial GeneMorph II Random Mutagenesis Kit (Agilent Technologies). The wild type (WT) *TfuDyP* coding sequence cloned into the pCTcon2 vector was used as the template for ep-PCRs. The ep-PCR amplified fragment of *TfuDyP* was used as a megaprimer to amplify the whole plasmid (MEGAWHOP) (Miyazaki & Takenouchi, 2002). The MEGAWHOP-PCR was carried out with different megaprimer : template amounts (250 ng : 150 ng, 500 ng : 300 ng, 250 ng : 300 ng) to optimize the yield of the PCR product and the transformation efficiencies. The PCR products obtained out of these reactions were first treated with DpnI and then transformed into the ultracompetent XL10 Gold cells. Approximately 670, 830, and 3500 transformants were obtained for the megaprimer:template ratios 250 ng:150 ng, 500 ng:300 ng, 250 ng:300 ng, respectively (Figure 35). In order to assure the diversity of the library and to reach a number of $\sim 10^5$ clones, transformation of the ultracompetent XL10 Gold cells was repeated with the PCR product of 250 ng:300 ng ratio several times. Five colonies were picked and cultures were prepared for sequence analysis to verify the mutagenesis frequency of the variants (Table 16). The sequence analysis showed that 4 out of 5 clones have mutations at least at the DNA level, therefore proving that the creation of the mutant libraries was successful. The remaining colonies obtained out of the transformations were collected and glycerol stocks were prepared accordingly. The DNA library was further amplified in the bacterial strain, plasmids were isolated and used for the transformation of EBY100 yeast cell line so that more than 10^5 different cell variants were obtained and further used for the FACS screening.

Results

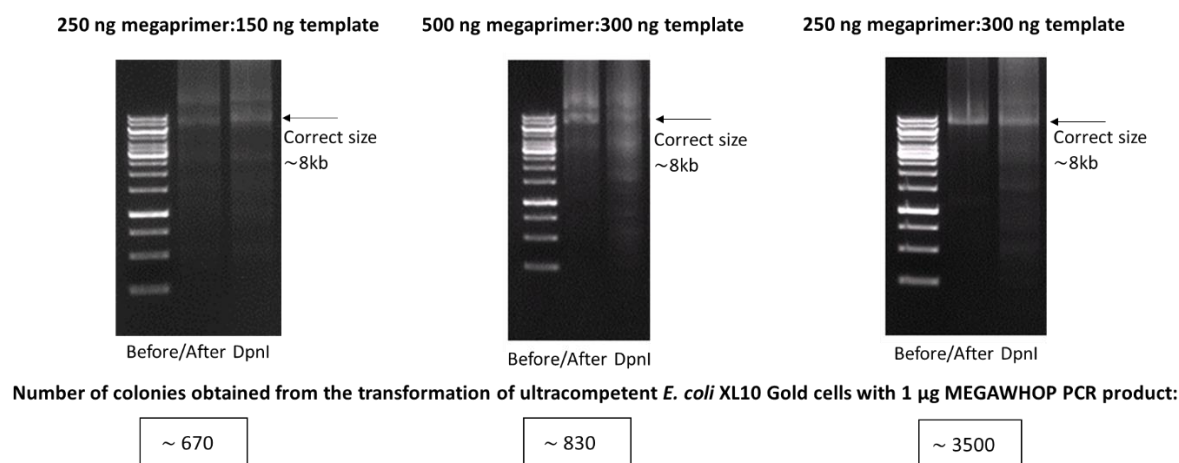


Figure 35: Analysis of the MEGAWHOP-PCR for the creation of mutant *TfuDyP* library. MEGAWHOP-PCRs were carried out with three different megaprimer:template ratios: 250 ng:150 ng (left), 500 ng:300 ng (middle), and 250 ng:300 ng (right), in order to reach maximum PCR product concentration and number of colonies following the transformation of competent XL10 Gold cells with the PCR products. The approximate length of the PCR product expected from the MEGAWHOP-PCR is 8 kb. Numbers of colonies obtained from XL10 Gold cells transformed with the corresponding PCR products are given below each agarose gel image (6.2.23).

Table 16: The sequence analysis of randomly selected five colonies from the transformation plates of MEGAWHOP-PCR products (6.2.23).

CLONES	Total number of mutations in codon exchange level	Amino acid changes
1	1	-
2	-	-
3	3	F→Y; Q→H; V→I
4	4	M→V; A→P; A→V; Q→P
5	3	A→V; E→G; A→F

2.7.2.3 FACS screening of mutant *TfuDyP* library

The feasibility of the adapted FACS screening method on the real mutant *TfuDyP* library was tested by an artificially created reference library, using a mixture of empty vector control (negative) cells and WT-*TfuDyP* expressing (positive) cells. The tyramide reaction was performed using the negative, the positive and the artificial library cells. When staining the cells only with tyramide based on enzyme activity (without antibody staining), we could not see a clear separation between the positive and negative population that was confirmed by no enrichment obtained after sorting (Figure 36-39 A, B, C). On the contrary, staining with both tyramide and antibody helped distinguishing the active population from the negative ones in the gates P4 (Figure 36-37) and P2 (Figure 38-39). The reaction time with tyramide was also an important parameter and was optimized using the timepoints 1, 5, 15 and 30 min. Five thousand events on the P4 and P2 gates were sorted for the reference libraries on YNB CAA glucose plates and were compared with the cells from the libraries before sorting. The cells before and after sorting were transferred to MTPs and their activity was evaluated using the ABTS assay. The results showed that the screening method was successful in enriching positive cells from a starting population of ~2% to a final purity of ~56%, when the reference library (5%) was incubated

Results

with tyramide for 1 min (Figure 40 A). The longer reaction times resulted in cross-reactivity between positive and negative cells therefore, no enrichment could be observed.

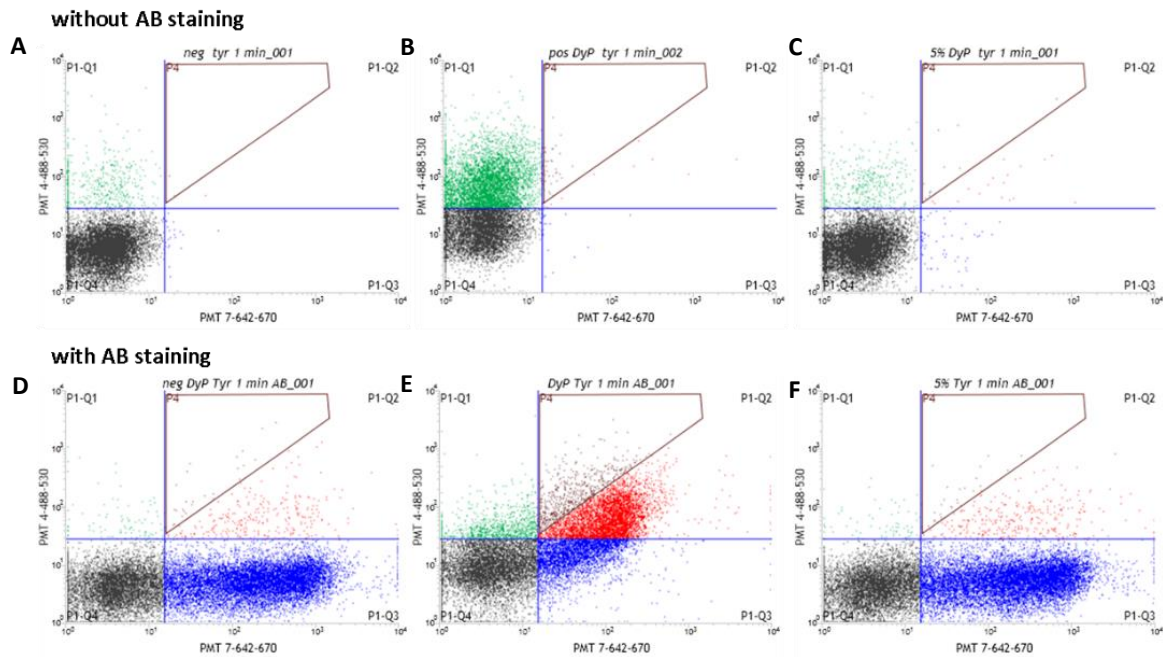


Figure 36: Optimization of reaction time (1 min) for tyramide assay using the artificial reference library. A-C: Samples without antibody staining (only tyramide stained); A: Negative cells, B: Positive cells, C: Artificial reference library (5%). D-F: Samples with both antibody and tyramide staining; D: Negative cells, E: Positive cells, F: Artificial reference library containing 5% positive cells (6.2.24). P4 gate (marked in red) used for the sorting.

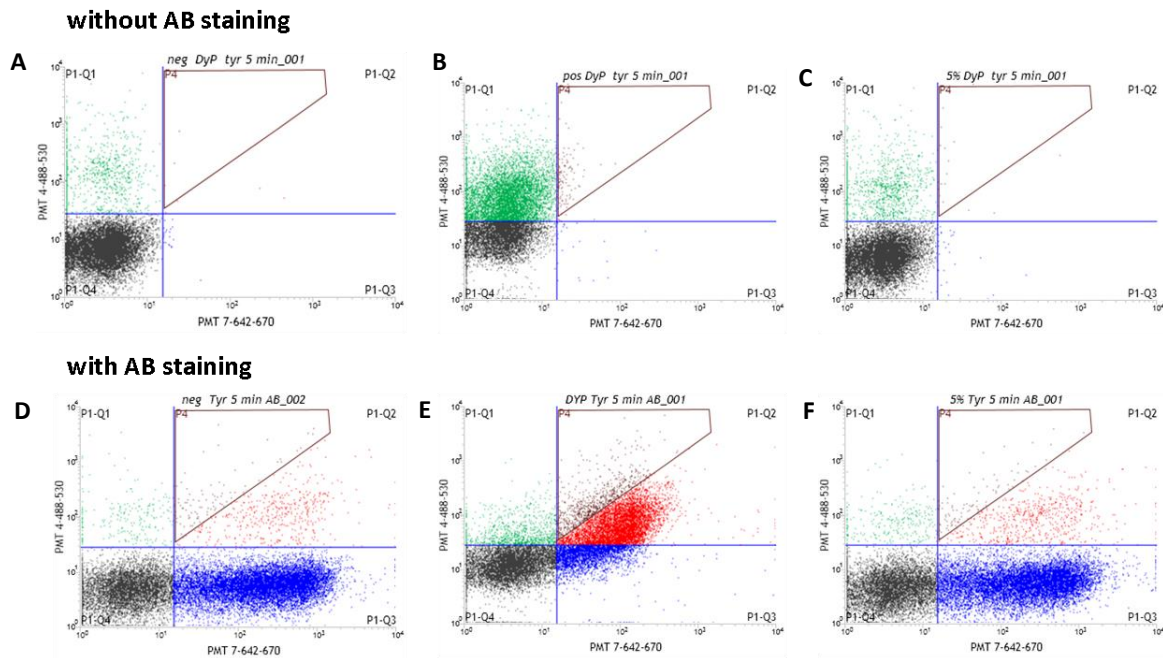


Figure 37: Optimization of reaction time (5 min) for tyramide assay using the artificial reference library. A-C: Samples without antibody staining (only tyramide stained); A: Negative cells, B: Positive cells, C: Artificial reference library (5%). D-F: Samples with both antibody and tyramide staining; D: Negative cells, E: Positive cells, F: Artificial reference library containing 5% positive cells (6.2.24). P4 gate (marked in red) used for the sorting.

Results

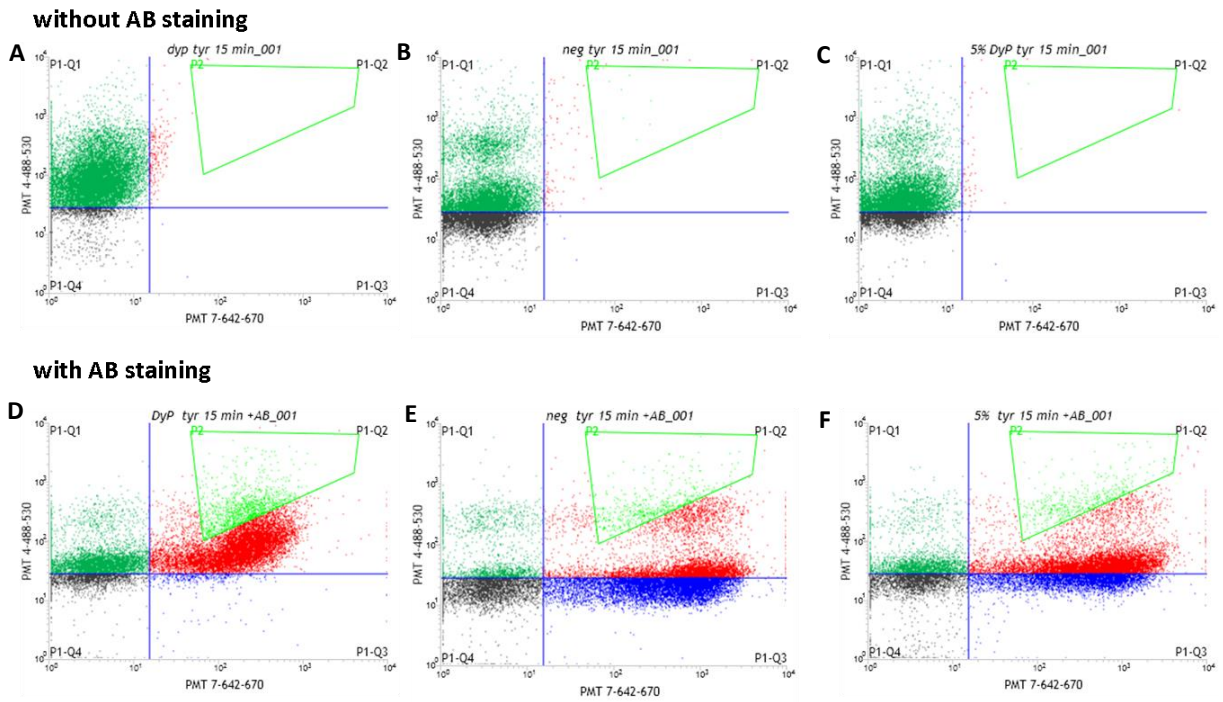


Figure 38: Optimization of reaction time (15 min) for tyramide assay using the artificial reference library. A-C: Samples without antibody staining (only tyramide stained); A: Negative cells, B: Positive cells, C: Artificial reference library (5%). D-F: Samples with both antibody and tyramide staining; D: Negative cells, E: Positive cells, F: Artificial reference library containing 5% positive cells (6.2.24). P2 gate (marked in green) used for the sorting.

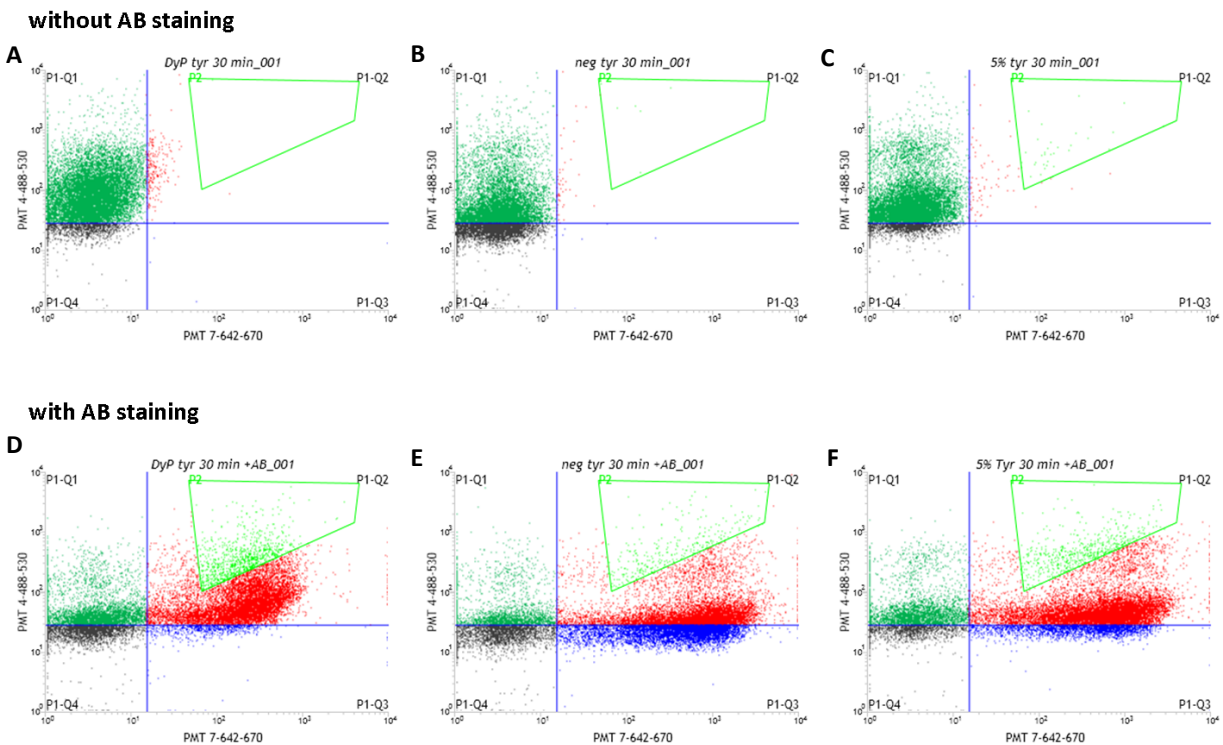
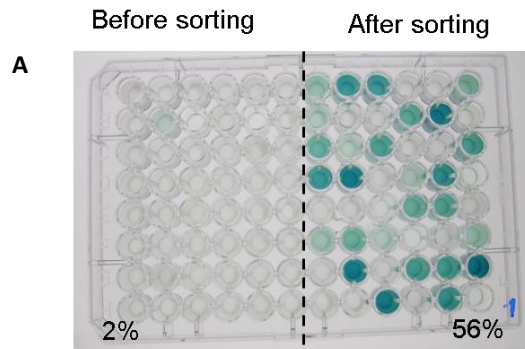


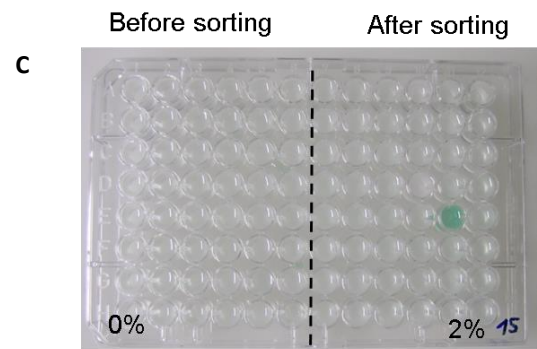
Figure 39: Optimization of reaction time (30 min) for tyramide assay using the artificial reference library. A-C: Samples without antibody staining (only tyramide stained); A: Negative cells, B: Positive cells, C: Artificial reference library (5%). D-F: Samples with both antibody and tyramide staining; D: Negative cells, E: Positive cells, F: Artificial reference library containing 5% positive cells (6.2.24). P2 gate (marked in green) used for the sorting.

Results

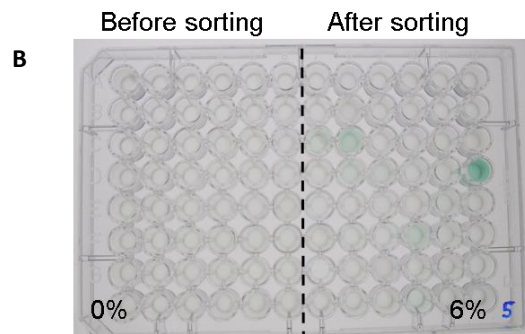
1 min tyr+ab



15 min tyr+ab



5 min tyr+ab



30 min tyr+ab

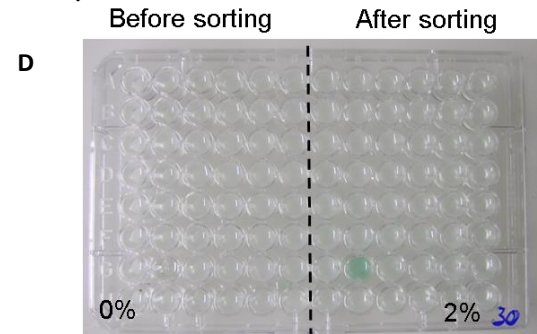


Figure 40: ABTS MTP assays of 5% reference libraries incubated with tyramide for 1 min (A), 5 min (B), 15 min (C), and 30 min (D) before and after sorting (6.2.24). In the presence of ABTS and H₂O₂, color change from transparent to blue-green shows the activity of the cells.

After proving on the artificial reference library that the screening and sorting method was successful, the mutant *TfuDyP* library was screened for oxidative stability by pretreating the cells with 5 mM H₂O₂ (6.2.24). The variants, which showed higher activity during FACS analysis were sorted (Figure 41) and analyzed first by the ABTS MTP assays and subsequently by the DNA sequencing. This yielded four mutant variants with higher activity, and H₂O₂ stability (Table 17). The positions of the mutations (blue) were highlighted individually on the homodimer structure of *TfuDyP* (Figure 42-right) together with the conserved residues (yellow) that are significant for the heme-binding and the catalytic activity (Figure 42-left).

Results

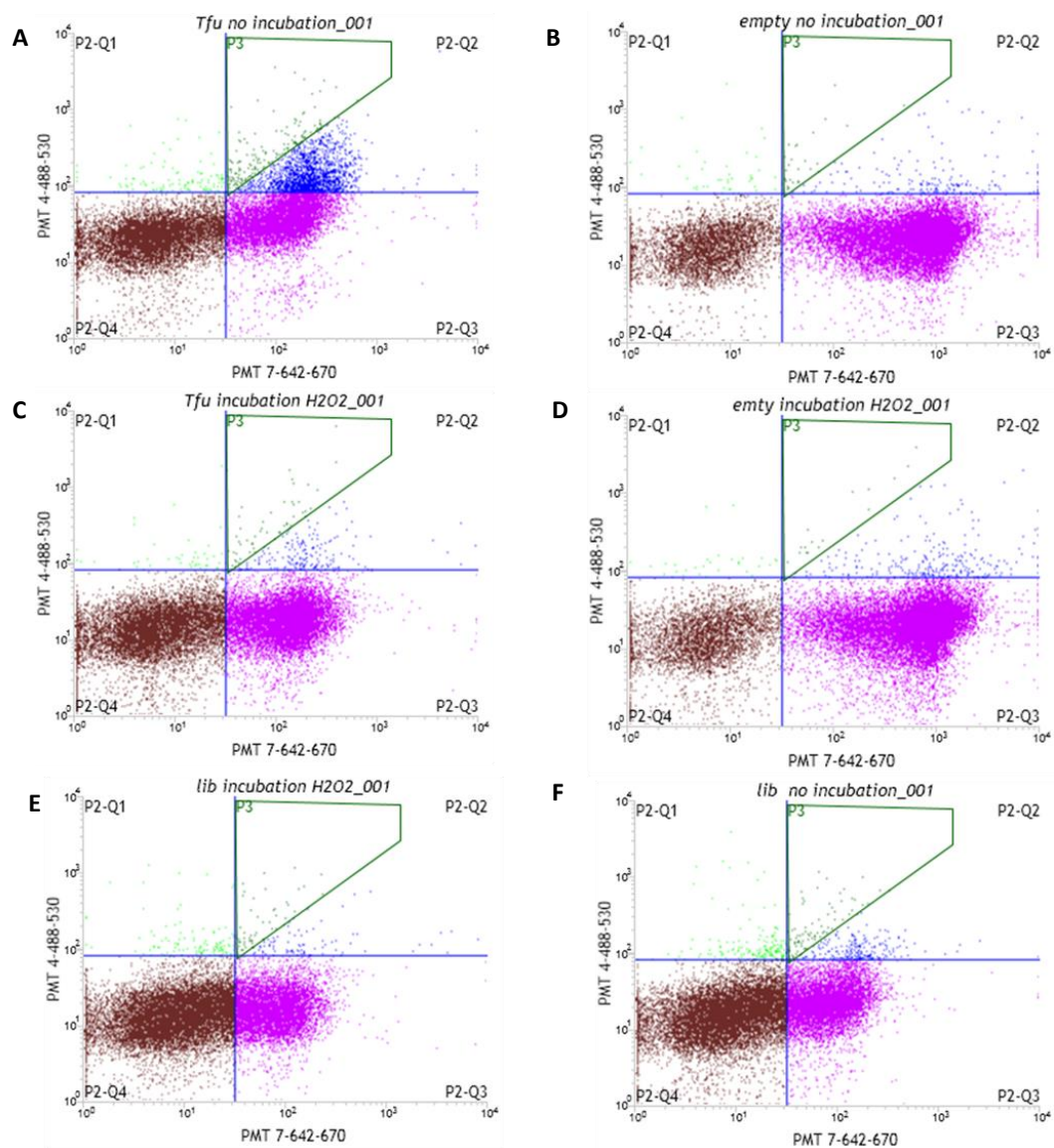


Figure 41: FACS analysis of *TfuDyP* library with (E) or without (F) H₂O₂ pretreatment together with positive (A, C) and negative controls (B, D). The library samples both with and without H₂O₂ pretreatment were sorted for the analysis by ABTS MTP assay.

Table 17: Sequencing analysis of the variants that showed higher activity in comparison to the WT-*TfuDyP* in the ABTS MTP assay after the pretreatment with 5 mM H₂O₂ (6.2.24). *Based on ABTS MTP assays.

Variant	Mutation	Increase in the activity in comparison to the WT- <i>TfuDyP</i> (fold)*
1	R315H	2.28
2	P154S and Q357R	1.67
3	V165I	1.39
4	S274C	1.39

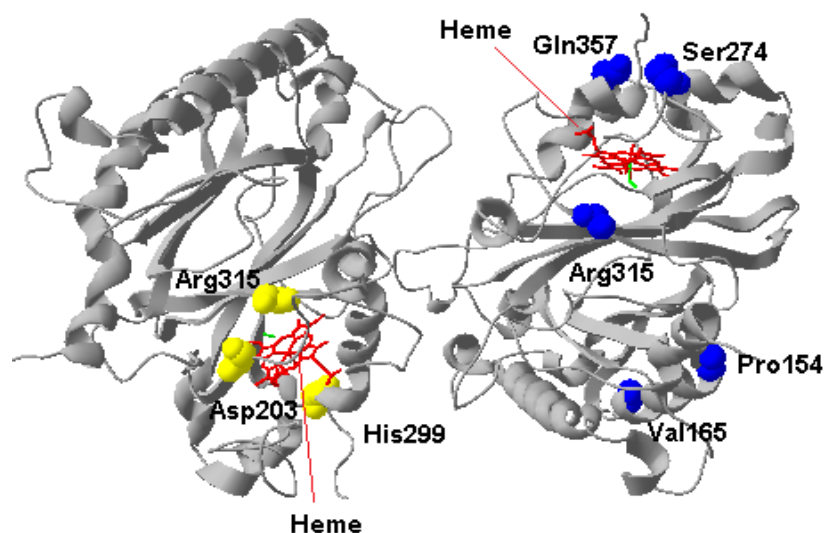


Figure 42: The homodimer structure of *TfuDyP* (PDB: 5FW4). The conserved residues (yellow) that are significant for heme-binding and catalytic activity are demonstrated on the monomer on the left. On the other monomer (right), the mutations (blue) carried by the sorted variants with higher H₂O₂ stability were demonstrated as a comparison with the conserved residues. The conserved residues and the mutational exchanges on the homodimer structure were indicated on the structure via Swiss-PdbViewer version 4.1.0.

Heterologous expression of mutant *TfuDyP* variants and WT-*TfuDyP* in *E.coli* for a detailed enzymatic characterization revealed differences in the expression yields (8.16). The variants with the single mutations R315H, V165I and S274C were expressed in higher yields (Table 18) in comparison to the WT-*TfuDyP*. However, an approximately 5-fold decrease in the heterologous expression yield (Table 18) was observed for the double mutant variant with the aminoacid exchanges of P154S and Q357R. Functional characterization assays indicated that the optimum temperature, which was determined as 60°C for all variants, was not affected by any of the mutational exchanges. However, the double mutation (P154 and Q357R) resulted in a slight optimum pH shift from 5.0 to 4.5 and the single R315H exchange shifted the optimum pH dramatically from 5.0 to 8.5 (Figure 60). For other variants and WT-*TfuDyP* the highest activities were recorded at pH 5.0. Analysis of the kinetic parameters of the mutant variants and the WT enzyme did not show significant changes in the turnover numbers (k_{cat}). The K_M of the V165I variant increased significantly suggesting a decrease in the specificity of the variant towards guaiacol. Interestingly, the lowest K_M was determined for the double mutant P154S and Q357R, which was expressed with the lowest yields. The heterologous expression yields, optimum pH and temperature values and the kinetic parameters are summarized for all the mutant *TfuDyP* variants and WT-*TfuDyP* in Table 18.

Results

Table 18: Characterization of the isolated mutant *TfuDyP* variants (6.2.24) and WT-*TfuDyP* (6.2.24) expressed in *E. coli* (6.2.6) for expression yield (mg protein per L⁻¹ expression culture), pH and temperature profiles (6.2.21) and kinetic parameters (6.2.17) (K_M , k_{cat} and k_{cat}/K_M) for guaiacol.

	Mutation	Expression yield (mg L ⁻¹)	Optimum pH	Optimum temperature (°C)	K_M (μM)	k_{cat} (s ⁻¹)	k_{cat}/K_M (μM ⁻¹ s ⁻¹)
1	R315H	78.3	8.5	60	20.9	1.8x10 ⁻³	8.5x10 ⁻⁵
2	P154S and Q357R	11.3	4.5	60	6.5	1.1x10 ⁻³	1.6x10 ⁻⁴
3	V165I	85.0	5.0	60	407.3	3.4x10 ⁻³	8.2x10 ⁻⁶
4	S274C	83.8	5.0	60	15.8	1.4x10 ⁻³	8.9x10 ⁻⁵
5	WT	57.8	5.0	60	11.7	1.4x10 ⁻³	1.2x10 ⁻⁴

3.0 Discussion

3.1 Heterologous expression of lignin-degrading enzymes

The structure of lignin is derived from the methoxylated hydroxycinnamyl alcohol building blocks ending up with a complex, unordinary and heterogeneous polymer composed of many different linkages (Rinaldi et al., 2016). The difficulties in the depolymerization of lignin hampers the efficient exploitation of the polymer and hinders the utilization of cellulose and hemicellulose. However, the high carbon content of lignin still makes it an attractive source to produce sustainable biofuels and chemicals.

Back in 1980s, white-rot fungi were identified to break lignin slowly by producing extracellular lignin-degrading peroxidases. Upon the findings, research about the lignin-degrading enzymes focused mainly on white-rot fungi such as *Phanerochaete chrysosporium* (Andrawis et al., 1988; Holzbaur et al., 1988; Kirk, 1987; Ulmer et al., 1983). Many more enzymes of fungal origin with the potential to degrade lignin were identified such as manganese peroxidases and laccases (Chen et al., 2012c; Hattikaul & Ibrahim, 2012). Despite the intensive work and deep investigations, there is no example yet of a fungal enzyme being commercially used for an effective lignin-degradation process. In the recent years, lignin-degrading enzymes of bacterial origin have attracted the attention as promising alternatives to fungal counterparts regarding the differences in functional parameters, their potential showed on complex lignin-model compounds and polymeric lignin, and the facilities in expression procedures. Unlike fungal enzymes, there is no requirement for post-translational modifications. Therefore, the heterologous expression of the bacterial enzymes can be carried out by well-defined, easy-to-handle bacterial host organisms such as *E. coli*. Bacterial enzymes present certain properties, which can be advantageous over the fungal counterparts (Ausec et al., 2011; Bugg et al., 2011a; Chandra & Chowdhary, 2015). For instance, bacterial laccases possess a wide range of pH optima and some of them are active at neutral or even basic pH values (Ece et al., 2017). However, fungal laccases show activity only in a narrow window of pH range and the large-scale production of fungal laccases can be challenging because of the slow growth rates of fungi or the requirements of the post-translational modifications, which complicate the successful heterologous expression (Lambertz et al., 2016).

The main purpose of this thesis was to express a set of bacterial lignin-degrading enzymes with high yields to be able to characterize the functional and kinetic parameters of the enzymes in detail using simple and complex lignin-model compounds and polymeric lignin samples. To achieve a better degradation of the recalcitrant lignin polymer, possible modification approaches such as immobilization and protein engineering were investigated. For this purpose, six knowledge-based bacterial enzymes from three different families of lignin-degrading enzymes were chosen (Table 1).

The coding sequences of all enzymes were previously reported either in the databases such as Uniprot and NCBI or in the literature.

3.1.1 *E. coli* as the heterologous expression host

Previous studies showed that, if present, the efficiency of the heterologous expression depends considerably on the existence of the leader peptide (Sletta et al., 2007). Furthermore, the stability and the activity of the recombinant protein are also affected by the presence or absence of the leader peptide (Singh et al., 2013). For the heterologous expression, the type of the signal sequence plays an important role since the native signal sequences might not be recognized by every host organism (Pines & Inouye, 1999; Rosano & Ceccarelli, 2014). In some cases, it is possible to optimize the signal sequences or to create an artificial one to improve the efficiency of the heterologous expression and the targeting to the desired compartment, such as the periplasm or to enable secretion (Clerico et al., 2008; Samant et al., 2014; Velaithan et al., 2014).

In this work, the *TfuDyP* coding sequence was expressed in the presence of the native Tat signal peptide, the *pelB* leader peptide provided on the pET-22b(+) vector system or without any leader peptides. Judging initially from the expression yields (Table 2), the existence of the Tat or *pelB* leader peptide limits the expression in comparison to the version without any signal sequence. Considering that all three versions of *TfuDyP* (-Tat, -*pelB* and -cp) were purified from the soluble fractions represented successful heme incorporation, and showed activity towards DMP, it can be concluded that the leader peptide does not play a crucial role in the folding process of *TfuDyP*. The coding sequence of *TfuDyP* bears merely one cysteine residue, which suggests there is no possibility and requirement to form any disulfide bridges. This might have an effect on the successful expression of *TfuDyP* without any leader peptides. *TfuDyP* was previously expressed in *E. coli* with the native Tat-sequence (van Bloois et al., 2010) and the expression yield was determined as 3 mg L⁻¹ expression culture after one step IMAC purification. It was shown that *TfuDyP* was exported to the periplasmic space when expressed in an *E. coli* strain, which was deficient in its Tat translocation system. SDS-PAGE analysis of purified *TfuDyP* sample revealed one unprocessed and one mature form of the recombinant enzyme, which is comparable to the results presented here for *TfuDyP*-Tat and -*pelB* (Figure 10). Recently, Rahmanpour and colleagues expressed *TfuDyP* that lacks any signal sequence in *E. coli* BL 21 (DE3) (Rahmanpour et al., 2016). The yield obtained after one-step IMAC purification and a following His₆-tag removal step was reported as 9 mg protein L⁻¹ expression culture. The increase in the expression yield achieved by removing the Tat signal sequence from the coding sequence reported in this study is comparable to the data obtained from the literature and indicates clearly that signal sequences might not always be required for the efficient heterologous expression in *E. coli*. Thus, the

Discussion

expression without any leader peptide can be an alternative strategy, when periplasmic or extracellular location is not crucial for a proper protein folding.

DyPB was expressed previously (Roberts et al., 2011) in the cytoplasm of *E. coli*. Although the expression yield of the recombinant DyP was not reported, the results indicate a successful expression. The results obtained in this thesis show that DyPB was expressed less efficiently in the cytoplasm of *E. coli* than *TfuDyP* (Table 2). The coding sequence of DyPB contains three cysteine residues. Although there has been no experimental proof so far, the expression of DyPB in the periplasm might have favored the formation of the disulfide bridges and consequently higher yields of recombinant active protein in the soluble fraction.

The coding sequence of *SSHGDyP* was revealed by the genome analysis of *Streptomyces albus* JA10, which is often used as heterologous expression host for bacterial proteins. The expression of the enzyme was not reported thus far. Although, the enzyme is reported as an extracellular enzyme, the analysis of the purified enzyme without any leader peptide does not indicate an unprocessed and a mature form of the enzyme. Adding the pelB leader peptide to the coding sequence of the enzyme did not make a significant change in the expression yields of the purified proteins.

Such as *SSHGDyP*, the coding sequence of *ScLac* was also suggested to harbor a leader peptide regarding its extracellular expression in its native host. However, the existence of the leader peptide has never been proved. The extracellular expression of *ScLac* by *Streptomyces cyaneus* CECT 3335 was previously carried out for 10 days in a submerged culture, yielding 8.19 mg protein from 100 mL of culture supernatant following five purification steps (Arias et al., 2003; Margot et al., 2013). In contrast, here, the heterologous expression of *ScLac* in *E. coli* achieved higher yields up to 104 mg L⁻¹ (Figure 13) in a shorter cultivation time and required only a single IMAC step. In the first report of the native expression of *ScLac* (Arias et al., 2003), the bacterial laccase was reported to be an extracellular laccase and it was purified from the culture supernatant. *ScLac* was later produced in its native host and compared with a native fungal laccase based on its activity on micropollutants (Margot et al., 2013). The *ScLac* activity was also detected in the extracellular fraction of *S. cyaneus*. The analysis of the *ScLac* sequence by databases such as SignalP and UniProt indeed did not indicate the presence of any leader peptides. Therefore, it was concluded that *ScLac* is not an extracellular enzyme and it was not secreted by the organism. It was actually released into the extracellular media throughout the cultivation because of the increasing rate of cell death (Margot et al., 2013). SDS-PAGE and western blot analysis of purified *ScLac*-cp did not yield two close bands as observed for *TfuDyP*, when *ScLac* was expressed without pelB leader peptide agreeing with the abovementioned findings. The expression of the enzyme with pelB leader peptide decreased the yields drastically (Table 2).

Discussion

Despite of the potential of the microbial β -etherases regarding their cleavage activity of the β -aryl ether linkages, very few members of the enzyme family was identified and characterized into details, such as LigE and LigF (Masai et al., 1991; Masai et al., 1993; Masai et al., 1999). More recently, ligE and LigF were also expressed in *E. coli* BL21(DE3) together with other novel bacterial β -etherases (Picart et al., 2014). The recombinant β -etherases were purified by one-step IMAC benefitting from the interaction between the His₆-tag at the N-terminus and the Ni²⁺-NTA agarose resin. The expression yields of the β -etherases were reported to be in the range of 75 to 150 mg protein L⁻¹ expression culture. In comparison to the yields reported by Picart et al., the yields obtained in this work (up to 16 mg L⁻¹) is lower, although the expression host was *E. coli* in both cases. However, the *E. coli* strain used in this work was BL21-CodonPlus(DE3)-RIL, which supplies rare codons for argU (AGA, AGG), ileY (AUA) and leuW (CUA), instead of BL21(DE3). Studies about heterologous expression of prokaryotic and eukaryotic proteins showed that the type of host strain can make great differences in the expression levels (Rosano & Ceccarelli, 2014). Therefore, many different strains and conditions should ideally be tested to express the protein of interest in desired amounts.

3.1.2 *P. fluorescens* as the heterologous expression host

E. coli has been used most of the time for the expression of bacterial lignin-degrading enzymes since it is most well-established, easy and simple organism to work with (Rosano & Ceccarelli, 2014). There are many molecular biology tools available that provide flexibility. However, the production levels of soluble recombinant proteins might be too low to be able to carry out further analyses of the recombinant enzymes. *P. fluorescens* is known to be a robust expression host particularly for pharmaceutical proteins. A wide range of molecular biology tools are also available and appropriate fermentation technics are tested successfully for up scaling procedures (Retallack et al., 2012). First studies have already revealed that *P. fluorescens* might be more effective for the heterologous expression of bacterial proteins when compared to *E. coli* under similar conditions (Retallack et al., 2005). Therefore, *P. fluorescens* might be an alternative for *E. coli*, when one cannot overcome the low expression yield issue for the target recombinant protein.

Except DyPB and SSHGDyP, all enzymes were expressed successfully in *P. fluorescens* and the yields after one-step IMAC were increased by 2 to 70-fold in comparison to the expression in *E. coli*. DyPB was not expressed at all and SSHGDyP was expressed in form of inclusion bodies. The expression yields of the β -etherases were improved up to 70-folds, particularly the yields for LigF reached to the gram levels indicating the great potential of *P. fluorescens* as a heterologous expression host for bacterial lignin-degrading enzymes.

Discussion

The biggest obstacle standing between the enzymes with high potential and real-life applications is generally the poor number of available enzymes. Problems occurring at the native, homologous or heterologous expression steps which arise from submerged cultures, low expression yields due to codon usage bias, leader peptides or accumulation of the protein of interest as inclusion bodies due to lack of the posttranslational modifications might comparatively affect the isolation or purification steps (Brijwani et al., 2010; Piscitelli et al., 2010). Relatively simple bacterial expression hosts such as *E. coli* provides higher productivity, low cost, short expression times and less laborious processes which are favorable routine processes and industrial applications. That is why *E. coli* is still the most commonly used expression host for the heterologous expression of broad range of enzymes from eukaryotic and prokaryotic origins. Using both *E. coli* and *P. fluorescens* as expression hosts, substantial expression yields were achieved in comparison to the previously reported studies about recombinant lignin-degrading enzymes with bacterial origin.

To compare the expression yields obtained for *E. coli* and *P. fluorescens* in this study (Table 19), the reported bacterial DyP-type peroxidases, laccases and β -etherases were summarized in Table 20, Table 21 and Table 22 together with the origins of the enzymes and the expression yields (when possible). The expression yields achieved in *E. coli* are in the range of the yields reported in the literature. However, the yields achieved in *P. fluorescens* outrun the reported yields in *E. coli*.

Table 19: Comparison of the expression yields obtained in *E. coli* and *P. fluorescens* with the yields reported in the literature obtained by heterologous expression. IB: Inclusion bodies, NE: Not expressed successfully, NR: Not reported. **TfuDyP* expressed with the yield of 200 mgL⁻¹ was almost inactive (Colpa & Fraaije, 2016).

Enzyme	Expression yields in <i>E. coli</i> ~mg protein L ⁻¹ expression culture	Expression yields in <i>P. fluorescens</i> ~mg protein L ⁻¹ expression culture	Expression yields reported in the literature~mg protein L ⁻¹ expression culture	Reference
<i>TfuDyP</i>	20.0	130.0	3.0-200.0*	(van Bloois et al., 2010); (Rahmanpour et al., 2016); (Colpa & Fraaije, 2016)
DyPB	18.0	NE	NR	(Ahmad et al., 2011)
<i>SSHGDyP</i>	5.0	IB	NR	NR
ScLac	104.0	234.0	NR	NR
LigE	5.5	490.0	75.0-150.0	(Picart et al., 2014)
LigF	16.0	1123.5	75.0-150.0	(Picart et al., 2014)

Table 20: Bacterial laccases, laccase-like phenol oxidases, and multi-copper oxidases produced by heterologous expression in *E. coli* and the corresponding expression yields (if reported). If not mentioned otherwise, the enzyme yield is the amount of enzyme recovered after purification. NR: not reported.

Enzyme	Origin	Yield	Comments	Reference
PpoA	<i>Marinomonas mediterranea</i>	NR		(Sanchez-Amat et al., 2001)
Cot A	<i>Bacillus subtilis</i>	NR	10% of total recombinant CotA expressed by <i>E. coli</i> was purified successfully	(Martins et al., 2002)
CotA	<i>B. subtilis</i>	20 mg L ⁻¹ (aerobic) 23 mg L ⁻¹ (anaerobic)		(Durao et al., 2006; Durao et al., 2008a; Durao et al., 2008b; Pereira et al., 2009)
EpoA	<i>Streptomyces griseus</i>	NR		(Endo et al., 2003)
STSL	<i>Streptomyces lavendulae</i>	10 mg L ⁻¹		(Suzuki et al., 2003)
Lbh1	<i>Bacillus halodurans</i>	NR		(Ruijssenaars & Hartmans, 2004)
SLAC	<i>Streptomyces coelicolor</i>	NR		(Machczynski et al., 2004)
Tth laccase	<i>Thermus thermophilus</i>	10 mg L ⁻¹		(Miyazaki, 2005)
McoA	<i>Aquifex aeolicus</i>	NR	Expressed as insoluble protein and recovered by unfolding and refolding	(Fernandes et al., 2007)
CotA	<i>Bacillus licheniformis</i>	10 mg L ⁻¹		(Koschorreck et al., 2008)
SilA	<i>Streptomyces ipomea</i>	NR	4.8-fold purification of the protein corresponding to a final yield of 85.6%	(Molina-Guijarro et al., 2009)

Discussion

Enzyme (continued)	Origin (continued)	Yield (continued)	Comments (continued)	Reference (continued)
LCMOs	<i>Bacillus coagulans</i> <i>Bacillus clausii</i> <i>Bacillus pumilus</i> <i>Streptomyces pristinaespiralis</i> <i>Gramella forsetii</i> <i>Marivirga tractuosa</i> <i>Spirosoma linguale</i>	NR		(Ihssen et al., 2015)
SCLAC SLLAC SVLAC AMLAC	<i>S. coelicolor</i> <i>Streptomyces lividans</i> <i>Streptomyces viridosporus</i> <i>Amycolatopsis</i> sp	15–20 mg L ⁻¹		(Majumdar et al., 2014)
Cot A	<i>B. clausii</i>	NR		(Brander et al., 2014)
Ssl1	<i>Streptomyces sviveus</i>	40–50 mg L ⁻¹		(Gunne & Urlacher, 2012b)
BALL	<i>B. licheniformis</i>	20 mg L ⁻¹		(Tonin et al., 2016)
MmPPO	<i>Marinomonas mediterranea</i>	NR	Recovered from membrane fraction and partially purified to 34 U L ⁻¹	(Tonin et al., 2016)

Table 21: Bacterial DyP-type peroxidases produced by heterologous expression in *E. coli* and the corresponding expression yields (if reported). If not mentioned otherwise, the enzyme yield is the amount of enzyme recovered after purification. NR: not reported.

Enzyme	Origin	Yield	Comments	Reference
AnaPX	<i>Anabaena sp.</i>	10 mg L ⁻¹		(Ogola et al., 2009)
BIDyP	<i>Brevibacterium linens</i>	NR		(Sutter et al., 2008)
BsDyP	<i>Bacillus subtilis</i>	NR		(Sezer et al., 2013)
BtDyP	<i>Bacteroides thetaiotaomicron</i>	NR		(Zubieta et al., 2007b)
DyP2	<i>Amycolatopsis sp.</i> 75iv2	25 mg L ⁻¹		(Brown et al., 2012)
DyP1B	<i>Pseudomonas fluorescens</i> Pf-5	30 mg 2 L ⁻¹		(Rahmanpour & Bugg, 2015b)
DyPA	<i>Rhodococcus jostii</i> RHA1	NR		(Ahmad et al., 2011)
DyPB	<i>R. jostii</i> RHA1	NR		(Ahmad et al., 2011)
dypPa	<i>Pseudomonas aeruginosa</i> PKE117	NR		(Li et al., 2012)
DyP2B	<i>P. fluorescens</i> Pf-5	26 mg 2 L ⁻¹		(Rahmanpour & Bugg, 2015b)
DyPA	<i>P. fluorescens</i> Pf-5	5 mg 2 L ⁻¹		(Rahmanpour & Bugg, 2015b)
FepB	<i>Staphylococcus aureus</i>	NR		(Turlin et al., 2013)
PpDyP	<i>Pseudomonas putida</i>	NR		(Sezer et al., 2013)
TyrA	<i>Shewanella oneidensis</i>	NR		(Zubieta et al., 2007a; Zubieta et al., 2007b)
TfuDyP	<i>Thermobifida fusca</i> YX	3 mg L ⁻¹		(van Bloois et al., 2010)
TfuDyP	<i>T. fusca</i> YX	9 mg L ⁻¹		(Rahmanpour et al., 2016)
TfuDyP	<i>T. fusca</i> YX	Up to 200 mg L ⁻¹	Low activity / inactive	(Colpa & Fraaije, 2016)

Table 22: Bacterial β -etherases produced by heterologous expression in *E. coli* and the corresponding expression yields (if reported). If not mentioned otherwise, the enzyme yield is the amount of enzyme recovered after purification. NR: not reported.

Enzyme	Origin	Yield	Comments	Reference
LigD	<i>Sphingomonas paucimobilis</i> SYK-6	NR		(Masai et al., 1991)
LigE	<i>S. paucimobilis</i>	NR		(Masai et al., 1991)
LigF	<i>S. paucimobilis</i>	2.66 mg 200 mL ⁻¹	2-step purification	(Masai et al., 2003; Masai et al., 1993)
LigG	<i>S. paucimobilis</i>	NR		(Masai et al., 2003)
LigE LigF LigG LigP	<i>Sphingobium</i> sp.	NR	2 rounds of IMAC	(Gall et al., 2014)
LigE LigE-NS LigE-NA LigF LigF-NS LigF-NA LigP LigP-SC	NA: <i>Novosphingobium</i> sp. PP1Y NS: <i>Novosphingobium</i> <i>aromaticivorans</i> DSM1244.	75-150 mg L ⁻¹	1-step IMAC	(Picart et al., 2014)

3.2 Functional and structural characterization of the purified enzymes

The Soret band scans assist in calculating Reinheitszahl (RZ) values of peroxidases, which give information about correct heme incorporation and initial hint about the enzymatic activity. The band analyses carried out here (Figure 18 A, B) showed that the heme B group was incorporated into the *TfuDyP* structure expressed in *E. coli* and *P. fluorescens* successfully. The corresponding RZ values (Table 4) were lower for the DyP that was expressed with leader peptides in *E. coli* compared to the same protein that was expressed without leader peptide. The highest RZ value of *TfuDyP* is obtained when the enzyme was expressed in *E. coli* without any leader peptides. A successful heme

Discussion

incorporation into *TfuDyP* via *P. fluorescens* expression shows that *P. fluorescens* is able to synthesize sufficient amount of heme without providing any precursors into the expression medium. Precursors are known to be crucial for the heterologous expression of heme-containing recombinant enzymes that are expressed in bacteria and yeast (Colpa & Fraaije, 2016). Here, the heme incorporation into the *TfuDyP* structure was successfully performed by the host without any additional precursors or laborious experimental steps. The same variation in the RZ values is also observed for DyPB. A lower RZ value (half) was obtained when the enzyme was expressed with pelB leader peptide in *E. coli* (Table 4). However, both DyPB samples with or without pelB leader peptide yielded lower RZ values in comparison to the *TfuDyP* samples. Although the heterologous expression of *SSHGDyP* yielded soluble proteins, the Soret scans showed no peaks for the existence of the heme B group (Figure 18 D). Thus, no RZ values could be calculated for the purified protein samples. This was already a sign that the enzymes were expressed in their inactive form. Following the structural analysis results, *in vitro* heme incorporation was attempted using hemin (no data shown), which was not successful. The calculated RZ values for *TfuDyP* and DyPB expressed in *E. coli* or *P. fluorescens* are comparable to those obtained for other fungal and bacterial DyP-type peroxidases (Kim & Shoda, 1999; Li et al., 2012).

The visible spectra analyses of Sclac indicated strongly that the laccases were expressed as apoproteins in *E. coli* and *P. fluorescens*. The addition of copper to the purified samples was necessary for the maturation and activation of the enzyme (Figure 19 A, B). The results suggest that incorporation of copper into the laccase structures can be complicated regardless from the heterologous expression host. A similar situation was observed for the recombinant EpoA that was only active when expressed in the presence of 10 μM CuSO_4 . Otherwise, the recombinant EpoA accumulated in an inactive monomeric form of the enzyme within the cells (Endo et al., 2003). However, the addition of copper ions to the expression medium is a critical issue since excess amount of copper shows toxic effect on the cell growth (Bird et al., 2013; Grey & Steck, 2001). Following the *in vitro* copper incorporation step, it was shown by the MTP assays (Figure 19 C, D) or zymography assays (Figure 20) that at least the T1-copper was incorporated into the protein structures and the recombinant laccases gained activity.

In the previous studies about the identification and characterization of *TfuDyP*, the enzyme was reported to show activity against Reactive Blue 19 (RB 19) between pH 3-4 with a maximum activity observed at pH 3.5 (van Bloois et al., 2010) and between pH 4.0-8.0 against 2,4-dichlorophenol (DCP) with a maximum activity observed around pH 5.0-5.5 (Rahmanpour et al., 2016). In this study, *TfuDyP* showed the highest activity at pH 4.0 using DMP as substrate. A shift in the optimal pH value towards different substrates was also observed with a DyP from *Irpex lacteus* (Salvachua et al., 2013). The fungal DyP showed maximum activity towards veratryl alcohol at pH 2.0, towards ABTS and DMP at pH 3.0 and towards RB 19 at pH 4.0. Although the reason for the pH shift remains unclear, it can be

Discussion

interpreted that phenolic or non-phenolic nature of the substrate together with the residues at the catalytic center on the distal face of heme cofactor play a major role in determining the optimal pH. The same is conceivable for the variations in the temperature optima using different substrates. The optimum temperature assays resulted in 25°C when *TfuDyP* was assayed with RB 19 (van Bloois et al., 2010), in a range of 45-60°C when the recombinant enzyme was assayed with DCP (Rahmanpour et al., 2016) and 60°C against DMP (this study). As typically observed for DyP-type peroxidases, DyPB showed the highest activity in the acidic pH region. The enzyme reached its maximum activity towards DMP at pH 4.5 and remained active until pH 6.5. (Ahmad et al., 2011) reported the optimal pH for DypB as pH 3.6 using ABTS as the substrate, however, the activity was retained at pH 5-6. Surprisingly, DyPB reached its maximum activity at 80°C and remained active when incubated at the temperatures up to 90°C. The recombinant ScLac showed a broad optimum pH and temperature profiles. ScLac showed its maximum activity at pH 5.5 and it retained its stability at neutral and basic pH values, in agreement with the reports of other bacterial laccases. This leads to the suggestion that ScLac also might be ideal for biotechnological applications where neutral or basic pH values are required over a longer period (Brander et al., 2014; Gunne & Urlacher, 2012b; Ruijssenaars & Hartmans, 2004). An activity at neutral or basic pH values is often observed for bacterial laccases and laccase-like enzymes but less frequently for the fungal laccases (Christopher et al., 2014). For example, *B. halodurans* Lbh1 showed maximum activity against SGZ at pH 7.5–8.0, *Streptomyces sviveus* Ssl1 showed maximum activity against phenolic substrates such as DMP and guaiacol at pH 9.0 and against SGZ at pH 8.0, and a halotolerant alkaline laccase from *Streptomyces psammoticus* showed maximum activity at pH 8.5 and retained 97% of its initial activity after 90 min at pH 9.0 (Gunne & Urlacher, 2012b; Niladevi et al., 2008; Ruijssenaars & Hartmans, 2004). High activities in alkaline solutions are ideal for industrial applications such as bio-bleaching of Kraft pulp during paper production, lignin modification or total biomass degradation (Pometto & Crawford, 1986; Ruijssenaars & Hartmans, 2004; Si et al., 2015). Laccases often remain active for a short time at high temperatures (Reiss et al. 2011; Zhang et al. 2013) but industrial applications usually require prolonged reactions. Although ScLac lost most of its activity following the incubation at 90°C, it showed promising stability profiles at 30°C and 60°C. A phenomenon known as heat activation, which has already been reported for a *Bacillus clausii* LMCO expressed in *E. coli* (Brander et al., 2014), was observed for ScLac after incubation at 30°C. Consistent with the previous reports of LigE and LigF, the recombinant β -etherases showed optimal pH values around pH 9.0 and pH 9.5 and optimal temperature values around 25°C (Picart et al., 2014). An incubation of the enzymes around 30°C-60°C caused almost total loss of the enzymatic activity suggesting that the enzymes are more convenient for the reactions carried at relatively mild conditions.

3.3 Activity analyses of the purified recombinant lignin-degrading enzymes

3.3.1 Activity assays with common lignin-model compounds

DMP and guaiacol are two of the well-known peroxidase substrates (van Bloois et al., 2010) and ABTS is a well-known synthetic mediator of laccases (Cabana et al., 2007a; Mishra & Bisaria, 2006). These three substrates are often used to test the activities of lignin-degrading peroxidases and laccases. The initial activity assays with the recombinant DyPs and the laccase were carried out using DMP to compare the specific activities. The values in Table 5 and Table 6 show that the leader peptides might affect the enzymatic activity. As observed for all three oxidoreductases, *TfuDyP*, *DyPB* and *ScLac*, the highest specific activities towards DMP were observed when the enzymes were targeted to the periplasm. The activity analyses of the recombinant enzymes on these three common substrates were further analyzed by kinetic measurements using *TfuDyp-cp* (expressed in *P. fluorescens*), *DyPB-pelB* (expressed in *E. coli*) and *ScLac-cp* (expressed in *E. coli*). The calculated kinetic parameters (Table 8, Table 9 and Table 10) resembled those reported previously (Chandra & Chowdhary, 2015; Ihssen et al., 2015; van Bloois et al., 2010). The highest k_{cat}/K_M values were obtained with ABTS for *TfuDyP* and *DyPB* consistent with the previous reports (Rahmanpour & Bugg, 2016; Roberts et al., 2011), whereas the lowest activity levels were observed with guaiacol. DyPs show highest oxidation activity towards anthraquinone dyes followed by typical peroxidase substrates and azo dyes such as ABTS (Kim & Shoda, 1999; Zubieta et al., 2007a). Although oxidation of guaiacol was reported previously for *TfuDyP* (van Bloois et al., 2010), the specific activity towards guaiacol was the lowest among all tested substrates. *ScLac* showed the highest k_{cat}/K_M with guaiacol, which is a natural mediator of the laccases and laccase-like phenol oxidases (Morozova et al., 2007). Many fungal and bacterial laccases are reported to present higher catalytic efficiencies for guaiacol rather than catechol, DMP or pyrogallol (Pardo & Camarero, 2015). In addition to the abovementioned substrates, *ScLac* was also tested against the non-phenolic substrate VA in the presence of two different mediator systems. *ScLac* showed oxidation activity towards the substrate in the presence of both mediator systems (Appendix Figure 49 -Figure 52). Veratraldehyde was obtained as the main product of the electron transfer route (Bourbonnais et al., 1998) provided by *ScLac*-ABTS LMS, however the conversion yield was not 100%. Although the quantification was not carried out for HPLC analyses, the area of the product peaks indicate higher product formation yields in the presence of ABTS as observed for many other bacterial laccases (Christopher et al., 2014).

Unlike for the lignin-degrading peroxidases and the laccases, there is no substrate that is commercially available for β -etherases. Therefore, the activity of *LigE* and *LigF* was tested merely against MUAV compound for specific activity determination and kinetic analyses. The expression of the β -etherases

with N-terminus His₆-tag yielded higher specific activities towards MUAV. Specific activities, which were significantly higher than the previously reported values (Picart et al., 2014), as well as the catalytic properties showed that LigF was more active on MUAV than LigE in accordance with the prior knowledge (Masai et al., 1991; Picart et al., 2014).

3.3.2 Activity assays with complex lignin-model compounds

Using simple model compounds that are commercially available gives an idea about the substrate preferences of the enzymes and its catalytic properties facilitating the comparison with the other reported enzymes. However, the activity assays with the aromatic phenolic or non-phenolic lignin-model compounds bears high significance because, unlike the commercial substrates, they reflect the structure and the properties of the natural lignin polymer partly. Four different aromatic phenolic and non-phenolic model compounds (Figure 26) were tested with the recombinant DyPs and the laccase. Among all the model compounds, significant activity levels were obtained merely with the phenolic SS β -O-4 OH model compound under certain conditions. A ketone product was obtained out of the reactions with *TfuDyP*, DyPB and SCLac (Table 13 and Table 14). However, SCLac showed significantly higher formation yields for the ketone product than the other enzymes. Furthermore, the conversion of the secondary alcohol moiety of the SS- β -O-4 OH to the corresponding the SS- β -O-4 ketone by SCLac was improved by saturating the reaction mix with O₂ prior to the incubation. A commercial laccase from *T. versicolor* was tested under the same conditions using equal amount of specific activities as the recombinant SCLac. The results show that the ketone formation yields of SCLac is comparable to the commercial laccase, therefore, promises high potential for further assays with lignocellulosic biomass. Most studies about biomass and lignin modification using laccases are of fungal origin. Many fungal enzymes were shown to oxidize or depolymerize lignin-model compounds, lignin polymers or lignocellulosic samples using different mediator systems (Camarero et al., 2005; Chandra & Chowdhary, 2015; Chen et al., 2012b; Gutierrez et al., 2012). However, there are only a few successful examples of bacterial laccases such as small laccases from *Streptomyces* sp. shown to produce acid precipitable lignin polymeric lignin from *Miscanthus x giganteus* lignocellulose (Majumdar et al., 2014). SCLAC from *S. coelicolor* was shown to degrade a similar dimeric phenolic β -O-4 model compound and oxidize a non-phenolic lignin-model compound (Majumdar et al., 2014) in the presence of different redox mediators. Although the redox mediators ABTS and HBT were used with SCLac on the non-phenolic SS β -O-4 model here, no oxidation or degradation product was obtained. However, this might be due to the requirement of a more comprehensive optimization work including more synthetic or natural laccase redox mediators.

The potential of *TfuDyP* and DyPB on the β -aryl ether lignin-model compound were known by previous reports (Ahmad et al., 2011; Rahmanpour et al., 2016). These two enzymes represent few of the most

comprehensively characterized bacterial DyP-type peroxidases. Their activity on the phenolic SS β -O-4 OH model compound increases the potential of the recombinant DyPs for future biomass valorization processes and makes the enzymes more attractive for industrial applications.

The ketone product which was obtained from the DyP and laccase reactions was purified and used in the activity assays of LigE and LigF. Initial assays indicated no cleavage of the dimeric ketone product. The results were unexpected because the activity of both LigE and LigF were shown on dimeric model compounds resulted in the cleavage of the model via nucleophilic attack by the tripeptide GSH on the carbon atom at the β position of substrates containing β -aryl ether linkages to produce guaiacol and a GSH-conjugated aromatic compound (Gall et al., 2014; Picart et al., 2014). The purified ketone was mixed with the rest of the unreacted phenolic SS β -O-4 OH model compound and this might have interfered with the β -etherase reactions.

3.3.3 Activity assays with Kraft lignin

The assays with commercial Kraft lignin resulted in an increase in the absorbance at 465 nm for *TfuDyP*, DyPB and ScLac. The control reactions carried out under the same conditions excluding the enzymes did not yield significant increase in the absorbance at the same wavelength. This indicates that the observed increase in the absorbance was due to reactions between the enzymes and the lignin sample. Kraft lignin is a commercial by-product of paper manufacturing and might be relatively rich in sulfonated groups. The results suggest that some parts of the substrate solution go through an oxidation process, however, it is not clear yet which groups of the polymer are attacked by the enzymes (Rahmanpour & Bugg, 2016). The reactions with increasing concentrations of Kraft lignin revealed Michaelis-Menten kinetic behavior for *TfuDyP*, DyPB and ScLac, which suggests that the enzymes might be able to bind certain parts of the polymeric lignin (Ahmad et al., 2011). As reported for DyPB previously, its activity towards Kraft lignin was improved in the presence of Mn^{2+} .

The oxidative enzymatic activities on Kraft lignin can be exploited for further functionalization of the commercial lignin by coupling water-soluble phenols (Lund & Ragauskas, 2001) or ester and ether derivatives (Kalliola et al., 2014). Functionalization of Kraft lignin can be directed in such a way to change the properties of the recalcitrant polymer for the benefit of the valorization protocols such as increased water solubility or even repolymerization of the lignin polymer. Nevertheless, the saturation kinetic behavior towards Kraft lignin is unusual for lignin-degrading enzymes regarding its recalcitrant structure rich in C-C linkages. Some argued that the kinetic behavior could be caused by a physical phenomenon rather than an enzymatic activity, however, no experimental evidence was shown.

3.4 Modification of the selected enzymes for enzymes for higher stability and/or activity

3.4.1 Immobilization of ScLac

The immobilization of ScLac was performed via two distinct methods: The immobilization on agarose beads and via cross-linked enzyme aggregates (CLEA). The recovery of the immobilized enzyme samples was determined as 71.5% (of initial activity) and 33% (bound protein) for CLEA procedure and immobilization on the agarose beads, respectively. The immobilized enzyme samples could be used at least five times in the sequential activity assays, if the samples were washed between the activity assays. Immobilization harbors not only the advantage of recycling but also a possible increase in stability and activity due to enhanced structural rigidity and decreased possibility of the dissociation-related inactivation (Guzik et al., 2014). Although the immobilized ScLac can be reused at least five times, neither the stability nor the activity of the immobilized enzyme improved compared to the free enzyme, which contrasts with previous studies of other laccases (Cabana et al., 2007b; Sinirlioglu et al., 2013). The pH optima of the immobilized enzymes differed from the free enzyme preparation most likely due to changes in the structural conformation of the enzyme or the microenvironment induced by the immobilization method or the matrix (Bussamara et al., 2012; Guzik et al., 2014; Kumar et al., 2014).

3.4.2 Protein engineering for improved H₂O₂ stability

Directed evolution mimics the natural evolution process in wet-lab in considerably shorter time and increases the chance of obtaining highly enhanced variants in comparison to the rational protein design (Turner, 2009). However, the directed evolution studies of lignin-degrading enzymes have been hampered by the lack of successful heterologous expression hosts, and efficient and rapid high-throughput methods (Garcia-Ruiz et al., 2014). *TfuDyP* represents one of the best-characterized bacterial DyP-type peroxidases. The potential of *TfuDyP* in oxidizing simple and complex lignin-model compounds and Kraft lignin has been shown and the three dimensional structure has been determined (Rahmanpour et al., 2016; van Bloois et al., 2010). In this study, *TfuDyP* was used for directed evolution to improve its stability and activity in the presence of higher H₂O₂ concentrations and to develop a high-throughput screening method that can be applied to other lignin-degrading oxidoreductases as well. The WT-*TfuDyP* gene was cloned in a surface display vector, which expresses the enzyme of interest on the cell surface by a covalent linkage. The surface display of *TfuDyP* provided the connection between phenotype and genotype throughout the screening and sorting experiments (Ostafe, 2013) and ruled out the requirement of the compartmentalization of the cells by encapsulation. In order to screen the mutant library of *TfuDyP*, a method that was previously developed for glucose oxidase was modified and applied successfully using the effective analytical cell

Discussion

biology technique based on FACS (Ostafe et al., 2014). The method used a fluorescent substrate to stain the cells via covalent binding. To distinguish the population with higher activity successfully a second staining technique was applied. A fluorescent secondary antibody, DyLight 647, was used for simultaneous detection of the enzyme expression while tyramide-fluorescein was used for monitoring the enzyme activity. Regarding the difference in the excitation and emission spectra of both dyes, the simultaneous usage did not result in the cross-talk between the channels.

Most of the DyPs are active in the presence of 1 mM H₂O₂ and beyond this concentration, the enzymes start losing their activity (Roberts et al., 2011; Shrestha et al., 2016). The screening of the *Tfu*DyP library resulted in four variants (Table 17) with higher activity towards ABTS than the WT-*Tfu*DyP after the pretreatment with 5 mM H₂O₂.

Among the mutations, the Arg315His exchange represents the most critical one. The Arg315 residue is on the distal face of the heme cofactor (Figure 42) and responsible for the stabilization of the compound I intermediate via hydrogen bonding (Hiner et al., 2002). This residue was previously exchanged by site-directed mutagenesis to Gln and the resulting mutant did not show any activity against ABTS in the presence of 1 mM H₂O₂ (Rahmanpour et al., 2016). As compared to Gln, His shows similar properties to Arg with a relatively less bulky side group. It can be concluded that the exchange to His did not disturb the cofactor-binding pocket and the hydrogen bonding and enhanced the stability instead. Moreover, this exchange resulted in a dramatic shift in the optimum pH value of the variant from acidic (5.0) to the basic (8.5) region. Activity at elevated pH values is not a known property for DyPs. So far, reported DyPs usually performed their best activity in the acidic pH range from 3.0 to 5.0 (Kim & Shoda, 1999; Shakeri et al., 2008). However, an optimal activity at basic pH can be advantageous for the applicability of the enzyme in alkali-based biomass pretreatment procedures (Xu et al., 2016). Pro154 and Val165 residues are located on the α -helix secondary structure (Figure 58). Ser274 and Gln357 do not correspond to any significant residues on the secondary structure, however, they are in the vicinity of the larger and smaller tunnels that provide access to the distal face of the heme cofactor and H₂O₂ (Rahmanpour et al., 2016). All three exchanges, Arg315His, Val165Ile and Ser274Cys, occur between the aminoacids within the same group of properties except the variant 2 with the double exchange Pro154Ser and Gln357Arg. Here, both residues are located on the protein surface (Figure 42), which might have affected the interaction between the enzyme and the environment in the reaction media. Interestingly, the double exchange resulted in a slight shift of optimum pH towards the acidic region and decreased the K_M value of the enzyme against guaiacol accompanied with a significant decrease in the heterologous expression yield (~5-fold).

4.0 Conclusions

Lignocellulosic material offers a vast amount of sources and possibilities for the production of sustainable chemicals, materials and value-added biofuels. It is more appropriate than most of other common biomass feedstocks used for biofuel production such as corn stover and sugarcane bagasse because it does not compete with the food supply. The cellulosic part of the lignocellulosic material is built by well-defined subunits and regular interlinking organized by β -1,4-glycosidic bonds. Unlike the cellulosic part, the lignin part of the lignocellulosic material is built by 3 different monomeric units linked by at least 7 types of bonding motifs. The complex structure of lignin requires complex conditions for complete degradation. The main drawback of biological lignin depolymerization originates from the variety in the subunits and linkages, which require wide range of reactions catalyzed by many different enzymes. The analysis of the enzymes on the complex lignin sub-structures and linkages require complicated technics and expertise as well. Regarding these difficulties arisen from the structure of lignin, the research in the field of biological lignin valorization developed relatively slow. First lignin-degrading organisms, thus lignin-degrading enzymes, were identified from white-rot fungi. Although, several bacteria were identified as lignin-degraders synchronously, the superior features of fungal enzymes such as high redox potential overshadowed the research in lignin-degrading bacteria and bacterial enzymes. The requirement of post-translational modifications, low expression yields and complicated fermentation procedures have emerged the bacterial lignin-degrading enzymes as valuable alternatives to the fungal enzymes in the last decade. Distinct functional parameters, facilities in the expression protocols and the availability of the heterologous expression hosts, helped in reaching higher amounts of bacterial lignin-degrading enzymes that resulted in characterization of the enzymes in more detail. Nevertheless, the potential of bacterial lignin-degrading enzymes on complex lignin-model compounds, polymeric lignin and lignocellulosic substrates is still limited to very few but promising examples from each class of enzymes. Nowadays, bacterial enzymes are still not included in most recent reviews about lignin-degrading enzymes, although certain classes are originally predominant in the bacteria. This clearly indicates the research in the field of lignin-degrading enzymes and biological lignin valorization should focus on the bacterial families as well to exploit the potential of the bacterial enzymes and to develop further optimization and protein engineering methods to increase their potential for degradation of recalcitrant lignin polymer.

To investigate the potential into more detail and to contribute to the field of the bacterial lignin-degrading, six bacterial enzymes were selected from DyP-type peroxidase, laccase and β -etherase families. 5 out of 6 selected enzymes were successfully expressed in *E. coli*, suggesting that despite its simplicity it still serves as an effective host system. The effects of the leader peptides for the

Conclusions

heterologous expression of the oxidoreductases or the position of the affinity tag for the β -etherases were also investigated in *E. coli*. The existence of the leader peptide affected the expression yields differently for each DyP and the laccase. The results showed that although the coding sequence of an enzymes consists of a leader peptide, the expression of the particular enzyme discarding the leader peptide might result in higher expression yields without losing the enzymatic activity or vice versa. The contradictions in the databases were revealed by the heterologous expression results for ScLac and SSHGDyP. Although the enzymes were reported as extracellular enzymes, SDS-PAGE and western blot analyses of the purified enzymes that were expressed without any additional leader peptide yielded merely one form of the enzymes. Therefore, it can be concluded that a comprehensive heterologous expression optimization should include both conditions, including and excluding the leader peptides. Locating the His₆-tag at the C-terminus of the β -etherases decreased the expression yields and affected the enzymatic activity reversely. On the contrary, locating the His₆-tag at the N-terminus resulted in higher expression yields and enzymatic activities for both of the β -etherases indicating that the position of the affinity tags might also be an important parameter for the successful heterologous expression of a lignin-degrading enzyme.

So far, *P. fluorescens* was not used as the heterologous expression host for lignin-degrading enzymes. In this thesis, 4 out of 6 selected enzymes were expressed successfully in *P. fluorescens*. The expression yields reached up to gram values showing that *P. fluorescens* can be a powerful alternative to *E. coli* for the expression of the bacterial lignin-degrading enzymes, particularly for β -etherases. This can certainly provide a great advantage over other expression hosts to avoid repeated expressions and purification cycles that can decrease the process costs substantially.

The recombinant enzymes expressed in *E. coli* or *P. fluorescens* were purified by one-step affinity chromatography successfully and characterized for functional and catalytic parameters. The structural characterization assays showed that both *E. coli* (in the presence of the precursor 5-ALA) and *P. fluorescens* (no precursor required) were able to synthesize the heme and incorporate it into the structure of the DyP-type peroxidases as the prosthetic group successfully. However, incorporation of the copper into ScLac structure failed in both of the expression hosts. Purified recombinant laccase expressed in both systems showed no activity without an *in vitro* T1-copper incorporation step, which was achieved by incubation of the recombinant enzyme solutions in the presence of copper. Functional parameter assays showed great differences of the optimal pH and temperature values among the classes of the enzymes. The results pointed out the bottleneck towards preparation of a single enzyme cocktail and suggested stepwise application of various enzyme cocktails for effective lignin depolymerization. Sets of enzyme cocktails can be prepared and the interaction and the potential synergism between the cocktail sets can be analyzed by Design of Experiments (DoE) software

Conclusions

approach. This approach reduces the number of the experiments required to optimize the cocktail contents and the conditions (Zhou et al., 2009).

The recombinant purified enzymes were tested with simple and complex lignin-model compounds and polymeric Kraft lignin. The assays with the simple lignin-model compounds such as DMP, ABTS or guaiacol yielded specific activities and kinetic parameters in the range of the previous similar reports. In addition to the abovementioned substrates, ScLac was also tested against the non-phenolic simple substrate veratryl alcohol in the presence of two common mediator systems ABTS and HBT. The recombinant laccase catalyzed the conversion of the non-phenolic substrate to the aldehyde product preferably in the presence of ABTS. All recombinant oxidoreductases showed oxidative activity towards phenolic SS β -O-4 OH lignin-model compound. However, ScLac showed the highest product formation percentage that was comparable to the activity of the commercial laccase from *Trametes versicolor*, proving the high potential of the bacterial laccases again. This is a very promising result, keeping in mind that the conversion of the complex model compounds can be very difficult especially with the individual enzymes. The same successful results were not observed with the non-phenolic complex lignin-model compounds suggesting that the redox potential of the bacterial oxidoreductases might be too low to oxidize the complex non-phenolic substrates or more optimization studies should be carried out. This issue can be overcome, for instance, by modifying the enzymatic structures via protein engineering approaches. In addition to the activity towards the phenolic model compound, the recombinant oxidoreductases showed oxidative activity and saturation kinetics behavior with the commercial Kraft lignin sample. The activity towards Kraft lignin is significant for functionalization of the polymeric lignin sample, which can further facilitate the modification of the polymer.

The cost of enzyme production is a major factor in the economics of enzyme-based biomass degradation processes and is dependent on the host cells and purification strategy (Klein-Marcuschamer et al., 2012). Such costs can be minimized if the enzyme is reused in multiple process cycles by means of immobilization. In this study, ScLac was immobilized using two distinct methods. The recovery and reusability of the enzyme were demonstrated successfully, suggesting that ScLac could be used for the development of cost-efficient biotechnological processes (Robinson, 2015). Two distinct immobilization methods were successfully applied to ScLac, which gives a chance to recycle the enzymes to decrease the expenses. Nevertheless, immobilized enzymes still need to be tested against more complex model compounds. Also the methods need to be applied to the rest of the enzymes in order to judge its overall applicability.

Protein engineering studies on lignin-degrading enzymes are focused mostly on variants originating from fungal sources. The majority of protein engineering studies on bacterial lignin-degrading enzymes consist of site-directed mutagenesis of certain residues to investigate the significant motives in the

Conclusions

enzyme structures such as heme-binding groups in order to reveal the active center of the enzymes or to figure out the residues that play a role in the conversion of the substrates. *TfuDyP* was chosen as the platform enzyme in our study as a proof of principle on which we can develop and fine tune the FACS based screening system. Once the screening system is developed it can be applied to other peroxidases as well. The directed evolution library of the DyP-type peroxidase, which contained approximately 10^5 variants, was created by combining ep-PCR and MEGAWHOP-PCR methods. A high-throughput screening method was developed to screen the mutant library via advanced FACS technique. This high-throughput screening method facilitates the screening procedure and increases the rate considerably in comparison to the common MTP assays. The cost related to material consumption is also decreased and the method can be applied to other bacterial or fungal DyP-type peroxidases and laccases or any lignin-degrading oxidoreductases. The screening of the mutant library of *TfuDyP* yielded four variants with five different mutations, which showed up to 2.3 times more activity in the presence of 5 mM H_2O_2 . The results give a hint for further development of the sequential mutant libraries of *TfuDyP*. The protein engineering study of *TfuDyP* contributes to the literature of lignin-degrading enzymes in two ways. First, the high-throughput screening method fills the gap in the field of time- and cost-efficient high-throughput screening assays. Second, the optimized method for creating directed evolution library together with the high-throughput screening method opens the door to further improve enzymatic activities and stabilities and to increase the potential of the bacterial enzymes for a better degradation of recalcitrant lignin part of the lignocellulosic biomass. In addition to all these, the approach of displaying the enzyme of interest on the cell surface of *S. cerevisiae* provides an alternative and robust immobilization system, which does not require protein purification and immobilization.

5.0 Outlook

The successful over-expression of the enzymes carried out in this study has given the possibility to test them on single and complex lignin-model compounds and polymeric Kraft lignin. As a future work, more assays could be carried out with other lignin-model compounds and polymeric lignin samples that possess different characteristics or isolated from different sources and vary in the type of linkages (Abdelaziz & Hultberg, 2017; Miles-Barrett et al., 2017; Rinaldi et al., 2016). These assays would reveal more about the potential of the recombinant enzymes for developing efficient lignin valorization methods. Despite the remarkable progress made with the fungal laccases (Maijala et al., 2012; Mattinen et al., 2011), those from bacteria have not received that much of attention yet. Sclac demonstrated a pronounced catalytic activity towards the phenolic SS β -O-4 OH lignin model compound and it should be tested on many more substrates to explore its potential further. The behavior of the recombinant laccase towards the non-phenolic lignin-model compounds should be analyzed in more detail by using different synthetic and natural mediator systems and the amount of the mediators used in the assays should be also optimized (Bourbonnais et al., 1998).

The biochemical and functional analyses of the recombinant lignin-degrading enzymes revealed the differences between the optimal conditions of the oxidoreductases and the β -etherases. Thus far, the enzymes were merely used in the individual activity assays towards simple and complex lignin-model compounds and polymeric Kraft lignin. Although promising results obtained from the assays carried out with single enzymes, the effective depolymerization of the lignin polymer requires a wide range of linkage catalysis that cannot be achieved by a single class of lignin-degrading enzymes (Chen et al., 2011). In recent years, the idea of using enzyme cocktails to reach escalated activity levels and wider spectrum of activity has attracted the attention and several strategies have been developed for both cellulosic and the lignin part of the biomass (Alvarez et al., 2016; Benoit et al., 2015; Mohanram et al., 2013). According to the information obtained from the functional parameter analyses, the recombinant enzymes can be grouped based on their optimal pH and temperature values and used together in the form of enzyme cocktails. Ideally, the enzyme cocktails can be prepared by mixing the DyP-type peroxidases and the laccase in one cocktail mixture and the β -etherases LigE and LigF in another cocktail mixture regarding their functional parameters. Sequential activity assays with those two enzyme cocktails might increase the activity on the substrates, as they might also widen the range of catalysis and provide complete depolymerization of dimeric or polymeric substrates. Furthermore, the content of the enzyme cocktails can be optimized via a Design of Experiments software approach, which would help to reduce the number of the experiments for the optimization assays. The approach would also assist in the analysis of the interaction and potential synergism between the lignin-

Outlook

degrading enzymes. This would provide a comprehensive optimization study in a relatively short time, which might not be possible using classical trial-and-error approaches in the wet laboratory.

Lignin is a complex polymer and degradation of this complex polymer requires high biological activities. High biological activities could be achieved by increasing the amount of the biological catalysts used in the assays. However, an important issue to pay attention is to use economically feasible production methods or to find a way to recycle and reuse the enzymes. The reuse of *ScLac* was demonstrated by two immobilization methods successfully, which was possible for at least 5 sequential activity assays. Those two immobilization techniques could be also applied to the DyP-type peroxidases and the β -etherases in order to further decrease the enzyme production costs. The activity of immobilized enzymes on the complex lignin-model compounds and polymeric lignin-model compounds should be also tested eventually.

The bottleneck of the protein engineering studies for lignin-degrading enzymes has always been the lack of efficient and rapid high-throughput screening methods. Most of the libraries have been screened by using conventional MTP assays, which are time-consuming, labor-intensive and expensive due to the high amounts of disposable material and substrates used in the screening. The ultra-high-throughput screening method, which was developed for *TfuDyP* in this thesis, should serve as an example for other oxidoreductases studied herein as well as in the literature. Directed evolution libraries could also be created for DyPB and *ScLac* in order to improve their catalytic properties or stabilities and the ultra-high-throughput method developed in this thesis could be applied to screen their libraries as well. The activity and stability of *TfuDyP* variants could be further improved by taking the obtained mutants from the first round of screening and performing a couple of iterative mutagenesis-screening cycles. The variants presented in this study that showed higher activity and stability were cloned in *E. coli* for higher-level expression followed by purification and functional and kinetic characterization. Although the kinetic parameters of the variants did not show dramatic changes in comparison to the WT-*TfuDyP*, a variant was characterized with a strong optimum pH shift to pH 8.5, which is not common for DyP-type peroxidases. However, this variant could be a valuable candidate for potential applications of the enzyme in alkali pretreatment methods and preparation of the enzyme cocktails with β -etherases with optimum pH levels in basic environment.

6.0 Experimental procedures

6.1 Materials

6.1.1 Chemicals and consumables

All chemicals were purchased from the following companies: Acro Organics (New Jersey, USA), Bio-Rad (Munich, Germany), Boehringer (Mannheim, Germany), Dianova (Hamburg, Germany), Duchefa (Haarlem, Netherlands), EMD Millipore (Darmstadt, Germany), Eurofins Genomics (Ebersberg, Germany), Fisher Scientific (Schwerte, Germany), GE Healthcare (Freiburg, Germany), Hybrid Catalysis (Eindhoven, The Netherlands), Invitek (Berlin, Germany), Lifetechnologies (Carlsbad, USA), Merck (Darmstadt, Germany), New England Biolabs (Frankfurt am Main, Germany), Pall Corporation (Port Washington, NY, USA), Promega (Madison, USA), Roche (Mannheim, Germany), Roth (Karlsruhe, Germany), Serva Electrophoresis (Heidelberg, Germany), Sigma-Aldrich (Munich, Germany), Stratagene (La Jolla, USA) and VWR International (Darmstadt, Germany).

Consumables were obtained from Bio-Rad (Munich, Germany), Biozym (Oldendorf, Germany), Eppendorf (Hamburg, Germany), Fisher Scientific (Schwerte, Germany), GE Healthcare (Freiburg, Germany), Greiner (Solingen, Germany), Hartenstein (Würzburg, Germany), Merck (Darmstadt, Germany), Millipore (Eschborn, Germany), NerbePlus (Winsen, Germany), Novodirect (Kehl/Rhein, Germany), PeqLab (Erlangen, Germany), Qiagen (Hilden, Germany), Roth (Karlsruhe, Germany), Sarstedt (Nümbrecht, Germany), Schott (Mainz, Germany) and VWR International (Darmstadt, Germany).

6.1.2 Primers

Primers were designed using Clone Manager 9 Professional and were ordered from Eurofins Genomics. The lyophilized primers were dissolved to 100 μ M in distilled water and were diluted to 10 μ M before they were used for PCR. All sequences are listed in the Appendix (8.1).

6.1.3 Plasmids

Plasmids were isolated from *E. coli* cells using the Pure Yield™ Plasmid Miniprep Kit for small amounts of DNA and the Pure Yield™ Midiprep Kit (Promega) for larger amounts. Plasmid integrity was verified by restriction digests and sequencing (6.2.1).

6.1.3.1 pET-22b(+) and pET-21d(+)

The expression vector pET-22b(+) was originally developed by (Studier & Moffatt, 1986). The commercial expression vector provides cloning of target genes under control of strong bacteriophage T7 transcription and translation signals, if required (Rosenberg et al., 1987; Rosenberg & Studier, 1987; Studier et al., 1990). The heterologous expression is induced by IPTG providing a source of T7 RNA polymerase in the host cell. The vector carries the coding sequence for the lactose-inducible lac operon

transcriptional repressor (LacI). Targeting of protein of interest to the periplasmic space can be achieved by a *pelB* leader sequence provided on the vector backbone. The vector also provides an optional C-terminal His₆-tag for protein purification. In the multiple cloning site, there are a number of restriction sites (*NcoI-XhoI*) present. The origin of replication (pBR322) ensures a medium copy number. *bla* gene provides resistance to ampicillin. Different from pET-22b(+), the pET-21d(+) vector carries an N-terminal T7-Tag sequence and an optional C-terminal His-Tag sequence. A plasmid map for each vector is provided in Appendix (Figure 43 and Figure 44).

6.1.3.2 pBB540, pBB541, pBB550 vectors expressing molecular chaperons

pBB540 (pSC101 origin) plasmid expresses chaperones *grpE* and *clpB* genes, pBB541 (p15A origin) plasmid expresses *groESL* gene and pBB550 (p15A origin) plasmid expresses *dnaK*, *dnaJ* and *groESL* genes under the control of the IPTG-regulated promoter PA1/*lacO*-1 or Plac (de Marco et al., 2007; de Marco et al., 2005b; Tomoyasu et al., 2001). pBB540 plasmid harbors *cat* gene that provides resistance to chloramphenicol. pBB541 and pBB550 plasmids contain *spect* gene for spectinomycin resistance.

6.1.3.3 pCTcon2

A version of pCTcon2 plasmid was developed by the group of Prof. K. Dane Wittrup (Koch Institute for Integrative Cancer Research, MIT) for yeast expression and includes CD20 sequence (183 bp) between *NheI* and *BamHI* restriction sites (Chao et al., 2006). The plasmid was kindly provided by Dr. Raluca Ostafe (Bio7, RWTH Aachen University). The expression plasmids provides an N-terminal AGA2 tag for surface display and a C-terminal c-myc tag for antibody staining. *Bla* gene on the vector backbone provides resistance to ampicillin. A plasmid map for the vector is provided in Appendix (Figure 45).

6.1.4 *Escherichia coli* strains

E. coli strain DH5 α was used for general cloning and the large-scale production of plasmids for DNA rub inoculation. This strain has the genotype *fhuA2 lac(del)U169 phoA glnV44 Φ 80' lacZ(del)M15 gyrA96 recA1 relA1 endA1 thi-1 hsdR17* (Hanahan, 1983).

E. coli BL21-CodonPlus(DE3)-RIL strain was used for the overexpression of certain constructs of lignin-degrading enzymes. This strain has the genotype *E. coli B F⁻ ompT hsdS(r_B⁻ m_B⁻) dcm⁺ Tet^r gal λ (DE3) endA Hte [argU ileY leuW Cam^r]* (Weiner et al., 1994).

E. coli BL21 Star (DE3) strain was used for the overexpression of certain constructs of lignin-degrading enzymes. This strain has the genotype *F⁻ ompT hsdS_B (r_B⁻, m_B⁻) gal dcmrne131 (DE3)* (Grunberg-Manago, 1999; Kido et al., 1996; Lopez et al., 1999).

E. coli Shuffle T7 express strain was used for the optimization studies *SSHGDyP* expression. The strain has the genotype *fhuA2 lacZ::T7 gene1 [lon] ompT ahpC gal λ att::pNEB3-r1-cDsbC (Spec^R, lacI^q) Δ trxB*

Experimental procedures

sulA11 R(mcr-73::miniTn10--Tet^S)2 [dcm] R(zgb-210::Tn10 --Tet^S) endA1 Δgor Δ(mcrC-mrr)114::IS10 (Bessette et al., 1999; Boyd et al., 2000; Chen et al., 1999; De Marco, 2009; Levy et al., 2001).

E. coli ArcticExpress (DE3) was used for the optimization studies SSHGDyP expression. The strain has the genotype *E. coli* B F⁻ *ompT hsdS*(r_B⁻ m_B⁻) *dcm*⁺ Tet^r *gal λ*(DE3) *endA Hte [cpn10 cpn60 Gent^r]* (Ferrer et al., 2003; Grodberg & Dunn, 1988; Jerpseth et al., 1997; Jerpseth et al., 1998; Schein, 1989).

One Shot[®] chemically competent *E. coli* Top 10 cells (Life Technologies) were used to transform and maintain directed evolution libraries. This strain has the genotype *mcrA, Δ(mrr-hsdRMS-mcrBC), Phi80lacZ(del)M15, ΔlacX74, deoR, recA1, araD139, Δ(ara-leu)7697, galU, galk, rpsL(SmR), endA1, nupG*.

XL10-Gold[®] Ultracompetent *E. coli* cells were used to transform and maintain directed evolution libraries. This strain has the genotype Tet^rΔ(*mcrA*)183 Δ(*mcrCB-hsdSMR-mrr*)173 *endA1 supE44 thi-1 recA1 gyrA96 relA1 lac Hte [F' proAB lacIqZΔM15 Tn10 (Tet^r) Amy Cam^r]*.

6.1.5 *Saccharomyces cerevisiae* EBY100 cells and yeast display system

EBY100 expresses the *AGA1* gene under control of the *GAL1* promoter. The strain was originally created by integrating the vector pIU211 into the *AGA1* locus of the *Saccharomyces cerevisiae* strain BJ5465 with the genotype MAT a *ura 3-52 trp 1 leu2Δ1 his3Δ200 pep4:HIS3 prb1Δ1. 6R can1 GAL* (Boder & Wittrup, 1997). pIU211 contains the *AGA1* gene regulated by the *GAL* promoter and a *URA3* selectable marker. The vector was linearized for integration *AGA1* using *BsWI*. *BsWI* cuts in the *AGA1* gene, ensuring that the construct integrates at the *AGA1* locus.

Together with the pCTcon2 plasmid, EBY100 cells construct the yeast display system. The system uses the *S. cerevisiae* α-agglutinin receptor to display heterologous proteins on the cell surface (Ostafe, 2013). The *AGA1* subunit of the system is expressed by EBY100 cells using the *GAL1* promoter (Lu et al., 1995) and *AGA2* subunit is encoded by the pCTcon2 vector as an N-terminal fusion to the protein of interest. The N-terminal region of *AGA2* binds to *AGA1* on the surface of the yeast cell by disulfide bond formation (Cappellaro et al., 1991). The c-myc tag expressed as a fusion to the C-terminal of the protein of interest can be used for immunodetection.

6.2 Methods

6.2.1 Vector construction

The constructs were prepared according to the standard guidelines provided by (Sambrook & Russell, 2001). The restriction enzymes used in the vector construction protocols were purchased from New England Biolabs (NEB). If the chosen restriction enzymes could not be used in the same buffer, DNA was cut sequentially and was purified between reactions using the Wizard® SV Gel and PCR Clean-Up System (Promega). Various DNA polymerases such as *Pfu* DNA polymerase (Promega), Phusion® High-Fidelity DNA Polymerase (NEB), Q5® High-Fidelity DNA Polymerase (NEB), Herculase II Fusion DNA Polymerase (Agilent Genomics) and *Pfu*Ultra II Fusion HS DNA Polymerase (Agilent Genomics) were used for PCR experiments and control PCRs were carried out using *GoTaq*® DNA polymerase (Promega). All vectors were dephosphorylated with calf intestinal phosphatase (CIP, NEB) after digestion and ligations were carried out using T4 DNA ligase (Promega) overnight at 16°C.

Some of the constructs were prepared according to the Gibson assembly protocol, which was developed by Dr. Daniel Gibson (J. Craig Venter Institute, USA) (Gibson et al., 2010; Gibson et al., 2009). The protocol was applied using the Gibson Assembly® Master Mix (NEB) and Q5® High-Fidelity DNA Polymerase (NEB) according to the protocol provided with the kit. The ligation or assembly products were transformed into *E. coli* DH5α cells and colonies were selected on LB plates supplemented with 100 µg/ml ampicillin for the residual vectors overnight at 37°C. Plasmids were isolated from overnight cultures and sequenced by Fraunhofer sequencing services (Fraunhofer IME Aachen). DNA was resolved by 1.2% (w/v) agarose gel electrophoresis in 1x TAE buffer (40 mM Tris base, 20 mM acetic acid, 1 mM EDTA). The GeneRuler™ 100 bp plus and 1-kb ladders from Fermentas (Thermo Fisher Scientific) were used as standards 8.4. Ethidium bromide was used for gel staining and DNA was visualized under UV light. Gel pictures were color inverted for higher contrast. DNA was isolated from agarose gels using the Wizard® SV Gel and PCR Clean-Up System (Promega).

Construction of pET-22b(+) vectors

TfuDyP constructs were amplified from the isolated genomic DNA of *Thermobifida fusca* YX. *TfuDyP* encoding nucleotide sequence (UniProt Q47KB1) was amplified using *Tfu1* and 2 primers for periplasmic localization via the native Tat leader peptide, and using *Tfu2* and 3 via *pelB* leader peptide. For the cytoplasmic expression, the coding sequence was amplified using *Tfu4-7* primers by Bachelor student Laura Grabowski. The amplified sequences were ligated into the pET-22b(+) vector via *NdeI-XhoI*, *HindIII-XhoI* and *NdeI-XhoI* sites *TfuDyP*-Tat, *TfuDyP*-*pelB* and *TfuDyP*-cp constructs, respectively. *DyPB* coding sequence (UniProt Q0SE24) was amplified using *DyPB1* and 2 primers for localization in the periplasmic space of *E. coli* and ligated into the pET-22b(+) vector via *EcoRI-XhoI*. The cytoplasmic

Experimental procedures

expression construct (DyPB-cp) was cloned by Gibson assembly between *NdeI* and *XhoI* sites using the primers DyPB3 and 4. *SSHGDyP* coding sequence (UniProt D6B600) was amplified using *SSHG1* and 2 primers to obtain the cytoplasmic expression construct (*SSHGDyP*-cp) in the pET-22b(+) vector (*NdeI*-*XhoI*). The construct for periplasmic localization was obtained by Gibson assembly using the primers *SSHG3* and 4 (*NcoI*-*XhoI*). *ScLac* coding sequence (UniProt F6L7B5) was amplified using *Sc1* and 2 primers and ligated into the pET-22b(+) vector between *NdeI*-*XhoI* sites for expression in the cytoplasm. To localize *ScLac* in the periplasm of *E. coli*, the coding sequence was amplified and ligated into the pET-22b(+) vector using the *Sc3-6* primers by Bachelor student Louisa Kauth (Institute for Molecular Biotechnology, RWTH Aachen University). The coding sequences of DyPB, *SSHGDyP* and *ScLac* were obtained from Genscript (USA) as codon-optimized synthetic genes. The coding sequences of *LigE* and *LigF* were kindly provided by Dr. Pere Picart (Institute of Biotechnology, RWTH Aachen University) and Prof. Dr. Annett Schallmey (Institute for Biochemistry, Biotechnology and Bioinformatic, Technical University of Braunschweig) in the artificial vector pMA-T between the restriction sites *HindIII* and *NdeI*. The coding sequences were cut using the abovementioned restriction sites and transferred into the pET-22b(+) vector between the same sites to obtain the constructs with C- terminus His₆-tag. The constructs with N-terminus His₆-tag were prepared by Gibson assembly introducing the His₆-tag sequence within the primers E1-2 and F1-2 primers (*NdeI*-*XhoI*). All the constructs were checked by applying colony PCR following ligation reactions or assembly protocol using the T7 pro and T7 ter primers for initial confirmation of the colonies with correct insert. Afterwards, final confirmations were carried out by sequence analysis using the same primer set (Sequencing services, Fraunhofer IME Aachen).

Construction of pD1 expression vector

The coding sequences for *TfuDyP* (UniProt Q47KB1), DyPB (UniProt Q0SE24), *SSHGDyP* (UniProt D6B600), *ScLac* (UniProt F6L7B5), *LigE* (UniProt P27457) and *LigF* (G2IN92) were codon optimized for expression in *P. fluorescens* and synthesized by “GeneArt (Thermo Fischer)” to contain *SpeI*/*XhoI* restriction sites at 5′ and 3′ regions. The synthetic genes were cloned into the *P. fluorescens* expression vector pD1 via given restriction sites. Due to legal restrictions, the construction of the pD1 expression vector was carried out by Dr. Stefan Rasche at Fraunhofer IME (Aachen).

Construction of pCTcon2 expression vector

TfuDyP, DyPB, *SSHGDyP* and *ScLac* coding sequences were amplified using the corresponding pET-22b(+) constructs as templates for the preparation of pCTcon2 constructs. The primers pCT1-8 were used in the PCR reactions and the inserts were ligated into the pCTcon2 vector via *NheI*-*SaII* sites. All the constructs were checked by applying colony PCR following ligation reactions or assembly protocol

Experimental procedures

using the pCT fw and pCT rev primers for initial confirmation of the colonies with correct insert. Afterwards, final confirmations were carried out by sequence analysis using the same primer set (Sequencing services, Fraunhofer IME Aachen).

6.2.2 Genomic DNA extraction from *Thermobifida fusca* XY

Glycerol stocks of *T. fusca* XY strain was kindly provided by Dr. Johannes Klinger (former affiliation Institute for Molecular Biotechnology, RWTH Aachen University) and the cells were cultivated as described by Leibniz Institute DSMZ. The genomic DNA was isolated using Wizard® SV Genomic DNA Purification System (Promega) according to the protocol provided with the kit. The isolated genomic DNA was resolved by 1.2% agarose gel electrophoresis in 1x TAE buffer.

6.2.3 Colony PCR

Colony-PCR is carried out to test recombinant colonies after transformation of ligation products into the electro- or chemically competent cells. The primer set used in the PCR can be insert-specific, backbone-specific or orientation-specific. In this study, backbone-specific primers were used for colony-PCRs and the protocol was applied as follows: The colonies were picked with a sterile toothpick, streaked on an LB agar plate (master plate) containing appropriate antibiotic and subsequently swirled into the PCR mix. The PCR products were resolved by 1.2% (w/v) agarose gel electrophoresis in 1x TAE buffer.

6.2.4 Transformation of competent *E. coli* cells

pUC19 plasmid (NEB) was used as a positive control to assess the efficiency of the transformations. Long-term cryocultures of transformed cells were prepared by adding 20% (v/v) glycerol and were stored at -80°C .

Heat shock

The chemically competent cells were thawed on ice for at least 15 minutes. When the cells were completely thawed, 1-5 μL of the ligation/assembly product or isolated plasmid sample (10 μg –100 ng) was added to the cells and the mixtures were incubated on ice for 30 minutes. The heat shock was applied on a 42°C heat block for 30 seconds and transferred to ice for another 2 minutes. Subsequently 250 μL SOC medium was added and the cells were incubated for 1 hour at 37°C on an orbital shaker (250 rpm). 50 μL –300 μL of the transformation mixture were plated onto pre-warmed LB agar plates containing appropriate antibiotic for selection and incubated at 37°C overnight.

Electroporation

Self-prepared electrocompetent cells were thawed on ice for at least 15 minutes. Once the cells were thawed completely, the ligation/assembly product was added and the cells were transferred to a pre-chilled electroporation cuvette. The electroporation was carried out at 2500 V for 5 ms and 900 μ L pre-warmed SOC medium was immediately added to the cell-DNA mixture in the cuvettes. The cell mixtures were transferred into 2 mL-Eppendorf tubes for incubation at 37 °C on an orbital shaker (250 rpm). Following 1 hour incubation, the cells were harvested by centrifugation (6000 rpm, 1 min, RT) and resuspended in 300 μ L SOC medium. The entire volume was plated on pre-warmed LB agar plates containing appropriate antibiotic for selection and incubated overnight at 37 °C.

6.2.5 Preparation and transformation of competent *S. cerevisiae* EBY100 cells

Preparation of competent EBY100 cells and transformation of the competent cells with pCTcon2 plasmid was carried according to the protocol described by (Gietz & Schiestl, 2007) by heat shock at 42°C. After transformation, the cells were grown directly in YNB-CAA glucose medium for 48 h at 30°C, 160 rpm. For short term storage cells were kept on YNB-CAA agar plates containing glucose and for long term storage, cell stocks were prepared with 20 % (v/v) glycerol and stored at -80°C.

6.2.6 Cultivation of *E. coli* and *P. fluorescens* cells for protein expression

Transformed *E. coli* cells were incubated overnight at 37°C shaking at 180 rpm in 50 mL lysogeny broth (LB) containing 100 μ g mL⁻¹ ampicillin and/or 50 μ g mL⁻¹ chloramphenicol as pre-cultures. The overnight cultures were then used to inoculate 500 mL terrific broth (TB) supplemented with the same antibiotics, and the cultures were incubated as described above until the optical density (OD₆₀₀) reached 0.6. Recombinant gene expression was then induced by adding 0.04 or 0.5 mM IPTG depending on the strain. Furthermore, 10 mM benzyl alcohol was added to the cultures 20 min before the IPTG to induce the expression of native chaperones (de Marco et al., 2005a). The cultures were incubated under the optimal conditions determined by optimization experiments (at 20°C for 20 h at 180 rpm or at 30 °C for 16 h at 180 rp).

Transformed *P. fluorescens* cells were cultivated in 1000 mL scale in a defined High-Throughput medium (HTP-medium; Teknova, USA). After 24 h incubation at 30°C and 250 rpm, protein expression was induced by the addition of IPTG (0.3 mM) and incubated for an additional 24 h incubation at 30°C and 250 rpm. Due to the use restrictions, the construction of the pD1 expression vector was carried out by Dr. Stefan Rasche at Fraunhofer IME (Aachen).

6.2.7 Cultivation of *S. cerevisiae* EBY100 cells

EBY100 cells were inoculated from YNB-CAA agar plates containing 2% (w/v) glucose and 50 $\mu\text{g mL}^{-1}$ chloramphenicol into liquid YNB-CAA medium containing 2% (w/v) glucose and 50 $\mu\text{g mL}^{-1}$ chloramphenicol. The cells were grown for 24 h at 30°C, 160 rpm. To induce protein expression, the cells were transferred to YNB-CAA media containing 2% (w/v) galactose and 50 $\mu\text{g mL}^{-1}$ chloramphenicol to OD₆₀₀ 1.0 and grown at 30°C, 160 rpm, for 16 h and then used for FACS experiments.

6.2.8 Protein extraction from *E. coli* and *P. fluorescens* cells

E. coli cells were harvested by centrifugation (5000 x g, 15 min, 4°C). The cell pellet was re-suspended in 20 mM potassium phosphate buffer (pH 7.4) containing 20 mM imidazole and 300 mM NaCl. Cells were disrupted by sonication in the presence of 0.5 mM phenylmethylsulfonyl fluoride, 1 mg mL⁻¹ lysozyme and 10 $\mu\text{g mL}^{-1}$ DNaseI. The cell suspension was centrifuged (30 000 x g, 30 min, 4°C), the supernatant was separated from the cell debris and filtrated with 0.45 μm filter prior to the IMAC.

P. fluorescens cells were harvested by centrifugation (11,000 x g, 20 min) after additional 24 h incubation at 30°C and 250 rpm. The supernatant was discarded and the remaining cell pellet was extracted by adding “BugBuster MasterMix” (Merck-Millipore) in phosphate-buffered saline (PBS, pH 7.4). Following protein extraction, the remaining cell debris was removed by centrifugation (16,000 x g, 10 min, 4°C).

6.2.9 IMAC purification of recombinant lignin-degrading enzymes

Proteins expressed in *E. coli* were purified via IMAC using 5 mL “HiTrap Chelating Sepharose FF” (GEHealthcare). The cell extracts were applied onto the column with 3 mL min⁻¹ velocity using potassium phosphate buffer (pH 7.4) containing 20 mM imidazole and 300 mM NaCl as the running and the washing buffer. Bound proteins were eluted in an increasing imidazole gradient from 0 mM to 500 mM over 50 mL total volume. The elutions were collected in 2 mL fractions and checked by SDS-PAGE and western blot analysis. All fractions containing the target protein were pooled and dialyzed against 100 mM HEPES (pH 7.5) overnight at 4°C. During the dialysis step, dialysis buffer was changed once.

Proteins expressed in *P. fluorescens* were purified via IMAC using 1 mL “HiTrap Chelating Sepharose FF” (GEHealthcare). The cell extracts were applied onto the column with 1 mL min⁻¹ velocity and PBS (pH 7.4) was used as the running and the washing buffer. Bound proteins were eluted in an increasing imidazole gradient between 0 mM and 250 mM over 30 mL total volume. The elutions were collected in 1 mL fractions and checked by SDS-PAGE and western blot analysis. All fractions containing the target protein were pooled and the buffer was exchanged with PBS (pH 7.4) by using PD-10 desalting

Experimental procedures

columns (GE-Healthcare). After the final desalting step the protein concentration was determined densitometrically using a well characterized and quantified protein standard. The purified and quantified proteins were stored at 4°C.

6.2.10 Sodium dodecyl sulfate polyacrylamide gel electrophoresis (SDS-PAGE)

Protein samples obtained in test expressions and IMAC purifications were resolved by SDS-PAGE (Laemmli, 1970). The samples were mixed with 5x reducing buffer (62.5 mM Tris-HCl pH 6.8, 30% (v/v) glycerol, 4% (w/v) SDS, 10% (v/v) 2-mercaptoethanol, 0.05% (w/v) bromophenol blue) and boiling for 5–10 min. Samples were separated on 12% polyacrylamide-SDS gels (stacking gel T = 4%, C = 2.7%, pH 6.8; resolving gel T = 12%, C = 2.7%, pH 8.8). The ColorPlus Prestained Protein Ladder Broad Range (P7711S, NEB) was used as a protein standard (Figure 46). The gel was run at 100 V until the samples reached the resolving gel and then at 200 V for approximately 40 minutes. 1x SDS buffer (25 mM Tris, 2 M glycine, 1 % (w/v) SDS) was used as running buffer. The resolved samples were analyzed by staining the gel with Coomassie Brilliant Blue staining solution (0.25 % (v/v) Coomassie Brilliant blue G-250, 50 % (v/v) methanol, 10 % (v/v) acetic acid) for 15 minutes shaking. Destaining step was repeated until clear bands are observed in destaining solution (5 % (v/v) methanol, 7.5 % (v/v) acetic acid).

6.2.11 Western blot

All constructs were designed to carry a His₆-tag either on the C- or on the N-terminus of the proteins of interest. For the specific detection of the proteins, the polyacrylamide gels were blotted onto a nitrocellulose membrane (HybondC, Amersham) and blocked for 1 h with 5% (w/v) skimmed milk in PBS. They were incubated with the primary and secondary antibodies and the signal was visualized with nitroblue tetrazolium chloride/5-bromo-4-chloro-3-indolylphosphate p-toluidine salt (NBT/BCIP) (Roth). The western blot was carried out semi-dry using Turbo TransBlot system (Bio-Rad, 25 V and 1 A for 30 minutes). Anti 6x his epitope tag (rabbit, Rockland) was used as the first antibody and Goat Anti Rabbit (GAR^{AP}, Dianova) was used as the second antibody.

6.2.12 Zymography assays

For zymography analysis, a native protein gel electrophoresis was performed using 4-12% Native-PAGE Tris-Glycine gels. 25 µg of protein sample was mixed with 5x non-reducing buffer and loaded on the non-denaturing gels. SDS-PAGE was carried out as described above (6.2.10). For each substrate, a separate gel was run. The gels were soaked in 10 mM ABTS (Sigma) or L-3,4-dihydroxyphenylalanine (L-DOPA; Sigma) or caffeic acid (Sigma) solutions prepared in 100 mM 2-(N-morpholino) ethanesulfonic acid (MES; Sigma) buffer (pH 5.5) and incubated at 37°C for 5 min. Reactions were stopped by the addition of 1:1 ethanol-water mixture (Ramachandra et al., 1987; Thomas et al., 1998).

6.2.13 Determination of protein concentration

For IMAC purified lignin-degrading enzyme samples, protein concentration was determined by the Edelhoch method (Edelhoch, 1967). However, the protein concentrations for immobilization studies of Sclac were determined by bicinchoninic acid assay (Pierce™ BCA Protein Assay Kit, Thermo Fisher Scientific) according to the protocol provided by the manufacturer.

6.2.14 UV-Vis Spectra for Soret band and T1-copper detection

The ultraviolet-visible (UV-Vis) spectra of 1 μM of purified *TfuDyP*-Pf preparation was recorded using Tecan Microplate Reader between the wavelengths of 300 and 800 nm. RZ value (A_{403}/A_{280}) of enzyme sample was calculated as described elsewhere (Hofbauer et al., 2015).

The ultraviolet-visible (UV-Vis) spectra of Sclac were recorded using 1 μM of IMAC-purified Sclac before and after the incubation with 0.1 mM CuSO_4 by Tecan Microplate Reader between 230 nm and 700 nm (Shleev et al., 2004). The activity assays before and after the incubation with CuSO_4 was performed against DMP.

6.2.15 Activity assays using simple lignin-model compounds

Enzymatic activity of purified recombinant enzymes were initially determined against simple lignin-model compounds by microtiter plate (MTP) assays. For the activity analysis of DyP-type peroxidases and laccase, ABTS, DMP and guaiacol was used as substrates. For β -etherases, MUAV was used as the substrate. Activity assays were carried out in the optimal buffer system of each enzyme and the reactions were followed by a plate reader (Infinite® 200 plate reader, Tecan). The oxidation of the following substrates was tested at the given wavelengths: guaiacol (Sigma) at 465 nm ($\epsilon=26.6 \text{ mM}^{-1} \text{ cm}^{-1}$) (Sakamoto et al., 2012; Singh et al., 2009), 2,6-dimethoxyphenol (DMP; Sigma) at 469 nm ($\epsilon=49.6 \text{ mM}^{-1} \text{ cm}^{-1}$) (Pandey, 2006; Yoshida et al., 2012) and ABTS (Sigma) ($\epsilon= 36 \text{ mM}^{-1} \text{ cm}^{-1}$) at 420 nm (Galai et al., 2012; Salvachua et al., 2013). For DyP-type peroxidases, the reaction mixtures were prepared in the presence of 0.2 mM H_2O_2 .

The β -etherase activity of LigE and LigF towards MUAV was measured fluorometrically in a plate reader (Infinite® 200 plate reader, Tecan) using an excitation wavelength of 360 nm and an emission wavelength of 450 nm (Masai et al., 1989; Picart et al., 2014). Reaction mixtures were prepared with 1 mM GSH (reduced) in the optimal buffer system of each enzyme. Formation of 4-methylumbelliferone (4MU) was monitored continuously over 15-30 min. The calibration of 4-MU formation was carried out with commercial 4-MU (Sigma) as the standard. The standard curve is provided in Appendix (Figure 47).

Control reactions for the activity assays were prepared under the same conditions with combinations of related purified enzyme and buffer, related substrate (and H_2O_2 or GSH) and buffer or buffer only. All activity assays were performed in triplicates. A significant increase in the absorbance was observed

merely in the presence of all of the components; the enzyme, the substrate (and H₂O₂ or GSH) and the buffer. Specific activity was expressed as units per milligram of protein.

6.2.16 Synthesis of MUAV compound

The fluorogenic substrate MUAV was synthesized in collaboration with Cristoph R. Müller and Mareike M. A. Honickel (ITMC, RWTH Aachen University) according to the protocol reported by (Weinstein & Gold, 1979).

6.2.17 Determination of enzyme kinetics

Kinetic parameters K_M , V_{max} and k_{cat} of purified DyP-type peroxidases and laccase were analyzed by measuring the activities towards ABTS, DMP and guaiacol with the concentrations ranging from 0.5 μ M to 1000 μ M. Kinetic parameters of purified β -etherases were analyzed by measuring the activity towards MUAV with the concentrations ranging from 1 μ M to 100 μ M. The measurement results were analysed and the kinetic constants were calculated using GraphPad Prism 6 software (Statcon, Germany).

6.2.18 Activity assays using complex lignin-model compounds

In the model compound assays, 20 mg phenolic SS- β -O-4 model (SS β -O-4 OH synthesised as reported by Lancefield et al. (Lancefield et al., 2015) and kindly provided by Dr. Christopher S. Lancefield (Chemistry, Debye Institute for Nanomaterials Science, Inorganic Chemistry and Catalysis, Utrecht University (current address)) was used with the released purified enzyme (with or without 500 μ M H₂O₂). The model compound was dissolved in 600 μ L of 100 % DMSO prior to the addition in the reaction mix. The reaction mix was incubated at 30 °C for 3 hours under constant rotation. After that time, it was extracted three times with ethyl acetate. The organic extracts were then combined, dried over MgSO₄, filtered and concentrated *in vacuo*. The residue was analysed by NMR spectroscopy.

Nuclear magnetic resonance (NMR, School of Chemistry, University of St Andrews and Inorganic Chemistry and Catalysis, Utrecht University) spectra were recorded at room temperature on Bruker Avance 500 (¹H 500 MHz, ¹³C 126 MHz) and Bruker Avance 400 (¹H 400 MHz, ¹³C 101 MHz) instruments. Deuterated solvents were used and ¹H NMR shifts were internally referenced to CDCl₃ (7.26 ppm) in d-chloroform. Data processing was performed using TopSpin and MestReNova 9.0 NMR software (Mestrelab Research S.L.). Quantification experiments were performed by adding 2-nitrophenol as internal standard following extraction of the reaction mixture.

6.2.19 Activity assays of ScLac towards veratryl alcohol

1 μ M ScLac expressed *E. coli* or *P. fluorescens* were tested towards 5 mM VA in the presence of 20 mM of a mediator system. As the mediator system both ABTS and HBT were used in the assays. The reaction mixtures were prepared in 100 mM MES (pH 5.5) buffer system and mixed by a rotator at 30°C for 16

Experimental procedures

h. After stopping the incubations, the reaction mixtures were extracted with ethyl acetate 3 times and the extraction products were analyzed by HPLC. The measurements were conducted on an Agilent Infinity 1260 HPLC apparatus using an Agilent Eclipse XDB-C18 (4.6 mm ID x 150 mm, 5 μ m) column with a H₂O/MeOH eluent and a flow rate of 1 mL min⁻¹. Reference solutions were prepared with the possible products of ScLac with VA, veratraldehyde and veratric acid, and analyzed under the same conditions as the enzymatic and the control reactions. The retention times of the peaks were compared with the reference peaks.

6.2.20 Activity assays using Kraft lignin

Oxidation of alkali Kraft lignin (Sigma) were analyzed spectrophotometrically with a plate reader (Infinite® 200 plate reader, Tecan) in the optimal buffer system of each enzyme. The reaction mixtures for DyP-type peroxidases were prepared in the presence of 1 mM H₂O₂. The initial reactions of DyP-type peroxidases were carried out both without MnCl₂ and with 1 mM MnCl₂ to check if MnCl₂ enhances the reaction rate. The reactions were followed spectrophotometrically at 465 nm (Ahmad et al., 2011; Rahmanpour & Bugg, 2016). The kinetic parameters K_M and V_{max} were analyzed as described above (6.2.17) with a concentration range of the substrate 2-50 μ M for *TfuDyP* and DyPB and 2-35 μ M for ScLac.

6.2.21 Characterization of the enzymes

The optimal reaction conditions of purified enzymes were analyzed by using one of the simple lignin-model compound. For DyP-type peroxidases and laccase, DMP was used as the substrate. Activity assays were carried out as described in section (6.2.15) using appropriate amounts of purified enzyme samples (0.1-1 μ M). pH profiles were determined by measuring the activity in a set of buffers with pH values ranging from 3.5 to 10.0. For the pH range from 3.5 to 5.0, 100 mM sodium acetate buffer; from pH 5.5 to 7.5, 100 mM 3-(N-morpholino) propanesulfonic acid buffer (MOPS); from pH 8.0 to 8.5, 100 mM 2-Amino-2-hydroxymethyl-propane-1,3-diol hydrochloric acid buffer (Tris-HCl) and from pH 9.0 to 10.0, 100 mM Glycine sodium hydroxide buffer was used.

To analyze the temperature profiles, appropriate amounts of purified enzyme samples (0.1-1 μ M) were incubated with related substrate in the optimal buffer system at various temperatures ranging from 25°C to 90°C for 5 min. The resulting absorbance or fluorescence values were measured as described above (6.2.15).

For short time (5 min) temperature dependent enzyme stabilities, appropriate amounts of purified enzyme samples (0.1-1 μ M) were incubated in the optimal buffer system at 30°C, 40°C, 50°C, 60°C, 70°C, 80°C and 90°C. Subsequent to the heat treatment, the samples were cooled down and the residual activities were assayed as described above (6.2.15). For long time (1 h) temperature

Experimental procedures

dependent enzyme stabilities, appropriate amounts of purified enzyme samples (0.1-1 μM) were incubated in the optimal buffer system at 30°C, 60°C, and 90°C. The residual activities were determined as described for the short time stability assay. pH stability assays were carried out the same way as described temperature dependent stability assays by incubating the enzymes in the optimal buffer system at approximately 25°C for 1 h, 6 h and 24 h and assaying the residual activities afterwards.

Organic solvent stability assays were carried out by assaying the activities of appropriate amounts of purified enzyme samples (0.1-1 μM) in the presence of 1%, 5%, 10%, 20%, 50% and approximately 67% (max) (v/v) ethanol, methanol and DMSO. The diagrams for the characterization assays were generated based on the relative activities, which were calculated by assigning the highest value of the data set as 100%.

6.2.22 Immobilization of ScLac

A sample of IMAC-purified ScLac was immobilized via two distinct methods. In the first method, cross-linked enzyme aggregates (CLEAs) were formed and in the second one, AminoLink™ Plus Coupling Resin (Thermo Fisher Scientific) was used as carrier material benefiting from Schiff base reaction between the primary amines of the protein and the aldehyde groups of the resin.

In order to obtain CLEAs, 2.5 mL of 1 g mL⁻¹ polyethylene glycol (PEG) 4000 solution was added dropwise to 5 mg of purified ScLac sample. The mixture was constantly mixed on an orbital shaker while adding the PEG solution (on ice) and afterwards incubated at 20°C for 2 h, 200 rpm. Following the incubation in the presence of PEG 4000, 5 mM glutaraldehyde was added and the sample was incubated overnight under the same conditions. On the next day, the sample was centrifuged to collect the CLEAs (5000x g, 10 min, 4°C). The supernatant was removed and an activity assay with DMP was performed to check for free laccase in the washing fraction. The washing steps were repeated until no activity was detected in the washing buffer and in the final step CLEAs were re-suspended in 1 mL of 0.1 M MES buffer (pH 5.5). Activity recovery after CLEAs protocol was calculated via dividing the activity (U) expressed by CLEAs by the activity of free enzyme (U L⁻¹) multiplied with the volume of the free enzyme used for the immobilization and then the resulting value was multiplied with 100 (Eq. 1) (Lopez-Gallego et al., 2005).

$$\text{Activity recovery (\%)} = \frac{A_{\text{CLEA}}}{A_{\text{free}} \times V_{\text{free}}} \times 100$$

Equation 1. Calculation of the activity recovery (%) of prepared CLEAs. A_{CLEAs} : activity (U) of prepared CLEAs; A_{Free} : activity (U mL⁻¹) of free enzyme; V_{Free} : volume (mL) of free enzyme used to prepare CLEAs.

For immobilization on AminoLink™ Plus Coupling Resin (Thermo Fischer), approximately 5 mg of purified ScLac-Ec was used with the resin consisting of agarose beads (10-50 μm) which are functionalized with aldehyde groups. The beads were provided as a 50% slurry in 0.02% (w/v) sodium

Experimental procedures

azide buffer. The immobilization protocol was performed in 10 mL gravity-flow columns from Bio-Rad and throughout the protocol the beads were never ran dry. 500 μ L of the bead slurry was pipetted into a 10 mL gravity-flow column. After the beads settled, the storage solution was drained and the beads were equilibrated with 6 mL of Coupling buffer (0.1 M sodium phosphate, 0.15 M NaCl, pH 7.2). Following the equilibration 4.5 mL of the protein sample (1.11 mg mL⁻¹) was added to the beads and the slurry was mixed for 3-4 hours at 4°C. Afterwards the samples were drained and the beads were equilibrated with 3 mL of pH 7.2 Coupling buffer. Then 1 mL of a 0.1 M sodium cyanoborohydride solution in Coupling buffer was added to the beads and the slurry was mixed overnight at 4°C. The reaction buffer was drained and the beads were equilibrated with 2 mL Quenching buffer (1 M Tris-HCl, pH 7.4). Following the equilibration, 1 mL of a 0.1 M sodium cyanoborohydride solution in Quenching buffer was added to the beads and the slurry was mixed further for 90 min. To finish the immobilization, the beads were washed with 6 mL washing buffer and stored in 500 μ L immobilization storage buffer.

The protein concentration on the beads was calculated by subtracting the mass of protein after the first reaction step and mass of the protein lost at washing steps from the initial mass of protein and dividing this by the resulting volume of bead slurry after the immobilization. Protein concentrations for immobilization experiments were determined by bicinchoninic acid assay (Pierce™ BCA Protein Assay Kit, Thermo Fisher Scientific) according to the protocol provided by the manufacturer. All samples and standards were measured either in duplicates or triplicates.

The reusability capacities of immobilized laccases were assessed in sequential activity assays against DMP which were repeated five times. Immediately prior to the reusability assay, the enzyme samples were mixed vigorously. Subsequent to each activity assay, beads and CLEAs were collected either by gravity or centrifugation (15000x g, 5 min, 4°C), washed thrice and used in the following activity assays. Temperature stability and pH optima profiles were obtained as described previously. The diagrams for the characterization of the immobilized ScLac were generated based on the relative activities which were calculated by assigning the highest value of the data set of each immobilization method as 100% (except for the reusability assay). For the reusability assay, first measurement result of each data set was taken as 100%.

6.2.23 Creation of *TfuDyP* Libraries

The directed evolution library of *TfuDyP* was created by error-prone PCR technique, which was carried out by GeneMorph II Random Mutagenesis Kit (Agilent Technologies). The kit comprises Mutazyme II DNA polymerase, a blend of two error prone DNA polymerases Mutazyme I DNA polymerase and a novel *Taq* DNA polymerase mutant that exhibits increased misinsertion and misextension frequencies compared to wild type *Taq*, providing mutation rates of 1–16 mutations per kb. A set of primers

Experimental procedures

(Eurofins MWG Operon) was design for random mutagenesis and *TfuDyP* sequence was amplified according to the manufacturer's instructions using the *TfuDyP* sequence cloned in pCTcon2. Amplified DNA was resolved on agarose gel and isolated using Wizard® SV Gel and PCR Clean-Up System (Promega). This product was used as a megaprimer for whole plasmid amplification (MEGAWHOP) in a following PCR step (Miyazaki & Takenouchi, 2002). Three different megaprimer/template ratio (250 ng/150 ng, 500 ng/300 ng, 250 ng/300 ng) was used to optimize MEGA-WHOHAP PCR with Q5® High-Fidelity DNA Polymerase (NEB). The cycling conditions were 98°C for 1 min, 1 cycle; 98°C for 10 sec/61°C for 30 sec/72°C for 4 min, 30 cycles; 72°C for 5 min, 1 cycle, after which the products were digested with DpnI for 1.5 h at 37°C and stored at 4°C until required. MEGAWHOP PCR products were transformed into *E. coli* XL10 Gold cells according to the manufacturer's protocol and the transformants were plated on LB Amp agar plates and grown at 37°C ON. 5 colonies were picked and inoculated in LB medium and plasmid DNA was isolated using the Pure Yield™ Midiprep Kit (Promega). Isolated DNA was analyzed by sequencing for mutation frequency. The rest of the colonies from the XL10 Gold plate were collected in liquid LB Amp media and re-grown for another 16 h at 37°C, 160 rpm. The DNA was then isolated the Pure Yield™ Midiprep Kit (Promega) and transformed into the competent *S. cerevisiae* EBY100 cell yielding the final directed evolution library of *TfuDyP*.

6.2.24 High-throughput screening of *TfuDyP* libraries

Tyramide fluorescein assay for FACS

EBY 100 cells expressing *TfuDyP* were harvested and washed three times with 100 mM sodium acetate buffer pH 4.5. Just before starting the activity assays, the diluted cells were washed for the last time with 0.1% (w/v) BSA in 100 mM sodium acetate buffer pH 4.5. 200 µL cell suspension containing 2×10^6 cells mixed with 1 mM H₂O₂ and 0.02 mM tyramide-fluorescein and incubated at RT for 1 min. The reaction was stopped by adding 0.5% (w/v) BSA with 10 mM ascorbic acid in 10X PBS and the cells were washed with 0.1% (w/v) BSA in 1X PBS 3 times. After washing the cells were resuspended in 200 µL 0.1% (w/v) BSA in 1X PBS. Half of the mixture was used for further antibody staining. 30 µg mL⁻¹ of mouse anti c-myc antibody (Abcam) was added to the cell suspension and incubated at 30°C for 30 min under constant shaking. The cells were washed again three times with 0.1% (w/v) BSA in PBS and resuspended in 100 µL of the same solution. The secondary anti-mouse IgG antibody was added and the mixture was incubated at 30°C for 30 min. The secondary antibody was either goat anti-mouse Fc IgG Dylight 650 (Abcam) (1:50 dilution) or Alexa Fluor 647 dye (Thermo Fisher) (1:50 dilution). Before FACS analysis, the cells were washed three times in 0.1% (w/v) BSA in PBS and finally resuspended in 1 mL PBS. The cells were analyzed using a BD FACS Diva flow cytometry system with the trigger parameter set on forward scattering. The analysis rate was 1000–5000 events/s and the sorting speed was 10–100 events/s. The 488 and 647 nm laser excitation wavelengths were used for detection and

Experimental procedures

emissions were detected using 530 and 670 nm filters. The positive cells were gated on a fluorescence double plot as specified in each experiment. The cells were sorted in the single cell mode onto YNB-CAA glucose chloramphenicol agar plates. The screening method was first tested with a reference library, which was prepared by mixing 95% empty vector control (negative) cells and 5% *TfuDyP* expressing cells (positive). To test the efficiency of the screening method, forty eight events of the sorted fraction were selected and the activities were assayed by an ABTS MTP assay (as described below) using ABTS as the substrate. Forty eight events were also selected from the unsorted reference library population and activity assays were carried out as described for the sorted events. The number of the cells that showed activity towards ABTS were compared to determine the level of enrichment, thus, the efficiency of the screening method.

The screening of real *TfuDyP* library was carried out with and without 5 mM H₂O₂ pretreated samples for a comparison, however, only H₂O₂ pretreated cells were sorted for variant analysis. The H₂O₂ pretreatment was applied as follows: Prior to starting the staining assay with tyramide-fluorescein, cells washed with 0.1% (w/v) BSA in 100 mM sodium acetate buffer pH 4.5 were incubated in the presence of 5 mM H₂O₂ at RT for 10 min. Following the incubation, 500 µL above mentioned sodium acetate buffer was added to dilute the cells and the cells were centrifuged (13 000 xg, 1 min, RT). The cells were washed three times with sodium acetate buffer and re-suspended in the same buffer to go on with the tyramide-fluorescein staining step as described above.

Synthesis of tyramide-fluorescein substrate

Fluorescein tyramide was synthesized as described (Gijlswijk et al., 1997; Ostafe, 2013) using 20 mM 5/6-carboxyfluorescein succinimidyl ester (Pierce) in dimethylformamide (DMF) mixed with 25 mM triethylamine and 20 mM tyramine HCl (Sigma-Aldrich Chemie GmbH) also in DMF. The mix was kept at room temperature for 2 h in the dark and ethanol was added in order to obtain a 2 mM fluorescein tyramide solution, which was kept at 4°C until required (Davidson et al., 2004; Davidson & Keller, 1999; Zhou & Vize, 2004).

Growing sorted EBY 100 cells and MTP assays with ABTS after FACS sorting

The EBY 100 cells sorted on YNB CAA glucose agar plates containing chloramphenicol was grown for 2 days at 30°C. Single colonies were inoculated on new YNB CAA glucose plates as masterplates and also into MTP plates containing 100 µL YNB CAA glucose medium with CM and grown for 24 h. 7 µL of the cell culture was transferred to new MTP wells containing 25 µL YNB CAA glucose medium and the cells were allowed to grow for a further 24 h before adding 84 µL YNB CAA galactose medium with CM and 5-ALA and growing for another 24 h. 7 µL of the cells were diluted in 84 µL 100 mM sodium acetate buffer pH 4.5 and the OD₆₀₀ was determined. After this point, 2 types of activity assays were carried

Experimental procedures

out to characterize the sorted cells. In the first assay, 5 mM H₂O₂ was added to the cell-buffer mixture and incubated for 20 min at RT. Following the incubation, 17 µL of 7 mM ABTS stock solution was added to the mixture and the increase in the absorbance was followed for 30 min at 420 nm with 1 min kinetic time intervals. In the second assay, 17 µL ABTS (7 mM) and 17 µL H₂O₂ was added to the cell-buffer mixture simultaneously and the increase in the absorbance was followed as described for the first assay. For each well measurement, the slope of the linear region was taken into account and the slopes were normalized to the OD₆₀₀ in each well and the values were compared with the values of the cells expressing the wild type enzyme. The best mutants were selected and the screening protocol was repeated using the same MTP assay with ABTS as described above. DNA was extracted from the best-performing *S. cerevisiae* mutants as described previously by Singh & Weil, 2002 and sequenced as described for other DNA samples in section 6.2.1.

Characterization of the isolated mutant *TfuDyP* variants

The isolated *TfuDyP* variants and the WT-*TfuDyP* were cloned into pET-21d(+) vector via *NheI* and *Sall* as described for pET-22b(+) vector in 6.2.1 for expression in the cytoplasm with a His₆-tag at the C-terminus. The plasmids carrying mutant variants or WT-*TfuDyP* were transformed into *E. coli* BL21 Star (DE3) strain. Recombinant gene expression (6.2.6) using 0.5 mM IPTG, extraction of the protein (6.2.8), following IMAC-purification (6.2.9) and further analysis of recombinant protein expression by SDS-PAGE (6.2.10) and Western blot (6.2.11) analyses were carried out as described previously. In order to characterize the functional parameters of the mutant variants and WT-*TfuDyP* guaiacol was used in the activity assays. The optimum pH values were determined using buffer systems between pH 3.5 and 10.0 (6.2.21). The optimum temperature values were determined in a temperature range from 25°C to 90°C. Kinetic parameters for guaiacol were determined as described previously (6.2.17) in a substrate concentration range of 10 µM – 1000 µM.

7.0 References

- Abdel-Hamid, A.M., Solbiati, J.O., Cann, I.K.O. 2013. Insights into lignin degradation and its potential industrial applications. *Advances in Applied Microbiology*, Vol 82, **82**, 1-28.
- Abdelaziz, O.Y., Hulteberg, C.P. 2017. Physicochemical characterisation of technical lignins for their potential valorisation. *Waste and Biomass Valorization*, **8**(3), 859-869.
- Adler, E. 1957. Structural elements of lignin. *Industrial & Engineering Chemistry*, **49**(9), 1377-1383.
- Aharoni, A., Amitai, G., Bernath, K., Magdassi, S., Tawfik, D.S. 2005. High-throughput screening of enzyme libraries: thiolactonases evolved by fluorescence-activated sorting of single cells in emulsion compartments. *Chemistry & Biology*, **12**(12), 1281-1289.
- Ahmad, M., Roberts, J.N., Hardiman, E.M., Singh, R., Eltis, L.D., Bugg, T.D.H. 2011. Identification of DypB from *Rhodococcus jostii* RHA1 as a lignin peroxidase. *Biochemistry*, **50**(23), 5096-5107.
- Alam, M., Islam, M.S., Hossen, M.M., Haque, M.S., Alam, M.M. 2014. Lignin degrading enzymes from *Macrophomina phaseolina* and uses thereof, Google Patents.
- Allocati, N., Federici, L., Masulli, M., Di Ilio, C. 2009. Glutathione transferases in bacteria. *Febs Journal*, **276**(1), 58-75.
- Alvarez, C., Reyes-Sosa, F.M., Diez, B. 2016. Enzymatic hydrolysis of biomass from wood. *Microbial Biotechnology*, **9**(2), 149-156.
- Anbu, P. 2016. Enhanced production and organic solvent stability of a protease from *Brevibacillus laterosporus* strain PAP04. *Brazilian Journal of Medical and Biological Research*, **49**(4), e5178.
- Andrawis, A., Johnson, K.A., Tien, M. 1988. Studies on compound I formation of the lignin peroxidase from *Phanerochaete chrysosporium*. *Journal of Biological Chemistry*, **263**(3), 1195-1198.
- Arias, M.E., Arenas, M., Rodriguez, J., Soliveri, J., Ball, A.S., Hernandez, M. 2003. Kraft pulp biobleaching and mediated oxidation of a nonphenolic substrate by laccase from *Streptomyces cyaneus* CECT 3335. *Applied and Environmental Microbiology*, **69**(4), 1953-1958.
- Ausec, L., van Elsas, J.D., Mandic-Mulec, I. 2011. Two- and three-domain bacterial laccase-like genes are present in drained peat soils. *Soil Biology & Biochemistry*, **43**(5), 975-983.
- Balan, V. 2014. Current challenges in commercially producing biofuels from lignocellulosic biomass. *ISRN Biotechnology*, **2014**, 463074.
- Baniel, A., Eyal, A. 2010. process for the recovery of hcl from a dilute solution thereof, Google Patents.
- Baucher, M., Monties, B., Van Montagu, M., Boerjan, W. 1998. Biosynthesis and genetic engineering of lignin. *Critical Reviews in Plant Sciences*, **17**(2), 125-197.
- Bauer, N., Mouratiadou, I., Luderer, G., Baumstark, L., Brecha, R.J., Edenhofer, O., Kriegler, E. 2016. Global fossil energy markets and climate change mitigation - an analysis with REMIND. *Climatic Change*, **136**(1), 69-82.
- Becker, S., Schmoltdt, H.U., Adams, T.M., Wilhelm, S., Kolmar, H. 2004. Ultra-high-throughput screening based on cell-surface display and fluorescence-activated cell sorting for the identification of novel biocatalysts. *Current Opinion in Biotechnology*, **15**(4), 323-329.
- Benoit, I., Culleton, H., Zhou, M.M., DiFalco, M., Aguilar-Osorio, G., Battaglia, E., Bouzid, O., Brouwer, C.P.J.M., El-Bushari, H.B.O., Coutinho, P.M., Gruben, B.S., Hilden, K.S., Houbraeken, J., Barboza, L.A.J., Levasseur, A., Majoor, E., Makela, M.R., Narang, H.M., Trejo-Aguilar, B., van den Brink, J., vanKuyk, P.A., Wiebenga, A., McKie, V., McCleary, B., Tsang, A., Henrissat, B., de Vries, R.P. 2015. Closely related fungi employ diverse enzymatic strategies to degrade plant biomass. *Biotechnology for Biofuels*, **8**, 107.
- Bessette, P.H., Åslund, F., Beckwith, J., Georgiou, G. 1999. Efficient folding of proteins with multiple disulfide bonds in the *Escherichia coli* cytoplasm. *Proceedings of the National Academy of Sciences*, **96**(24), 13703-13708.
- Bird, L.J., Coleman, M.L., Newman, D.K. 2013. Iron and copper act synergistically to delay anaerobic growth of bacteria. *Applied and Environmental Microbiology*, **79**(12), 3619-3627.
- Boder, E.T., Wittrup, K.D. 1997. Yeast surface display for screening combinatorial polypeptide libraries. *Nature Biotechnology*, **15**(6), 553-557.

References

- Boerjan, W., Ralph, J., Baucher, M. 2003. Lignin biosynthesis. *Annual Reviews for Plant Biology*, **54**, 519-546.
- Bornscheuer, U., Buchholz, K., Seibel, J. 2014. Enzymatic degradation of (Ligno) cellulose. *Angewandte Chemie-International Edition*, **53**(41), 10876-10893.
- Bourbonnais, R., Leech, D., Paice, M.G. 1998. Electrochemical analysis of the interactions of laccase mediators with lignin model compounds. *Biochimica Et Biophysica Acta-General Subjects*, **1379**(3), 381-390.
- Boyd, D., Weiss, D.S., Chen, J.C., Beckwith, J. 2000. Towards single-copy gene expression systems making gene cloning physiologically relevant: lambda InCh, a simple *Escherichia coli* plasmid-chromosome shuttle system. *Journal of Bacteriology*, **182**(3), 842-847.
- Brander, S., Mikkelsen, J.D., Kepp, K.P. 2014. Characterization of an alkali- and halide-resistant laccase expressed in *E. coli*: CotA from *Bacillus clausii*. *PLoS One*, **9**(6), e99402.
- Brecha, R.J. 2008. Emission scenarios in the face of fossil-fuel peaking. *Energy Policy*, **36**(9), 3492-3504.
- Brijwani, K., Rigdon, A., Vadlani, P.V. 2010. Fungal laccases: production, function, and applications in food processing. *Enzyme Research*, **2010**, 149748.
- Brissos, V., Pereira, L., Munteanu, F.D., Cavaco-Paulo, A., Martins, L.O. 2009. Expression system of CotA-laccase for directed evolution and high-throughput screenings for the oxidation of high-redox potential dyes. *Biotechnology Journal*, **4**(4), 558-563.
- Brown, M., Wittwer, C. 2000. Flow cytometry: principles and clinical applications in hematology. *Clinical Chemistry*, **46**(8 Pt 2), 1221-1229.
- Brown, M.E., Barros, T., Chang, M.C. 2012. Identification and characterization of a multifunctional dye peroxidase from a lignin-reactive bacterium. *ACS Chemical Biology*, **7**(12), 2074-2081.
- Bruijninx, P.W., B; Gruter, GJ; Westenbroek, A; Engelen-Smeets, E. 2016. Lignin valorisation - The importance of a full value chain approach, (Ed.) D.B. Cluster, pp. 22.
- Bugg, T.D., Ahmad, M., Hardiman, E.M., Singh, R. 2011a. The emerging role for bacteria in lignin degradation and bio-product formation. *Current Opinion in Biotechnology*, **22**(3), 394-400.
- Bugg, T.D.H., Ahmad, M., Hardiman, E.M., Singh, R. 2011b. The emerging role for bacteria in lignin degradation and bio-product formation. *Current Opinion in Biotechnology*, **22**(3), 394-400.
- Bussamara, R., Dall'agnol, L., Schrank, A., Fernandes, K.F., Vainstein, M.H. 2012. Optimal conditions for continuous immobilization of *Pseudozyma hubeiensis* (Strain HB85A) lipase by adsorption in a packed-bed reactor by response surface methodology. *Enzyme Research*, **2012**, 329178.
- Cabana, H., Jiwan, J.-L.H., Rozenberg, R., Elisashvili, V., Penninckx, M., Agathos, S.N., Jones, J.P. 2007a. Elimination of endocrine disrupting chemicals nonylphenol and bisphenol A and personal care product ingredient triclosan using enzyme preparation from the white rot fungus *Coriopsis polyzona*. *Chemosphere*, **67**(4), 770-778.
- Cabana, H., Jones, J.P., Agathos, S.N. 2007b. Preparation and characterization of cross-linked laccase aggregates and their application to the elimination of endocrine disrupting chemicals. *Journal of Biotechnology*, **132**(1), 23-31.
- Call, H.P. 1992. Process, using enhanced-action laccase enzymes, for the delignification or bleaching of lignocellulose-containing material or for the treatment of waste water, Google Patents.
- Call, H.P., Mucke, I. 1997. History, overview and applications of mediated lignolytic systems, especially laccase-mediator-systems (Lignozym(R)-process). *Journal of Biotechnology*, **53**(2-3), 163-202.
- Camarero, S., Ibarra, D., Martinez, M.J., Martinez, A.T. 2005. Lignin-derived compounds as efficient laccase mediators for decolorization of different types of recalcitrant dyes. *Applied and Environmental Microbiology*, **71**(4), 1775-1784.
- Canas, A.I., Camarero, S. 2010. Laccases and their natural mediators: Biotechnological tools for sustainable eco-friendly processes. *Biotechnology Advances*, **28**(6), 694-705.
- Cappellaro, C., Hauser, K., Mrsa, V., Watzele, M., Watzele, G., Gruber, C., Tanner, W. 1991. *Saccharomyces cerevisiae* a-agglutinin and alpha-agglutinin - Characterization of Their Molecular Interaction. *Embo Journal*, **10**(13), 4081-4088.
- Chakar, F.S., Ragauskas, A.J. 2004. Review of current and future softwood kraft lignin process chemistry. *Industrial Crops and Products*, **20**(2), 131-141.

References

- Chandra, R., Chowdhary, P. 2015. Properties of bacterial laccases and their application in bioremediation of industrial wastes. *Environmental Science-Processes & Impacts*, **17**(2), 326-342.
- Chao, G., Lau, W.L., Hackel, B.J., Sazinsky, S.L., Lippow, S.M., Wittrup, K.D. 2006. Isolating and engineering human antibodies using yeast surface display (vol 1, pg 755, 2006). *Nature Protocols*, **1**(2).
- Chen, J., Song, J.-l., Zhang, S., Wang, Y., Cui, D.-f., Wang, C.-c. 1999. Chaperone activity of DsbC. *Journal of Biological Chemistry*, **274**(28), 19601-19605.
- Chen, M., Zeng, G.M., Tan, Z.Y., Jiang, M., Li, H., Liu, L.F., Zhu, Y., Yu, Z., Wei, Z., Liu, Y.Y., Xie, G.X. 2011. Understanding lignin-degrading reactions of ligninolytic enzymes: binding affinity and interactional profile. *Plos One*, **6**(9).
- Chen, Q., Marshall, M.N., Geib, S.M., Tien, M., Richard, T.L. 2012a. Effects of laccase on lignin depolymerization and enzymatic hydrolysis of ensiled corn stover. *Bioresource Technology*, **117**, 186-192.
- Chen, Q., Marshall, M.N., Geib, S.M., Tien, M., Richard, T.L. 2012b. Effects of laccase on lignin depolymerization and enzymatic hydrolysis of ensiled corn stover. *Bioresour Technol*, **117**, 186-192.
- Chen, Y.R., Sarkanen, S., Wang, Y.Y. 2012c. Lignin-degrading enzyme activities. *Methods in Molecular Biology*, **908**, 251-268.
- Cherry, J.R., Lamsa, M.H., Schneider, P., Vind, J., Svendsen, A., Jones, A., Pedersen, A.H. 1999. Directed evolution of a fungal peroxidase. *Nature Biotechnology*, **17**(4), 379-384.
- Christopher, L.P., Yao, B., Ji, Y. 2014. Lignin biodegradation with laccase-mediator systems. *Frontiers in Energy Research*, **2**, 12.
- Claus, H. 2003. Laccases and their occurrence in prokaryotes. *Archives of Microbiology*, **179**(3), 145-150.
- Clerico, E.M., Maki, J.L., Gierasch, L.M. 2008. Use of synthetic signal sequences to explore the protein export machinery. *Biopolymers*, **90**(3), 307-319.
- Colpa, D.I., Fraaije, M.W. 2016. High overexpression of dye decolorizing peroxidase TfuDyP leads to the incorporation of heme precursor protoporphyrin IX. *Journal of Molecular Catalysis B-Enzymatic*, **134**, 372-377.
- Colpa, D.I., Fraaije, M.W., van Bloois, E. 2014. DyP-type peroxidases: a promising and versatile class of enzymes. *Journal of Industrial Microbiology and Biotechnology*, **41**(1), 1-7.
- d'Errico, C., Jorgensen, J.O., Krogh, K.B.R.M., Spodsberg, N., Madsen, R., Monrad, R.N. 2015. Enzymatic degradation of lignin-carbohydrate complexes (LCCs): Model studies using a fungal glucuronoyl esterase from *Cerrena unicolor*. *Biotechnology and Bioengineering*, **112**(5), 914-922.
- Davidson, L.A., Keller, R., DeSimone, D. 2004. Patterning and tissue movements in a novel explant preparation of the marginal zone of *Xenopus laevis*. *Gene Expression Patterns*, **4**(4), 457-466.
- Davidson, L.A., Keller, R.E. 1999. Neural tube closure in *Xenopus laevis* involves medial migration, directed protrusive activity, cell intercalation and convergent extension. *Development*, **126**(20), 4547-4556.
- Dayer, M.R., Moosavi-Movahedi, A.A., Dayer, M.S. 2010. Band assignment in hemoglobin porphyrin ring spectrum: Using four-orbital model of Gouterman. *Protein and Peptide Letters*, **17**(4), 473-479.
- De Marco, A. 2009. Strategies for successful recombinant expression of disulfide bond-dependent proteins in *Escherichia coli*. *Microbial cell factories*, **8**(1), 26.
- de Marco, A., Deuerling, E., Mogk, A., Tomoyasu, T., Bukau, B. 2007. Chaperone-based procedure to increase yields of soluble recombinant proteins produced in *E. coli*. *BMC Biotechnology*, **7**, 32.
- de Marco, A., Vigh, L., Diamant, S., Goloubinoff, P. 2005a. Native folding of aggregation-prone recombinant proteins in *Escherichia coli* by osmolytes, plasmid- or benzyl alcohol-overexpressed molecular chaperones. *Cell Stress & Chaperones*, **10**(4), 329-339.

References

- de Marco, A., Vigh, L., Diamant, S., Goloubinoff, P. 2005b. Native folding of aggregation-prone recombinant proteins in *Escherichia coli* by osmolytes, plasmid- or benzyl alcohol-overexpressed molecular chaperones. *Cell Stress Chaperones*, **10**(4), 329-339.
- Deshpande, S. 2012. Enzyme immunoassays: from concept to product development. *Springer Science & Business Media*.
- Durao, P., Bento, I., Fernandes, A.T., Melo, E.P., Lindley, P.F., Martins, L.O. 2006. Perturbations of the T1 copper site in the CotA laccase from *Bacillus subtilis*: structural, biochemical, enzymatic and stability studies. *Journal of Biological Inorganic Chemistry*, **11**(4), 514-526.
- Durao, P., Chen, Z., Fernandes, A.T., Hildebrandt, P., Murgida, D.H., Todorovic, S., Pereira, M.M., Melo, E.P., Martins, L.O. 2008a. Copper incorporation into recombinant CotA laccase from *Bacillus subtilis*: characterization of fully copper loaded enzymes. *Journal of Biological Inorganic Chemistry*, **13**(2), 183-193.
- Durao, P., Chen, Z.J., Silva, C.S., Soares, C.M., Pereira, M.M., Todorovic, S., Hildebrandt, P., Bento, I., Lindley, P.F., Martins, L.O. 2008b. Proximal mutations at the type 1 copper site of CotA laccase: spectroscopic, redox, kinetic and structural characterization of I494A and L386A mutants. *Biochemical Journal*, **412**, 339-346.
- Ece, S., Lambertz, C., Fischer, R., Commandeur, U. 2017. Heterologous expression of a *Streptomyces cyaneus* laccase for biomass modification applications. *AMB Express*, **7**(1), 86.
- Edelhoch, H. 1967. Spectroscopic determination of tryptophan and tyrosine in proteins. *Biochemistry*, **6**(7), 1948-1954.
- Endo, K., Hayashi, Y., Hibi, T., Hosono, K., Beppu, T., Ueda, K. 2003. Enzymological characterization of EpoA, a laccase-like phenol oxidase produced by *Streptomyces griseus*. *Journal of Biochemistry*, **133**(5), 671-677.
- Farrell, R., Kirk, T., Tien, M. 1987. Novel enzymes for degradation of lignin, Google Patents.
- Fernandes, A.T., Soares, C.M., Pereira, M.M., Huber, R., Grass, G., Martins, L.O. 2007. A robust metallo-oxidase from the hyperthermophilic bacterium *Aquifex aeolicus*. *FEBS J*, **274**(11), 2683-2694.
- Ferrer, M., Chernikova, T.N., Yakimov, M.M., Golyshin, P.N., Timmis, K.N. 2003. Chaperonins govern growth of *Escherichia coli* at low temperatures. *Nature biotechnology*, **21**(11), 1266-1267.
- Galai, S., Touhami, Y., Marzouki, M.N. 2012. Response surface methodology applied to laccases activities exhibited by *Stenotrophomonas maltophilia* Aap56 in different growth conditions. *Bioresources*, **7**(1), 706-726.
- Gall, D.L., Kim, H., Lu, F.C., Donohue, T.J., Noguera, D.R., Ralph, J. 2014. Stereochemical features of glutathione-dependent enzymes in the *Sphingobium* sp Strain SYK-6 beta-aryl etherase pathway. *Journal of Biological Chemistry*, **289**(12), 8656-8667.
- Garcia-Ruiz, E., Gonzalez-Perez, D., Ruiz-Duenas, F.J., Martinez, A.T., Alcalde, M. 2012. Directed evolution of a temperature-, peroxide- and alkaline pH-tolerant versatile peroxidase. *Biochemical Journal*, **441**, 487-498.
- Garcia-Ruiz, E., Mate, D.M., Gonzalez-Perez, D., Molina-Espeja, P., Camarero, S., Martínez, A.T., Ballesteros, A.O., Alcalde, M. 2014. Directed evolution of ligninolytic oxidoreductases: From functional expression to stabilization and beyond. *Cascade Biocatalysis*, 1-22.
- Ghaffar, S.H., Fan, M.Z. 2014. Lignin in straw and its applications as an adhesive. *International Journal of Adhesion and Adhesives*, **48**, 92-101.
- Gibson, D.G., Smith, H.O., Hutchison III, C.A., Venter, J.C., Merryman, C. 2010. Chemical synthesis of the mouse mitochondrial genome. *Nature methods*, **7**(11), 901-903.
- Gibson, D.G., Young, L., Chuang, R.-Y., Venter, J.C., Hutchison, C.A., Smith, H.O. 2009. Enzymatic assembly of DNA molecules up to several hundred kilobases. *Nature methods*, **6**(5), 343-345.
- Gierer, J., Ljunggren, S. 1979. Reactions of lignins during sulfate pulping .16. Kinetics of the cleavage of beta-aryl ether linkages in structures containing carbonyl groups. *Svensk Papperstidning-Nordisk Cellulosa*, **82**(3), 71-81.
- Gierer, J., Wannstrom, S. 1986. Formation of ether bonds between lignins and carbohydrates during alkaline pulping processes. *Holzforschung*, **40**(6), 347-352.

References

- Gietz, R.D., Schiestl, R.H. 2007. High-efficiency yeast transformation using the LiAc/SS carrier DNA/PEG method. *Nature protocols*, **2**(1), 31-34.
- Gijlswijk, R.P.v., Zijlmans, H.J., Wiegant, J., Bobrow, M.N., Erickson, T.J., Adler, K.E., Tanke, H.J., Raap, A.K. 1997. Fluorochrome-labeled tyramides: use in immunocytochemistry and fluorescence in situ hybridization. *Journal of Histochemistry & Cytochemistry*, **45**(3), 375-382.
- Giovannetti, R. 2012. The use of spectrophotometry UV-Vis for the study of porphyrins. *Edited by Jamal Uddin*, **87**.
- Givan, A.L. 2001. Principles of flow cytometry: an overview. *Methods in Cell Biology*, **63**, 19-50.
- Givaudan, A., Effosse, A., Faure, D., Potier, P., Bouillant, M.L., Bally, R. 1993. Polyphenol oxidase in *Azospirillum lipoferum* isolated from rice rhizosphere - Evidence for laccase activity in nonmotile strains of *Azospirillum lipoferum*. *Fems Microbiology Letters*, **108**(2), 205-210.
- Glenn, J.K., Morgan, M.A., Mayfield, M.B., Kuwahara, M., Gold, M.H. 1983. An extracellular H₂O₂-requiring enzyme preparation involved in lignin biodegradation by the white rot basidiomycete *Phanerochaete chrysosporium*. *Biochemical and Biophysical Research Community*, **114**(3), 1077-1083.
- Gonzalez-Perez, D., Garcia-Ruiz, E., Alcalde, M. 2012. *Saccharomyces cerevisiae* in directed evolution: An efficient tool to improve enzymes. *Bioengineered*, **3**(3), 172-177.
- Gratzl, J.S., Chen, C.L. 2000. Chemistry of pulping: Lignin reactions. *Lignin : Historical, Biological, and Materials Perspectives*, **742**, 392-421.
- Green, T.R. 1977. Significance of glucose oxidase in lignin degradation. *Nature*, **268**(5615), 78-80.
- Grey, B.N., Steck, T.R. 2001. Concentrations of copper thought to be toxic to *Escherichia coli* can induce the viable but nonculturable condition. *Applied and Environmental Microbiology*, **67**(11), 5325-5327.
- Grodberg, J., Dunn, J.J. 1988. ompT encodes the *Escherichia coli* outer membrane protease that cleaves T7 RNA polymerase during purification. *Journal of bacteriology*, **170**(3), 1245-1253.
- Grunberg-Manago, M. 1999. Messenger RNA stability and its role in control of gene expression in bacteria and phages. *Annual review of genetics*, **33**(1), 193-227.
- Gunne, M., Urlacher, V.B. 2012a. Characterization of the alkaline laccase Ssl1 from *Streptomyces sviveus* with unusual properties discovered by genome mining. *Plos One*, **7**(12).
- Gunne, M., Urlacher, V.B. 2012b. Characterization of the alkaline laccase Ssl1 from *Streptomyces sviveus* with unusual properties discovered by genome mining. *PLoS One*, **7**(12), e52360.
- Gupta, M.N. 1992. Enzyme function in organic solvents. *European Journal of Biochemistry*, **203**(1-2), 25-32.
- Gupta, N., Farinas, E.T. 2009. Narrowing laccase substrate specificity using active site saturation mutagenesis. *Combinatorial Chemistry & High Throughput Screening*, **12**(3), 269-274.
- Gupta, N., Lee, F.S., Farinas, E.T. 2010. Laboratory evolution of laccase for substrate specificity. *Faseb Journal*, **24**.
- Gupta, N., Sheng, S.L., Farinas, E.T. 2011. Directed evolution of CotA laccase for increased substrate specificity using *Bacillus subtilis* spores. *Abstracts of Papers of the American Chemical Society*, **241**.
- Gutierrez, A., Rencoret, J., Cadena, E.M., Rico, A., Barth, D., del Rio, J.C., Martinez, A.T. 2012. Demonstration of laccase-based removal of lignin from wood and non-wood plant feedstocks. *Bioresource Technology*, **119**, 114-122.
- Guzik, U., Hupert-Kocurek, K., Wojcieszynska, D. 2014. Immobilization as a strategy for improving enzyme properties-Application to oxidoreductases. *Molecules*, **19**(7), 8995-9018.
- Hanahan, D. 1983. Studies on transformation of *Escherichia coli* with plasmids. *Journal of Molecular Biology*, **166**(4), 557-580.
- Harreither, W., Sygmund, C., Augustin, M., Narciso, M., Rabinovich, M.L., Gorton, L., Haltrich, D., Ludwig, R. 2011. Catalytic properties and classification of cellobiose dehydrogenases from ascomycetes. *Applied and Environmental Microbiology*, **77**(5), 1804-1815.
- Hatakka, A.I. 1984. Biological Pretreatment of lignocellulose for enzymatic-hydrolysis of cellulose. *Applied Biochemistry and Biotechnology*, **9**(4), 363-364.

References

- Hatti-Kaul, R., Ibrahim, V. 2012. Lignin-Degrading Enzymes: An Overview. *Bioprocessing Technologies in Biorefinery for Sustainable Production of Fuels, Chemicals, and Polymers*, 167-192.
- Hayes, J.D., Flanagan, J.U., Jowsey, I.R. 2005. Glutathione transferases. *Annual Review of Pharmacology and Toxicology*, **45**, 51-88.
- Hiner, A.N., Raven, E.L., Thorneley, R.N., García-Cánovas, F., Rodríguez-López, J.N. 2002. Mechanisms of compound I formation in heme peroxidases. *Journal of inorganic biochemistry*, **91**(1), 27-34.
- Hofbauer, S., Hagmuller, A., Schaffner, I., Mlynek, G., Krutzler, M., Stadlmayr, G., Pirker, K.F., Obinger, C., Daims, H., Djinovic-Carugo, K., Furtmuller, P.G. 2015. Structure and heme-binding properties of HemQ (chlorite dismutase-like protein) from *Listeria monocytogenes*. *Archives of Biochemistry and Biophysics*, **574**, 36-48.
- Hofrichter, M., Ullrich, R., Pecyna, M.J., Liers, C., Lundell, T. 2010. New and classic families of secreted fungal heme peroxidases. *Applied Microbiology and Biotechnology*, **87**(3), 871-897.
- Holzbour, E.L., Andrawis, A., Tien, M. 1988. Structure and regulation of a lignin peroxidase gene from *Phanerochaete chrysosporium*. *Biochemical and Biophysical Research Community*, **155**(2), 626-633.
- Houborg, K., Harris, P., Poulsen, J.C.N., Schneider, P., Svendsen, A., Larsen, S. 2003. The structure of a mutant enzyme of *Coprinus cinereus* peroxidase provides an understanding of its increased thermostability. *Acta Crystallographica Section D-Biological Crystallography*, **59**, 997-1003.
- Ihssen, J., Reiss, R., Luchsinger, R., Thony-Meyer, L., Richter, M. 2015. Biochemical properties and yields of diverse bacterial laccase-like multicopper oxidases expressed in *Escherichia coli*. *Scientific Reports*, **5**.
- Isikgor, F.H., Becer, C.R. 2015. Lignocellulosic biomass: a sustainable platform for the production of bio-based chemicals and polymers. *Polymer Chemistry*, **6**(25), 4497-4559.
- Isroi, Millati, R., Syamsiah, S., Niklasson, C., Cahyanto, M.N., Lundquist, K., Taherzadeh, M.J. 2011. Biological pretreatment of lignocelluloses with white-rot fungi and its applications: A Review. *Bioresources*, **6**(4), 5224-5259.
- Jeffries, T.W. 1990. Biodegradation of lignin-carbohydrate complexes. *Biodegradation*, **1**(2-3), 163-176.
- Jerpseth, B., Callahan, M., Greener, A. 1997. New competent cells for highest transformation efficiencies. *Strategies*, **10**(2), 37-38.
- Jerpseth, M., Jerpseth, B., Briester, L., Greener, A. 1998. Codon bias-adjusted BL21 derivatives for protein expression. *Strateg*, **11**, 3-4.
- Johansson, A., Aaltonen, O., Ylinen, P. 1987. Organosolv Pulping - Methods and pulp properties. *Biomass*, **13**(1), 45-65.
- Jorgensen, H., Kristensen, J.B., Felby, C. 2007. Enzymatic conversion of lignocellulose into fermentable sugars: challenges and opportunities. *Biofuels Bioproducts & Biorefining-Biofpr*, **1**(2), 119-134.
- Kalliola, A., Asikainen, M., Talja, R., Tamminen, T. 2014. Experiences of Kraft lignin functionalization by enzymatic and chemical oxidation. *Bioresources*, **9**(4), 7336-7351.
- Kido, M., Yamanaka, K., Mitani, T., Niki, H., Ogura, T., Hiraga, S. 1996. RNase E polypeptides lacking a carboxyl-terminal half suppress a mukB mutation in *Escherichia coli*. *Journal of Bacteriology*, **178**(13), 3917-3925.
- Kim, S.J., Shoda, M. 1999. Purification and characterization of a novel peroxidase from *Geotrichum candidum* dec 1 involved in decolorization of dyes. *Applied and Environmental Microbiology*, **65**(3), 1029-1035.
- Kirk, T.K. 1987. The lignin-degrading enzyme-system of *Phanerochaete chrysosporium*. *Abstracts of Papers of the American Chemical Society*, **194**, 157-Mbtd.
- Klein-Marcuschamer, D., Oleskowicz-Popiel, P., Simmons, B.A., Blanch, H.W. 2012. The challenge of enzyme cost in the production of lignocellulosic biofuels. *Biotechnology and Bioengineering*, **109**(4), 1083-1087.
- Kondo, R., Sarkanen, K.V. 1984. Kinetics of Lignin and Hemicellulose dissolution during the initial-stage of alkaline pulping. *Holzforschung*, **38**(1), 31-36.

References

- Koschorreck, K., Richter, S.M., Ene, A.B., Roduner, E., Schmid, R.D., Urlacher, V.B. 2008. Cloning and characterization of a new laccase from *Bacillus licheniformis* catalyzing dimerization of phenolic acids. *Applied Microbiology and Biotechnology*, **79**(2), 217-224.
- Koschorreck, K., Schmid, R.D., Urlacher, V.B. 2009. Improving the functional expression of a *Bacillus licheniformis* laccase by random and site-directed mutagenesis. *BMC Biotechnology*, **9**, 12.
- Kumar, A., Dhar, K., Kanwar, S.S., Arora, P.K. 2016. Lipase catalysis in organic solvents: advantages and applications. *Biological Procedures Online*, **18**, 2.
- Kumar, V.V., Sivanesan, S., Cabana, H. 2014. Magnetic cross-linked laccase aggregates-bioremediation tool for decolorization of distinct classes of recalcitrant dyes. *Science of the Total Environment*, **487**, 830-839.
- Laemmli, U.K. 1970. Cleavage of structural proteins during the assembly of the head of bacteriophage T4. *Nature*, **227**(5259), 680-685.
- Lambertz, C., Ece, S., Fischer, R., Commandeur, U. 2016. Progress and obstacles in the production and application of recombinant lignin-degrading peroxidases. *Bioengineered*, **7**(3), 145-154.
- Lancefield, C.S., Ojo, O.S., Tran, F., Westwood, N.J. 2015. Isolation of functionalized phenolic monomers through selective oxidation and C-O bond cleavage of the β -O-4 linkages in lignin. *Angewandte Chemie International Edition*, **54**(1), 258-262.
- Leemhuis, H., Kelly, R.M., Dijkhuizen, L. 2009. Directed evolution of enzymes: Library screening strategies. *IUBMB Life*, **61**(3), 222-228.
- Levy, R., Weiss, R., Chen, G., Iverson, B.L., Georgiou, G. 2001. Production of correctly folded Fab antibody fragment in the cytoplasm of *Escherichia coli* trxB gor mutants via the coexpression of molecular chaperones. *Protein expression and purification*, **23**(2), 338-347.
- Li, J., Liu, C., Li, B., Yuan, H., Yang, J., Zheng, B. 2012. Identification and molecular characterization of a novel DyP-type peroxidase from *Pseudomonas aeruginosa* PKE117. *Applied Biochemistry and Biotechnology*, **166**(3), 774-785.
- Lipovsek, D., Antipov, E., Armstrong, K.A., Olsen, M.J., Klibanov, A.M., Tidor, B., Wittrup, K.D. 2007. Selection of horseradish peroxidase variants with enhanced enantioselectivity by yeast surface display. *Chemistry & Biology*, **14**(10), 1176-1185.
- Liu, S.J. 2010. Woody biomass: Niche position as a source of sustainable renewable chemicals and energy and kinetics of hot-water extraction/hydrolysis. *Biotechnology Advances*, **28**(5), 563-582.
- Longwell, C.K., Labanieh, L., Cochran, J.R. 2017. High-throughput screening technologies for enzyme engineering. *Current Opinion in Biotechnology*, **48**, 196-202.
- Lopez-Gallego, F., Betancor, L., Hidalgo, A., Alonso, N., Fernandez-Lafuente, R., Guisan, J.M. 2005. Co-aggregation of enzymes and polyethyleneimine: a simple method to prepare stable and immobilized derivatives of glutaryl acylase. *Biomacromolecules*, **6**(4), 1839-1842.
- Lopez, P.J., Marchand, I., Joyce, S.A., Dreyfus, M. 1999. The C-terminal half of RNase E, which organizes the *Escherichia coli* degradosome, participates in mRNA degradation but not rRNA processing *in vivo*. *Molecular microbiology*, **33**(1), 188-199.
- Lora, J.H., Glasser, W.G. 2002. Recent industrial applications of lignin: A sustainable alternative to nonrenewable materials. *Journal of Polymers and the Environment*, **10**(1-2), 39-48.
- Lu, C.F., Montijn, R.C., Brown, J.L., Klis, F., Kurjan, J., Bussey, H., Lipke, P.N. 1995. Glycosyl phosphatidylinositol-dependent cross-linking of alpha-agglutinin and beta 1,6-glucan in the *Saccharomyces cerevisiae* cell wall. *Journal of Cell Biology*, **128**(3), 333-340.
- Luis, P., Walther, G., Kellner, H., Martin, F., Buscot, F. 2004. Diversity of laccase genes from basidiomycetes in a forest soil. *Soil Biology & Biochemistry*, **36**(7), 1025-1036.
- Lund, M., Ragauskas, A.J. 2001. Enzymatic modification of kraft lignin through oxidative coupling with water-soluble phenols. *Applied Microbiology and Biotechnology*, **55**(6), 699-703.
- Machczynski, M.C., Vijgenboom, E., Samyn, B., Canters, G.W. 2004. Characterization of SLAC: a small laccase from *Streptomyces coelicolor* with unprecedented activity. *Protein Science*, **13**(9), 2388-2397.

References

- Maijala, P., Mattinen, M.L., Nousiainen, P., Kontro, J., Asikkala, J., Sipila, J., Viikari, L. 2012. Action of fungal laccases on lignin model compounds in organic solvents. *Journal of Molecular Catalysis B-Enzymatic*, **76**, 59-67.
- Majumdar, S., Lukk, T., Solbiati, J.O., Bauer, S., Nair, S.K., Cronan, J.E., Gerlt, J.A. 2014. Roles of small laccases from *Streptomyces* in lignin degradation. *Biochemistry*, **53**(24), 4047-4058.
- Marechal, F., Favrat, D., Jochem, E. 2005. Energy in the perspective of the sustainable development: The 2000 W society challenge. *Resources Conservation and Recycling*, **44**(3), 245-262.
- Margot, J., Bennati-Granier, C., Maillard, J., Blanquez, P., Barry, D.A., Holliger, C. 2013. Bacterial versus fungal laccase: potential for micropollutant degradation. *AMB Express*, **3**(1), 63.
- Martinez, A.T., Speranza, M., Ruiz-Duenas, F.J., Ferreira, P., Camarero, S., Guillen, F., Martinez, M.J., Gutierrez, A., del Rio, J.C. 2005. Biodegradation of lignocellulosics: microbial, chemical, and enzymatic aspects of the fungal attack of lignin. *International Microbiology*, **8**(3), 195-204.
- Martins, L.O., Soares, C.M., Pereira, M.M., Teixeira, M., Costa, T., Jones, G.H., Henriques, A.O. 2002. Molecular and biochemical characterization of a highly stable bacterial laccase that occurs as a structural component of the *Bacillus subtilis* endospore coat. *Journal of Biological Chemistry*, **277**(21), 18849-18859.
- Masai, E., Ichimura, A., Sato, Y., Miyauchi, K., Katayama, Y., Fukuda, M. 2003. Roles of the enantioselective glutathione S-transferases in cleavage of beta-aryl ether. *Journal of Bacteriology*, **185**(6), 1768-1775.
- Masai, E., Katayama, Y., Fukuda, M. 2007. Genetic and biochemical investigations on bacterial catabolic pathways for lignin-derived aromatic compounds. *Bioscience, biotechnology, and biochemistry*, **71**(1), 1-15.
- Masai, E., Katayama, Y., Kawai, S., Nishikawa, S., Yamasaki, M., Morohoshi, N. 1991. Cloning and sequencing of the gene for a *Pseudomonas paucimobilis* enzyme that cleaves beta-aryl ether. *Journal of Bacteriology*, **173**(24), 7950-7955.
- Masai, E., Katayama, Y., Kubota, S., Kawai, S., Yamasaki, M., Morohoshi, N. 1993. A bacterial enzyme degrading the model lignin compound beta-etherase is a member of the glutathione-S-transferase superfamily. *FEBS Letters*, **323**(1-2), 135-140.
- Masai, E., Katayama, Y., Nishikawa, S., Fukuda, M. 1999. Characterization of *Sphingomonas paucimobilis* SYK-6 genes involved in degradation of lignin-related compounds. *Journal of Industrial Microbiology and Biotechnology*, **23**(4-5), 364-373.
- Masai, E., Katayama, Y., Nishikawa, S., Yamasaki, M., Morohoshi, N., Haraguchi, T. 1989. Detection and localization of a new enzyme catalyzing the β -aryl ether cleavage in the soil bacterium (*Pseudomonas paucimobilis* SYK-6). *FEBS letters*, **249**(2), 348-352.
- Matsuura, T., Yomo, T. 2006. In vitro evolution of proteins. *Journal of Bioscience and Bioengineering*, **101**(6), 449-456.
- Mattinen, M.L., Maijala, P., Nousiainen, P., Smeds, A., Kontro, J., Sipila, J., Tamminen, T., Willfor, S., Viikari, L. 2011. Oxidation of lignans and lignin model compounds by laccase in aqueous solvent systems. *Journal of Molecular Catalysis B-Enzymatic*, **72**(3-4), 122-129.
- Miles-Barrett, D.M., Montgomery, J.R., Lancefield, C.S., Cordes, D.B., Slawin, A.M., Lebl, T., Carr, R., Westwood, N.J. 2017. Use of bisulfite processing to generate high- β -O-4 content water-soluble lignosulfonates. *ACS Sustainable Chemistry & Engineering*, **5** (2), 1831-1839 .
- Mishra, S., Bisaria, V. 2006. Production and characterization of laccase from *Cyathus bulleri* and its use in decolourization of recalcitrant textile dyes. *Applied microbiology and biotechnology*, **71**(5), 646-653.
- Miyazaki-Imamura, C., Oohira, K., Kitagawa, R., Nakano, H., Yamane, T., Takahashi, H. 2003. Improvement of H₂O₂ stability of manganese peroxidase by combinatorial mutagenesis and high-throughput screening using in vitro expression with protein disulfide isomerase. *Protein Engineering*, **16**(6), 423-428.
- Miyazaki, K. 2005. A hyperthermophilic laccase from *Thermus thermophilus* HB27. *Extremophiles*, **9**(6), 415-425.

References

- Miyazaki, K., Takenouchi, M. 2002. Creating random mutagenesis libraries using megaprimer PCR of whole plasmid. *Biotechniques*, **33**(5), 1033-1034.
- Mohanram, S., Amat, D., Choudhary, J., Arora, A., Nain, L. 2013. Novel perspectives for evolving enzyme cocktails for lignocellulose hydrolysis in biorefineries. *Sustainable Chemical Processes*, **1**(1), 15.
- Molina-Guijarro, J.M., Perez, J., Munoz-Dorado, J., Guillen, F., Moya, R., Hernandez, M., Arias, M.E. 2009. Detoxification of azo dyes by a novel pH-versatile, salt-resistant laccase from *Streptomyces ipomoea*. *International Microbiology*, **12**(1), 13-21.
- Morawski, B., Quan, S., Arnold, F.H. 2001. Functional expression and stabilization of horseradish peroxidase by directed evolution in *Saccharomyces cerevisiae*. *Biotechnology and Bioengineering*, **76**(2), 99-107.
- Moreno, A.D., Ibarra, D., Alvira, P., Tomas-Pejo, E., Ballesteros, M. 2015. A review of biological delignification and detoxification methods for lignocellulosic bioethanol production. *Critical Reviews in Biotechnology*, **35**(3), 342-354.
- Morozova, O.V., Shumakovich, G.P., Shleev, S.V., Yaropolov, Y.I. 2007. Laccase-mediator systems and their applications: A review. *Applied Biochemistry and Microbiology*, **43**(5), 523-535.
- Munk, L., Sitarz, A.K., Kalyani, D.C., Mikkelsen, J.D., Meyer, A.S. 2015. Can laccases catalyze bond cleavage in lignin? *Biotechnology Advances*, **33**(1), 13-24.
- N, K.T. 1971. Organosolv pulping and recovery process, Google Patents.
- Nichols, J.M., Bishop, L.M., Bergman, R.G., Ellman, J.A. 2010. Catalytic C-O bond cleavage of 2-aryloxy-1-arylethanol and its application to the depolymerization of lignin-related polymers. *Journal of the American Chemical Society*, **132**(46), 16725-16725.
- Niladevi, K.N., Jacob, N., Prema, P. 2008. Evidence for a halotolerant-alkaline laccase in *Streptomyces psammoticus*: Purification and characterization. *Process Biochemistry*, **43**(6), 654-660.
- Ogola, H.J., Kamiike, T., Hashimoto, N., Ashida, H., Ishikawa, T., Shibata, H., Sawa, Y. 2009. Molecular characterization of a novel peroxidase from the cyanobacterium *Anabaena* sp. strain PCC 7120. *Applied Environmental Microbiology*, **75**(23), 7509-7518.
- Olsen, M., Iverson, B., Georgiou, G. 2000. High-throughput screening of enzyme libraries. *Current Opinion in Biotechnology*, **11**(4), 331-337.
- Ostafe, R. 2013. Development of high throughput screening systems of mutant libraries for sugar modifying enzymes (glucose oxidase and cellulases), Aachen, Techn. Hochsch., Diss., 2013.
- Ostafe, R., Prodanovic, R., Nazor, J., Fischer, R. 2014. Ultra-high-throughput screening method for the directed evolution of glucose oxidase. *Chemical Biology*, **21**(3), 414-421.
- Otsuka, Y., Sonoki, T., Ikeda, S., Kajita, S., Nakamura, M., Katayama, Y. 2003. Detection and characterization of a novel extracellular fungal enzyme that catalyzes the specific and hydrolytic cleavage of lignin guaiacylglycerol β -aryl ether linkages. *European journal of biochemistry*, **270**(11), 2353-2362.
- Pandey, A. 2006. *Enzyme technology*. Springer Science & Business Media.
- Pardo, I., Camarero, S. 2015. Exploring the oxidation of lignin-derived phenols by a library of laccase mutants. *Molecules*, **20**(9), 15929-15943.
- Patel, S.C., Hecht, M.H. 2012. Directed evolution of the peroxidase activity of a de novo-designed protein. *Protein Engineering Design & Selection*, **25**(9), 445-451.
- Pereira, L., Coelho, A.V., Viegas, C.A., Santos, M.M., Robalo, M.P., Martins, L.O. 2009. Enzymatic biotransformation of the azo dye Sudan Orange G with bacterial CotA-laccase. *Journal of Biotechnology*, **139**(1), 68-77.
- Picart, P., de Maria, P.D., Schallmeyer, A. 2015. From gene to biorefinery: microbial beta-etherases as promising biocatalysts for lignin valorization. *Frontiers in Microbiology*, **6**.
- Picart, P., Muller, C., Mottweiler, J., Wiermans, L., Bolm, C., Dominguez de Maria, P., Schallmeyer, A. 2014. From gene towards selective biomass valorization: bacterial beta-etherases with catalytic activity on lignin-like polymers. *ChemSusChem*, **7**(11), 3164-3171.
- Pines, O., Inouye, M. 1999. Expression and secretion of proteins in *E. coli*. *Molecular Biotechnology*, **12**(1), 25-34.

References

- Piscitelli, A., Pezzella, C., Giardina, P., Faraco, V., Giovanni, S. 2010. Heterologous laccase production and its role in industrial applications. *Bioengineered Bugs*, **1**(4), 252-262.
- Pollegioni, L., Tonin, F., Rosini, E. 2015. Lignin-degrading enzymes. *FEBS Journal*, **282**(7), 1190-1213.
- Pometto, A.L., Crawford, D.L. 1986. Effects of pH on lignin and cellulose degradation by *Streptomyces viridosporus*. *Applied and Environmental Microbiology*, **52**(2), 246-250.
- Qiu, W.H., Chen, H.Z. 2012. Enhanced the enzymatic hydrolysis efficiency of wheat straw after combined steam explosion and laccase pretreatment. *Bioresource Technology*, **118**, 8-12.
- Rahmanpour, R., Bugg, T.D. 2015a. Characterisation of Dyp-type peroxidases from *Pseudomonas fluorescens* Pf-5: Oxidation of Mn(II) and polymeric lignin by Dyp1B. *Archives of Biochemistry and Biophysics*, **574**, 93-98.
- Rahmanpour, R., Bugg, T.D.H. 2016. Chapter 14 structure and reactivity of the Dye-decolorizing Peroxidase (DyP) family in Heme Peroxidases, *The Royal Society of Chemistry*, 334-357.
- Rahmanpour, R., Bugg, T.D.H. 2015b. Characterisation of Dyp-type peroxidases from *Pseudomonas fluorescens* Pf-5: Oxidation of Mn(II) and polymeric lignin by Dyp1B. *Archives of Biochemistry and Biophysics*, **574**, 93-98.
- Rahmanpour, R., Rea, D., Jamshidi, S., Fulop, V., Bugg, T.D.H. 2016. Structure of *Thermobifida fusca* DyP-type peroxidase and activity towards Kraft lignin and lignin model compounds. *Archives of Biochemistry and Biophysics*, **594**, 54-60.
- Ramachandra, M., Crawford, D.L., Pometto, A.L. 1987. Extracellular enzyme activities during lignocellulose degradation by *Streptomyces* spp.: A Comparative Study of wild-type and genetically manipulated strains. *Applied and Environmental Microbiology*, **53**(12), 2754-2760.
- Retallack, D.M., Jin, H.F., Chew, L. 2012. Reliable protein production in a *Pseudomonas fluorescens* expression system. *Protein Expression and Purification*, **81**(2), 157-165.
- Retallack, D.M., Squires, C.H., Watkins, D.C., Gaertner, F.H., Lee, S.L., Shutter, R. 2005. Expression of mammalian proteins in *Pseudomonas fluorescens*, Google Patents.
- Rinaldi, R., Jastrzebski, R., Clough, M.T., Ralph, J., Kennema, M., Bruijninx, P.C.A., Weckhuysen, B.M. 2016. Paving the way for lignin valorisation: Recent advances in bioengineering, biorefining and catalysis. *Angewandte Chemie-International Edition*, **55**(29), 8164-8215.
- Rippert, P., Puyaubert, J., Grisolle, D., Derrier, L., Matringe, M. 2009. Tyrosine and phenylalanine are synthesized within the plastids in *Arabidopsis*. *Plant Physiology*, **149**(3), 1251-1260.
- Roberts, J.N., Singh, R., Grigg, J.C., Murphy, M.E., Bugg, T.D., Eltis, L.D. 2011. Characterization of dye-decolorizing peroxidases from *Rhodococcus jostii* RHA1. *Biochemistry*, **50**(23), 5108-5119.
- Robinson, P.K. 2015. Enzymes: principles and biotechnological applications. *Understanding Biochemistry: Enzymes and Membranes*, **59**, 1-41.
- Rodriguez Couto, S., Toca Herrera, J.L. 2006. Industrial and biotechnological applications of laccases: a review. *Biotechnology Advances*, **24**(5), 500-513.
- Rosano, G.L., Ceccarelli, E.A. 2014. Recombinant protein expression in *Escherichia coli*: advances and challenges. *Frontiers in Microbiology*, **5**, 172.
- Rosenberg, A.H., Lade, B.N., Chui, D.S., Lin, S.W., Dunn, J.J., Studier, F.W. 1987. Vectors for selective expression of cloned DNAs by T7 RNA-Polymerase. *Gene*, **56**(1), 125-135.
- Rosenberg, A.H., Studier, F.W. 1987. T7 RNA-polymerase can direct expression of Influenza-Virus capsid-binding protein (Pb2) in *Escherichia coli*. *Gene*, **59**(2-3), 191-200.
- Roth, S., Spiess, A.C. 2015. Laccases for biorefinery applications: a critical review on challenges and perspectives. *Bioprocess Biosystems Engineering*, **38**(12), 2285-2313.
- Ruijsenaars, H.J., Hartmans, S. 2004. A cloned *Bacillus halodurans* multicopper oxidase exhibiting alkaline laccase activity. *Applied Microbiology Biotechnology*, **65**(2), 177-182.
- Rulli, M.C., Bellomi, D., Cazzoli, A., De Carolis, G., D'Odorico, P. 2016. The water-land-food nexus of first-generation biofuels. *Scientific Reports*, **6**, 22521.
- Ryu, K., Hwang, S.Y., Kim, K.H., Kang, J.H., Lee, E.K. 2008a. Functionality improvement of fungal lignin peroxidase by DNA shuffling for 2,4-dichlorophenol degradability and H₂O₂ stability. *Journal of Biotechnology*, **133**(1), 110-115.

References

- Ryu, K., Kang, J.H., Wang, L.S., Lee, E.K. 2008b. Expression in yeast of secreted lignin peroxidase with improved 2,4-dichlorophenol degradability by DNA shuffling. *Journal of Biotechnology*, **135**(3), 241-246.
- Sakamoto, T., Yao, Y., Hida, Y., Honda, Y., Watanabe, T., Hashigaya, W., Suzuki, K., Irie, T. 2012. A calmodulin inhibitor, W-7 influences the effect of cyclic adenosine 3', 5'-monophosphate signaling on ligninolytic enzyme gene expression in *Phanerochaete chrysosporium*. *Amb Express*, **2**.
- Salvachua, D., Prieto, A., Martinez, A.T., Martinez, M.J. 2013. Characterization of a novel dye-decolorizing peroxidase (DyP)-type enzyme from *Irpex lacteus* and its application in enzymatic hydrolysis of wheat straw. *Applied Environmental Microbiology*, **79**(14), 4316-4324.
- Samant, S., Gupta, G., Karthikeyan, S., Haq, S.F., Nair, A., Sambasivam, G., Sukumaran, S. 2014. Effect of codon-optimized *E. coli* signal peptides on recombinant *Bacillus stearothermophilus* maltogenic amylase periplasmic localization, yield and activity. *Journal of Industrial Microbiology Biotechnology*, **41**(9), 1435-1442.
- Sambrook, J., Russell, D. 2001. Molecular cloning: A laboratory manual, *Cold Spring Harbor Laboratory Press*, **3**, 17-32.
- Sanchez-Amat, A., Lucas-Elio, P., Fernandez, E., Garcia-Borron, J.C., Solano, F. 2001. Molecular cloning and functional characterization of a unique multipotent polyphenol oxidase from *Marinomonas mediterranea*. *Biochimica et Biophysica Acta*, **1547**(1), 104-116.
- Saritha, M., Arora, A., Lata. 2012. Biological pretreatment of lignocellulosic substrates for enhanced delignification and enzymatic digestibility. *Indian Journal of Microbiology*, **52**(2), 122-130.
- Schein, C.H. 1989. Production of soluble recombinant proteins in bacteria. *Nature Biotechnology*, **7**(11), 1141-1149.
- Schubert, C. 2006. Can biofuels finally take center stage? *Nature Biotechnology*, **24**(7), 777-784.
- Sezer, M., Santos, A., Kielb, P., Pinto, T., Martins, L.O., Todorovic, S. 2013. Distinct structural and redox properties of the heme active site in bacterial dye decolorizing peroxidase-type peroxidases from two subfamilies: Resonance Raman and electrochemical study. *Biochemistry*, **52**(18), 3074-3084.
- Shakeri, M., Sugano, Y., Shoda, M. 2008. Stable repeated-batch production of recombinant dye-decolorizing peroxidase (rDyP) from *Aspergillus oryzae*. *Journal of Bioscience and Bioengineering*, **105**(6), 683-686.
- Shivange, A.V., Marienhagen, J., Mundhada, H., Schenk, A., Schwaneberg, U. 2009. Advances in generating functional diversity for directed protein evolution. *Current Opinion in Chemical Biology*, **13**(1), 19-25.
- Shleev, S.V., Morozova, O.V., Nikitina, O.V., Gorshina, E.S., Rusinova, T.V., Serezhenkov, V.A., Burbaev, D.S., Gazaryan, I.G., Yaropolov, A.I. 2004. Comparison of physico-chemical characteristics of four laccases from different basidiomycetes. *Biochimie*, **86**(9-10), 693-703.
- Shrestha, R., Chen, X.J., Ramyar, K.X., Hayati, Z., Carlson, E.A., Bossmann, S.H., Song, L.K., Geisbrecht, B.V., Li, P. 2016. Identification of surface-exposed protein radicals and a substrate oxidation site in A-class dye-decolorizing peroxidase from *Thermomonospora curvata*. *Acs Catalysis*, **6**(12), 8036-8047.
- Si, W., Wu, Z., Wang, L., Yang, M., Zhao, X. 2015. Enzymological characterization of Atm, the first laccase from *Agrobacterium* sp. S5-1, with the ability to enhance *in vitro* digestibility of maize straw. *PLoS One*, **10**(5), e0128204.
- Singh, G., Batish, M., Sharma, P., Capalash, N. 2009. Xenobiotics enhance laccase activity in alkali-tolerant gamma-*Proteobacterium* JB. *Brazilian Journal of Microbiology*, **40**(1), 26-30.
- Singh, M.V., Weil, P.A. 2002. A method for plasmid purification directly from yeast. *Analytical Biochemistry*, **307**(1), 13-17.
- Singh, P., Sharma, L., Kulothungan, S.R., Adkar, B.V., Prajapati, R.S., Ali, P.S., Krishnan, B., Varadarajan, R. 2013. Effect of signal peptide on stability and folding of *Escherichia coli* thioredoxin. *PLoS One*, **8**(5), e63442.

References

- Singh, R., Eltis, L.D. 2015. The multihued palette of dye-decolorizing peroxidases. *Archives of Biochemistry and Biophysics*, **574**, 56-65.
- Sinirlioglu, Z.A., Sinirlioglu, D., Akbas, F. 2013. Preparation and characterization of stable cross-linked enzyme aggregates of novel laccase enzyme from *Shewanella putrefaciens* and using malachite green decolorization. *Bioresource Technology*, **146**, 807-811.
- Sletta, H., Tondervik, A., Hakvag, S., Aune, T.E.V., Nedal, A., Aune, R., Evensen, G., Valla, S., Ellingsen, T.E., Brautaset, T. 2007. The presence of N-terminal secretion signal sequences leads to strong stimulation of the total expression levels of three tested medically important proteins during high-cell-density cultivations of *Escherichia coli*. *Applied and Environmental Microbiology*, **73**(3), 906-912.
- Statistics, I. 2011. CO₂ emissions from fuel combustion-highlights. IEA, Paris <http://www.iea.org/co2highlights/co2highlights.pdf>. Cited July.
- Studier, F.W., Moffatt, B.A. 1986. Use of bacteriophage-T7 RNA-polymerase to direct selective high-level expression of cloned genes. *Journal of Molecular Biology*, **189**(1), 113-130.
- Studier, F.W., Rosenberg, A.H., Dunn, J.J., Dubendorff, J.W. 1990. Use of T7 RNA-polymerase to direct expression of cloned genes. *Methods in Enzymology*, **185**, 60-89.
- Sugano, Y. 2009. DyP-type peroxidases comprise a novel heme peroxidase family. *Cellular and Molecular Life Sciences*, **66**(8), 1387-403.
- Sukumaran, R.K., Singhanian, R.R., Pandey, A. 2005. Microbial cellulases - Production, applications and challenges. *Journal of Scientific & Industrial Research*, **64**(11), 832-844.
- Sutter, M., Boehringer, D., Gutmann, S., Guenther, S., Prangishvili, D., Loessner, M.J., Stetter, K.O., Weber-Ban, E., Ban, N. 2008. Structural basis of enzyme encapsulation into a bacterial nanocompartment. *Nature Structural & Molecular Biology*, **15**(9), 939-947.
- Suzuki, T., Endo, K., Ito, M., Tsujibo, H., Miyamoto, K., Inamori, Y. 2003. A thermostable laccase from *Streptomyces lavendulae* REN-7: Purification, characterization, nucleotide sequence, and expression. *Bioscience Biotechnology and Biochemistry*, **67**(10), 2167-2175.
- Tanamura, K., Abe, T., Kamimura, N., Kasai, D., Hishiyama, S., Otsuka, Y., Nakamura, M., Kajita, S., Katayama, Y., Fukuda, M. 2011. Characterization of the third glutathione S-transferase gene involved in enantioselective cleavage of the β -aryl ether by *Sphingobium* sp. strain SYK-6. *Bioscience, biotechnology, and biochemistry*, **75**(12), 2404-2407.
- Tao, Z. 2012. Cellulose hydrolysis with ph adjustment, Google Patents.
- Tapin, S., Sigoillot, J.C., Asther, M., Petit-Conil, M. 2006. Feruloyl esterase utilization for simultaneous processing of nonwood plants into phenolic compounds and pulp fibers. *Journal of Agricultural and Food Chemistry*, **54**(10), 3697-3703.
- Thomas, M., Barker, G., Furness, P.N. 1998. A semi-quantitative approach to in situ zymography using tissue sections. *Journal of Pathology*, **186**, 4a-4a.
- Thurston, C.F. 1994. The structure and function of fungal laccases. *Microbiology-Sgm*, **140**, 19-26.
- Tien, M., Kirk, T.K. 1983. Lignin-degrading enzyme from the hymenomycete *Phanerochaete chrysosporium* burds. *Science*, **221**(4611), 661-663.
- Tomoyasu, T., Mogk, A., Langen, H., Goloubinoff, P., Bukau, B. 2001. Genetic dissection of the roles of chaperones and proteases in protein folding and degradation in the *Escherichia coli* cytosol. *Molecular Microbiology*, **40**(2), 397-413.
- Tonin, F., Melis, R., Cordes, A., Sanchez-Amat, A., Pollegioni, L., Rosini, E. 2016. Comparison of different microbial laccases as tools for industrial uses. *Nature Biotechnology*, **33**(3), 387-398.
- Turlin, E., Debarbouille, M., Augustyniak, K., Gilles, A.M., Wandersman, C. 2013. *Staphylococcus aureus* FepA and FepB proteins drive heme iron utilization in *Escherichia coli*. *PLoS One*, **8**(2), e56529.
- Turner, N.J. 2009. Directed evolution drives the next generation of biocatalysts. *Nature Chemical Biology*, **5**(8), 568-574.
- Ulmer, D.C., Leisola, M.S., Schmidt, B.H., Fiechter, A. 1983. Rapid degradation of isolated lignins by *Phanerochaete chrysosporium*. *Applied and Environmental Microbiology*, **45**(6), 1795-1801.

References

- Uzal, E.N., Ros, L.V.G., Pomar, F., Bernal, M.A., Paradela, A., Albar, J.P., Barcelo, A.R. 2009. The presence of sinapyl lignin in Ginkgo biloba cell cultures changes our views of the evolution of lignin biosynthesis. *Physiologia Plantarum*, **135**(2), 196-213.
- Valentine, J., Clifton-Brown, J., Hastings, A., Robson, P., Allison, G., Smith, P. 2012. Food vs. fuel: the use of land for lignocellulosic next generation' energy crops that minimize competition with primary food production. *Global Change Biology Bioenergy*, **4**(1), 1-19.
- van Bloois, E., Pazmino, D.E.T., Winter, R.T., Fraaije, M.W. 2010. A robust and extracellular heme-containing peroxidase from *Thermobifida fusca* as prototype of a bacterial peroxidase superfamily. *Applied Microbiology and Biotechnology*, **86**(5), 1419-1430.
- Van Dyk, J.S., Pletschke, B.I. 2012. A review of lignocellulose bioconversion using enzymatic hydrolysis and synergistic cooperation between enzymes-Factors affecting enzymes, conversion and synergy. *Biotechnology Advances*, **30**(6), 1458-1480.
- van Groenestijn, J.W., Jetten, J.M., van Deventer, H.C., Slomp, R., Slaghek, T.M. 2012. Novel method for processing lignocellulose containing material, Google Patents.
- Vanholme, R., Demedts, B., Morreel, K., Ralph, J., Boerjan, W. 2010. Lignin biosynthesis and structure. *Plant Physiology*, **153**(3), 895-905.
- Velaithan, V., Chin, S.C., Yusoff, K., Illias, R.M., Rahim, R.A. 2014. Novel synthetic signal peptides for the periplasmic secretion of green fluorescent protein in *Escherichia coli*. *Annals of Microbiology*, **64**(2), 543-550.
- Weiner, M., Anderson, C., Jerpseth, B., Wells, S., Johnson-Browne, B., Vaillancourt, P. 1994. Studier pET system vectors and hosts. *Strategies in Molecular Biology*, **7**(4).
- Weinstein, D.A., Gold, M.H. 1979. Synthesis of guaiacylglycol and glycerol- β -O (- β -methyl umbelliferyl) ethers: Lignin model Substrates for the possible fluorometric assay of β -etherases. *Holzforchung*, **33**, 134-135.
- Widsten, P., Kandelbauer, A. 2008. Laccase applications in the forest products industry: A review. *Enzyme and Microbial Technology*, **42**(4), 293-307.
- Wong, T.S., Wu, N., Roccatano, D., Zacharias, M., Schwaneberg, U. 2005. Sensitive assay for laboratory evolution of hydroxylases toward aromatic and heterocyclic compounds. *Journal of Biomolecular Screening*, **10**(3), 246-252.
- Wong, T.S., Zhurina, D., Schwaneberg, U. 2006. The diversity challenge in directed protein evolution. *Combinatorial Chemistry and High Throughput Screening*, **9**(4), 271-288.
- Woolridge, E.M. 2014. Mixed enzyme systems for delignification of lignocellulosic biomass. *Catalysts*, **4**(1), 1-35.
- Xu, H.F., Li, B., Mu, X.D. 2016. Review of Alkali-based pretreatment to enhance enzymatic saccharification for lignocellulosic biomass conversion. *Industrial & Engineering Chemistry Research*, **55**(32), 8691-8705.
- Yoshida, T., Sugano, Y. 2015. A structural and functional perspective of DyP-type peroxidase family. *Archives of Biochemistry and Biophysics*, **574**, 49-55.
- Yoshida, T., Tsuge, H., Hisabori, T., Sugano, Y. 2012. Crystal structures of dye-decolorizing peroxidase with ascorbic acid and 2,6-dimethoxyphenol. *FEBS Lett*, **586**(24), 4351-4356.
- Yu, Y., Lou, X., Wu, H.W. 2008. Some recent advances in hydrolysis of biomass in hot-compressed, water and its comparisons with other hydrolysis methods. *Energy & Fuels*, **22**(1), 46-60.
- Zaburanyi, N., Rabyk, M., Ostash, B., Fedorenko, V., Luzhetskyy, A. 2014. Insights into naturally minimised *Streptomyces albus* J1074 genome. *Bmc Genomics*, **15**:97.
- Zakzeski, J., Jongorius, A.L., Bruijninx, P.C., Weckhuysen, B.M. 2012. Catalytic lignin valorization process for the production of aromatic chemicals and hydrogen. *ChemSusChem*, **5**(8), 1602-1609.
- Zhou, J., Wang, Y.H., Chu, J., Luo, L.Z., Zhuang, Y.P., Zhang, S.L. 2009. Optimization of cellulase mixture for efficient hydrolysis of steam-exploded corn stover by statistically designed experiments. *Bioresource Technology*, **100**(2), 819-825.
- Zhou, X.L., Vize, P.D. 2004. Proximo-distal specialization of epithelial transport processes within the *Xenopus* pronephric kidney tubules. *Developmental Biology*, **271**(2), 322-338.

References

- Zubieta, C., Joseph, R., Krishna, S.S., McMullan, D., Kapoor, M., Axelrod, H.L., Miller, M.D., Abdubek, P., Acosta, C., Astakhova, T., Carlton, D., Chiu, H.J., Clayton, T., Deller, M.C., Duan, L., Elias, Y., Elsliger, M.A., Feuerhelm, J., Grzechnik, S.K., Hale, J., Han, G.W., Jaroszewski, L., Jin, K.K., Klock, H.E., Knuth, M.W., Kozbial, P., Kumar, A., Marciano, D., Morse, A.T., Murphy, K.D., Nigoghossian, E., Okach, L., Oommachen, S., Reyes, R., Rife, C.L., Schimmel, P., Trout, C.V., van den Bedem, H., Weekes, D., White, A., Xu, Q., Hodgson, K.O., Wooley, J., Deacon, A.M., Godzik, A., Lesley, S.A., Wilson, I.A. 2007a. Identification and structural characterization of heme binding in a novel dye-decolorizing peroxidase, TyrA. *Proteins*, **69**(2), 234-243.
- Zubieta, C., Krishna, S.S., Kapoor, M., Kozbial, P., McMullan, D., Axelrod, H.L., Miller, M.D., Abdubek, P., Ambing, E., Astakhova, T., Carlton, D., Chiu, H.J., Clayton, T., Deller, M.C., Duan, L., Elsliger, M.A., Feuerhelm, J., Grzechnik, S.K., Hale, J., Hampton, E., Han, G.W., Jaroszewski, L., Jin, K.K., Klock, H.E., Knuth, M.W., Kumar, A., Marciano, D., Morse, A.T., Nigoghossian, E., Okach, L., Oommachen, S., Reyes, R., Rife, C.L., Schimmel, P., van den Bedem, H., Weekes, D., White, A., Xu, Q., Hodgson, K.O., Wooley, J., Deacon, A.M., Godzik, A., Lesley, S.A., Wilson, I.A. 2007b. Crystal structures of two novel dye-decolorizing peroxidases reveal a beta-barrel fold with a conserved heme-binding motif. *Proteins*, **69**(2), 223-233.

8.0 Appendix

8.1 Primer list

Primer number	Primer name	Sequence (5'→3') (Letters in lower case indicate overlapping regions for Gibson clonings)
<i>Tfu1</i>	<i>TfuDyP-Tat-NdeI</i>	GGAATTCATATGGAATTCGATGACCGAACCCAGAC
<i>Tfu2</i>	<i>TfuDyP-Tat-XhoI</i>	AAGCTCGAGTCCTTCGATCAGGTCCTGTCC
<i>Tfu3</i>	<i>TfuDyP-pelB-HindIII</i>	CCCAAGCTTCACCCCTGCTGCCCGACTC
<i>Tfu4</i>	<i>TfuDyP-pelB-XhoI</i>	TAAACTCGAGTCCTTCGATCAGGTCCTG
<i>Tfu5</i>	<i>TfuDyP-cp-NdeI</i>	GGGTTTCATATGCCCTGCTGCCCGACTCCGAC
<i>Tfu6</i>	<i>TfuDyP-cp-XhoI</i>	CCGCTCGAGTCCTTCGATCAGGTCCTGTC
<i>Tfu7</i>	<i>TfuDyP-cp-SDM fw</i>	TGGATGGACGGCGGCAGCTACCTGGTCGTGCGACGGATCCGCATG
<i>Tfu8</i>	<i>TfuDyP-cp-SDM rv</i>	CATGCGGATCCGTCGACGACCAGGTAGCTGCCGCCGTCCATCCA
DyPB1	DyPB-pelB-EcoRI	CCGGAATTCACCGGGCCCGGTGGCGCGCC
DyPB2	DyPB-pelB-XhoI	AAGCTCGAGCTGGCTCACGCCTTTCAGGC
DyPB3	GA-DyPB-cp-(NdeI)	ctttaagaaggagatatacaATGCCGGGCCCGGTGGCG
DyPB4	GA-DyPB-cp-(XhoI)	agtgggtggtggtggtgctGCTGCTCACGCCTTTCAGGCCGC
SSHG1	SSHGDyP-cp-NdeI	GGAATTCATATGGAATTCAACTGACCATTGATCCGGGGC
SSHG2	SSHGDyP-cp-XhoI	AAGCTCGAGGCTGGTGCGGCGCGGG
SSHG3	GA-SSHGDyP-pelB-(NcoI)	gctgcccagccggcgatggcATGCTGACCATTGATCCGGGGCGG
SSHG4	GA-SSHGDyP-pelB-(XhoI)	agtgggtggtggtggtgctGCTGGTGCGGCGCGGGTT
Sc1	ScLac-cp-NdeI	CCATATGGAAACCGATATTATTGAACGCCTG
Sc2	ScLac-cp-XhoI	CCTCGAGGAAGCCGGTATGGCCCCG
Sc3	GA-22b fw	TAGTTAGCCGTAGTTAGGCCACCACTTCAAGAACTCTGTAGCACCGCC
Sc4	GA-22b rev	AGGCGTTCAATAATATCGGTGGCCATCGCCGGCTGGGC
Sc5	GA-22b ScLac fw	ACCGATATTATTGAACGCC
Sc6	GA-22b ScLac rev	GCCTAACTACGGCTACAC
E1	GA-LigE-Nhis-(NdeI)	ttaactttaagaaggagatatacatatgcaccaccaccaccaccacGCACGCAATAATACC ATC
E2	GA-LigE-Nhis-(XhoI)	atctcagtgggtggtggtggtgctcagTTAATCTGCTTTTTCTGCAAC
F1	GA-LigF-Nhis-(NdeI)	ttaactttaagaaggagatatacatatgcaccaccaccaccaccacACCCTGAACTGTAT AGC
F2	GA-LigF-Nhis-(XhoI)	atctcagtgggtggtggtggtgctcagTTATGCAACTTTTTCTGTTT
pCT1	<i>TfuDyP-NheI-fw</i>	CTAGCTAGCCCCCTGCTGCCCGACTCC
pCT2	<i>TfuDyP-SalI-rv</i>	CGCGTCGACTCCTTCGATCAGGTCCTGTCC
pCT3	DyPB-NheI-fw	CTAGCTAGCCCCGGGCCCGGTGG
pCT4	DyPB-SalI-rv	CGCGTCGACTGGCTCACGCCTTTCAGG
pCT5	SSHGDyP-NheI-fw	CTAGCTAGCCTGACCATTGATCCGGG
pCT6	SSHGDyP-SalI-rv	CGCGTCGACTGGTGCGGCGCGGGTTC
pCT7	ScLac-NheI-fw	CTAGCTAGCACCGATATTATTGAACGCC
pCT8	ScLac-SalI-rv	CGCGTCGACCGGTATGGCCCCG
T7 pro	T7 promoter	TAATACGACTCACTATAGG
T7 ter	T7 terminator	GCTAGTTATTGCTCAGCGG
Sc seq	ScLac sequencing	AGAAGATGCGCTGCATCTGCC
pCT fw	pCT vector specific forward	AGTAACGTTTGTGAGTAATTGC
pCT rv	pCT vector specific reverse	GTCGATTTTGTACATCTACAC

8.2 List of equipment

Name	Type	Manufacturer
BD FACS Diva (NJ, USA)	Flow cytometry system	BD Biosciences, USA
JEOL GSX Delta 270	NMR	JEOL, USA
Waters LCT ESI mass spectrometer and 2795 HPLC	LC-MS	Waters, UK
Agilent Infinity 1260 (with Agilent Eclipse XDB-C18 (4.6 mm ID x 150 mm, 5µm) column)	HPLC	Agilent Technologies, USA
-20°C premium	Freezer	Liebherr-International AG, Switzerland
Allegra X15R	Centrifuge	Beckman Coulter, Germany
Beckmann Avanti 30	Centrifuge	Beckman Coulter, Germany
Beckmann Avanti J-30i	Centrifuge	Beckman Coulter, Germany
Beckmann Avanti J-E	Centrifuge	Beckman Coulter, Germany
Biophotometer	Photometer	Eppendorf, Germany
Canon PowerShot SX220 HS	Camera	Canon, Germany
Eppendorf Centrifuge 5415 D	Centrifuge	Eppendorf, Germany
GE Äkta pure	FPLC	GE Healthcare, Germany
GE Fraction Collector F9-C	Automated sample collector	GE Healthcare, Germany
Heraeus B12 and UT12	Incubator	Heraeus, Germany
Heraeus HS9	Sterile bench	Heraeus, Germany
Herafreeze	-80°C freezer	Heraeus, Germany
Herolab E.A.S.Y. Win32-System	Gel documentation	Herolab GmbH, Germany
Herolab UVT-20M, wavelength: 302 nm	UV transilluminator	Herolab GmbH, Germany
Ikamag REC-G	Stirrer	IKA Labortechnik, Germany
Infinite M200	96 well plate reader	TECAN Group Ltd, Switzerland
UP200S	Ultrasonic processor	Hielscher Ultrasonics, Germany
Innova 4430 and 4340	Incubator/shaker	New Brunswick Scientific GmbH, Germany
Kuhner ShakerX	Incubator/shaker	Kuhner AG, Switzerland
Mastercycler gradient	PCR cyclers	Eppendorf, Germany
Microfuge R	Centrifuge	Beckman Coulter, Germany
Mini-Protean 3 cell devices	Gel electrophoresis supply	BioRad, Hercules, USA
Mini-Sub Cell GT	Electrophoresis supply	BioRad, Hercules, USA
Multiporator	Electroporation device	Eppendorf, Germany
Nikon CoolPix 4500	Camera	Nikon, Germany
PowerPac 300	Power supply	BioRad, Hercules, USA
Primus 25 advanced	PCR cyclers	MWG Biotech, Germany
Primus 96 Plus	PCR cyclers	MWG Biotech, Germany
Mastercycler	PCR cyclers	Eppendorf, Germany
Sartorius BP 610, 1202 MP and BP 121 S	Scales	Sartorius, Germany
Systemec DE-45	Autoclave	Systemec, Germany
Thermomixer comfort	Temperature controlled mixer	Eppendorf, Germany
Varioklav135 S and 300S EPZ	Autoclave	Thermo Fisher Scientific, USA
Vortex Genie 2	Vortex	Scientific Industries, USA
Wide Mini-Sub Cell GT	Electrophoresis supply	BioRad, USA

8.3 Plasmid maps

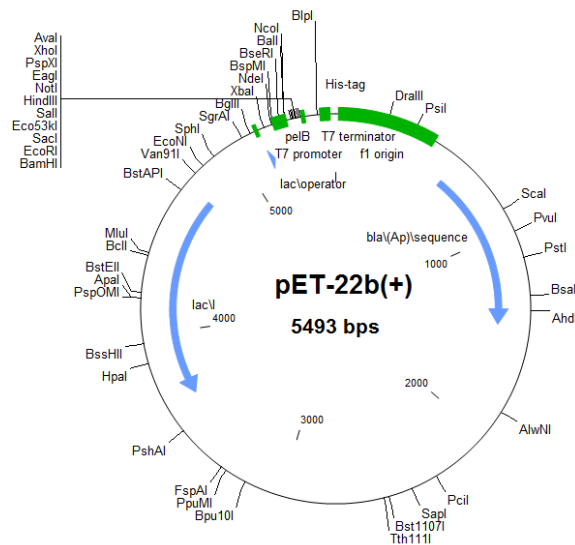


Figure 43: pET-22b(+) vector used as template for vector construction and expression in *E. coli*. Restriction enzyme sites are shown on the outer region of the vector. The vector comprises a number of restriction sites (NcoI-XhoI) present in the multiple cloning site. The origin of replication (pBR322) ensures a medium copy number. T7 promoter provides IPTG-inducible protein expression. lacI: lactose-inducible lac operon transcriptional repressor; pelB: 22-mer long N-terminal leader peptide for potential periplasm localization (pectate lyase B of *Erwinia carotovora* CE); His-tag: hexahistidin-tag at the C-terminus for potential affinity chromatography applications; bla: gene of β -lactamase; f1 origin: origin of phage replication.

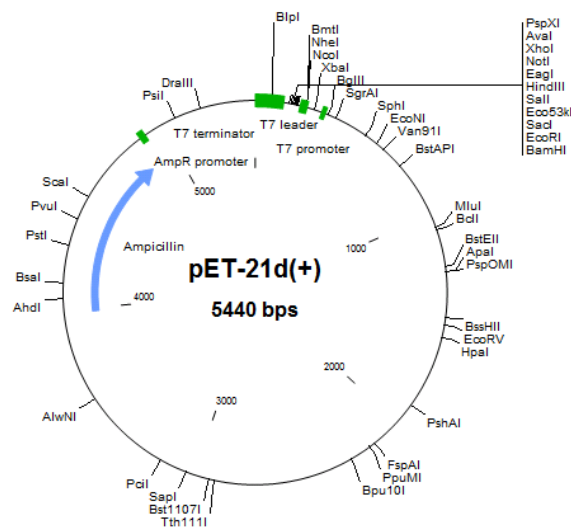


Figure 44: pET-21d(+) vector used as template for vector construction and expression of mutant *TfuDyP* variants and WT-*TfuDyP* in *E. coli*. Restriction enzyme sites are shown on the outer region of the vector. The vector comprises a number of restriction sites (NdeI-NcoI) present in the multiple cloning site. The origin of replication (pBR322) ensures a medium copy number. T7 promoter provides IPTG-inducible protein expression. lacI: lactose-inducible lac operon transcriptional repressor; T7-tag at the N-terminus and His-tag at the C-terminus for potential affinity chromatography applications.

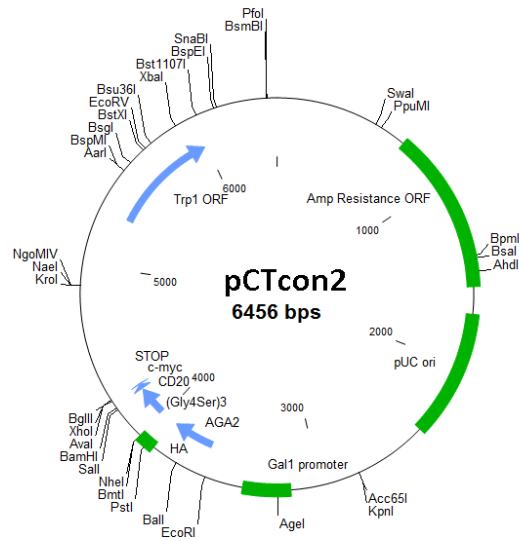


Figure 45: pCTcon2 vector used for construction and expression in *S. cerevisiae* EBV 100 cells for FACS screening. Restriction enzyme sites are shown on the outer region of the vector. Trp1 ORF: gene of phosphoribosylanthranilate isomerase; Amp Resistance ORF: ampicillin resistance gene; pUC ori: a variant of pMB1 origin of replication; Gal1 promoter: Yeast promoter with upstream activating sequence mediating Gal4-dependent induction; HA: Hemagglutinin tag; c-myc: an epitope tag derived from avian myelocytomatosis viral oncogene homolog; AGA2: A-agglutinin-binding subunit; (Gly₄Ser)₃: flexible peptide linker; CD20: B-lymphocyte antigen CD20 a non-glycosylated phosphoprotein expressed on the surface of all mature B-cells.

8.4 Protein and DNA ladder

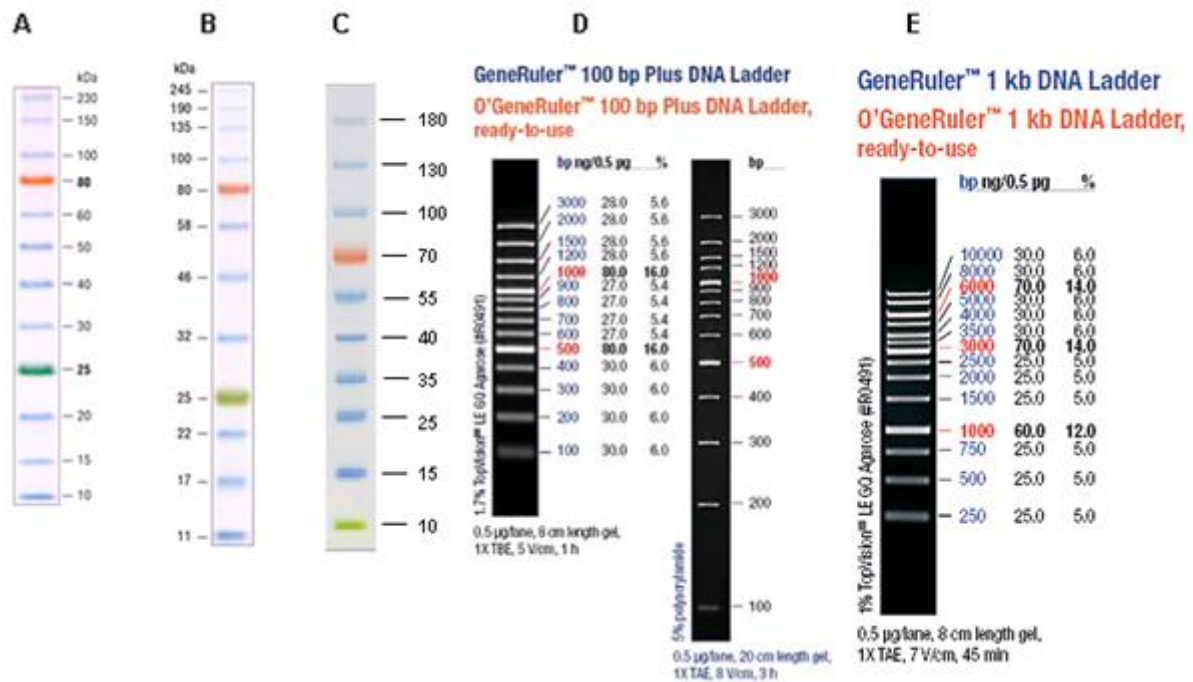


Figure 46: Protein and DNA ladders. A: P7711S ColorPlus™ Prestained Protein Ladder, Broad Range (10-230 kDa) (<https://www.neb.com/products/p7711-colorplus-prestained-protein-ladder-broad-range-10-230-kda>), B: P7712S ColorPlus™ Prestained Protein Ladder, Broad Range (10-230kDa) (<https://www.neb.com/products/p7712-color-prestained-protein-standard-broad-range-11-245-kda>), C: PageRuler™ Prestained Protein Ladder (10 to 180 kDa) (<https://www.thermofisher.com/order/catalog/product/26616>), D: GeneRuler™ 1 kb DNA Ladder (<http://www.thermoscientificbio.com/nucleic-acid-electrophoresis/generuler-1-kb-dna-ladder-ready-to-use-250-to-10000-bp/>), E: GeneRuler™ 100 bp Plus DNA Ladder (<http://www.thermoscientificbio.com/nucleic-acid-electrophoresis/generuler-100-bp-plus-dna-ladder-100-to-3000-bp/>).

8.5 Standard calibration curve of 4-MU (MUAV product)

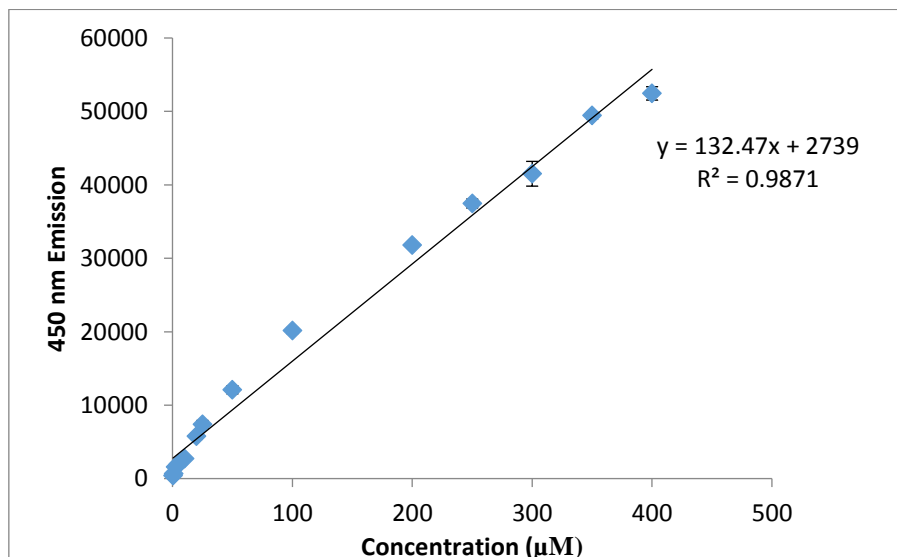


Figure 47: Standard calibration curve for quantification of 4-MU, which is produced as a result of the enzymatic activity of β -etherases on MUAV. Dilution series of stock commercial 4-MU (Sigma) solution was prepared in the range of 0.5-400 μ M and the fluorescence intensity was measured in a plate reader (Infinite® 200 plate reader, Tecan) using an excitation wavelength of 360 nm and an emission wavelength of 450 nm.

8.6 Representative IMAC chromatogram

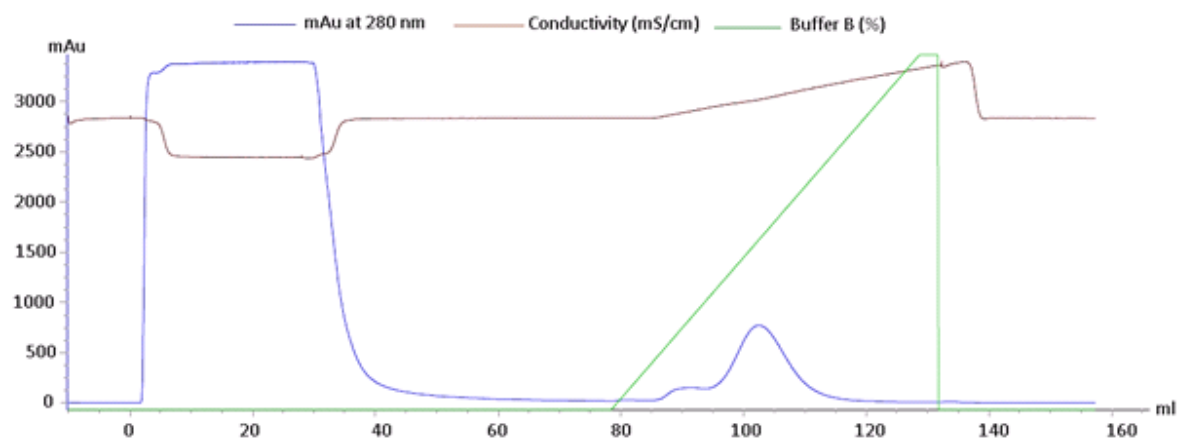


Figure 48: A representative IMAC chromatogram. In the chromatogram, the blue line shows the milliabsorbance (mAu) at 280 nm, the green line shows the buffer B concentration (imidazole gradient (%)), the brown line shows the conductivity (mS cm^{-1}) throughout the purification procedure. The elution of the protein is followed by an obvious increase in A_{280} that builds the elution peak. The elution fractions (95-120 mL), which correspond to that peak are later analysed by SDS-PAGE and western blot. Each construct of all enzymes was purified by IMAC after the heterologous expression. This chromatogram shows the IMAC purification ScLac-cp His₆-tag fusion protein (6.2.9).

8.7 Analysis of ScLac activity on veratryl alcohol by HPLC

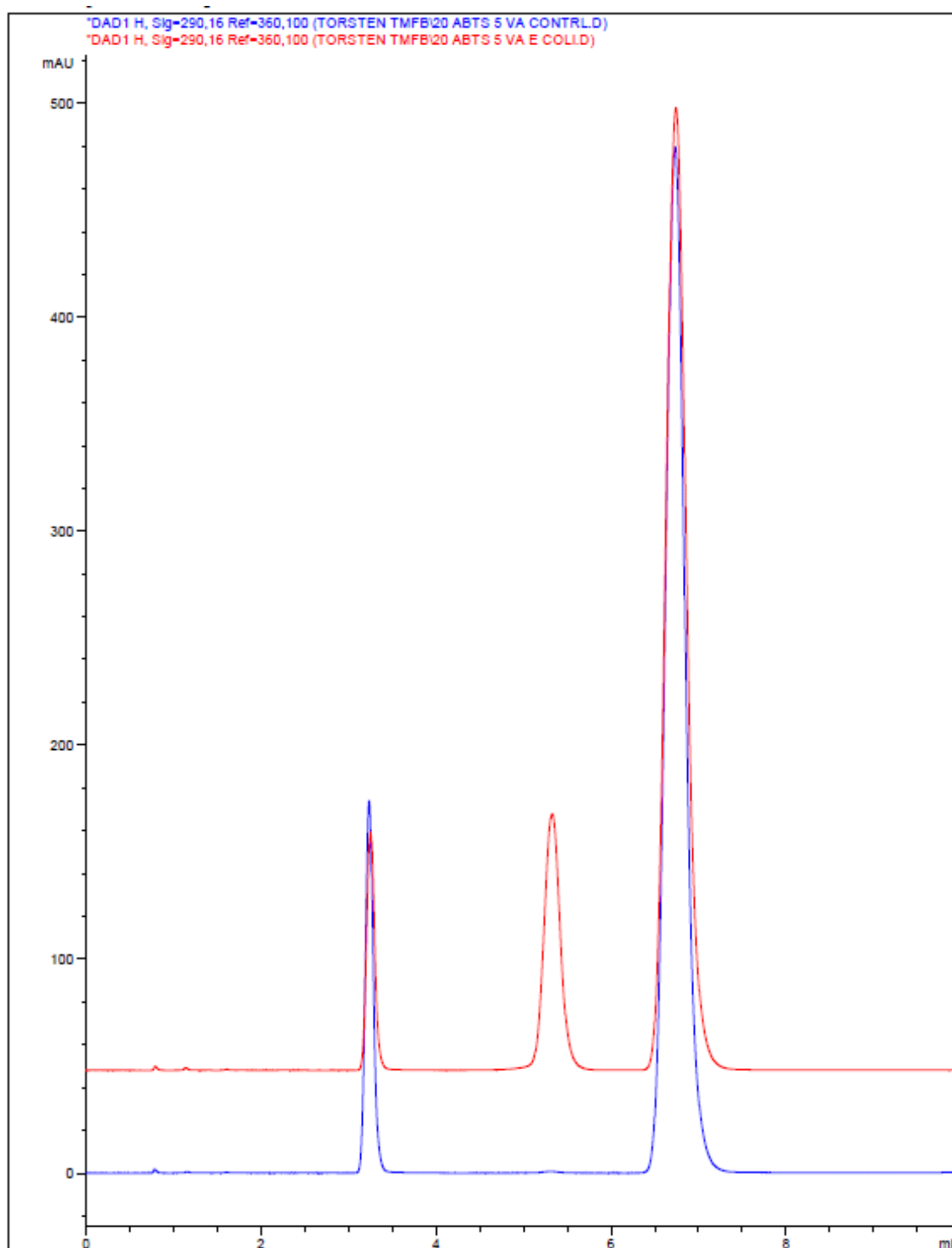


Figure 49: HPLC analysis of ScLac (6.2.19) activity on the non-phenolic substrate veratryl alcohol in the presence of ABTS as the mediator system. 1 μ M ScLac expressed in *E. coli* (6.2.6) was used in the activity assays (6.2.19) towards 5 mM VA at 30°C. 20 mM ABTS was used as the mediator system for the oxidation of the non-phenolic model substrate. A control reaction mixture was also prepared under the same conditions as the enzymatic reaction excluding the enzyme. Red line: Enzymatic reaction. Blue line: Control reaction.

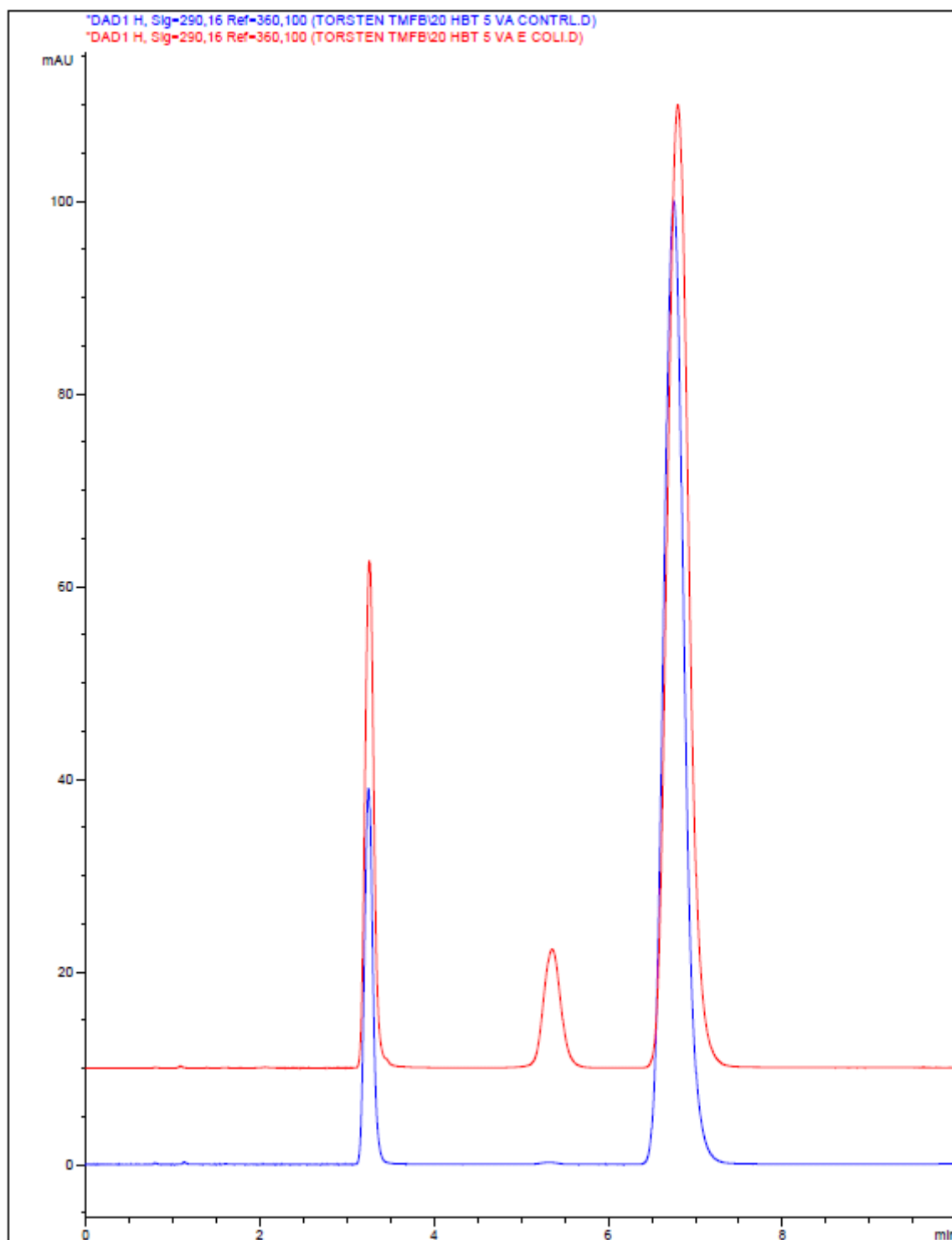


Figure 50: HPLC analysis of ScLac activity (6.2.19) on the non-phenolic substrate veratryl alcohol in the presence of HBT as the mediator system. 1 μ M ScLac expressed in *E. coli* (6.2.6) was used in the activity assays (6.2.19) towards 5 mM VA. 20 mM HBT was used as the mediator system for the oxidation of the non-phenolic model substrate. A control reaction mixture was also prepared under the same conditions as the enzymatic reaction excluding the enzyme. Red line: Enzymatic reaction. Blue line: Control reaction.

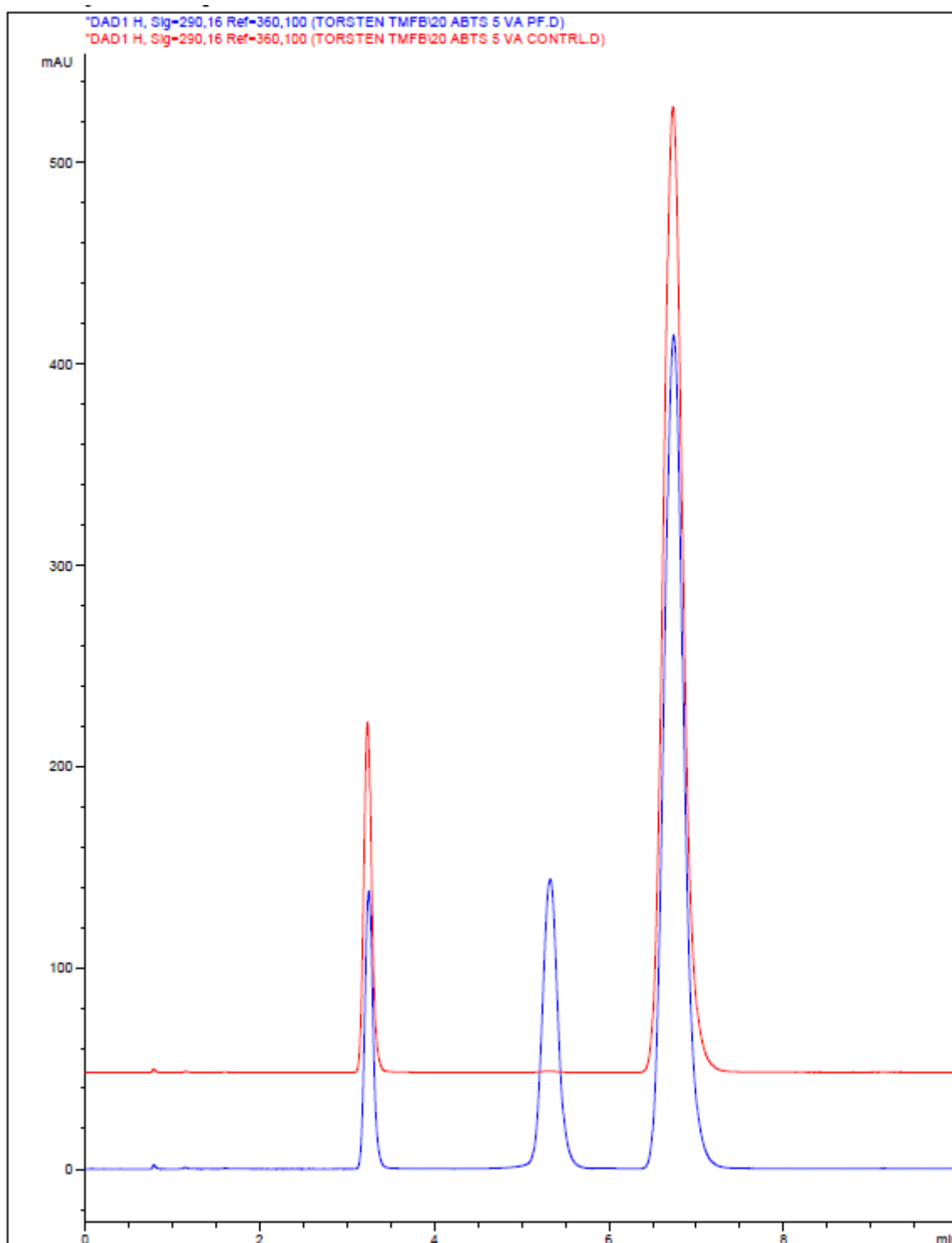


Figure 51: HPLC analysis of ScLac activity (6.2.19) on the non-phenolic substrate veratryl alcohol in the presence of ABTS as the mediator system. 1 μ M ScLac expressed in *P. fluorescens* (6.2.6) was used in the activity assays (6.2.19) towards 5 mM VA. 20 mM ABTS was used as the mediator system for the oxidation of the non-phenolic model substrate. A control reaction mixture was also prepared under the same conditions as the enzymatic reaction excluding the enzyme. Blue line: Enzymatic reaction. Red line: Control reaction.

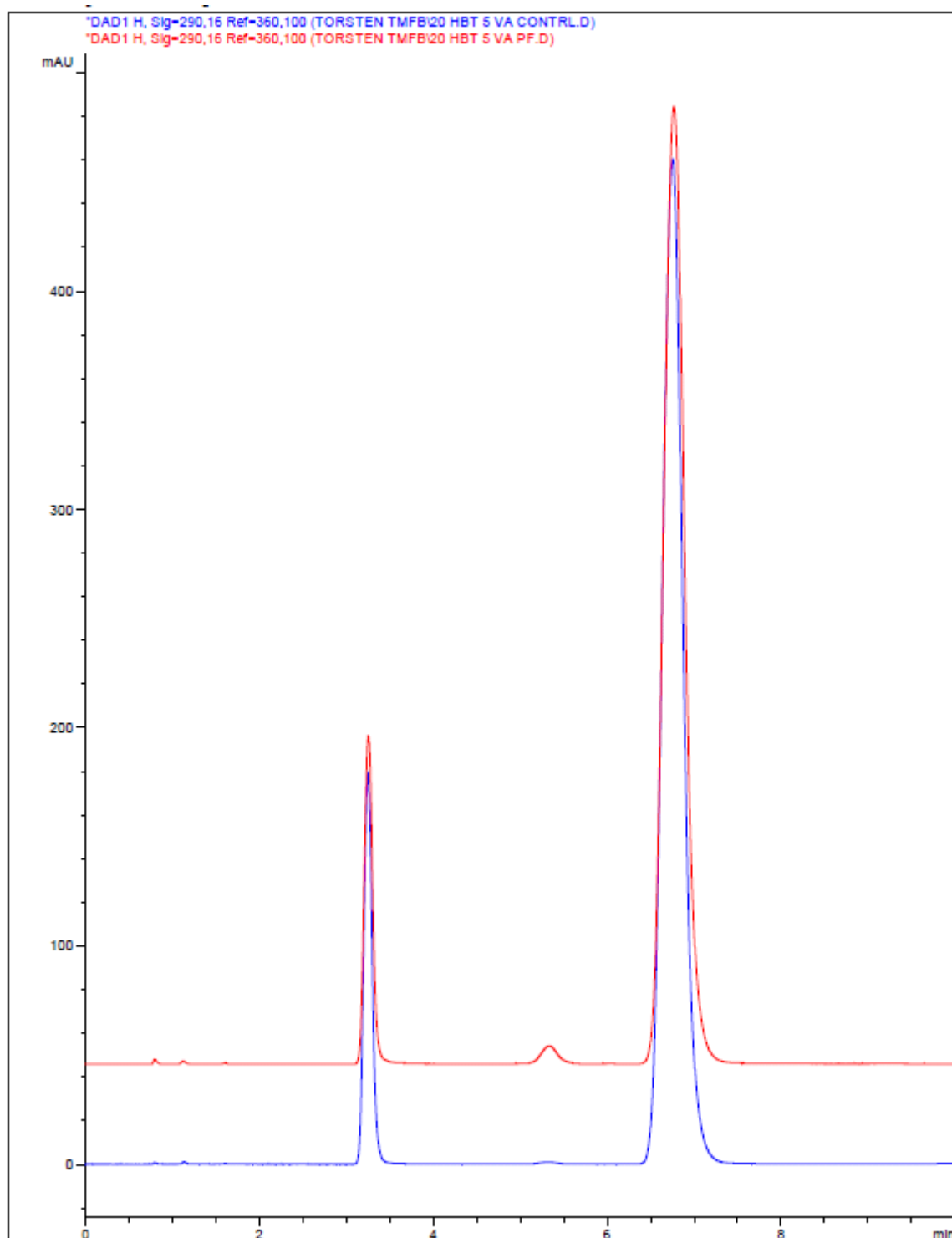


Figure 52: HPLC analysis of Sclac activity (6.2.19) on the non-phenolic substrate veratryl alcohol in the presence of HBT as the mediator system. 1 μ M Sclac expressed in *P. fluorescens* (6.2.6) was used in the activity assays (6.2.19) towards 5 mM VA. 20 mM HBT was used as the mediator system for the oxidation of the non-phenolic model substrate. A control reaction mixture was also prepared under the same conditions as the enzymatic reaction excluding the enzyme. Red line: Enzymatic reaction. Blue line: Control reaction.

8.8 Representative LC-MS analysis of ScLac reaction with the SS β -O-4 OH model

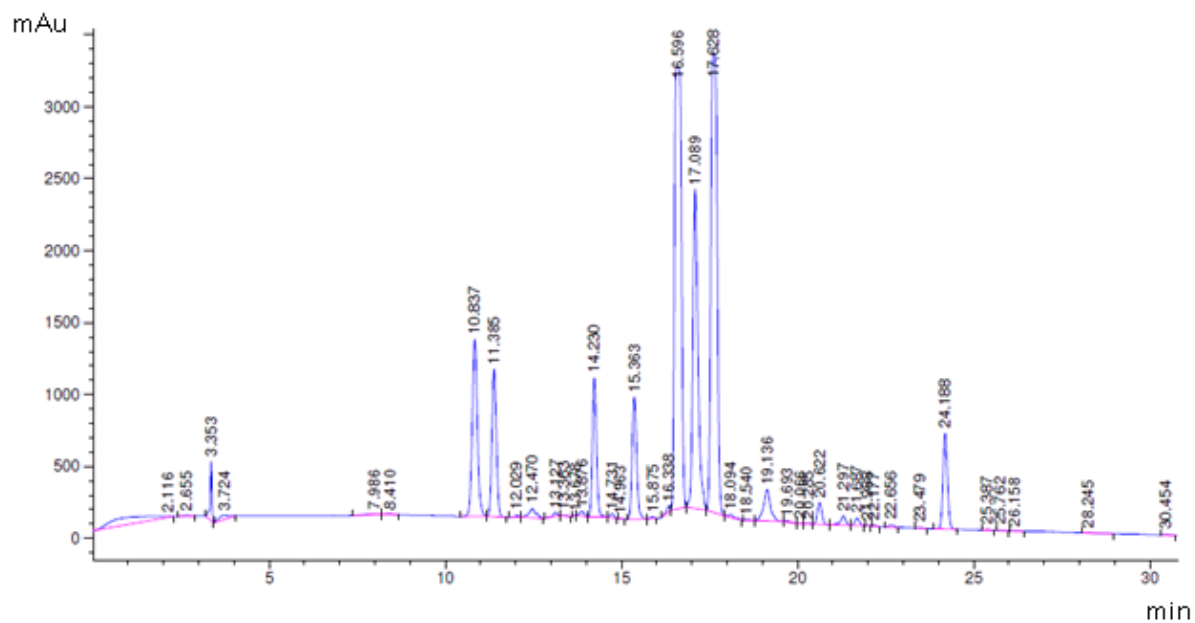


Figure 53: Representative LC-MS chromatogram of the analysis of ScLac reaction with the SS β -O-4 model compound (6.2.18). Peaks in the diagram correspond to the reaction components and putative products of the enzymatic reaction on the substrate and are compared with the theoretical mass calculations of the expected products.

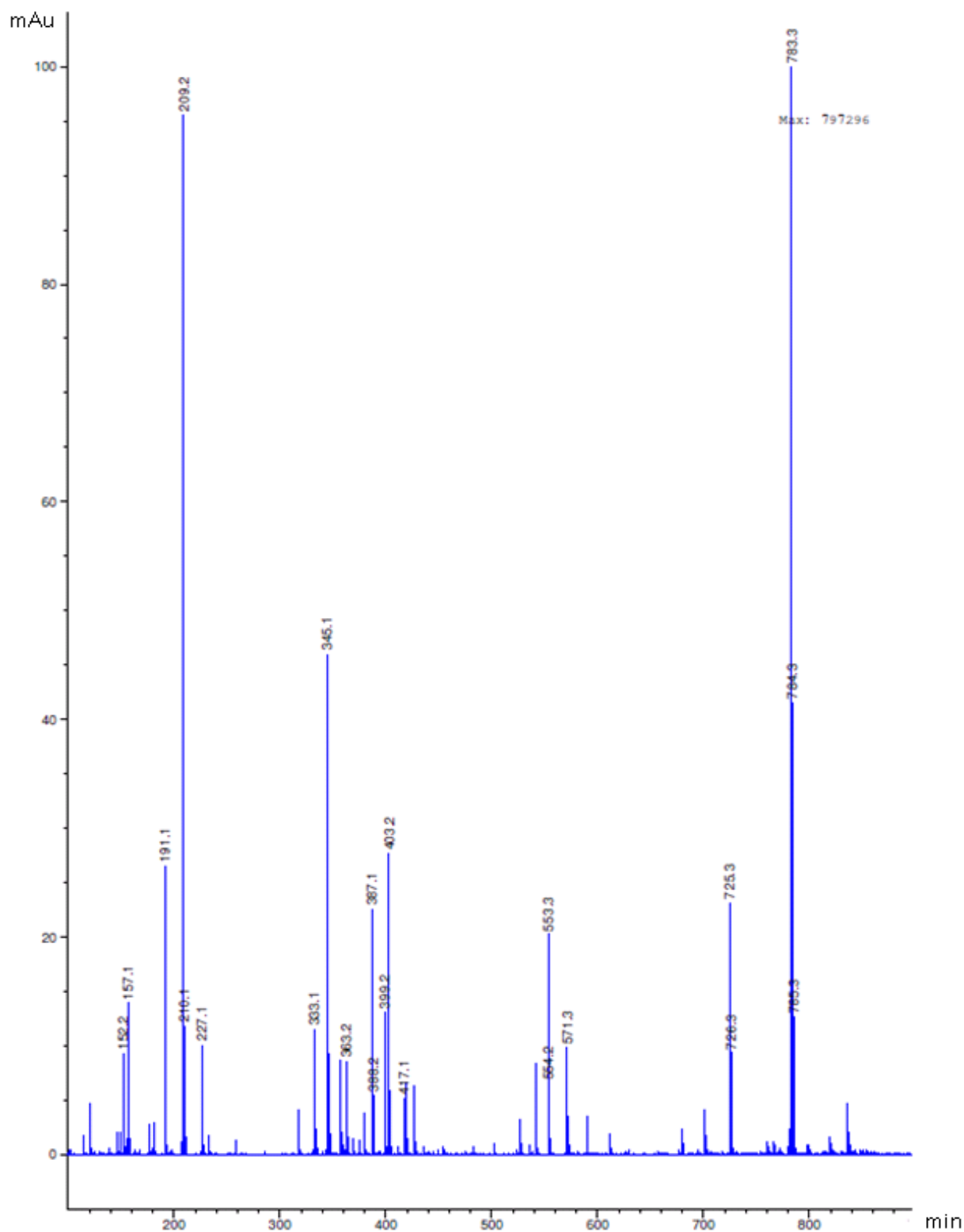


Figure 54: Representative LC-MS chromatogram of the analysis of S_cLac reaction with the SS β-O-4 model compound (6.2.18). Peaks in the diagram correspond to the reaction components and putative products of the enzymatic reaction on the substrate and are compared with the theoretical mass calculations of the expected products.

8.9 Activity analysis of commercial laccase from *T. versicolor* on phenolic SS β -O-4 OH lignin-model compound

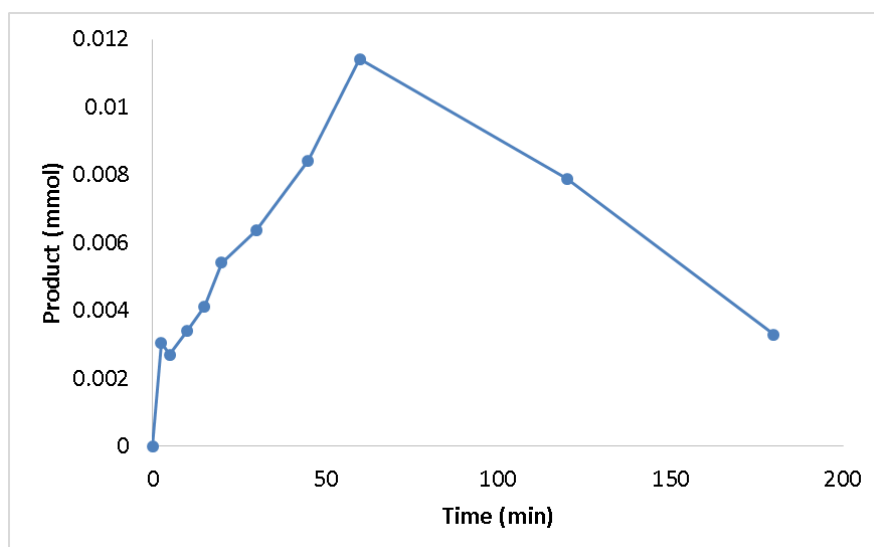


Figure 55: Activity analysis of laccase from *T. versicolor* towards the phenolic SS β -O-4 OH lignin-model compound (6.2.18). All conditions were kept similar to recombinant ScLac and equal amounts of specific activities were used in the activity assay for a better comparison.

8.10 Initial activity assays with Kraft lignin

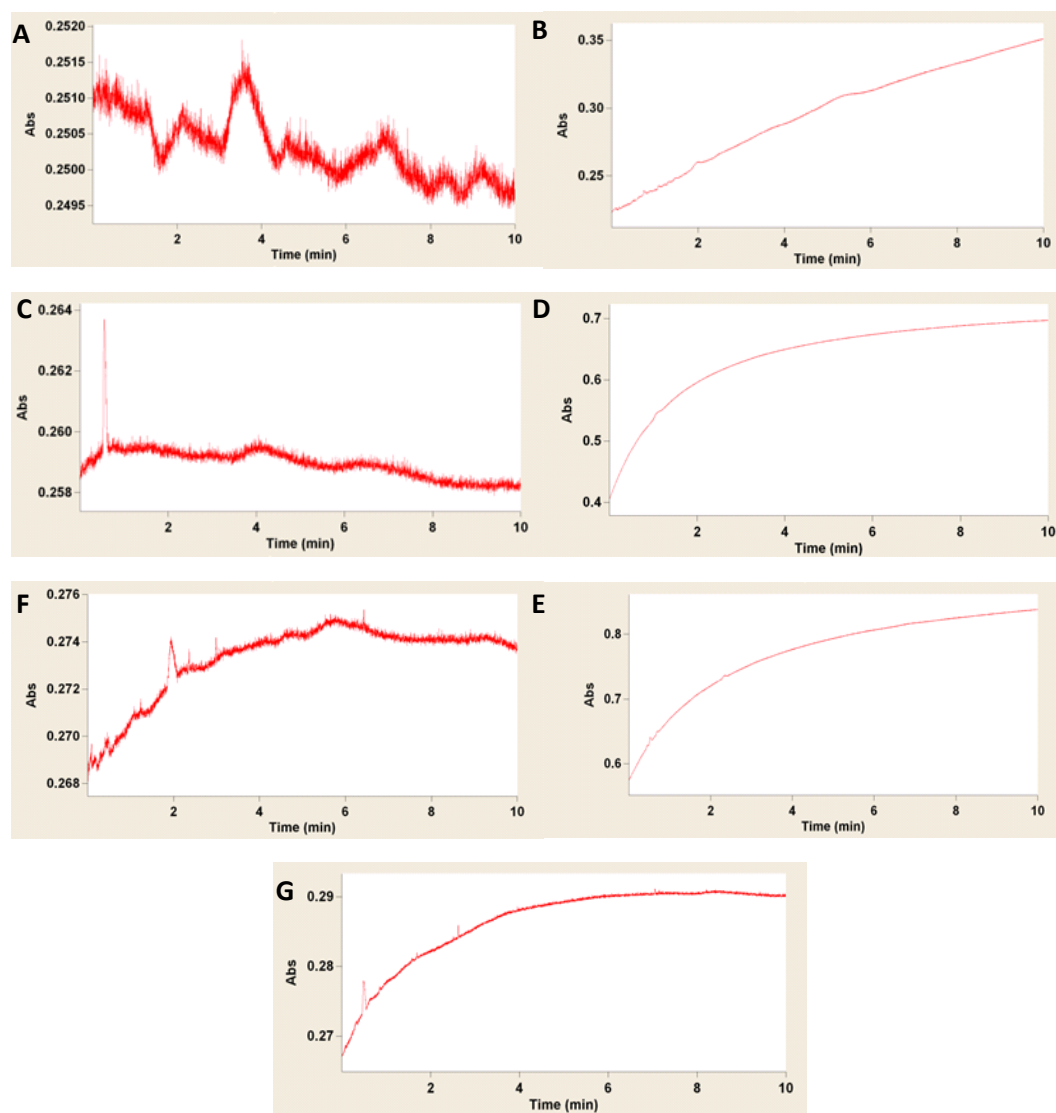


Figure 56: Preliminary activity assays of *TfuDyP*, *DyPB* and *Sclac* towards Kraft lignin (6.2.20). A: Control reaction for *Sclac* assay B: *Sclac* assay C: Control reaction for *DyP*-type peroxidases D: *TfuDyP* assay E: *DyPB* assay F: *TfuDyP* assay with 1 mM MnCl_2 G: *DyPB* assay with 1 mM MnCl_2 .

8.11 Optimization of *TfuDyP* expression time in *S. cerevisiae*

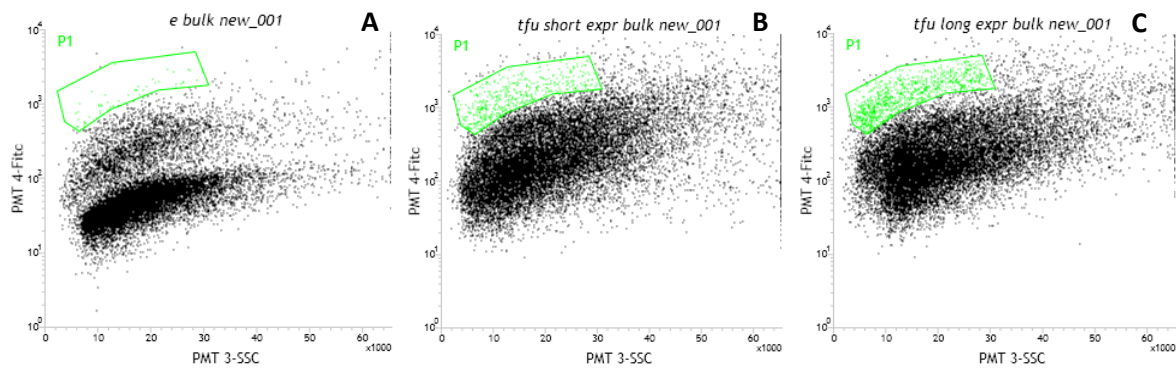


Figure 57: Optimization of *TfuDyP* expression time in *S. cerevisiae*. *S. cerevisiae* cells that express *TfuDyP* (6.2.7) were induced for 16 h (B) or 20 h (C) to optimize the expression time. Control expression was carried out with *S. cerevisiae* cells that contain empty pCTcon2 vector (A). The P1 gate (indicated in green) shows the region where positive cells would accumulate provide the comparison between *TfuDyP* expressing cells and empty vector control cells.

8.12 Secondary structure of *TfuDyP*

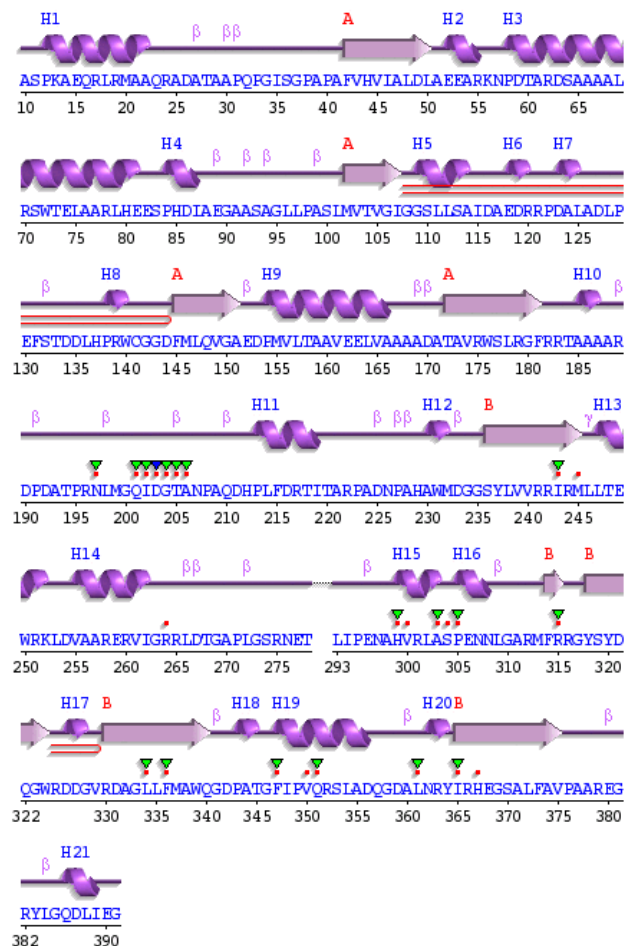


Figure 58: Secondary protein structure of *TfuDyP* (PDB: 5FW4) (via www.expasy.org). Secondary structures : Helix and strand. Motifs β : beta turn γ : gamma turn : beta hairpin. Residue contacts : to ligand. : PDB SITE records.

8.13 Characterization of isolated mutant *TfuDyP* variants and WT-*TfuDyP*

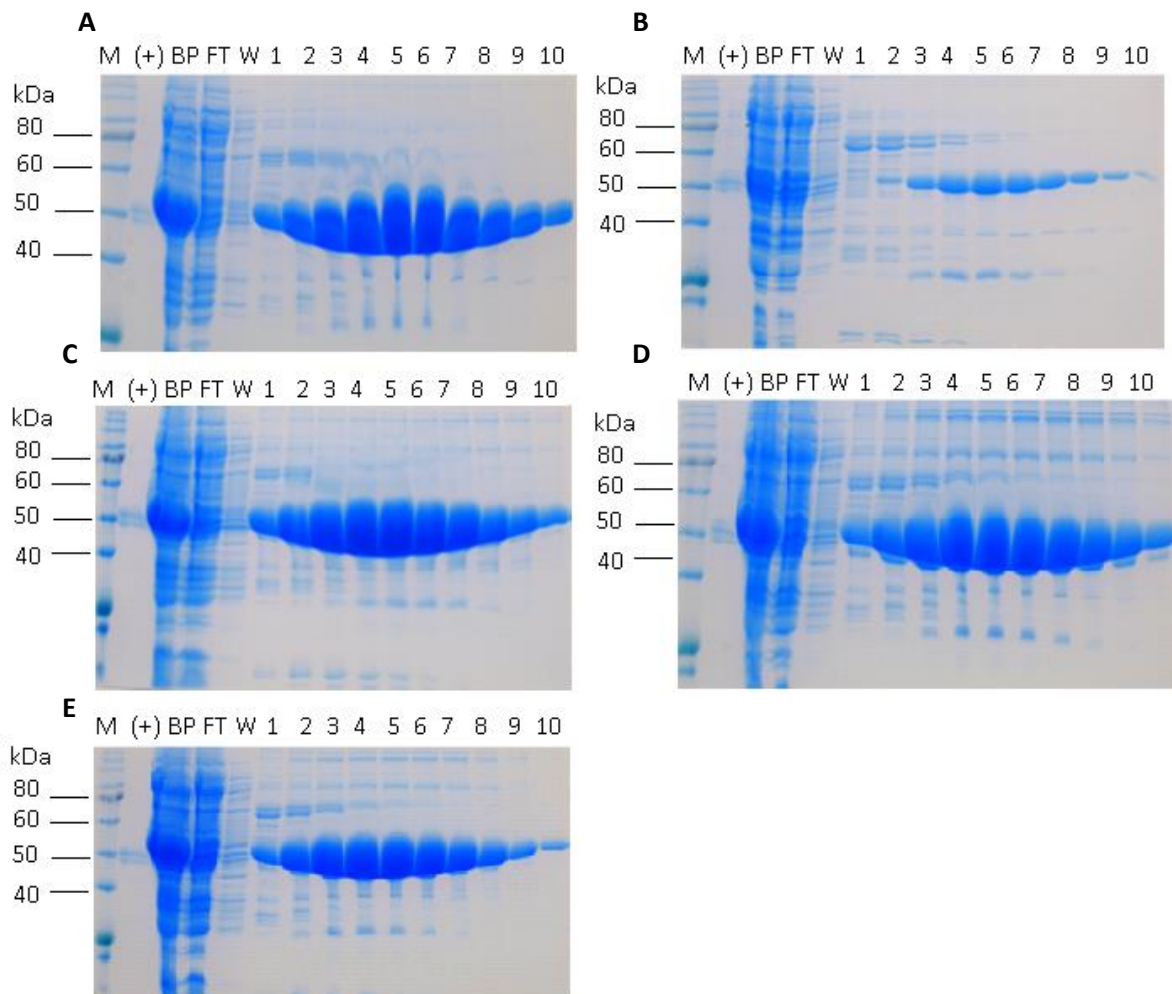


Figure 59: SDS-PAGE analyses of purified mutant *TfuDyP* variants and WT-*TfuDyP*. Elution fractions for R315H (A), P154S+Q357R (B), V165I (C), S274 (D) variants and WT-*TfuDyP* (E). M: Molecular mass marker (P7712S, NEB), C(+): Positive control (a His6-tagged recombinant protein sample), BP: Before purification, FT: Flow through, W: Washing after sample application, 1-10: Elution fractions. SDS-PAGE analyses (A-E) were carried out using 12% polyacrylamide gels (6.2.10).

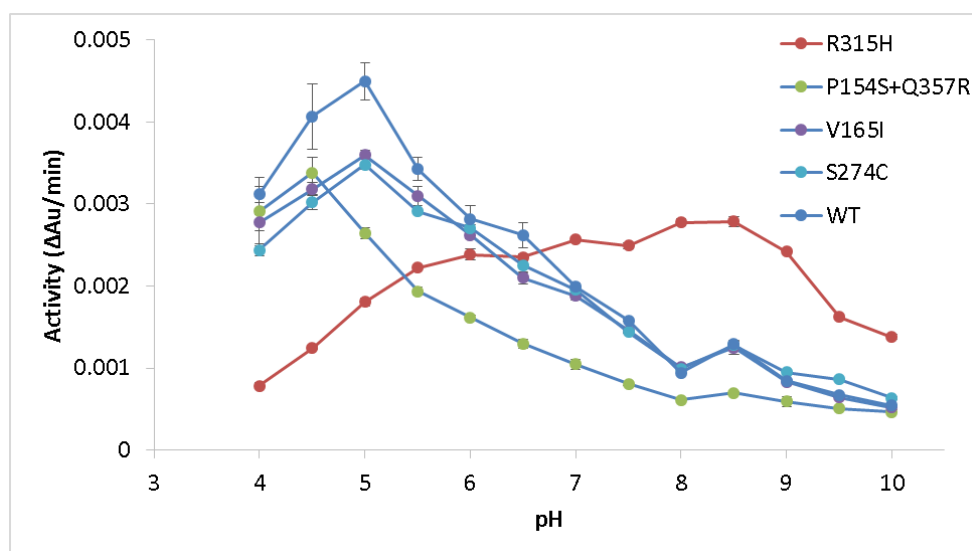


Figure 60: Optimum pH profile of mutant *TfuDyP* and WT-*TfuDyP* variants. The activities of the purified recombinant enzymes were measured against 200 μ M guaiacol (6.2.15) at 25°C in buffers with various pH values ranging from pH 3.5 to 10.0 at 25°C (6.2.21). All measurements were performed in triplicate (n = 3). Error bars indicate standard deviation ($\bar{x} \pm$ SD) from arithmetic mean.

8.14 List of publications

Publications:

Ece, S., Lambertz, C., Fischer, R., & Commandeur, U. (2017). Heterologous expression of a *Streptomyces cyaneus* laccase for biomass modification applications. *AMB Express*, 7(1), 86.

Lambertz, C., **Ece, S.**, Fischer, R., & Commandeur, U. (2016). Progress and obstacles in the production and application of recombinant lignin-degrading peroxidases. *Bioengineered*, 7(3), 145-154.

Manuscripts in preparation:

Ece S, Lambertz C, Rahman-Pour R, Rasche S, Tran F, Lancefield CS, Bugg TD, Westwood NJ and Commandeur U, Fischer R (2017) *Pseudomonas fluorescens* produces high yields of a recombinant *Thermobifida fusca* DyP-type peroxidase with activity against lignin model compounds and Kraft lignin.

Ece S, Tran F, Lancefield CS, Lambertz C, Commandeur U, Fischer R, Bruijninx P, Westwood NJ (2018) Analysis of ScLac activity on a phenolic SS-β-O-4 lignin model compound.

Ece S, Lambertz C, Commandeur U, Fischer R, Ostafe R (2018) Ultra-High-Throughput Screening of a Dye-decolorizing peroxidase/laccase library created by directed evolution.

Poster Presentations:

Ece S, Lambertz C, Commandeur U, Fischer R (2014) Recombinant production of lignin-degrading enzymes, 2nd TMFB International Conference, Aachen, Germany.

Ece S, Lambertz C, Commandeur U, Fischer R (2014) Recombinant expression of a DyP-type Peroxidase in an *E. coli* host system for effective lignin degradation, BIOCAT, Hamburg, Germany.

List of non-PhD related publications

Ece S, Evran S, Janda JO, Merkl R, Sterner R (2015) Improving thermal and detergent stability of *Bacillus stearothermophilus* neopullulanase by rational enzyme design. *Protein Engineering, Design & Selection*, (28): 6, 147–151.

Kozgus Guldu O, **Ece S**, Evran S, Medine EI, Odaci Demirkol D, Unak P & Timur S (2014) Isolation and Immobilization of His-Tagged Alcohol Dehydrogenase on Magnetic Nanoparticles in One Step: Application as Biosensor Platform, *Journal of Macromolecular Science, Part A: Pure and Applied Chemistry*, (51): 9, 699-705.

Ozturk H, **Ece S**, Gundeger E, Evran S (2013) Site-Directed Mutagenesis of Methionine Residues for Improving Oxidative Stability of α-amylase from *Thermotoga maritima*. *Journal of Bioscience and Bioengineering*, (116): 4, 449–451.

8.15 List of figures

Figure 1: The big picture of energy consumption and its adverse outcomes on economics and environment (Bauer et al., 2016; Statistics, 2011)..	5
Figure 2: The main components of lignocellulose and their building blocks (Isikgor & Becer, 2015)..	6
Figure 3: The monomers, which build lignin polymers and corresponding units within the incorporated lignin polymer structure (modified from Abdel-Hamid et al., 2013).....	7
Figure 4: Phenylpropanoid linkages in lignin polymer structure (modified from Abdel-Hamid et al., 2013).....	8
Figure 5: A scheme of ideal lignocellulosic biomass exploitation by the conversion of the subunits into the value-added products (adapted from Jorgensen et al., 2007).....	9
Figure 6: Biomass pretreatment methods and the type of lignin obtained from each method (adapted from Bruijninx et al., 2016).....	10
Figure 7: The lignin subunits that are attacked by lignin-degrading enzymes and the most common reaction mechanisms for each enzyme (modified from Lambertz et al., 2016).....	12
Figure 8: β -aryl ether cleavage pathway in <i>S. paucimobilis</i> via guaiacyl- α -veratrylglycerol (GVL) model compound (Picart et al., 2014).	16
Figure 9: The flowchart of the work described in this thesis.	19
Figure 10: SDS-PAGE and western blot analysis of the IMAC purification fractions of <i>TfuDyP</i> -cp (A, B), <i>TfuDyP</i> -Tat (C, D) and <i>TfuDyP</i> -pelB (E, F).....	23
Figure 11: SDS-PAGE and western blot analyses of the IMAC purification fractions of <i>DyPB</i> -cp (A, B) and <i>DyPB</i> -pelB (C, D).....	24
Figure 12: SDS-PAGE and western blot analyses of the IMAC purification fractions of <i>SSHGDyP</i> -cp (A, B) and <i>SSHGDyP</i> -pelB (C, D).	25
Figure 13: SDS-PAGE and western blot analyses of the IMAC purification fractions of <i>Sclac</i> -cp (A, B) and <i>Sclac</i> -pelB (C, D).	26
Figure 14: SDS-PAGE and western blot analyses of the IMAC fractions of <i>LigE</i> with C-terminus His ₆ -tag (A, B) and with N-terminus His ₆ -tag (C, D).....	27
Figure 15: SDS-PAGE and western blot analyses of the IMAC purification fractions of <i>LigF</i> with C-terminus His ₆ -tag (A, B) and <i>LigF</i> with N-terminus His ₆ -tag (C, D).....	27

Appendix

Figure 16: SDS-PAGE and Western-Blot analyses of the IMAC purification fractions of <i>E. coli</i> BL21 Star (DE3) cells (A, B) and <i>E. coli</i> BL21-CodonPlus(DE3)-RIL (C, D) carrying the empty pET-22b(+) vector.	28
Figure 17: SDS-PAGE of IMAC purified <i>TfuDyP</i> , <i>ScLac</i> , <i>LigE</i> and <i>LigF</i> expressed in <i>P. fluorescens</i>	29
Figure 18: Soret band analyses of DyP-type peroxidases expressed in <i>E. coli</i> and <i>P. fluorescens</i> (Pf).	31
Figure 19: Visible spectra analyses and activity assays of <i>ScLac</i> -cp expressed in <i>E. coli</i> (A, C) and in <i>P. fluorescens</i> (B, D).	32
Figure 20: Zymogram analysis of purified laccases expressed in <i>E. coli</i> (lane 1) and in <i>P. fluorescens</i> (lane 2).	33
Figure 21: pH (A) and temperature (B) profiles of the recombinant lignin-degrading enzymes.	34
Figure 22: Short term (A) and long term (B) thermal stability assays of the recombinant lignin-degrading enzymes.	36
Figure 23: pH stability profiles of the recombinant lignin-degrading enzymes.	37
Figure 24: Stability profiles of the recombinant lignin-degrading enzymes in the presence of DMSO.	40
Figure 25: Stability profiles of the recombinant lignin-degrading enzymes in the presence of ethanol and methanol.	41
Figure 26: The phenolic and non-phenolic, aromatic complex lignin-model compounds.	42
Figure 27: Conversion of the secondary alcohol moiety of the SS- β -O-4 OH (left) to the corresponding SS- β -O-4 ketone (right) in the presence of laccase enzymes.	43
Figure 28: Representative analysis of the activity against the SS β -O-4 OH model compound by NMR using <i>ScLac</i>	43
Figure 29: Demonstration of the quantification of the phenolic SS β -O-4 OH model compound conversion to the corresponding ketone product by the addition of an internal standard to the reaction mixtures after the reactions are stopped.	44
Figure 30: Kinetic analysis of the <i>ScLac</i> -Ec activity on the phenolic SS β -O-4 OH model compound. .	46
Figure 31: Change of <i>TfuDyP</i> , <i>DyPB</i> and <i>ScLac</i> activity (Abs s^{-1}) by increasing Kraft lignin concentration (μM).	47
Figure 32: The reusability of immobilized <i>ScLac</i> samples.	48
Figure 33: Characterization of immobilized and free <i>ScLac</i> samples.	49

Appendix

Figure 34: Ultra-high-throughput screening method for FACS.	50
Figure 35: Analysis of the MEGAWHOP-PCR for the creation of mutant <i>TfuDyP</i> library.	52
Figure 36: Optimization of reaction time (1 min) for tyramide assay using the artificial reference library.	53
Figure 37: Optimization of reaction time (5 min) for tyramide assay using the artificial reference library.	53
Figure 38: Optimization of reaction time (15 min) for tyramide assay using the artificial reference library.	54
Figure 39: Optimization of reaction time (30 min) for tyramide assay using the artificial reference library.	54
Figure 40: ABTS MTP assays of 5% reference libraries incubated with tyramide for 1 min (A), 5 min (B), 15 min (C), and 30 min (D) before and after sorting (6.2.24).	55
Figure 41: FACS analysis of <i>TfuDyP</i> library with (E) or without (F) H ₂ O ₂ pretreatment together with positive (A, C) and negative controls (B, D).	56
Figure 42: The homodimer structure of <i>TfuDyP</i> (PDB: 5FW4).	57
Figure 43: pET-22b(+) vector used as template for vector construction and expression in <i>E. coli</i>	114
Figure 44: pET-21d(+) vector used as template for vector construction and expression of mutant <i>TfuDyP</i> variants and WT- <i>TfuDyP</i> in <i>E. coli</i>	114
Figure 45: pCTcon2 vector used for construction and expression in <i>S. cerevisiae</i> EBY 100 cells for FACS screening.	115
Figure 46: Protein and DNA ladders.	116
Figure 47: Standard calibration curve for quantification of 4-MU, which is produced as a result of the enzymatic activity of β -etherases on MUAV.	116
Figure 48: A representative IMAC chromatogram.	117
Figure 49: HPLC analysis of ScLac (6.2.19) activity on the non-phenolic substrate veratryl alcohol in the presence of ABTS as the mediator system.	118
Figure 50: HPLC analysis of ScLac activity (6.2.19) on the non-phenolic substrate veratryl alcohol in the presence of HBT as the mediator system.	119
Figure 51: HPLC analysis of ScLac activity (6.2.19) on the non-phenolic substrate veratryl alcohol in the presence of ABTS as the mediator system.	120

Appendix

Figure 52: HPLC analysis of ScLac activity (6.2.19) on the non-phenolic substrate veratryl alcohol in the presence of HBT as the mediator system.....	121
Figure 53: Representative LC-MS chromatogram of the analysis of ScLac reaction with the SS β -O-4 model compound (6.2.18).	122
Figure 54: Representative LC-MS chromatogram of the analysis of ScLac reaction with the SS β -O-4 model compound (6.2.18).	123
Figure 55: Activity analysis of laccase from <i>T. versicolor</i> towards the phenolic SS β -O-4 OH lignin-model compound (6.2.18).	124
Figure 56: Preliminary activity assays of <i>TfuDyP</i> , DyPB and ScLac towards Kraft lignin (6.2.20).....	125
Figure 57: Optimization of <i>TfuDyP</i> expression time in <i>S. cerevisiae</i>	126
Figure 58: Secondary protein structure of <i>TfuDyP</i> (PDB: 5FW4) (via www.expasy.org).	126
Figure 59: SDS-PAGE analyses of purified mutant <i>TfuDyP</i> variants and WT- <i>TfuDyP</i>	127
Figure 60: Optimum pH profile of mutant <i>TfuDyP</i> and WT- <i>TfuDyP</i> variants.	128

8.16 List of tables

Table 1: Enzymes that have been chosen for heterologous expression in an <i>E. coli</i> and a <i>Pseudomonas fluorescens</i> host system.	20
Table 2: Optimal culture conditions (Induction OD ₆₀₀ , IPTG concentration, expression temperature and expression duration), <i>E. coli</i> strain used for the heterologous expression of the lignin-degrading enzyme constructs and the corresponding expression yields.....	22
Table 3: The initial and optimized heterologous expression yields of the lignin-degrading enzymes in <i>P. fluorescens</i>	30
Table 4: Reinheitszahl (RZ) values (6.2.14) calculated for DyP-type peroxidases expressed in <i>E. coli</i> and <i>P. fluorescens</i> with or without leader peptides.	31
Table 5: Specific activities of recombinant DyP-type peroxidases towards DMP (6.2.15) expressed by various heterologous expression strategies.	37
Table 6: Specific activities of the recombinant ScLac towards DMP (6.2.15) expressed by various heterologous expression strategies.....	38
Table 7: Specific activities of the recombinant β -etherases towards MUAV (6.2.15) expressed by various heterologous expression strategies.	38
Table 8: Kinetic parameters (6.2.17) of <i>TfuDyP</i> towards DMP, ABTS and guaiacol.	38

Appendix

Table 9: Kinetic parameters (6.2.17) of DyPB towards DMP, ABTS and guaiacol.....	38
Table 10: Kinetic parameters (6.2.17) of Sclac towards DMP, ABTS and guaiacol.....	39
Table 11: Kinetic parameters (6.2.17) of LigE towards MUAV.....	39
Table 12: Kinetic parameters (6.2.17) of LigF towards MUAV.....	39
Table 13: Percentage formation of SS β -O-4 OH ketone by purified Sclac expressed in <i>E. coli</i> or <i>P. fluorescens</i>	45
Table 14: Percentage formation of SS β -O-4 OH ketone by purified <i>TfuDyP</i> and DyPB expressed in <i>E. coli</i> or <i>P. fluorescens</i>	45
Table 15: Kinetic parameters of <i>TfuDyP</i> , DyPB and Sclac towards Kraft lignin (6.2.17).....	47
Table 16: The sequence analysis of randomly selected five colonies from the transformation plates of MEGAWHOP-PCR products (6.2.23).....	52
Table 17: Sequencing analysis of the variants that showed higher activity in comparison to the WT- <i>TfuDyP</i> in the ABTS MTP assay after the pretreatment with 5 mM H ₂ O ₂ (6.2.24).....	56
Table 18: Characterization of the isolated mutant <i>TfuDyP</i> variants (6.2.24) and WT- <i>TfuDyP</i> (6.2.24) expressed in <i>E. coli</i> (6.2.6) for expression yield (mg protein per L ⁻¹ expression culture), pH and temperature profiles (6.2.21) and kinetic parameters (6.2.17) (K_M , k_{cat} and k_{cat}/K_M) for guaiacol.....	58
Table 19: Comparison of the expression yields obtained in <i>E. coli</i> and <i>P. fluorescens</i> with the yields reported in the literature obtained by heterologous expression.....	63
Table 20: Bacterial laccases, laccase-like phenol oxidases, and multi-copper oxidases produced by heterologous expression in <i>E. coli</i> and the corresponding expression yields (if reported).....	64
Table 21: Bacterial DyP-type peroxidases produced by heterologous expression in <i>E. coli</i> and the corresponding expression yields (if reported).....	66
Table 22: Bacterial β -etherases produced by heterologous expression in <i>E. coli</i> and the corresponding expression yields (if reported).....	67

Acknowledgements

I would like to thank all the people who contributed in some way to the work described in this thesis. First and foremost, I thank my academic advisor, Prof. Dr. Rainer Fischer, for giving me the opportunity to conduct my research towards my PhD degree in his group. During my work, he contributed to a great research experience by giving me intellectual freedom and providing me the great opportunities at Fraunhofer IME, engaging me in new ideas, and demanding a high quality of work in all my endeavors. Additionally, I would like to thank my second examiner Prof. Dr. Lars M. Blank for his interest in my work.

I am grateful to Dr. Ulrich Commandeur for giving me the chance to work at Bio7 and to benefit from all the opportunities provided by the institute. Thanks for the challenging progress report presentations, I have comprehended how important the controls are and how easily they can be forgotten. I would like to thank Dr. Camilla Lambertz for taking part in my supervision and for her constant help with the revisions carried out on my reports, manuscripts and dissertation. I acknowledge Dr. Birgit Orthen for her invaluable feedback and insightful comments on my PhD Outline discussions, PhD seminars and dissertation. I would like to thank Dr. Richard Twyman for his rigorous revisions on the spelling and grammar of my manuscripts.

I would be remiss if I did not thank Karolin Richter, who deserves the credit for providing much needed help with the technical issues and the practical difficulties that I faced in the lab. I acknowledge Ingrid Wildrath for always helping me with the administrative issues.

I acknowledge all my current and former colleagues at Bio7, particularly Camilla, Christian, Dirk, Holger, Hormoz, Johannes, Julie, Mareike, Megan, Niklas and Tini, for sharing the office and the labs, for their support in daily lab-life and for the friendly atmosphere throughout the challenging times. I would like to thank Bachelor students Laura and Louisa for contributing to the greater picture of my thesis and helping me to gain organizational and supervisor skills.

Every result described in this thesis was accomplished with the help and support of fellow lab-mates and collaborators. I would like to thank Dr. Raluca Ostafe for helping me with the directed evolution studies and FACS screenings and for being patient long hours in the lab trying to solve the practical difficulties with me. I greatly benefited from her solid scientific insights. The secondments that I experienced helped me a lot to develop an interdisciplinary background and have made indispensable contributions to the work described in this thesis. I would like to thank various members of the groups with whom I had the opportunity to work: Prof. Dr. Nicholas Westwood and Dr. Fanny Tran Lancefield for supervising me and helping me with the enzymatic reactions on lignin-model compounds and NMR analyses and Dr. Brunello Nardone for helping me with the LC-MS measurements during my

Acknowledgements

secondment at the School of Chemistry (University of St Andrews), Assoc. Prof. Dr. Pieter Bruijninx and Dr. Christopher Lancefield for providing me the lignin-model compounds, helping with the NMR measurements and for their supervision during my exchange at Debye Institute for Nanomaterials Science (Utrecht University) and Prof. Dr. Timothy Bugg and Dr. Rahman Rahmanpour for kindly hosting me in their lab and helping me to gain more insight into the lignin-degrading enzyme activities at the Department of Chemistry (University of Warwick). I would like to thank Torsten Rinesch (Organic Chemistry, RWTH Aachen University) for helping with the HPLC analyses of certain enzymatic reactions and Christoph Müller (ITMC, RWTH Aachen University) for synthesizing MUAV compound.

I am grateful for the funding sources from SuBiCat ITN via Marie Skłodowska-Curie Actions (EC) and Cluster of Excellence TMFB that allowed me to pursue my studies, attend conferences and meetings and gain an international background. I acknowledge all SuBiCat members and colleagues for useful workshops, fruitful discussions and sharing challenging times under a very friendly atmosphere.

Finally, I would like to acknowledge all my friends and family who supported me over the years. I would like to cordially thank Mom, Dad, my brother and Turgay for their constant love and support. Thank you for supporting me wholeheartedly with every decision I made and encouraging me always to do my best.

Declaration

Declaration

I hereby declare that all information in this document has been obtained and presented in accordance with academic rules and ethical conduct. I also declare that as required by these rules and conduct I have fully cited and referenced all material and results that are not original to this work.

Selin Ece, Aachen 07.02.2018

Curriculum vitae

Name: Selin Ece

Date of birth: 27.05.1987

Place of birth: Izmir, Turkey

Education

2001-2005: High School: Sidika Rodop High School, Izmir, Turkey

2005-2010: Undergraduate studies: Bachelor of Biochemistry, Ege University, Izmir, Turkey
with a special focus on Biotechnology

Minor studies: Food Engineering, Ege University, Izmir, Turkey

Bachelors thesis: Heterologous expression, purification and investigation of bio-electrochemical parameters of an (C-His₆ Tag) alcohol dehydrogenase.

2010-2013: Graduate studies: Master of Science in Biochemistry, Ege University, Izmir, Turkey

Masters thesis: Increasing the thermal and chemical stability of a neopullulanase for its use in biotechnology.

2013 onwards: PhD in molecular biotechnology with a Marie Skłodowska-Curie Early Stage Researcher Fellowship

Working title: Heterologous expression of lignin-degrading enzymes for biological depolymerization of lignin